eman ta zabal zazu

Universidad del País Vasco

Euskal Herriko Unibertsitatea

Saretze erreakzioaren kontrola proteinazko filmen eta biokonpositeen propietateak egokitzeko

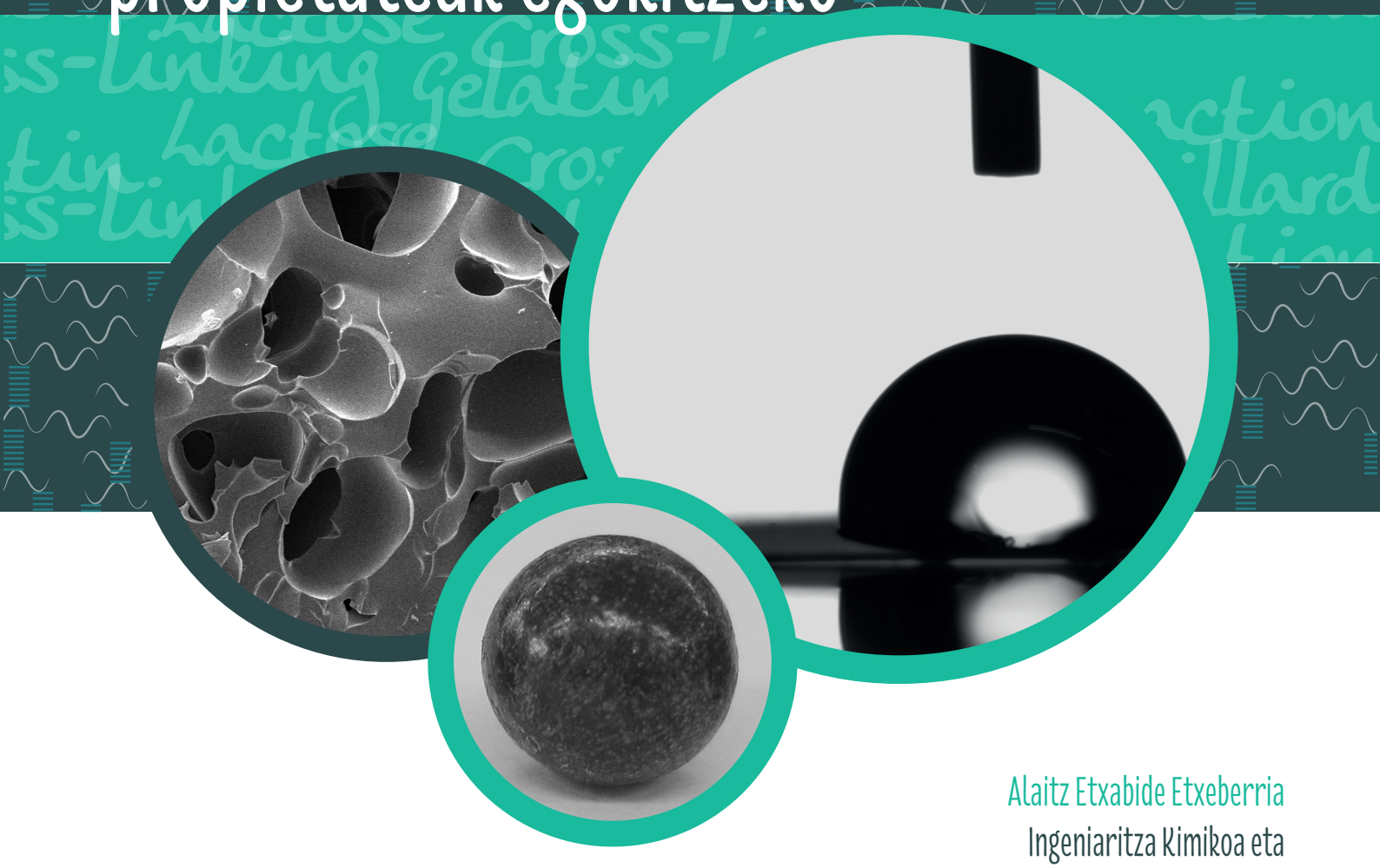

Alaitz Etxabide Etxeberria

Ingeniaritza Kimikoa eta Ingurumenaren Ingeniaritza saila

Donostia-San Sebastián, 2017

Saretze erreakzioaren kontrola proteinazko filmen eta biokonpositeen propietateak egokitzeko

Alaitz Etxabide Etxeberria

Tesi Zuzendariak: Koro de la Caba eta Pedro Guerrero

Ingeniaritza Kimikoa eta Ingurumenaren Ingeniaritza Saila

Donostia-San Sebastián, 2017

eman ta zabal zazu

Universidad del País Vasco

Euskal Herriko Unibertsitatea

Saretze erreakzioaren kontrola proteinazko filmen eta biokonpositeen propietateak egokitzeko

Alaitz Etxabide Etxeberria

Ingeniaritza Kimikoa eta Ingurumenaren Ingeniaritza Saila

Donostia-San Sebastián, 2017

Esker onak / Agradecimientos/ Remerciements/ Acknowledgements

Bizitzako bertze fase berri bati hasiera eman dion hiru urte t`erdiko etapa honen amaierara iristeko nire ondoan egon diren pertsona guztiei eskerrak eman nahi dizkiet.

Comenzar agradeciendo a Koro de la Caba y Pedro Guerrero, directores de mi tesis-doctoral. Gracias por ofrecerme esta oportunidad de dar los primeros pasos en la investigación junto a vosotros. Un placer haberos conocido y haber compartido con vosotros ese tiempo durante los proyectos fin de grado y máster. Gracias también por la confianza depositada en mí a la hora de iniciar esta tesis doctoral dentro del grupo BIOMAT. La orientación, el seguimiento y la supervisión continua junto con el apoyo recibido a lo largo de estos años han sido esenciales para mi desarrollo profesional como personal. Gracias, de nuevo por establecer en mí unos principios de trabajo sólidos e imprescindibles.

Bertzetik, doktorego-tesi honetan jardunean, nire ondoan egon diren hasieran lankide ziren eta orain lagun direnei, beraien laguntza eta pazientzia eskertu nahi dizkiet. Aldi berean, etxekoek emandako babesa eta bereziki niganako erakutsitako konfiantza eskertu nahiko nituzke, beraiek gabe lan honen bidea aldapatsuagoa izango litzateke eta. Orain arte aipatu ez ditudan lagun minak eta kuadrillakoak ere, eskerrak aunitz hor egoteagatik. Ahaztu gabe, Jose Emilio Txoperenari “Txoltxan” tesiaren euskarazko bertsioan emandako laguntza eskertu nahiko nizuke.

Je tiens à remercier infiniment Madame Véronique Coma et Monsieur Christian Gardrat pour m’avoir dirigée pendant mon séjour scientifique dans le Laboratoire de Chimie des Polymères Organiques (LCPO), à l’Université Bordeaux 1 (France). Leurs enseignements et conseils m’ont été d’une grande aide. I would also like to thank Dr. Piergiorgio Gentile and Dr. Ana Maria Ferreira-Duarte for giving me the chance to carry out scientific stay in the School of Mechanical and Systems Engineering at Newcastle

University (UK). Their good humor and wide knowledge were important and helpful for going on advancing in my investigation.

Azkenik, Euskal Herriko Unibertsitateak (UVP/EHU, PIF13/008 kontratua) eta Biomat ikerketa taldeak (UPV/EHU, GIU15/03) emandako diru-laguntza eskertzearekin batera, Gipuzkoako Foru Aldundia, UPV/EHU-ko Ikerkuntzarako Zerbitzu Orokorra (SGIker) eta NanoBioCell nahiz Enedi ikerketa taldeak eskertu nahiko nituzke.

Laburpena

Plastikoek eguneroko bizitza eraldatu dute eta onura ugari ekarri dizkiote gizarteari. Hala ere, plastikoen erabilerak eta hauen zabor-tratamenduak sortutako kezkek jasangarriagoak diren iturrien erabilera bultzatzeko ordezko materialen garapena sustatu dute, ekonomia zirkularraren kontzeptuarekin bat etorriz. Honi dagokionez, gelatina material berriztagarria eta biodegradagarria izateaz gain erabilgarria da, kostu baxua dauka, filma eratzeko gaitasuna du eta zentzumen onargarritasuna erakusten du. Testuinguru honetan, lan honen helburu orokorra, formulazioen konposizioaren eta prozesatze metodoen nahiz baldintzen arabera asmo ezberdinetarako, hala nola, paketatzeko edota aplikazio farmazeutikoetarako gelatinan oinarritutako materialak garatzea eta karakterizatzea izan da.

Lan hau 10 atalez osatuta dago. Lehenengo atala, film aktiboetan egin berri diren aurrerapenen ikuspegi orokorra da. Bertan, produktu eta aplikazio berrietarako industriako hondakinetatik eta azpi-produktuetatik lehengaiak lortzearen garrantzia azpimarratzen da. Ikerkuntza lan hau aurrera eramateko erabilitako materialak eta metodoak berriz, bigarren atalean azaltzen dira. Ondoren, hirugarren atalean, prozesatze baldintzen eragina gelatinazko filmen propietate funtzionalengan nahiz materialaren ingurumen-inpaktua aztertu dira, filmen abantailak eta hobetu beharreko alderdiak identifikatzeko helburuarekin.

Gelatinaren berezko hidrofilotasuna filmen hauskortasun altuaren eta urarekiko sentikortasunaren erantzule dela aintzakotzat hartuta, propietate funtzional hauen hobekuntza Maillard izeneko saretze erreakzioa ahalbidetzen duen laktosaren gehikuntzaren bidez aztertu da. Maillard erreakzioan, eta beraz filmen propietateetan laktosa kantitateak, berokuntzak eta soluzioaren pH-ak duten eragina laugarren eta bosgarren ataletan aztertu da. Kapitulu hauetan lortutako emaitzak kontuan izanda, seigarren atalean, pH basikoan Maillard erreakzioaren kontrola berokuntza denboraren

funtziopean burutu da. Maillard erreakzioan zehar konposatu antioxidatzaileak sortzen direnez, zazpigarren atalean saretutako gelatinazko filmen ahalmen antioxidatzailea aztertzearekin batera, filma eratzeko soluzioan gehituriko kurkumatik eratorritako konposatuak filmen propietate antioxidatzaileetan duen eragina ere aztertu da. Filmen azterketa sakon baten ostean, estrusio eta injekzio bidez lorturiko laktosarekin saretutako gelatinazko biokonpositeen propietateak zortzigarren atalean aztertu dira. Azkenik, bederatzigarren atalean ikerketa honen ondorio orokorrak laburtu dira eta testuan zehar aipatutako erreferentziak hamargarren atalean zerrendatu dira.

Helburuak

Ikerlan honen helburu orokorra, formulazioen konposizioaren eta prozesatze metodoen nahiz baldintzen arabera gelatinan oinarritutako materialak garatu eta karakterizatzea da.

Tesiaren helburu zehatzak ondorengoak dira:

- Film aktiboetan egindako hobekuntzen ikuspegi orokorra ematea.
- Gelatinazko filmen propietate funtzionaletan prozesatze baldintzen eragina aztertzea.
- Gelatinaren erauzketa prozesutik filma zakarretara bota arte gelatinazko filmen ingurumen-inpaktua ebaluatzea.
- Laktosa edukiaren, berokuntzaren eta disoluzioaren pH-aren eragina saretze erreakzioan eta gelatinazko filmen propietate funtzionaletan aztertzea.
- Saretutako gelatinazko filmen ahalmen antioxidatzailea aztertzea.
- Gelatinazko biokonpositeak lortzeko estrusio eta injekzio prozesuen parametroak optimizatzea.

Aurkibidea

1 Sarrera

1.1 Gelatina, ontziratze aktiborako lehengaia

2015 urtean Europako plastikoen merkatuak esponentzialki gora egin zuen, urteko 58 milioi tona ekoiztuz (PlasticsEurope, 2016); horietatik gutxi gora-behera % 39,9a paketatze-industriara bideratu zen. Paketatzea egunerokotasunerako beharrezko eta funtsezko kontsumogaia bihurtu da. Bilgarriek funtzio ezberdinak betetzen dituzte, hala nola, eustea, babestea, praktikoa izatea, komunikatzea, eta elikagaien kalitatea nahiz segurtasuna ziurtatzea (Roberston, 2013). Erabilera honetarako, plastiko sintetikoek propietate bikainak aurkezten dituzte. Hala ere, beraien iraunkortasunak zakarretarako hondakinetan arazo nabarmenak sortzen ditu, izan ere, material hauek ez-biodegradagarriak eta birziklatzeko zailak baitira.

Azken urteotan, iturri berriztagarrietatik eratorritako polimero biodegradagarriak, hala nola, nekazaritza-industriako eta itsasoko hondakin eta azpi-produktuak, petroliotik eratorritako polimeroak ordezkatzeko aukera jasangarritzat hartu dira (Leceta et al., 2014). Gainera, kontsumitzaileen osasun, elikatze balio eta elikagaien babesaren (konposatu toxikoen lekutzea bildukitik elikagaira) inguruan sorturiko kezkek, sintetikoak diren konposatuak naturalak diren substantziekin ordezkatuak izateko interesa areagotu dute (Bravin, Peressini, eta Sensidoni, 2006; López-Rubio, Lagarón, eta Ocio, 2008). Hori dela eta, elikagaiak babesteko biopolimero eta gehigarri naturalen erabilera ingurumenaren jasangarritasun eta kontsumitzaileen onargarritasun terminoetan abantaila izan daiteke. Landare eta animalietatik eratorritako material biodegradagarriek eta jangarriek, hala nola, proteinek, polisakaridoek eta lipidoek, bilduki moduan elikagaiekin kontaktuan erabiltzeko ahalmena erakutsi dute (Nur Hanani, Roos, eta Kerry, 2014; Wang et al., 2012).

Biopolimeroen artean, proteinen ugaritasunagatik, filma sortzeko gaitasunagatik, gardentasunagatik eta O_2, CO_2 eta lipidoen kontrako hesi-propietate bikainengatik, proteinak elikagaien paketatze produkziorako ezaugarri baliagarriak eskaintzen dituzten lehengaiak dira (Krochta, 2002; Lacroix eta Vu, 2014). Gainera,

proteinak heteropolimeroak direnez, talde funtzional ugari dituzte eta ondorioz, proteinetan oinarritutako materialen propietateak aldakuntza entzimatiko, kimiko edota fisikoen bidez eraldatu daitezke, aplikazio jakinetan behar diren amaierako propietateak lortzeko (Hammann eta Schmid, 2014). Horretaz gain, aipatzekoa da proteinetan oinarritutako filmak konposatu antioxidatzaileak, antimikrobiarrak, antifungikoak eta zaporedun moduko konposatuak eramateko garraiatzaile bikainak izan daitezkeela (Guadipati, 2013).

Azkeneko urteotan, proteinen ikerketaren arloan gelatinan oinarritutako materialenganako interesa handitu da (Gómez-Guillén et al., 2011). Gelatina animalia proteina bat da, lur eta itsasoko animalien hezur, azal eta ehun konektiboetako kolagenoari egindako hidrolisitik lortzen dena. Gelatinen artean, arrazoi soziokulturalak direla eta, arrain gelatinak arreta erakarri du ugaztun gelatinen ordez erabiltzeko (Benjakul, Kittiphattanabawon, eta Regenstein, 2012). Gelatinen ugaritasunak, erabilgarritasunak eta kostu baxuak material hau aplikazio ugarietan erabiltzera bultzatzen dute. Gelatina elikagai zaporegabea, biobateragarria, biodegradagarria eta ez-toxikoa denez (Ali et al., 2012), jangarriak diren filmetan erabiltzeko ahalmen handia erakusten du (Bergo eta Sobral, 2007; Karim eta Bhat, 2008). Gainera, gelatinazko filmak bioaktiboak garraiatzeko eramaile bezala erabili daitezke. Testuinguru honetan, kapitulu honen helburua elikagaien narriadura eragotzi edo atzeratzeko, eta hauen iraungitzea luzatzeko film aktibo moduan erabilitako gelatinan oinarritutako filmetan egin berri diren aurrerapenen ikuspegi orokorra ematea da.

Lipidoen erreakzio kimikoa, bereziki oxigenoarekin erreakzionatzen duten gantz-azido polisaturatugabeak, elikagaietan ematen den narriadura erreakzio nagusienetako bat da. Lipidoen oxidazioaz gain, elikagai produktuek nutriente ugari dituztenez, mikrobioengatik narriatzeko joera daukate (Kaewpprachu eta Rawdkuen, 2016). Narriadura prozesu hau elikadura produktuen produkzioko edozein urratsetan gerta daiteke, ontziratzean eta biltegiratzean esaterako, produktuan garraztasuna

eraginez. Lipidoen oxidazioak eta mikrobioen hazkuntzak elikagaien kalitatearen narriadura eragiten dute, horien egitura, itxura eta kolorea aldatuz, usain eta zapore txarrak sortuz, nutrizio-balioaren galtzea eraginez eta toxikoak diren konposatuak nahiz polimero oxidatuak sortuz (Anbinder et al., 2015; Tian, Decker, eta Goddard, 2013). Beraz, usteltzeak elikaduraren iraungitzea laburtzen du eta honek kontsumitzailearengan nahigabea eta kexak sortzen ditu, produktuaren onargarritasunean eta honen salmentetan eraginez. Ondorioz, bezeroen gaitzesteagatik elikagai-produktu kantitate handiak galtzen dira, ingurumenean eta ekonomian inpaktu negatiboak sortuz (Lin et al., 2013; Wardhani et al., 2013).

Elikagaien iraungitzea luzatzeko eta elikagaiak usteltzetik babesteko, gordetze teknika ezberdinak erabili dira, hala nola, izoztea, lehortzea, paketatzearen atmosfera aldatzea (MAP), hutsezko paketatzea eta konposatu aktiboen gehitzea, beste batzuen artean (Rahman, 2007). Elikagaietan zuzenenean gehituriko konposatu aktiboek lipidoen oxidazioa eta mikrobioen hazkuntza gutxitzen dituzten arren, babes-denbora laburrak erakusten dituzte (Costa et al., 2015; Bolumar, Andersen, eta Orlien, 2011). Gainera, elikagai asko daude, freskoak edo lehengaiak diren elikagaiak esaterako, konposatu aktiboak zuzenean gehitzeko baimenik ez dutenak (Tovar et al., 2005). Arazo hauek, paketatze aktiboaren ikerkuntza elikagai-industriako eskakizunak eta bezeroen beharrak betetzera bideratu dute (Roberston, 2013; Sanches-Silva et al., 2014). Konposatu antioxidatzaileak eta antimikrobiarrak filmen formulazioan gehitzea lipidoen oxidazioa eta mikrobioen hazkuntza arrakastaz geldiarazteko eta beraz, elikagaien usteltzea galarazteko etorkizun handiko metodoa da.

1.2 Gelatinazko filmentzat konposatu antioxidatzaileak

Antioxidatzaile sintetikoen (butil hidroxitoluenoa (BHT), butil hidroxianisola (BHA), terbutil hidrokinona (TBHQ) eta propil galato (PG)) osasun arrisku potentzialak, elikagaiak paketatzeko seguruagoak diren irtenbideen ikerketa burutzea behartu du (Boulekbache-Makhlouf, Slimani, eta Madani, 2013). Hortaz, oxidatzaile naturalak

erabiltzeko beharra izugarri zabaldu da eta horregatik, substantzia naturalak ikertuak izaten ari dira aktiboak diren konposatu naturalen iturri gisa (**1.1 taula**). Konposatu fenolikoak bereziki, egitura eta gai kimikoen aldaera ugariak eta propietate biologiko (anti-hantura, antimikrobiarra, antikantzerigenoa eta antimutagenikoa) bikainak erakusten dituzten antioxidatzaile naturalen talde garrantzitsuenetakoa kontsideratzen da. Konposatu hauek iturri ezberdinetatik eratortzen dira, hala nola, fruta, belar, espezie, barazki, lekari, intxaur, hazi, ale eta zerealetatik (Carlsen et al., 2010; Costa et al., 2015; Nollet eta Toldrá, 2015).

1.1 taula Film aktiboak sortzeko behi, txerri eta arrain gelatinari gehitutako antioxidatzaile naturalak.

Gelatina iturria	Antioxidatzailea	Erreferentzia
Behi gelatina	*Ascophyllum nodosum* alga marroi estraktua	Kadam et al., 2015
	Azenario-zuntz hondakina	Iahnke et al., 2015
	Zatoria multiflora	Kavoosi et al., 2014
	Eukaliptu egur lignosulfonatuak	Núñez-Flores et al., 2012
Txerri gelatina	Azido askorbikoa	Kowalzyk, 2016
	Etanol lupulu estraktua	Kowalczyk eta Biendl, 2016
	Kurkuma etanol estraktua	Bitencourt et al., 2014
Arrain gelatina	Kumarin, azido ferulikoa, tirosola, kerzitina	Benbettaïeb et al., 2016c
	Koko oskol etanol estraktua	Nagaranjan et al., 2015
	Kanela olio esentziala	Wu et al., 2015
	Te berde estraktua	Wu et al., 2013
	Sufre gabeko lignina uretan ez disolbagarria	Núñez-Flores et al., 2013
	Jengibre, kurkuma	Tongnuanchan et al., 2013
	Bergamota, limoia, lima	Tongnuanchan et al., 2012
	Iltze-kanela olio esentziala	Giménez et al., 2012
	C. barbata alga estraktua	Haddar et al., 2012
	Kanela, iltze-kanela, anis estraktua	Hoque et al., 2011

Substantzia aktiboen artean, olio esentzialek mikroorganismo ugarien kontrako ezaugarri antifungiko eta antiseptikoak erakusten dituztenez, aplikazio farmazeutikoetan asko erabiltzen dira (Djilani eta Dicko, 2012). Gainera, olio esentzial batzuk, beraien aktibitate antioxidatzaileengatik, elikagaiak babesteko ere erabiltzen dira. Iturri ezberdinetatik lortutako olio esentzial zitrikoak, bergamota, limoia eta lima esaterako, arrain gelatinazko filmen formulazioan gehituak izan dira (Tongnuanchan, Benjakul, eta Prodpran, 2012). Argiaren eta ur lurrunaren kontrako hesi-propietateak hobetzeaz gain, bergamota olio esentzialak 2,2-difenil-1-pikrilhidrazil (DPPH) erradikal

librea ezabatzeko aktibitaterik handiena erakutsi zuen. Sustraietatik eratorritako olio esentzialak, hala nola, jengibrea eta kurkuma, arrainen azaletatik lortutako gelatinazko filmetan ere gehitu dira (Tougnuanchan, Benjakul, eta Prodpran, 2013).

Gehitutako olio esentzialez gain, olioaren kontzentrazioak ahalmen antioxidatzailean eragina dauka. *Zatoria multiflora* olio esentziala behi gelatinazko filma eratzeko soluzioan kontzentrazio ezberdinetan gehitzerakoan, filmen ahalmen antioxidatzailea 2,6 ± 0,11tik 5,5 ± 0,51 mg azido galikoaren baliokidea/g filmeko igo zela ikusi zen, olio esentzialaren kontzentrazioa % 2tik % 8ra handitzerakoan (Kavoosi et al., 2014). Olio esentzial hauen aktibitate antioxidatzaileak, nitrogeno oxido eta malondialdehidoaren presentziarekin zerikusia du. Gainera, filmek aktibitate antimikrobiarra erakutsi zuten, bakterio Gram-positiboek (*Staphylococcus aureus, Bacillus subtilis*) bakterio Gram-negatiboek (*Pseudomonas aeruginosa, Escherichia coli*) baino eraginkortasun handiagoa erakutsiz.

Atarés eta Chiralt-ek (2016) elikagaiak paketatzeko film eta geruza jangarri/biodegradagarrien egituretan, propietate fisikoetan eta bioaktiboetan olio esentzialen gehikuntzaren eragina aztertu zuten. Olio esentzialak nagusiki emultsio bidez film eta geruzetan gehitu ziren, elikagaien teknologian erabilitako lurrunketaren ondorioz galdutako gehigarri kopurua txikitzeko erreminta egokia izateaz gain, polimeroaren matrizearen eta konposatu aktiboaren arteko kontaktua hobetzeko balio dezakeelako. Olio esentzialen gehikuntza bidez jangarriak diren film eta geruzen propietate antioxidatzaileetan edota antimikrobiarretan lortutako hobekuntzek, olio esentzialak elikagaien iraungitzea luzatu eta produktuaren balioa igo dezaketela adierazi zuten.

Olio esentzialez gain, belar eta espezieen estraktu gordinek konposatu fenolikoen kantitate handiak dituztenez, lipidoen oxidazioa atzeratzeko egokiak dira eta ondorioz, polimeroen matrizetan agente antioxidatzaile moduan erabiltzen dira

(Embuscado, 2015). Bitencourt eta lankideek (2014) kurkuma etanol estraktuaren ahalmen antioxidatzailea txerri gelatinazko filmetan aztertu zuten eta aktibitate antioxidatzailea gehituriko gehigarriaren kontzentrazioarekiko proportzionala zela ikusi zuten. Estraktuaren % 2 gehitzean, DPPH erradikala ezabatzeko aktibitatearen azterketak, antioxidatzaile ahalmena % 1,8tik % 79,2ra handitu zela erakutsi zuen. Ahalmen antioxidatzailea estraktuan dauden kurkumaren eta beste konposatu fenolikoen presentziarekin erlazionatzen da. Eragin antioxidatzaileaz gain, kurkuma etanol estraktuaren gehikuntzarekin tentsio erresistentzia eta urarekiko nahiz argiarekiko hesi-propietateak hobetu ziren. Beste estraktu batzuk, te berde estraktua bezalakoak, zilarrezko karpa arrainaren azaletik lortutako gelatinazko filmetan gehitzean, filmen propietate mekanikoak eta hesi-propietateak ere hobetu ziren (Wu et al., 2013). Estraktuaren ahalmen antioxidatzaileari dagokionez, te berde estraktuaren % 0,7ko gehikuntzak, fenolikoen guztizko edukia eta DPPH erradikalak ezabatzeko aktibitatea nabarmenki hobetu zituela ikusi zen, 39,05 mg azido galikoaren baliokidea/g film eta % 31,4ko inhibizioa aurkeztuz, hurrenez hurren. Hala ere, aktibitate antioxidatzailea biltegiratze denborarekin txikitu zen, % 22ko DPPH erradikalak ezabatzeko aktibitatea erakutsiz 180 egunez filmak biltegian gorde ostean. Denbora luzez filmak aktibo mantentzeko helburuarekin, Kowalczyk eta Biendl-ek (2016) txerri gelatinazko filmetatik etanol lupulu estraktuaren askatzea aztertu zuten. Emaitzek erakutsi zuten gelatinazko filmen handitzea kontrolatuz estraktuaren askatzea denbora luzeagoetara luzatu zitekeela. Antzeko emaitzak ikusi ziren azido askorbikoa (C bitamina) txerri gelatinazko filmak eratzeko soluzioan gehitu zenean (Kowalczyk, 2016). Algetan aurkitzen diren bitaminak, florotaninoak, laminaranak, sulfatatutako polisakaridoak, karotenoideak eta mineralak bioaktibo moduan ere erabili daitezke. Haddar eta lankideek (2012) *C. barbata* alga estraktua arrain gelatinazko filmetan gehitzerakoan, estraktuaren konposatu fenolikoengatik eta flabonoideengatik filmen aktibitate antioxidatzailea nabarmenki hobetu zela ikusi zuten. *Ascophyllum nodosum*

estraktua bezalako itsas belar estraktuak behi gelatinazko filmetan gehitu zirenean, filmen aktibitate antioxidatzailea sustatu zela ikusi zen (Kadam et al., 2015).

1.3 Gelatinazko filmentzat konposatu antimikrobiarrak

Aktibitate mikrobiarra elikagai askoren narriaduraren beste arrazoietako bat da eta elikagai-produktuen kalitatea eta babesa txikitzearen erantzule da (Rawdkuen et al., 2012). Elikagai-produktuen ekoizpen-katean zehar elikagaiari zuzenean konposatu antimikrobiarrak gehitzeak, mikrobioen hazkuntza eta elikagaiaren iraungitzea kontrolatu ditzake (Singh et al., 2016). Hala ere, konposatu antimikrobiarrak elikagaien paketatzean gehitzeak geroz eta arreta handiagoa erakarri du. Gelatinazko filmetan konposatu antimikrobiar naturalak gehitu dira, hala nola, olio esentzialak, belar estraktuak, landare eta espeziak, peptidoak eta kitosanoa (**1.2 taula)**.

Aktibitate antioxidatzaileaz gain, olio esentzialak gelatinazko film aktiboak prestatzeko filma eratzeko soluzioetan gehitzerakoan, efektu antimikrobiarra erakutsi dute. Arrain gelatinazko filmetan, bereziki limoi belar olioa gehitzerakoan, bakterio Gram-positiboekiko (*S. aureus*, *Listeria monocytogenes*) eta bakterio Gram-negatiboekiko (*E. coli*, *Salmonella typhimurium*) inhibizio efektua ikusi zen. Bergamota olio esentzialarekin prestatutako filmek aldiz, bakterio Gram-positiboekiko inhibizioa bakarrik erakutsi zuten (Ahmad et al., 2012). Olio esentzialen aktibitate antimikrobiarra bakterioen pareta zelularra hautsi dezaketen terpenoei egotzi zaie, hauek ondoren zelula barrura sartu eta proteinaren desnaturalizazioa, zelulen nahiz mintzen suntsiketa eta zelulen hiltzea eragiten dutelako. Aipaturikoa kontuan hartuz, olio esentzialen aktibitate antioxidatzailea txikiagoa izan daiteke bakterio hauen pareta zelularra inguratzen duen kanpoko mintz gehigarriarengatik. Izan ere, honek konposatu hidrofoboen difusioa mintzean zehar eragozten du eta beraz, konposatu antimikrobiarraren efektua murrizten du (Oussalah et al., 2007).

Lisozima bezalako peptido bioaktiboak ere elikagaiak babesteko gelatinazko filmetan gehitu daitezke. Beraien aktibitate antimikrobiarra pareta zelularretako peptidoglikano geruzen hidrolisiari elkartu zaio (Perez-Espitia et al., 2012). Lisozima konposatudun arrain gelatinazko filmek ez zuten *E. coli*-aren hazkuntza inhibitu, lisozimak bakterio Gram-negatiboen lipopolisakarido geruzan zehar sartu ezin zirelako (Bower et al., 2006). Hala ere, lisozima zuten gelatinazko filmek, nahiz eta gehigarriaren kontzentrazioa oso baxua izan (% 0,001), bakterio Gram-positiboen (*Bacillus subtilis, Streptoccocus cremoris*) kontra eraginkorrak zirela erakutsi zuten. Lisozimak katekinekin gelatinazko filma eratzeko soluzioan gehitzerakoan, lorturiko filmek bakterio Gram-positiboekiko eta Gram-negatiboekiko aktibitate antimikrobiarra erakutsi zuten, nahiz eta inhibiziorik altuena bakterio Gram-positiboekiko (*S. aureus*, *Listeria innocua*) eta legamiekiko (*Saccharomyces cerevisiae*) eta inhibiziorik txikiena berriz, bakterio Gram-negatiboekiko (*E. coli*) lortu zen (Rawdkuen et al., 2012). Legamia eta lizunen hazkuntzan katekina eta lisozima dituzten behi gelatinazko filmak izandako efektua txerri-haragi xehatuan aztertu zen (Kaewprachu et al., 2015). Emaitzek, gelatinazko filmetan bildutako laginek polibilin kloruro (PVC) bezalako film komertzialetan bildutako laginek baino legamia eta lizun kantitate gutxiago zituztela erakutsi zuten.

Kitosanoa gelatinazko filma eratzeko soluzioan gehitzean, elikagaiak usteltzen dituzten *S. aureus* bezalako mikroorganismoen kontrako film aktiboak ere lortu ziren (Gómez-Estaca et al., 2011). Autore hauek, gelatina kitosanoarekin nahastea gelatinazko filmen urarekiko erresistentzia eta propietate mekanikoak hobetzeko modua zela erakusteaz gain, filmak aktibitate antimikrobiarrarekin hornitzeko modua zela ere aztertu zuten. Te berdea estraktuarekin batera, gelatina agarra bezalako beste polisakaridoekin nahasi zen (Giménez et al., 2013). Konposatu aktiboen askatzea aztertzerakoan, te berde estraktua filma eratzeko soluzioan gehitu zenean, estraktuaren aktibitate antioxidatzailea mantendu egin zela ikusi zen, lorturiko filmek

Vibrio parahaemolyticus, Photobacterium phosphoreum, *Shewanella putrefaciens,* eta *Pseudomonas fluorescens* bakterioen hazkuntza inhibitzeko gai zirela erakutsi zutelako.

1.2 taula Behi, txerri eta arrain gelatinazko film aktiboak garatzeko gehituriko konposatu antimikrobiarrak.

Gelatina iturria	Konposatu antimikrobiarra	Mikroorganismoa	Erreferentziak
Behi gelatina	Erromero, oregano, zitriko estraktuak	*L. innocua, P. fluorescens, A. hydrophila/caviae*	Iturriaga et al., 2012
	Iltze-kanela, izpiliku, erromero, ezkai olio esentziala	*L. acidophilus, L. Monocytogenes*	Gómez-Estaca et al., 2010b
	Katekin-lisozima	Azido laktiko bakterio, legamiak eta lizunak	Kaewprachu et al., 2015
	Kitosanoa	*S. aureus*	Gómez-Estaca et al., 2011
Txerri gelatina	Oregano, erromero olio esentzialak	*Enterobacteriaceae*	Gómez-Estaca et al., 2010a
Arrain gelatina	Te berde estraktua	*V. parahaemolyticus, P. phosphoreum, S. putrefaciens, P. fluorescens*	Giménez et al., 2013
	Limoi belar olio esentziala	*S. aureus, L. monocytogenes, E. coli, S. typhimurium*	Ahmad et al., 2012
	Iltze-kanela, piper olio esentziala	*S. aureus, A. hydrophila, L. monocytogenes*	Shakila et al., 2015
	Basiliko hosto olio esentziala, ZnO nanopartikulak	*Pseudomonas, S. putrefaciens, Enterobacteriaceae*	Arfat et al., 2015
	Lisozima	*E. coli, B. subtilis, S. Cremoris*	Bower et al., 2006
	Katekin-lisozima	*E. coli, S. aureus, L. innocua, S. cerevisiae*	Rawdkuen et al., 2012

Espezie eta fruten beste estraktu batzuk ere, hala nola, uretan disolbagarriak diren erromero, oregano eta fruitu zitrikoen estraktuak, bakterio Gram-positiboen (*L. innocua*) eta Gram-negatiboen (*P. fluorescens*, *Aeromonas hydrophila/caviae*) kontrako aktibitate antimikrobiarra aztertzeko erabili ziren. Estraktu guztiekiko *L. innocua* sentiberena zen bitartean, *P. fluorescens* iraunkorrena zen (Iturriaga, Olabarrieta, eta de Marañón, 2012).

Eragile antimikrobiarren artean, konposatu inorganikoak, oxido metaliko batzuk esaterako, oro har segurutzat (generally recognized as safe, GRAS) hartzen dira eta gainera, elikagaien prozesamenduan eta paketatzean zehar erabiltzen diren tenperatura eta presio altuekiko egonkorrak dira. Honi dagokionez, ZnO nanopartikulen akzio mekanismoa aztertu zen eta emaitzek, nanopartikulek zelulen mintza hautsi eta estres oxidatiboa eragiten zutela iradoki zuten (Xie et al., 2011). Hau da, Zn^{2+} ioiak pareta zelularra zeharkatu, zelulen konposatuetaraino iritsi eta zelularen bideragarritasunean eragin dezake. Gainera, ZnO nanopartikulek hidrogeno peroxidoa sortu dezakete, oso ezaguna den eragile oxidatzailea, mintz zelularra kaltetuz (Tayel et al., 2011). Lupia arraina biltzeko erabilitako gelatinazko filmetan ZnO nanopartikulak gehitu zirenean, elikagaiaren iraungitzea 4 egunetatik 12 egunetara luzatzea lortu zen (Arfat et al., 2015).

1.4 Gelatinazko filmetatik konposatu aktiboen askatzearen kontrola

Filmetatik konposatu aktiboen askatzea aztertzeko, difusio bidezko migrazioaren neurketaz egin daiteke. Alde batetik, *in vitro* azterketa, filmen guztizko murgilketa elikagaiak simulatzen dituzten disolbatzaileetan, hau da, benetako elikagaien portaera emulatzen dituzten likidoetan (ur-simulatzaileak edo gantz-simulatzaileak) burutu daiteke. Beste aldetik berriz, konposatu aktiboaren askatzea aztertzeko, paketatze aktiboa elikagai-produktuarekin zuzenean erabili daiteke. Bi kasuetan, migrazio entseguen ostean, elikagai-simulatzailea edo elikagaia bera aztertu behar dira askatutako konposatu aktiboaren kantitatea eta efikazia determinatzeko.

Aktiboen kontrolatutako askatzea duten paketatze aktiboak prestatzeko metodo ezberdinak erabili daitezke, hala nola, konposatu aktiboen enkapsulazioa, biopolimeroaren saretzea edo nanobetegarrien gehitzea. Liposomak, partikula polimerikoak edo lipido nanopartikulak konposatu aktiboen askapena hasi arte hauek enkapsulatzeko eta ingurunetik isolatzeko banaketa-gailuak dira. Babestutako askatze teknika hauen bidez aktiboaren askapen-proportzioa kontrolatzeaz gain, konposatu aktiboa oxidazioa eragiten duten faktoreetatik (beroa, argia eta hezetasuna) babesten da, konposatu hegazkorren lurruntzea saihestu/atzeratzen da eta prozesatze eta biltegiratze bitartean materialaren erabilera errazten da (Martins et al., 2014; El Asbahani et al., 2015).

Konposatu aktiboen enkapsulazioa emultsifikazio eta lehortze-esprai, edo koazerbatze eta disolbatzailearen lurrunketa bidez egin daiteke (Da Silva, Barreira, eta Oliveira, 2016). Wu eta lankideek (2015) kanela olio esentziala zuten gelatinazko filmak prestatu zituzten eta olio esentzialaren askatzearen alderaketa egin zuten, hau zuzenean filma eratzeko soluziora gehituz edota konposatua nanopartikuletan enkapsulatu ondoren soluziora gehituz. Konposatu aktiboa enkapsulatuta zegoen laginetan, 99,5 orduren ostean, olio esentzialaren askatzea % 98tik % 87ra jaitsi zela Ikusi zen.

Enkapsulazioaz gain, konposatu aktiboaren askatzea kontrolatzeko irradiazio bidezko saretze erreakzioa erabili daiteke. Benbettaïeb eta lankideek (2016b) elektroi sorta irradiazioaren (60 kGy) ostean, ingurune urtsuan kumarina eta tirosola bezalako konposatu aktiboen difusio koefiziente eraginkorraren txikitzea gertatzen zela ikusi zuten, irradiazioagatik eratutako sareak eragindako eragozpenengatik. Antzeko emaitzak lortu ziren etanol simulatzailean kerzitina konposatu aktibodun eta kitosanodun arrain gelatinazko filmak murgiltzean (Benbettaïeb et al., 2016a). Irradiazioak filmetatik kerzitinaren askapena mantsotu zuen, irradiazio prozesuan sortutako interakzio berriek filmen egitura aldatu zutelako.

Nanobuztinen gehitzearekin gelatinaren sarean ere aldaketak eragin daitezke. Giménez eta lankideek (2012) iltze-kanela olio esentziala konposatu aktibo moduan arrain gelatinazko filmetan gehitu zuten eta olio esentzialaren askatzean, sepiolita nanobuztinaren eragina aztertu zuten, filma uretan denbora tarte ezberdinetan sartuz. Iltze-kanelaren osagai nagusietakoa eugenola denez, uretan eugenolaren askatzea gelatinazko filmetatik eta sepiolitadun gelatinazko filmetatik kontrolatu zen. Sepiolitadun filmek eugenolaren mailakako askatzea erakutsi zuten, gelatinazko filmetan eugenolaren gehienezko askatzea 45 minututan eman zen bitartean.

1.5 Etorkizuneko joerak eta aukerak ikuspuntu globaletik

Elikagaien prozesatze industrian sortutako elikagai-zaborretatik erauzitako konposatuei arreta berezia ematen ari zaie azken urteotan. Izan ere, ingurumen eta ekonomia ikuspuntutik elikagai-zaborren kantitate handien (azalak, oskolak, patsa osoak) kudeaketak arazo larriak eragiten ditu. Egoera hau gainditzeko, sehaskatik hilobira eta ekonomia zirkularra bezalako industri-kontzeptu ekologikoak garatu dira, industriako hondakinak produktu eta aplikazio berrietarako lehengai moduan erabiltzeko helburuarekin.

Azken urteotan linazi-olioaren enkapsulazioan eta azenarioaren prozesatze industrian sortutako hondakinetatik, gelatinazko kapsulen hondakinetatik eta azenario hondakinetako zuntzetatik konkretuki, gelatinazko filmak prestatzeko zenbait ikerketa burutu dira (Iahnke et al., 2015). % 8,5eko azenario hondakina zuten gelatinazko filmak eguzki-lore olioa paketatzeko erabili ziren eta azenarioko karotenoideen presentziak olioa oxidaziotik babestu zuela ikusi zen. Crizel eta lankideek (2016) masusta-urdin zukua lortzeko prozesuan lortutako konposatu aktibodun filmak prestatzeko kapsulen hondakinetako gelatina ere erabili zuten. Masusta-urdinaren zuntz dietetikoa filma eratzeko soluzioan gehitu zen eta zuntz kontzentrazio ezberdineko arrain gelatinazko filmak eguzki-lore olioa paketatzeko erabili ziren. Aktibitate antioxidatzailea 35 egun baino gehiagoz olioa biltegian gorde ostean aztertu zen eta 0,15 g/mL–ko zuntz

kontzentraziodun filmek aktibitate antioxidatzailerik handiena zutela ikusi zen, denboran zehar gelatinazko film hauek peroxido balio konstante eta egonkorrak erakutsi baitzituzten.

Hondakinen kudeaketaren legislazioak elikagai-industriako hondakinen balioztatzea nabarmentzen du (Ravindran eta Jaiswal, 2016). Hortaz, paketatze aktiboak garatzeko industria hondakinak lehengai moduan erabiltzea merkea eta ekologikoki erakargarria da. Hondakinak balio erantsidun produkzioan erabiltzea ekonomia zirkularraren izaerarekin dator, hau da, iturri biologiko berriztagarriak ekonomikoki bideragarriak diren produktu bilakatzea (**1.1 irudia**).

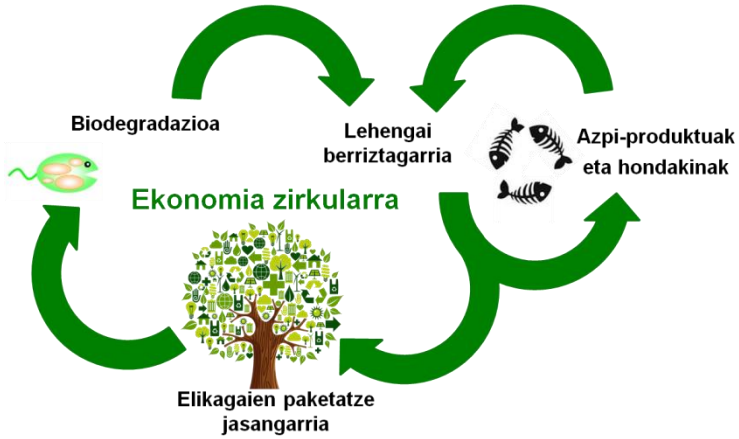

1.1 irudia Elikagaien prozesatze hondakinen eta azpi-produktuen balioztatzea ekonomia zirkularrerantz.

Honi dagokionez, lehengaien iturriez gain, fabrikatze prozesuek ere eginkizun garrantzitsua betetzen dute. Nahiz eta estrusioa ondo finkatutako industria teknika izan, ez da gelatinekin asko erabili. Hala ere, behi gelatinaren (Nur Hanani et al., 2013) eta arrain gelatinaren (Etxabide, Guerrero, eta de la Caba, 2016) estrusioan egin berri diren ikerketa lanek fabrikazio prozesu hau gelatina prozesatzeko metodo egokia dela iradokitzen dute. Gainera, gelatinaren urtze-puntu baxuak, material hau beste kontsumogaiak baino tenperatura baxuagotan estrusio bidez prozesatzea ahalbidetzen du, bere bideragarritasuna handitzeaz gain prozesuari jasangarritasuna gehituz.

Estrusio termoplastikoa erabilera askotakoa, oso eraginkorra eta fabrikazio teknologia etengabea dela kontuan edukiz eta, aldi berean, elikagaien prozesatze hondakinetatik gelatina oso erabilgarria denez, teknika honen erabilerak gelatinaren produkzioa handitu eta elikagaiak paketatzeko aplikazioetara gelatinazko filmen erabilera zabaldu dezake.

Azkenik, biodegradazioaren ebaluazioa gakoa da gaur egungo elikagaien paketatzearen merkatu-gaitasuna handitzeko. Nahiz eta poliesterretan oinarritutako elikagaien paketatzeen biodegradagarritasunari buruzko zenbait lan orain gutxi argitaratu diren (Arrieta et al., 2014; Song et al., 2016), gelatinazko filmekin lan gutxi burutu dira (Etxabide et al., 2016a; Uranga et al., 2016). Hortaz, elikagaiak paketatzeko disziplinarteko ikerkuntza arlo honi elkartutako film aktibo hauen bizi amaierako analisia etorkizunean burutuko den helburuetako bat izatea espero da.

Laburbilduz, aurretik aipaturiko ekonomia zirkularrekin zerikusia duten hiru mailei (erauzketa, produkzioa, eta zakarren tratamendua) dagokienez, errendimenduak handitzeko eta gai kimikoak gutxitzeko helburuarekin etorkizuneko lanetan hiru prozesu hauen hobekuntzan fokatzeko ahaleginak egingo dira, lehiakorrak eta jasangarriak diren elikagaien paketatzeari bidea emanez.

2 Materialak eta metodoak

2.1 Materialak

Arrain gelatina komertziala (A mota, 200 bloom, % 11,06ko hezetasuna eta % 0,147ko errautsak) eskuzabaltasunez Weishardt International-ek (Liptovsky Mikulas, Eslovakia) emandakoa zen. Glizerola eta laktosa Panreac Química S.A.-tik (Bartzelona, Espainia) erosi ziren, plastifikatzaile eta saretze erreaktibo gisa erabiltzeko, hurrenez hurren. Glutaraldehidoa (GTA, % 25 w/v uretan), Panreac Química S.A.-k. (Bartzelona, Espainia) eta genipina (GP, ≥ % 98 HPLC purutasuna), Sigma-Aldrich-ek (Madril, Espainia) hornitutakoak, filmen prestaketarako saretze erreaktibo gisa erabili ziren. Tetrahidrokurkumina (THC) Sabinsa Corporation-ek (New Jersey, USA) emandakoa, antioxidatzaile moduan erabili zen. 2,2-difenil-1-pikril hidrazil (DPPH), Folin Ciocalteu erreaktiboa eta azido galikoa Sigma-Aldrich-etik (Saint-Louis, USA) erosi ziren. Sodio karbonatoa (Na_2CO_3) Merck (Fontenary Sous Bois, France) eta 2,6-di-tert-butil-4-metilfenol (BHT) Sigma-Aldrich-ek (Saint-Louis, USA) hornitutakoak ziren. Metanola (MeOH) gradu analitikokoa zen eta ura berriz destilatua.

2.2 Filmen eta biokonpositeen prestaketa

2.2.1 Filmen prestaketa

Laktosa kantitate ezberdineko (% 10, 20 eta 30, ehunekoaren araberako pisua gelatina idorrarekiko) gelatinazko filmak disoluzio metodoa erabiliz prestatu ziren. Lehenengo, arrain gelatina 5 g eta beharrezko laktosa kantitatea 100 mL ur destilatuan disolbatu ziren, berogailu magnetiko batean nahastea 80 ºC-an eta 200 bira minutuko abiaduran 30 minutuz irabiatzen utziz. Ondoren, % 10 glizerola (gelatina idorrarekiko) disoluzioan gehitu zen eta 1 N HCl-rekin edo 1 N NaOH-rekin disoluzioaren pH-a 2,0ra (pH azidoa izendatua) edo 10,0era (pH basikoa izendatua) egokitu zen, hurrenez hurren, eta nahastea beste 30 minutuz 80 ºC-an irabiatzen utzi zen. pH-a aldatu gabeko filmak ere prestatu ziren eta pH berezkoa (5,4) izenez deitu ziren. Gero, filma eratzeko soluziotik 17 mL Petri ontzi bakoitzean isuri ziren eta hauek 48 orduz giro tenperaturan lehortzen utzi ziren tratatu gabeko (NH) filmak lortzeko. Ondoren, Petri

ontzietatik desitsatsitako film batzuk 105 ºC-an 24 orduz labean berotu ziren, tratatutako (HT) filmak lortuz.

Filmak GTA-rekin eta GP-rekin ere prestatu ziren. Horretarako, gelatinazko filmak (50 µm-tako lodiera) aurretik azaldu den bezala prestatu ziren. Laburbilduz, 5 g gelatina 100 mL ur destilatuan disolbatu ziren, nahastea berogailu magnetiko batean 80 ºC-an eta 200 bira minutuko abiaduran 30 minutuz irabiatzen utziz. Ondoren, % 10 glizerola (gelatina idorrarekiko) disoluzioan gehitu zen eta 1 N NaOH-rekin disoluzioaren pH-a 10,0era egokitu zen. Ondoren, saretze erreaktiboa (laktosa, GP edo GTA) disoluziora gehitu zen eta nahasteak 5 minutuz 37 ºC-an irabiatzen utzi ziren. Aurreko ikerketa batzuetan oinarrituz, % 20 laktosa (Etxabide et al., 2015b), % 0,75 GTA (Chiou et al., 2008), edo % 0,25 GP (Ma et al., 2013), denak gelatina idorrarekiko ehunekoak, saretze erreaktiboen kontzentrazio optimoak bezala soluziora gehitu ziren. Azkenik, filma eratzeko soluziotik 17 mL Petri ontzi bakoitzean isuri ziren eta disoluzioak 48 orduz giro tenperaturan lehortzen utzi ziren filmak lortzeko. Laktosarekin prestatutako filmen kasuan, hauek Petri ontzietatik desitsatsi ziren eta 105 ºC-an 24 orduz labean berotu ziren, saretutako filmak lortzeko.

THC-rekin prestatutako filmen kasuan, 5 g gelatina eta % 20 laktosa (gelatina idorrarekiko ehunekoa) 100 mL ur destilatuan disolbatu ziren, nahastea 80 ºC-an eta 200 bira minutuko abiaduran 30 minutuz berogailu magnetiko batean irabiatzen utziz. Ondoren, % 10 glizerola eta % 5 THC (gelatina idorrarekiko ehunekoak) duen nahastea gelatinazko disoluzioan gehitu zen eta 1 N NaOH-rekin disoluzioaren pH-a 10,0era egokitu zen. Gero, disoluzioa ultrasoinu ekipoan (Elmasonic S 30 (H), Singen, Germany) giro tenperaturan 5 minutuz utzi zen eta ondoren, nahastea beste 30 minutuz 80 ºC-an eta 200 bira minutuko abiaduran irabiatzen utzi zen. Azkenik, filma eratzeko soluziotik 17 mL Petri ontzi bakoitzean isuri ziren eta disoluzioak 48 orduz giro tenperaturan lehortzen utzi ziren filmak lortzeko. Filmak Petri ontzietatik desitsatsi ziren eta 105 ºC-an 24 orduz labean berotu ziren G filmak (laktosa gabeko

gelatinazko filmak), G-THC filmak (THC-dun laktosarik gabeko gelatinazko filmak), GL filmak (laktosadun gelatinazko filmak), eta GL-THC filmak (THC-dun eta laktosadun gelatinazko filmak) lortzeko.

Filmen karakterizazioa baino lehen, hauek ganbera klimatiko batean 25 ºC eta % 50eko hezetasun erlatiboko baldintzapean 48 orduz gorde ziren. Lodiera gertuenez 0,001 mm-ko QuantuMike digimatic mikrometroaren (Mitutoyo Espainia) bidez neurtu zen. Gutxienez hiru neurketa egin ziren lagin bakoitzeko puntu ezberdinetan eta batezbestekoa eta desbiderapena erakutsi ziren.

2.2.2 Biokonpositeen prestaketa

Batera biratzen duten torloju bikoitzeko estrusio-makina, Thermo Haake MiniLab II (Thermo Fisher Scientific) mikro nahasgailua, gelatinazko xaflak sortzeko erabili zen. Estrusio-elikadura 40 g gelatina, % 10 glizerola (gelatina idorrarekiko ehunekoa) eta laktosa kantitate ezberdinak (% 10, 20 eta 30, gelatina idorrarekiko ehunekoak) NaOH 1 M erabiliz pH-a 10.0era egokitutako ur destilatuan (% 50, gelatina idorrarekiko ehunekoak) nahasiz prestatu zen. Nahastea eskuz nahasi zen, nahaste homogeneo bat lortu arte. Ondoren, estrusio-makina 1,6 g/min-ko abiaduran elikatu zen, estrusio-zilindroaren tenperatura 90 ºC-an zehaztu zen, torlojuaren abiadura 70 bira minutuan egokitu zen, eta momentuaren balioak 25 eta 30 N·cm bitartekoak izan ziren.

Xaflak giro tenperaturara hoztu ondoren, gelatinazko laginak lauki txikitan moztu ziren eta ondoren, pelletak injektatu ziren. Thermo Haake MiniJet II (Thermo Fisher Scientific) injektorea arrain gelatinazko biokonpositeak lortzeko erabili zen. Azterturiko propietateen arabera, injekzio molde ezberdinak erabili ziren; molde esferikoak edo hezur-formako moldeak. Injektatutako biokonpositeak 105 ºC-an 270 minutuz berotu ziren. Berotze denbora Etxabide eta lankideek (2015b) egindako lanaren arabera aukeratu zen. Bertan, laktosadun gelatinaren egitura sekundarioan

aldaketak eragiteko 105 ºC-an % 30 laktosa kantitatea zuten laginak gutxienez 270 minutuz berotzea beharrezkoa zela erakutsi zen. Azkenik, laginak aztertu aurretik, hauek ganbera klimatiko batean 25 ºC eta % 50eko hezetasun erlatiboko baldintzapean 48 orduz gorde ziren.

2.3 Karakterizazio fisiko-kimikoa

2.3.1 Hezetasun edukia (MC) eta disolbaturiko masa totala (TSM)

Konposizio bakoitzeko hiru lagin pisatu ziren (m_w) eta jarraian laginak 105 ºC-an 24 orduz aire-zirkulazioko labe batean lehortu ziren. Ondoren, filmak berriro ere pisatu ziren (m_0) eta MC-ren balioak beheko formula bidez kalkulatu ziren:

$$MC\ (\%) = \frac{m_w - m_0}{m_w} \times 100$$

Gero, lagin lehorrak sodio azidadun (0,02 g/100 mL, mikrobioen hazkuntza ekiditeko) ur destilatuan (30 mL) murgildu ziren. Flaskoak, noizbehinkako agitazio geldopean 25 ºC-an 24 orduz ganbera klimatiko batean gorde ziren. Ez-disolbatutako materia pisatu aurretik (m_f), laginak 105 ºC-an 24 orduz aire-zirkulazioko labean lehortu ziren. TSM, 24 orduz ur destilatuan murgildutako film lehorren disolbatutako materiaren ehunekoa bezala azaldu zen (Cuq et al., 1996; Kunte et al., 1997):

$$TSM\ (\%) = \frac{m_0 - m_f}{m_0} \times 100$$

2.3.2 Ura xurgatzeko gaitasuna

Biokonpositeen ura xurgatzeko gaitasuna analisi grabimetriko bidez aztertu zen, ASTM D570-98 (ASTM, 1998) arauari jarraituz. Biokonposite bakoitzeko hiru lagin pisatu ziren (W_0) eta pH 7 zuen fosfato buffer soluzio gazian (PBS) laginak murgildu ziren. Ondoren, denbora zehatz batzuetan laginak buffer soluziotik atera, paperezko zapi batekin lehortu eta berriro ere pisatu ziren (W_t). Prozesua handitze-balio

konstanteak lortu arte errepikatu zen. Ura xurgatzeko gaitasuna (S) ondorengo ekuazioa erabiliz kalkulatu zen (Martínez-Ruvalcaba et al., 2009):

$$S\ (\%) = \frac{(W_t - W_0)}{W_0} \times 100$$

Ura xurgatzeko gaitasuna (S) denborarekiko (t) irudikatzen duen grafikoa marraztu zen, S-ren oreka determinatzeko.

2.3.3 Fourierren transformatuaren bidezko espektroskopia infragorria (FTIR)

FTIR analisia Nicolet Nexus FTIR espektrofotometroan burutu zen (Thermo Scientific), Golden Gate (Specac) ATR osagarria erabiliz. Guztira, 32 ekorketa egin ziren 4 cm^{-1}-eko erresoluzioarekin. Neurketak 4000 eta 800 cm^{-1}-eko tartean egin ziren. Espektro guztiak Savitzky-Golay funtzioa erabiliz leundu ziren. Kurben egokitze prozedurarako, banden posizioen gidan amida zonako espektroaren bigarren deribatua erabili zen, OriginPro 9.1 softwarearen laguntzaz.

2.4 Propietate optikoak

2.4.1 Distira-neurketak

Distira 60º-ko eraso-angeluan neurtu zen, ASTM D-523-14 (ASTM, 2014) arauari jarraituz eta gainazal laua duen Multi Gloss 268 plus distirametroa (Konica Minolta) erabiliz. Konposizio bakoitzeko laginetan hamar neurketa egin ziren 25 ºC-an.

2.4.2 Kolore-neurketak

Kolorea CR-400 Minolta Croma Meter (Konica Minolta) kolorea neurtzeko gailua erabiliz neurtu zen. Film zatiak plater zuri baten gainean jarri ziren (kalibrazio plater zuriaren balio estandarrak L*= 97,39, a*= 0,03 eta b*= 1,77 izan ziren) eta L*, a* eta b* kolore parametroak CIELAB kolore eskala erabiliz neurtu ziren: L*= 0-tik (beltza) L*= 100-era (zuria), -a*-tik (berdetasuna) +a*-ra (gorritasuna), eta –b*-tik (urdintasuna) +b*-ra (horitasuna). Laktosa kantitatearen funtziopean HT filmen kolore aldaketa (ΔE*) laktosa kantitate berdineko NH filmekiko ondorengo formula bidez kalkulatu zen:

$$\Delta E^{*}=\sqrt{(\Delta L^{*})^{2}+(\Delta a^{*})^{2}+(\Delta b^{*})^{2}}$$

Arrexka-indizeak (BI) kolore marroiaren purutasuna adierazten duenez eta arretze-prozesu ez-entzimatikoetan oso garrantzitsua den parametroa denez (Olivas et al., 2007; Palou et al., 1999), BI balioak ondorengo moduan kalkulatu ziren:

$$BI\ (\%)=\frac{x-0.31}{0.172}\times 100$$

non,

$$x=\frac{(a^{*}+1.75L^{*})}{(5.645L^{*}+a^{*}-3.012b^{*})}$$

2.4.3 Argia xurgatzeko gaitasuna

Filmen argiarekiko hesi-propietateak determinatzeko, V-630 ultramore ikuskorreko (UV-vis) espektrofotometroa (Jasco) erabili zen. Argiarekiko xurgatzea 200-800 nm bitarteko uhin-luzeretan neurtu zen eta konposizio bakoitzeko hiru lagin aztertu ziren.

2.4.4 Fluoreszentziako espektroskopia

Fluoreszentzia emisio neurketak kontrolatutako kubetadun (Holder TLC50, Quantum North West) Photon Technology International (PTI, Horiba ABX) espektrofotometroa erabiliz egin ziren eta espektroak FeliX32 softwarea erabiliz lortu ziren. Gelatinazko filmak 335 nm-an kitzikatu ziren eta espektroak 360-365 nm bitartean 105 ºC-an 30 minuturo neurtu ziren.

2.5 Hesi-propietateak

2.5.1 Uraren kontaktu-angelua (WCA)

WCA-ren neurketak OCA20 kontaktu-angelu sistema (DataPhysics Instruments) erabiliz egin ziren. Filmaren hidrofobotasuna aztertzeko 3 µL-ko ur

destilatu tanta bat filmaren gainazalean ezarri zen eta tantaren irudia SCA20 softwarea bidez lortu zen. Konposizio bakoitzeko bost neurketa egin ziren 25 ºC-an.

2.5.2 Ur lurrunaren iragazkortasuna (WVP)

WVP-ren balioak PERME™ W3/0120 (Labthink Instruments Co. Ltd.) hezetasuna kontrolatua zuen ganbera klimatiko batean neurtu ziren. Film bakoitza 7,4 cm-ko diametroko laginetan moztu zen, analisi-azalera 33 cm^2-koa izanik. Filmak 38 ºC-an eta % 90eko hezetasun erlatiboan mantendu ziren, ASTM E96-00 (ASTM, 2000) arauari jarraituz. WVP analisi grabimetriko bidez neurtu zen, pisua konstantea izan arte. Lehenengo ur lurrunaren transmisio-abiadura (WVTR) kalkulatu zen:

$$\mathrm{WVTR}\left(\frac{g}{s\cdot cm^2}\right)=\frac{G}{t\times A}$$

non, G pisu aldaketa (g), t denbora (s), eta A analisi-azalera (cm^2) diren.

Ur lurrunaren iragazkortasuna (WVP) honela kalkulatu zen:

$$\mathrm{WVP}\left(\frac{g}{s\cdot cm\cdot Pa}\right)=\frac{\mathrm{WVTR}\times L}{\Delta P}$$

non, L laginen lodiera (cm) eta ΔP filmean zehar ur lurrunaren presio partzialaren diferentzia (Pa) diren. Konposizio bakoitzeko hiru lagin neurtu ziren.

2.6 Propietate mekanikoak

Trakzio erresistentziaren (TS) eta haustura elongazioaren (EB) neurketak sistema elektromekaniko (MTS Insight 10) batean 25 ºC-an eta ASTM D1708-93 (ASTM, 1993) arauari jarraituz burutu ziren. Laginak 4,75 mm × 22,25 mm-ko tiretan moztu ziren eta film-konposizio bakoitzeko gutxienez bost lagin entseatu ziren.

2.7 Karakterizazio termikoa

2.7.1 Analisi termograbimetrikoa (TGA)

Neurketa termograbimetrikoak Mettler Toledo TGA SDTA 851 (Mettler Toledo S.A.E.) ekipoarekin egin ziren. Saiakuntzak 25 ºC-tik 800 ºC-ra gauzatu ziren, 10 ºC/min-ko berotze-abiadurarekin eta giro inertean (10 mL N_2/min) erreakzio termo-oxidatzaileak ekiditeko.

2.7.2 Ekorketa diferentzialeko kalorimetria (DSC)

DCS-ko neurketak beso-robot bat eta hozteko unitate bezala hozkailu elektrikoa zituen Mettler Toledo DSC 822 (Mettler Toledo S.A.E.) ekipoan egin ziren. Laginak (4,0 ± 0,1 mg) hermetikoki itxitako aluminiozko kapsuletan sartu ziren, -50 ºC-tik 250 ºC-ra 10 ºC/min-ko berotze-abiaduran giro inertean (10 mL N_2/min) laginak berotzerakoan masa galerak ekiditeko.

2.7.3 Analisi mekaniko-dinamikoa (DMA)

DMA-ko neurketak tentsio-moduan Eplexor 100N (Gabo Qualimeter) ekipoa erabiliz neurtu ziren. Entsegua 1 Hz-ko maiztasun konstantean burutu zen. Esfortzu anplitudea % 0,05-ean finkatu zen eta tenperatura tartea -100 ºC-tik 140 ºC-ra 2 ºC/min-ko berotze-abiaduran igo zen.

2.8 Gainazal eta egituraren karakterizazioa

2.8.1 Ekorketazko elektroi-mikroskopia (SEM)

Haustura-gainazalaren morfologia bistaratzeko emisio-eremuzko Hitachi S-4800 (Hitachi High-Technologies Corporation) ekorketazko elektroi-mikroskopioa 15 kV-tako azelerazio tentsiopean erabili zen. Konposizio bakoitzeko laginak bi aldeko zinta itsasgarriaren laguntzaz metalezko oinarrian kokatu ziren eta behaketa aurretik urrez estali ziren (JFC-1100) argoizko ingurune hutsean.

2.8.2 Indar atomikozko mikroskopia (AFM)

Laginen morfologia giro baldintzetan AFM bidez aztertu zen. AFM-ko irudiak ekorketazko zundazko mikroskopioa (Nanoscope IIIa Multimode™, Bruker) erabiliz lortu ziren. Aldizkako kontaktu metodoa erabili zen 200-400 kHz-tako maiztasun erresonantzian, 0,6-1,0 Hz-tako ekorketa tartean eta 10-80 N/m-ko indar konstanteko punta/kantileberra airean erabiliz. Laginen prestaketari dagokionez, konposizio bakoitzeko 80 ºC-an zegoen filma eratzeko soluzioaren bolumen txiki bat (10 µL) bi aldeko zinta itsasgarriarekin substratu (1,5 cm-ko diametroa) bati itsatsiriko eta 80 ºC-ra beroturiko mikazko xafla (1,0 cm-ko diametroa) baten gainen ezarri zen, gelatinaren konglomerazio posibleak ekiditeko. Ondoren, ondo hedaturiko film meheak lortzeko biraketa abiadura handia (200 rpm) 120 s-z erabili zen. Azkenik, Petri ontzietatik desitsatsitako film batzuk 105 ºC-an 24 orduz labean berotu ziren eta lagin guztiak ganbera klimatiko batean 25 ºC eta % 50eko hezetasun erlatiboko baldintzapean 48 orduz gorde ziren beraien egitura aztertu aurretik.

2.8.3 X-izpien bidezko espektroskopia fotoelektronikoa (XPS)

Filmen gainazalen analisi kimikorako K-Alpha espektroskopioa (ThermoFisher Scientific) erabili zen. AlKα iturri monokromatikoa (hv = 1486,6 eV) 200 µm-tako diametrotako puntuaz aktibatu zen. Espektro osoa (0-1350 eV) 200 eV-ko pasatze energia konstanteaz lortu zen eta bereizmen handiko espektroa aldiz 40 eV-ko pasatze energia konstanteaz lortu zen. Sakontasun-profila (3-10 nm inguruan) Ar^+-ren hauste bidez lortu zen. C 1s, N 1s eta O 1s espektroen kuantifikazioa eta kokapena ThermoFisher Scientific–ek emandako AVANTAGE softwarea bidez gauzatu zen.

2.8.4 Mikroskopia optikoa

Mikroskopio optikoa filmen gainazala aztertzeko erabili zen eta mikroskopio digitalaren (Leica) bidez 40X handitzea duten mikrografia optikoak lortu ziren.

2.8.5 X izpien difrakzioa (XRD)

XRD-ren azterketak 40 kV eta 40 mA-tan lan egin zuen difrakzio unitate (PANalytic Xpert PRO) batekin egin ziren. Erradiazioa Cu-Kα (λ = 1,5418 Å) iturritik sortu zen eta difrakzio datuak 2,5º eta 50º tarteko 2θ balioetatik lortu ziren. θ, laginarekiko X-izpiaren elektroi-sortaren eraso-angelua da.

2.8.6 Filmen porositatearen neurketa

Filmen porositatearen ehunekoa merkuriozko intrusio porosimetro (MIP) bidez lortu zen, merkuriozko intrusio porosimetroa (Autopore IV, Micromeritics Instrument) erabiliz. Lorturiko intrusio kurbek, aplikatutako merkurio-presio balio bakoitzeko filmean sarturiko merkurioaren bolumena merkurioaren intrusio seinalearekin erlazionatzen du. Porositatea, aplikatutako merkurio-presioa (0,0036-228 MPa) eta merkurioa sartu zen poroen tamaina erlazionatuz determinatu zen. MIP azterketa bitartean, hasierako hustuketa presioa 50 µm Hg-takoa zen, 5 minututako hustuketa denboran. Merkurioaren betetze presioa 0,53 psia-koa zen eta orekatzeko denbora 10 s-koa izan zen.

2.8.7 Biokonpositeen dentsitate eta porositate neurketak

Konposizio bakoitzeko hiru lagin esferikoen dentsitateen balioak, ura xurgatzeko gaitasunaren azterketa ondotik kalkulatu ziren. Lagin bakoitzaren diametroaren batezbestekoa (d), diametroak kalibragailu (Mitutoyo Corporation, Japan) bidez hiru aldiz neurtuz kalkulatu zen, eta masa (m), 5 dezimalen irakurketa ahalbidetzen zuen ES 125 SM balantza elektronikoa (Precisa Ldt.) erabiliz pisatu zen. Laginen dentsitatea (ρ) ondorengo moduan kalkulatu zen:

$$\rho\left(\frac{g}{cm^3}\right)=\frac{6m}{\pi d^3}$$

non, m laginaren masa (g) eta d esferaren diametroa (cm) ziren. Biokonpositeen dentsitateen (ρ_x) balioak 105 ºC-an 270 minutuz biokonpositeak berotu ondoren neurtu

ziren eta bero tratamendu gabeko biokonpositeak ($\rho_{kontrol}$) kontrol laginak bezala erabili ziren.

Porositatea ondorengo ekuazio bidez kalkulatu zen (Nakamatsu et al., 2006):

$$\text{Porositatea } (\%) = \left(1 - \frac{\rho_x}{\rho_{kontrol}}\right) \times 100$$

non, ρ_x eta $\rho_{kontrol}$ laktosa kantitate berdineko biokonpositeen dentsitateen balioak ziren.

2.9 Aktibitate antioxidatzailea

2.9.1 Tetrahidrokurkuminaren (THC) egonkortasun termikoa

TGA analisia, TGA-Q 500 (TA Instruments) ekipoan egin zen. Lagina (10 mg), platinozko kapsula batean sartu zen eta 24 ordutako azterketa 105 ºC-an giro inertean (60 mL N_2/min) burutu zen, oxidazio termikoa saihesteko.

2.9.2 THC-ren askatzea eta filmen masa galera

THC-ren askatzea, 25 ºC-an eta 250 bira minutuko abiaduran filmak (1,5 cm x 2,0 cm) 5 egunez MeOH disoluzioan (5 mL) murgildu ostean aztertu zen. Konposatu antioxidatzailea argitik babesteko, filmak beirazko ontzi ilunetan murgildu ziren. UV-vis espektrofotometro (Perkin-Elmer Lambda 18 spectrometer, Perkin-Elmer) bidez, argiarekiko xurgatzea 250-800 nm bitartean neurtu zen. MeOH-ren xurgatze espektroak 5 egunez 24 orduro neurtu ziren eta konposizio bakoitzeko hiru lagin aztertu ziren.

5 egunetako murgilketaren ostean, filmak soluziotik atera eta egun batez giro tenperaturan lehortzen utzi ziren. Ondoren, filmak ganbera klimatikoan 48 orduz gorde ziren eta azkenik beraien pisua neurtu zen. Konposizio bakoitzeko hiru lagin erabili ziren eta film bakoitzaren masa galera ondorengo ekuazioaz kalkulatu zen:

$$\text{Masa galera } (\%) = (1 - \frac{W_5}{W_0}) \times 100$$

non, W_0 murgilketa aurretik eta W_5 5 egunetako murgilketaren ostean filmen pisuak ziren.

2.9.3 Fenolikoen guztizko edukia (TPC)

TPC-ren balioak Folin-Ciocalteu entsegua erabiliz lortu ziren. 5 egunetako filmen murgilketaren ostean, MeOH soluzioaren 50 µL, 10 mL-tako ontzi batera pasa ziren eta Folin-Ciocalteu erreaktiboaren 500 µL gehitu ziren, soluzioa sutsuki astinduz. Ondoren, % 20 (w/v) Na_2CO_3 soluziotik 1000 µL gehitu ziren eta soluzioa berriro ere sutsuki astindu zen. Azkenik, ontziaren bolumena ur destilatuaz bete zen eta soluzioa 2 orduz giro tenperaturan eta iluntasunean geldi utzi zen. Ondoren, kontrol erreaktiboarekiko (MeOH) soluzioren xurgatzea 760 nm-an UV-vis espektrofotometroa bidez neurtu zen. Entsegu guztiak hirukoiztuta egin ziren eta TPC mg azido galikoaren baliokide (GAE) moduan azaldu zen.

2.9.4 DPPH erradikalak ezabatzeko aktibitatea

DPPH erradikalak ezabatzeko aktibitatea Molyneuxen (2004) metodoaren arabera neurtu zen. 5 egunetako filmen murgilketaren ostean, MeOH soluzioaren 2 mL DPPH soluzioaren (150 µM) 2 mL-rekin nahasi ziren. Nahastea sutsuki astindu zen eta ondoren, giro tenperaturan eta iluntasunean 30 minutuz geldi utzi zen. Erradikal askeak ezabatzeko aktibitatea erreferentzia moduan erabili zen butil hidroxitolueno (BHT) soluzioarekin alderatu zen. Inhibizio balioak (I) 517 nm-an emandako xurgatze balioen txikitzearekin kalkulatu ziren:

$$I\ (\%) = \frac{A_{kontrol} - A_{lagin}}{A_{kontrol}} \times 100$$

non, $A_{kontrol}$ MeOH soluzioaren xurgatzea eta A_{lagin} 5 egunetako murgilketaren ostean soluzioaren xurgatzea diren. Entsegu guztiak hirukoiztuta egin ziren.

2.10 Filmen desintegrazioa

Simulazio entsegu moduan, materialaren desintegrazioa laborategi-mailan aztertzeko, filmak lurrean lurperatu ziren (Prakash-Maran et al., 2014). Laburki azalduz, Petri ontziak lurra ontziratzeko erabili ziren eta lurraren mikroflora naturala degradaziorako ingurune moduan erabili zen. Hasierako mikrofloraren konposizioa pH-aren menpekoa da. Lurraren hasierako pH-a 1:5 masa/bolumen erlazio (1 g lur/5 mL ur destilatu) bidez neurtu zen eta 7,3-koa zen. Gelatinazko filmak angeluzuzen forman (2 cm x 3 cm) moztu ziren eta ondoren lurraren gainazaletik 4 cm-ra lurperatu ziren. Laginak giro tenperaturan inkubatu ziren eta entsegu guztian zehar (15 egun) lurraren hezetasuna % 100 izan zen. Filmen desintegrazioa FTIR bidez jarraitu zen.

2.11 Ingurumen analisia

Ingurumen analisia ISO 14014-ak (ISO 1404, 2006) ezarritako ildo nagusien eta gomendioen arabera egin zen. Hortaz, ebaluazioa lau fasetan bereizi zen: helburuaren eta helmenaren definizioa, bizi zikloaren inbentarioa (LCI), bizi zikloaren ingurumen eraginaren ebaluazioa (LCIA) eta emaitzen interpretazioa.

Analisi honen helburu nagusia ingurumen inpaktuak definituz arrain gelatinazko filmen ingurumen-karga kalkulatzea da, filmen paketatzea diseinatzerakoan egokiak diren neurriak proposatzeko eta honela, beraien merkatu ahalmena handitzeko. Paketatzeko filmetan egin berri diren analisietan ikusi den bezala (Günkaya eta Banar, 2016), aukeratutako unitate funtzionala 1 m^2 (50 μm-tako lodiera duen filma) izan zen. Lan honetan, “sehaskatik-sehaskara” ikuspuntua kontuan hartu zen eta hiru fase nagusi zehaztu ziren: lehengaien erauzketa, filmen manufaktura eta bizi amaiera.

Analisi hau egiteko SimaPro 7.3.3 softwarea erabili zen. Erauzketa fasea ez zenez gure laborategian egin, arrain gelatinaren kasurako LCI-rako datuak literaturatik lortu ziren (Karim eta Bhat, 2009) eta glizerolaren eta erauzketa prozesuan erabilitako gehigarrien kasuan SimaPro softwarean eskuragarri dagoen Ecoinvent 2.2. datu

basetik datuak lortu ziren. Filmen fabrikazioa gure laborategian egin zenez, lan honetan oinarrituta LCI datuak jaso ziren. Azkenik, bizi amaierako faserako datuak Euskal Herrian kokatutako Lapatx konpostaje-plantari esker lortu ziren. Ingurumen analisia egiterakoan, suposizio batzuk kontuan hartu ziren. Plastifikatzaile bezala erabilitako glizerola, biodiesela lortzeko soja-olioaren ekoizpenean lortutako azpi-produktutzat hartu zen. Bizi amaierako fasean, film hondakinen 1 kg-tik 200 g konpost bezala kontsideratu ziren eta gainerako materia organikoa biodegradazio-prozesuan parte hartzen duten mikroorganismoek digeritu zutela kontuan hartu zen. Gainera, lurraren hobekuntzarako sortutako konposta saihesturiko produktutzat hartu zen.

Inbentarioko datuetan oinarrituz, amaierako emaitzak Eco-indicator 99 metodologian erabilitako ingurumen-kategorietan aurkeztu ziren. Metodologia honek ingurumen-inpaktuak hiru kalte-kategoriatan edo amaiera-puntutan taldekatzen ditu: giza osasuna, ekosistemaren kalitatea eta baliabideak (Calderón et al., 2010). Lan honetan, tarteko puntuetan neurketak egin ziren, puntu hauek, faktoreen karakterizazioan emisioen garrantzia islatzen duten inpaktu-kategoriako kausa-efektu kateari lotuta daudelako (Bare et al., 2000). Giza osasunaren kategoriak tarteko puntuetan 6 inpaktu-kategoria biltzen ditu: kartzinogenoak, organiko arnasgarriak, ez-organiko arnasgarriak, klima-aldaketa, erradiazioa eta ozono-geruza. Inpaktu-kategoria hauek DALY eskala (ezintasunagatik egokitutako bizi urteak, *Disability Adjusted Life Year*) darabilte. Ekosistemaren kalitateak ekotoxikotasuna, azidotzea/eutrofizazioa eta lurraren erabilera kontuan edukitzen ditu. Ekotoxikotasuna eta lurraren erabilera potentzialki eragindako frakzioa (PAF m^{-2} $year^{-1}$, *Potentially Affected Fraction*) eta azidotzea/eutrofizazioa potentzialki desagertutako frakzioa (PDF m^{-2} $year^{-1}$, *Potentially Disappeared Fraction*) terminoetan adierazten dira. Gainera, baliabideen kategoriak mineralak eta erregai fosilak kontuan izan ditu; biak MJ gaineratiko energia bezala adierazten dira. Azterturiko inpaktu-kategorien garrantzi erlatiboa kontuan hartzeko, inpaktu balio normalizatuak irudikatu ziren. Normalizazioa, kategoria adierazleen

emaitzen eta europar mailako eguneratutako emisio garrantzitsuenen erreferentzien proportzioak determinatuz burutu zen.

2.12 Analisi estatistikoa

Datuei faktore bakar baten bariantza analisia (ANOVA) burutu zitzaien, SPSS softwarea (SPSS Statistic 20,0) erabiliz. Post hoc konparaketa anitzak Tukey-ren froga anizkoitzaren bidez determinatu ziren, $P < 0,05$-eko esangura mailarekin.

3 Arrain gelatinazko film jasangarriak

3.1 Laburpena

Erregai fosilen agortzearen eta giza jarduerak eragindako ingurumen kutsaduraren inguruan sortutako kezkek, bizi zikloan zehar ingurumen-karga baxuagoko material berriztagarrietan oinarritutako produktuen garapena bideratu dute (Yates eta Barlow, 2013). Aurretik aipatu moduan, Europan, 2015 urtean plastikoen eskaera 58 milioi tonara iritsi zen; horietatik % 39,9a paketatze-industriara bideratu zen eta ehuneko horretatik gehiengoa epe motzeko aplikazioetan erabili zen. Gainera, kontsumitutako 25,8 milioi tona zabortegietara eraman ziren, Europar Batasuneko (EB) herrialde gehienetan lurperatzea zaborren kudeaketarako lehenengo aukera delako (PlasticsEurope, 2016). Behar ugarietarako plastiko mota ezberdinak erabiltzen dira, polipropilenoa (PP), dentsitate baxuko polietilenoa (LDPE), dentsitate altuko polietilenoa (HDPE) edo polibinil kloruroa (PVC) merkatu ezberdin askotan erabiltzen diren plastiko sintetiko arruntenak izanik. Petroliotik eratorritako plastikoen inpaktua txikiagotzeko, film organikoetan arreta nabaria jarri da (Leceta et al., 2014), horien artean, gelatinazko filmak bezalako elikagaien prozesatze hondakinetatik lortzen diren proteinekin prestaturiko filmetan (Reddy eta Yang, 2013; Silva et al., 2014). Arrain hondakinetatik ekoitzitako gelatinaren gaiak berriki arreta handia bereganatu du. Arrain azalek eta hezurrek, arrainen pisu totalaren % 30a osatzen dutenez, arrain-industriako hondakinak gelatina ekoizteko etorkizun oneko bidea kontsideratzen dira (Gómez-Guillén et al., 2002). Gainera, hondakin horien balioztatzeak, zaborren kudeaketa arazoak gutxiagotu ditzake (Kittiphattanabawon et al., 2005), hondakinen maneiu desegokiagatik sorturiko arazo ekologiko larriak eta ingurumen-kutsadura ekidinez.

Kapitulu honen helburua, arrain gelatinazko filmen propietate funtzionaletan, hala nola, propietate mekanikoetan, optikoetan eta hesi-propietateetan, filmak prestatzeko baldintzen eragina aztertzea izan zen. Espektroskopia eta difrakzio metodoen bidez propietateetan ikusitako aldaketak gelatinazko egituran emandako

aldaketekin erlazionatu ziren. Gainera, ingurumen-inpaktuak neurtu ziren, filmen abantailak eta hobetu beharreko alderdiak identifikatzeko.

3.2 Emaitzak eta eztabaida

Paketatze teknologiak produktuaren babesarekin batera honen itxura, kontsumitzailearen onargarritasuna eta gizarte nahiz ingurumen kontzientzia bezalako arazoak modu orekatuan kontuan izan behar ditu. Alderdi hauek kontuan hartuz, pH-aren (azidoa, berezkoa, basikoa) eragina arrain gelatinazko filmen propietate mekanikoetan, optikoetan, hesi-propietateetan eta materialaren egituran aztertzeko helburuarekin, filmen karakterizazioa egin zen.

3.2.1 Filmen karakterizazioa

Ultramore (UV) argitik ondo babestua egoteak, paketatutako produktuan UV argiak eragindako oxidazio erreakzioak sorturiko narriadura ekidin dezake (Díaz-Visurraga et al., 2010). **3.1 irudia**n ikus daitekeen moduan, arrain gelatinazko filmek UV argia xurgatzeko gaitasun handia erakutsi zuten, arrain gelatinan dauden lotura peptidiko (200-250 nm) eta ohizko aminoazido aromatikoengatik, hala nola, tirosina eta fenilalanina bezalako kromoforoengatik (250-300 nm) (Samira, Thuan-Chew, eta Azhar, 2014; Hong et al., 2014).

UV argiarekiko erresistentziaz gain, gardentasuna eta kolorea bezalako propietate optikoek kontsumitzailearen erosteko gogoan eragiten dute eta beraz, hauek kontuan eduki beharreko propietateak dira. Filmak gardenak ziren, **3.1 irudia**n ikus daitekeen moduan 600 nm-an hauek UV argia xurgatu ez zutelako, filmen soluzioa prestatzeko erabilitako pH-a kontuan hartu gabe.

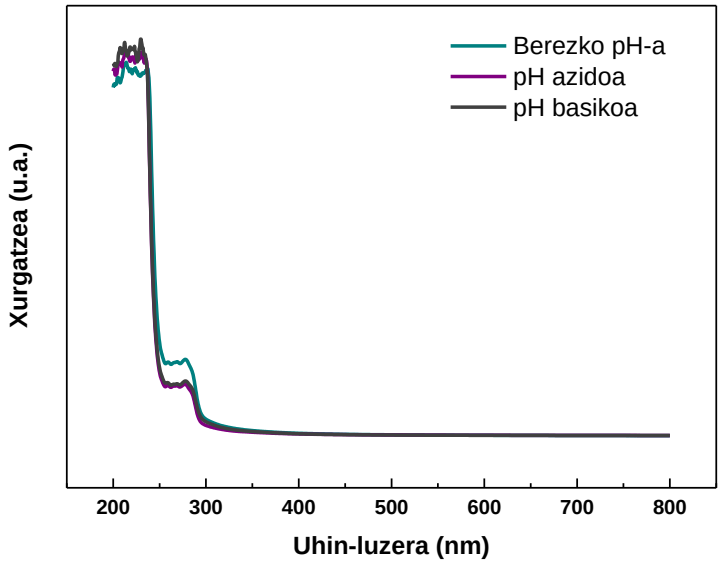

3.1 irudia Arrain gelatinazko filmen UV-vis espektroa, soluzioaren pH-aren funtziopean.

Era berean, kolore parametroetan ez zen aldaketa esanguratsurik (P > 0,05) ikusi, **3.1 taula**n zerrendatutako L*, a* eta b* balioek erakutsi zuten bezala. **3.1 taula**n distiraren balioak agertzen dira. Distira, filmen gainazalen laztasunarekin zuzenki erlazionatua dago eta beraz, distira balioak baxuak dira gainazala latza denean. 60º-etako eraso-angeluan neurtutako distira balioak 70 DU (distira unitateak) baino handiagoak badira, honek gainazala distiratsua eta leuna dela adierazten du (Keyf eta Etikan, 2004). Soluzioaren pH-a aldatzerakoan, filmek distira handiagoa erakutsi zuten eta beraz, berezko pH-an prestatutako filmak baino gainazal leunagoa aurkeztu zuten, pH-aren aldaketak filmen gainazala aldarazi zuela adieraziz.

3.1 taula Arrain gelatinazko filmen propietate optikoak, soluzioaren pH-aren funtziopean.

pH	L*	a*	b*	Distira$_{60º}$ (DU)
Berezkoa	96,13 ± 0,53^{a}	-0,18 ± 0,09^{a}	2,86 ± 0,41^{a}	35,89 ± 2,85^{a}
Azidoa	96,14 ± 0,44^{a}	-0,18 ± 0,04^{a}	2,65 ± 0,10^{a}	152,00 ± 1,58^{c}
Basikoa	96,19 ± 0,25^{a}	-0,10 ± 0,03^{a}	3,01 ± 0,10^{a}	119,75 ± 6,90^{b}

$^{a-c}$ Zutabe berean letra bera duten bi balio ez dira esanguratsuki (P > 0,05) desberdinak, Tukey-ren froga anizkoitzaren arabera.

UV argiarekiko hesi-propietateez gain, urarekiko hesi-propietateak neurtu ziren. Urarekiko kontaktu angelua (WCA) gainazalaren bustitze ahalmenaren neurketa da eta materialaren izaera hidrofiloa edo hidrofoboa definitzeko erabiltzen da. WCA-ren balio baxuek, 90º baino txikiagoek, bustitze ahalmena handia edo izaera hidrofiloa adierazten dute eta aldiz WCA-ren balio altuek, 90º baino handiagoek, bustitze ahalmen txikia edo izaera hidrofoboa adierazten dute (Yuan eta Lee, 2013). Arrain gelatinazko filmen WCA-ren balioak **3.2 taula**n erakusten dira. Ikus daitekeen moduan, pH-a aldatzerakoan WCA-ren balio handiagoak lortu ziren. Honen arrazoia, proteinan emandako konformazio aldaketek, gelatinaren talde ez polarrak filmaren gainazalerantz bideratu zituztela izan zitekeen.

3.2 taula Arrain gelatinazko filmen uraren kontaktu-angeluaren (WCA) eta ur lurrunaren iragazkortasunaren (VWP) balioak, soluzioaren pH-aren funtziopean.

pH	WCA (°)	WVP 10^{12} (g cm^{-1} s^{-1} Pa^{-1})
Berezkoa	76,85 ± 1,36[a]	1,48 ± 0,16[a]
Azidoa	91,35 ± 3,26[b]	1,52 ± 0,10[a]
Basikoa	88,61 ± 3,36[b]	1,81 ± 0,16[b]

[a-b] Zutabe berean letra bera duten bi balio ez dira esanguratsuki (P > 0,05) desberdinak, Tukey-ren froga anizkoitzaren arabera.

Ingurugirotik datorren edota ingurugirorantz doan hezetasunaren aldaketa kontrolatzeko, filmek erabileraren araberako ur lurrunaren iragazkortasunaren (WVP) balio egokiak erakutsi behar dituzte. Arrain gelatinazko filmen WVP-ren balioak **3.2 taula**n erakusten dira. Ikus daitekeen moduan, pH basikoan proteinaren desnaturalizazioa handiagoa denez, WVP-ren balioak handiagoak (P < 0,05) ziren, proteinaren egituraren destoleste handiago batek ur-molekulen irazkortasuna erraztu zuela adieraziz.

Azkenik, materialak erabiltzerakoan beraien osotasuna mantentzeko trakzio erresistentziaren (TS) eta haustura elongazioaren (EB) propietate egokiak izatea oso garrantzitsua denez, filmen propietate mekanikoak aztertu ziren. **3.3 taula**n ikusi

daitekeen moduan, propietate mekaniko hoberenak filmen prestaketan pH basikoa erabili zenean lortu ziren. pH-a aldatu zenean TS balioak nabarmenki ($P < 0,05$) handitu ziren eta pH basikoan prestatuko filmen kasuan, 50 MPa baino TS balio altuagoak lortu ziren. Hala ere, soluzioaren pH-ak ez zuen EB-n nabarmenki ($P > 0,05$) eragin.

3.3 taula Arrain gelatinazko filmen trakzio erresistentziaren (TS) eta haustura elongazioaren (EB) balioak, soluzioaren pH-aren funtziopean.

pH	TS (MPa)	EB (%)
Berezkoa	$36,52 \pm 2,98^{a}$	$1,79 \pm 0,54^{a}$
Azidoa	$43,02 \pm 0,52^{b}$	$2,31 \pm 0,33^{a}$
Basikoa	$52,39 \pm 3,16^{c}$	$2,88 \pm 0,68^{a}$

$^{a-c}$ Zutabe berean letra bera duten bi balio ez dira esanguratsuki ($P > 0,05$) desberdinak, Tukey-ren froga anizkoitzaren arabera.

Arrain gelatinazko filmen propietate funtzionalak filma eratzeko soluzioaren pH-ak eragindako egitura aldaketekin erlazionatzeko, proteinen egitura tertziarioa determinatzeko ohikoa den XRD teknika erabili zen eta arrain gelatinazko filmen difrakzio bandak soluzioaren pH-aren funtziopean **3.2 irudia**n erakusten dira.

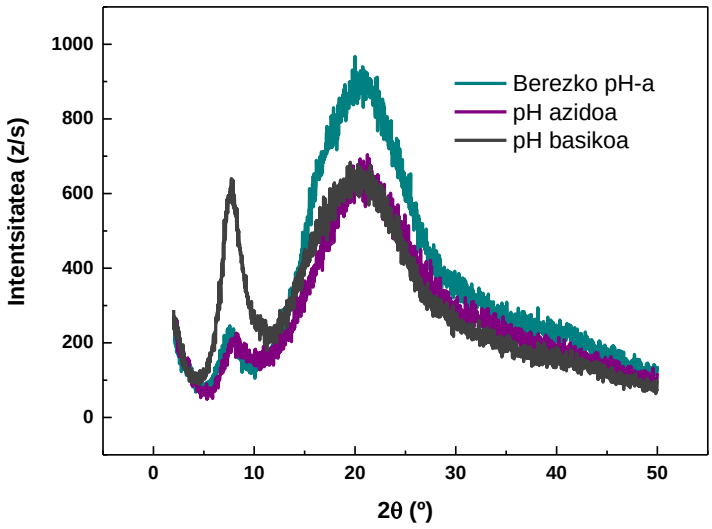

3.2 irudia Arrain gelatinazko filmen XRD ereduak, soluzioaren pH-aren funtziopean.

Eredu guztiek bi difrakzio banda erakutsi zituzten, 21º-etako banda, gelatinaren kristalinitatearekin erlazionatu zena, eta 7,4º-tako banda, kolageno natiboaren helize hirukoitzaren hondarrari egokitu zitzaiona (Learner et al., 2008; Schmidt, Giacomelli, eta Soldi, 2005). Soluzioaren pH-a aldatu zenean, kristalinitate baxuagoa ikusi zen eta honek desnaturalizazio handiagoagatik egitura nahaspilatuagoa lortu zela adierazi zuen, gelatinaren egitura tertziarioan aldaketak eragin zituena (Mikšovská eta Larsen, 2007). Proteinen egitura tertziarioa interakzioa ez-kobalenteez zehaztuta dagoenez, hala nola, hidrogeno zubizko loturak, interakzio hidrofoboak, eta erakarpen eta aldarapen kargak, soluzioaren pH-aren aldaketak interakzio fisiko hauek eten ditzake, **3.2 irudia**n ikus daitekeen kristalinitatearen bandaren intentsitatea txikiaraziz. Emaitza hauek WVP-ren emaitzekin bat egin zuten, desnaturalizazio maila handiagoak ur lurrunaren iragazkortasuna erraztu zuela ikusi zelako. Bestetik, pH azidoan eta berezkoan helize hirukoitzaren hondarra pH basikoan baino txikiagoa zen. Nahiz eta gelatina kolagenoaren hidrolisi partzialetik (helize hirukoitzaren haustura ematen da eta zorizko kiribil egitura osatzen da) lortzen den, gelatina kolageno natiboaren egitura partzialki berreskuratzeko gai da. Fenomeno honi kiribiletik helizerako transformazioa deritzo (Ghoshal, Stapf, eta Mattea, 2014). Emaitzek, arrain gelatinazko filmak lehortzen ziren bitartean kolagenoaren helize hirukoitzaren birtolestea baldintza basikoetan erraztu egin zela erakutsi zuten.

Proteinen bigarren egiturarekiko amida I bibrazioen sentiberatasunagatik espektroskopia infragorria proteinen egitura aztertzeko baliagarria den tresna da (Fabian eta Mäntele, 2002). Hortaz, gelatinaren egitura sekundarioa α-helize/nahaspilatua eta β-xafla konformazioen terminoetan aztertzeko, amida I banda (1600-1700 cm^{-1}), proteinen lotura peptidikoen karbonilo taldeen (C=O) bibrazioei elkarturikoa, FTIR espektroskopia bidez aztertu zen. **3.3 irudia**n ikusten den moduan, gelatinazko filmen bigarren egitura sekundarioa α-helize/nahaspilatua konformazioez, 1650 cm^{-1}-eko bandari elkartutakoa, eta β-xafla konformazio antiparaleloez,

1630-1615 cm^{-1} eta 1700-1680 cm^{-1}-eko bandei elkartutakoa, osatuta zegoen nagusiki (Guerrero, Kerry, eta de la Caba, 2014; Susi, Timasheff, eta Stevens, 1967).

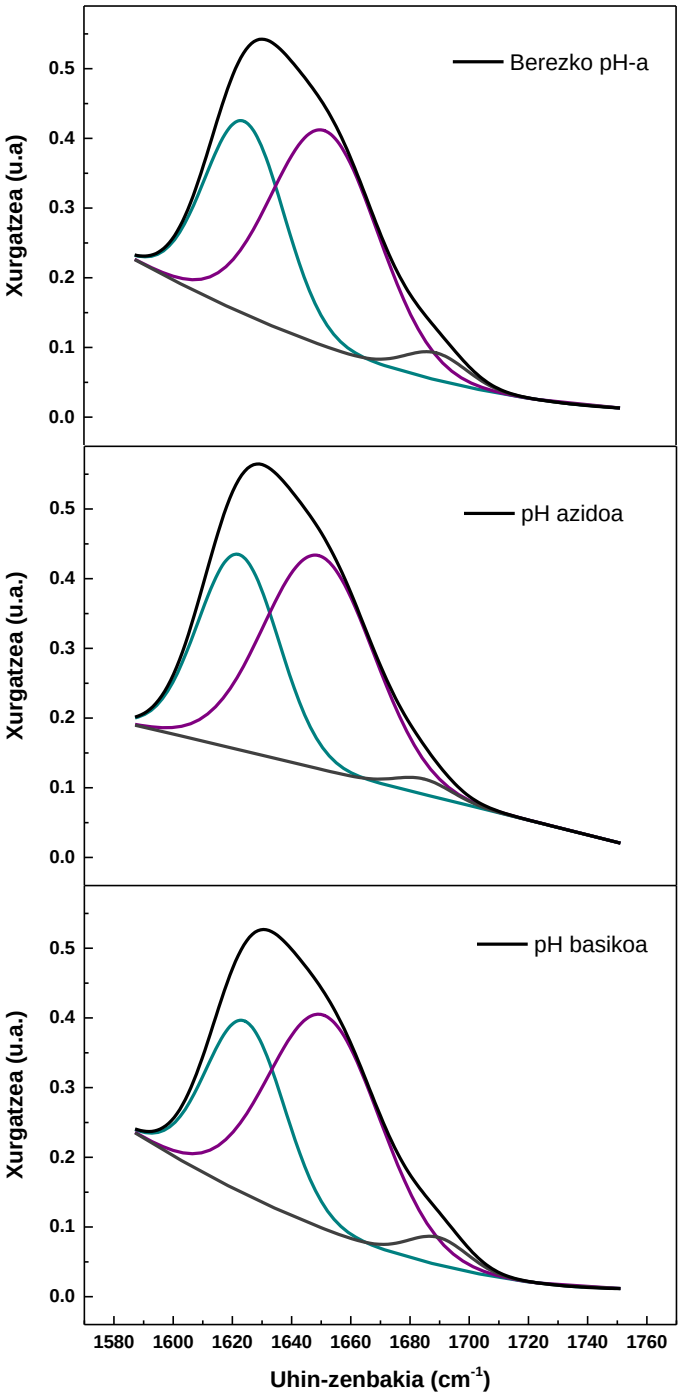

3.3 irudia Arrain gelatinazko filmen amida I bandaren egokitze kurbaren espektroak, soluzioaren pH-aren funtziopean.

α-helizea egitura nagusiena zen, soluzioaren pH-a kontuan hartu gabe. Hala ere, baldintza basikoetan prestatutako filmak azalera handiagoa erakutsi zuten (**3.4 taula**) eta hortaz, baldintza azidoetan prestatutako filmak baino α-helize egitura kantitate handiagoak zituzten. Bestalde, filmak baldintza azidoetan prestatu zirenean, β-xafla egituraren (1700-1680 cm^{-1}) xurgatze azaleraren gutxitzea ikusi zen. Beraz, emaitzek, soluzioaren pH-ak arrain gelatinazko filmen egitura sekundarioa aldatu zuela erakutsi zuten. Ur-disoluzioan, proteinaren aminoazidoak kargatuta daude eta horregatik proteinaren mugikortasuna pH-aren funtziopean dago. pH-a puntu isoelektrikotik urruti dagoenean, proteinaren karga positiborantz edo negatiborantz pH-aren arabera aldatzen da. Karga berdinak bata bestetik aldaratzen direnez, honek proteinaren agregazioak ekiditen ditu. Beraz, barruko interakzioak aldatu egiten dira proteinaren egitura zabalduz (desnaturalizazioa edo destolestea) (Hoque, 2011). Fenomeno horregatik, filmaren egitura aldatu zen eta beraz, aurretik aipaturiko zenbait propietate funtzional ere bai.

3.4 taula Amida I bandaren egokitze kurbaren emaitzen ehunekoak (%), soluzioaren pH-aren funtziopean.

pH	β-xafla/zorizko kiribila (1630-1615 cm^{-1})	α-helizea (1650 cm^{-1})	β-xafla/zorizko kiribila (1700-1680 cm^{-1})
Berezkoa	38,16	57,63	4,21
Azidoa	39,13	58,71	2,16
Basikoa	34,72	61,03	4,25

Gelatinazko filmen propietate funtzionalez gain, beraien biodegradagarritasuna garrantzizko abantaila da komertzialak diren polimero ez biodegradagarriekin alderatuz gero, azken hauek zakarretara bota eta ondorengo zaborren kudeaketan arazoak eta kostuak eragiten dituztelako. Gelatina eta glizerola konposatu biodegradagarriak direnez eta beraien artean erreakzio kimikorik ez dagoenez, filmen biodegradagarritasuna ziurtatzeko biodegradazio azterketa egitea ez da beharrezkoa (UNE-EN 13432, 2001). Hala ere, filmen desintegrazio azterketa filmak lurrean kontrolatutako baldintzetan lurperatuz burutu zen, gelatinazko filmen desintegrazioa

FTIR espektroen bidez aztertzeko. pH ezberdinetan prestaturiko filmen espektroetan (erakutsi gabeko datuak) ez zen aldaketa nabarmenik ikusi. Hortaz, baldintza basikoetan destoleste handiagoa zegoenez eta beraz, interakzioetarako talde eskuragarri gehiago zeudenez, desintegrazioren azterketa baldintza horietan prestatutako filmetan burutu zen eta emaitzak **3.4 irudia**n erakusten dira.

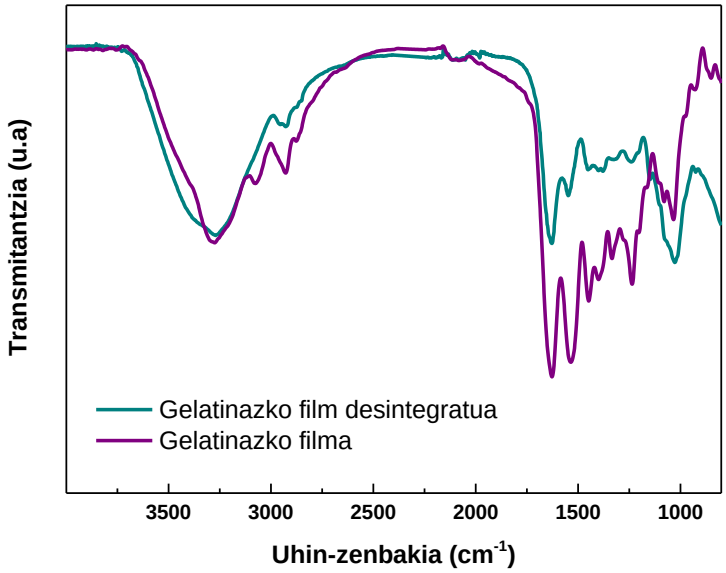

3.4 irudia Arrain gelatinazko filmen FTIR espektroak, hauek lurrean lurperatu aurretik eta desintegrazioaren ondoren.

Xurgatze banda nagusienak 1630-800 cm^{-1}-eko tartean kokatuta zeuden. Gelatinazko bandak, 1630 cm^{-1}-eko C=O loturaren luzatzearekin (amida I), 1530 cm^{-1}-eko N-H loturaren tolestearekin (amida II) eta 1230 cm^{-1}-eko C-N loturaren luzatzearekin (amida III) erlazionatu ziren (Schmidt, Giacomelli, eta Soldi, 2005). Glizerolaren banda nagusiak aldiz, 850, 940 eta 1000 cm^{-1}-eko C-C loturen eta 1050 eta 1100 cm^{-1}-eko C-O loturen bost bandekin erlazionatu ziren (Basu et al., 2011). Desintegrazioan zehar filmen banda esanguratsuen desplazamendurik ikusi ez zen arren, amida I, II eta III banden intentsitateen txikitzea gertatu zen. Gainera, xurgatze banden intentsitateen txikitzea amida II eta III bandetan amida I bandan baino

nabariagoa zen. Biodegradazio maila mikroorganismoak polimero-kateen zehar sartzeko erraztasunaren menpekoa denez, prozesu hau kateen malgutasunaren eta proteinaren zati amorfoaren funtziopean dago, besteen artean (Kijchavengkul eta Auras, 2008).

Emaitzek, mikroorganismoek nagusiki C-N loturaren luzapenean, ondoren N-H loturaren tolestean eta nekez C=O loturaren luzapenean erasotzen zutela erakutsi zuten. Hortaz, amida III (C-N) eta amida II (N-H) talde funtzional hidrolizagarriak amida I (C=O) taldea baino erasotuagoak izateko erraztasun handiagoa erakutsi zuten. Emaitza hauek, aurretik aipaturiko amida taldeen loturak puskatzeko behar den energia kantitatearekin bat datoz. Zehazki, C-N, N-H eta C=O lotura energiak 305 kJ/mol-etakoak, 390 kJ/mol-etakoak eta 799 kJ/mol-etakoak dira, hurrenez hurren. Gainera, aipatzekoa da glizerolaren banda analisian zehar ez zela ia aldatu, lurrean zeuden mikroorganismoek plastifikatzailea eraso egin ez zutela adieraziz. Izan ere, mikroorganismo ugari glizerolan hazi daitezke (Da Silva, Mack, eta Contiero, 2009) eta hortaz, plastifikatzailean emandako mikroorganismoen ugaritzeak proteinaren desintegrazioa sustatu zuen. Ondorioz, lurraren pH-a 7,9-ra igo zen. Handitze txiki hau filmen proteinen amonifikazioagatik izan zitekeen.

3.2.2 Ingurumen analisia

Arrain gelatinazko filmen ingurumen-inpaktuari dagokionez, 3 fase nagusi aztertu ziren: lehengaien erauzketa, filmen manufaktura eta bizi amaiera. **3.5 irudia**n sistemaren mugen diagrama eskematikoa erakusten da.

Arrain gelatinazko filmak prestatzea, arrainen prozesatze-industriako hondakinei balioa eransteko modua da. Hondakin horien % 30a kolageno kantitate handia duten azal eta hezurrez osatua dago (Gómez-Guillén et al., 2002). Erauzketa prozesua sodio hidroxidoan eta ondoren azido azetikoan emandako handitze arinetan datza. Jarraian, gelatinaren erauzketa ur destilatuan 70 ºC-an 90 minutuz burutzen da

eta gero, lagina 18 orduz 50 ºC-an dagoen labe batean lehortzen da. Arrain gelatinaren erauzketa-etekinaren batezbestekoan oinarrituta, lan honetan erabilitako etekina %15a izan zen (Karim eta Bhat, 2009). Prozesu hau ez zen gure laborategian burutu eta beharrezko datuak literaturatik hartu ziren (Karim eta Bhat, 2009). Gainera, arrainen zati jangarrien produkzioa sistemaren mugetatik at zegoen.

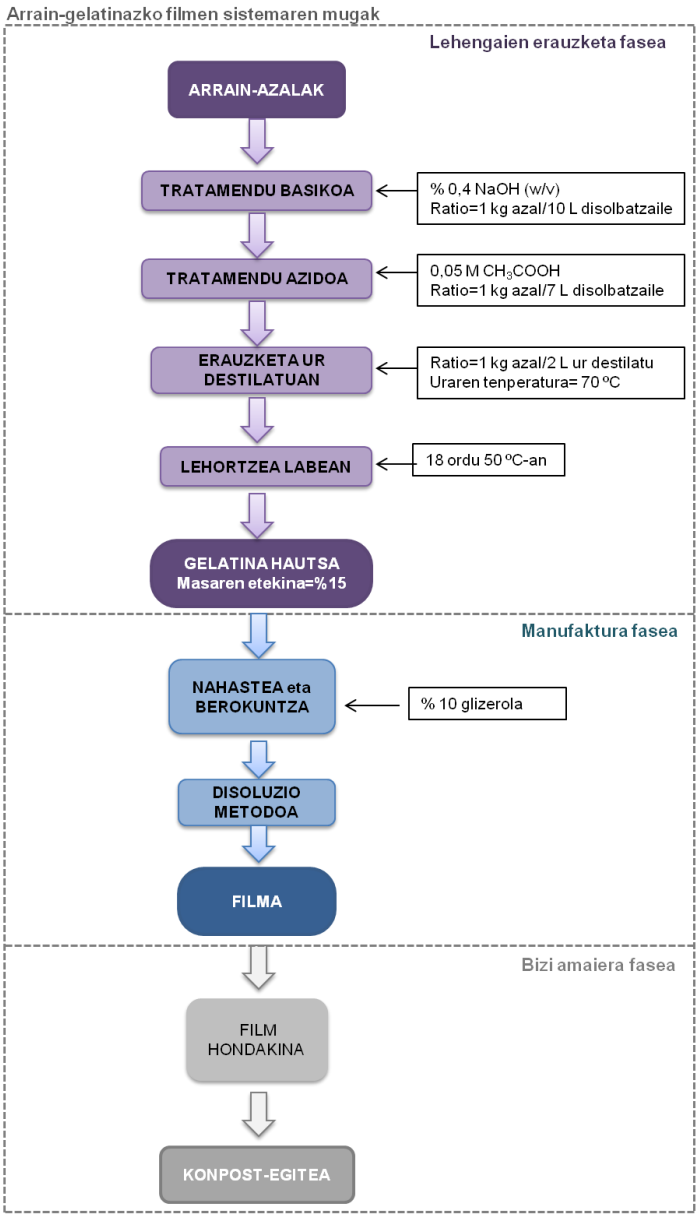

3.5 irudia Arrain gelatinazko filmen ingurumen-inpaktuaren sistemaren mugak.

Arrain gelatinazko filmen manufakturari dagokionez, datuak aurretik zehaztutako eta gure laborategian egindako atal esperimentalean erabilitako

prozesuetatik lortu ziren. Filmen manufakturan, lehengaietatik filmak lortzeko prozesuaren ingurumen-karga kontuan eduki zen eta beraz, prozesuan zehar erabilitako gehigarriak nahiz kontsumitutako energia aintzakotzat hartu ziren. Erabilitako glizerola biodiesela lortzeko soja-olioaren ekoizpenean lortutako azpi-produktutzat hartu zenez, soja-olioaren esterifikazio prozesua metil-esterra eta glizerola lortzeko aintzat hartu zen.

Azkenik, konposta, hondakinen biodegradatze aerobikoan oinarritutako prozesua, zakarretarako jokalekua izan zen. Filmen 1 kg hondakin bakoitzeko, 200 g konpost hartu ziren eta gainerako materia organikoa biodegradazio-prozesuan parte hartzen duten mikroorganismoek digeritu zutela kontsideratu zen. Konpost instalazioak energetikoki laguntza behar ez zuela aintzat hartu zen eta beraz, kontsumo elektrikorik ez zen kontuan hartu. Prozesu hau ez zen gure laborategian burutu eta aurretik aipatutako datuak Euskal Herrian kokatutako konpost-instalazio batek emandakoak izan ziren. Gainera, analisiaren faseetan ez zen garraiatzea kontuan hartu.

Arrain gelatinazko filmen ingurumen-inpaktuen analisirako Eco-indicator 99 metodoa erabili zen. Metodologia hau oro har Europan erabiltzen da, emaitzak tarteko puntu edo inpaktu-kategorietatik amaiera-puntu edo kalte-kategorietaraino lotzen dituelako, analisian erabilitako iturri eta igorritako substantziek eragindako ingurumen efektu negatiboak emanez (Ingrao et al., 2015). Ingurumen analisi honen helburuen arabera, 3 fase nagusien inpaktu-kategoriak **3.6 irudia**n erakusten dira.

Ikus daitekeen moduan, azterturiko inpaktu-kategoria gehienetan lehengaiaren erauzketa faserik kutsagarriena izan zen. Zehazki, arrain gelatinazko filmek erregai fosilen eta ez-organiko arnasgarrien inpaktu-kategorietan ingurumena gehien kaltetu zuten. Gelatinaren erauzketa prozesuan kontsumitutako energia kategoria horien ingurumen-kargaren erantzule izan zen.

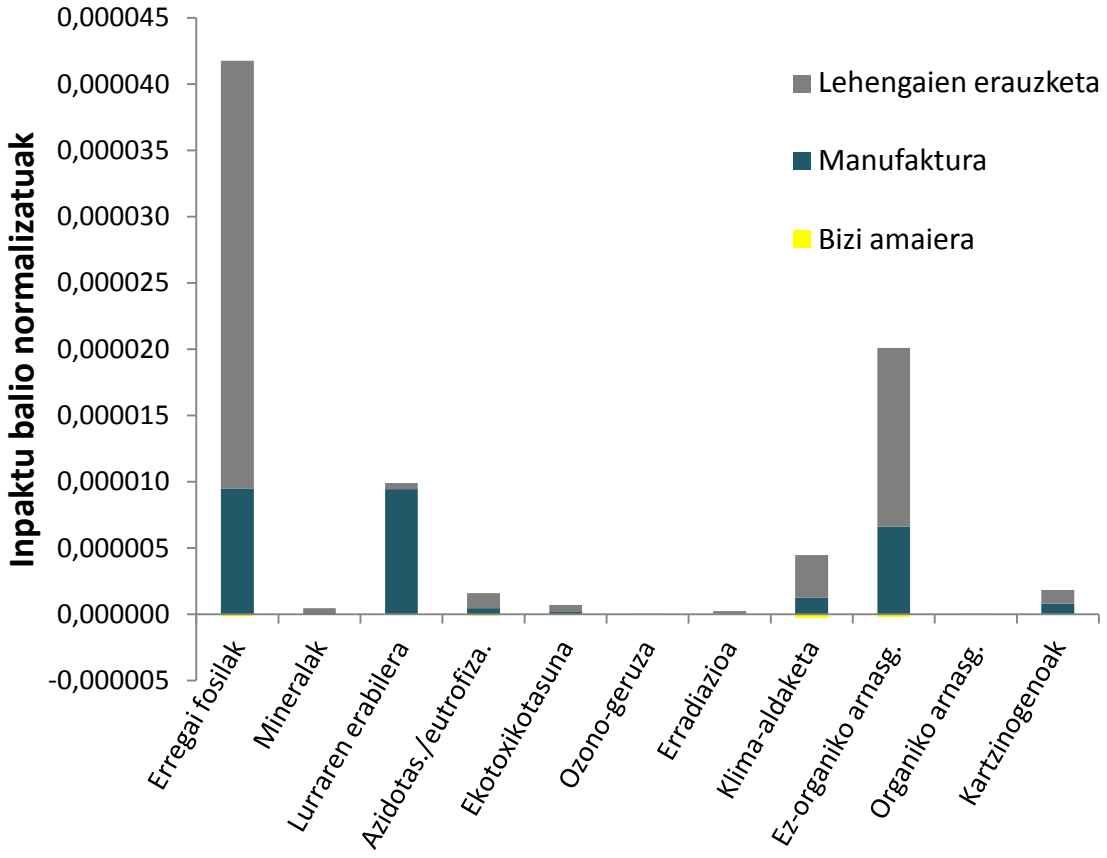

3.6 irudia Arrain gelatinazko filmen ingurumen-inpaktuen balio normalizatuak.

Manufaktura faseari dagokionez, energiaren kontsumoa eta glizerola lortzeko sojaren lantze-prozesua erregai fosilen, lurraren erabileraren eta ez-organiko arnasgarrien ingurumen-kargen erantzule nagusiak izan ziren. Lurraren erabilerari dagokionez, ingurumen-karga hori glizerola, biodiesela lortzeko soja-olioaren ekoizpenean lortutako azpi-produktutzat hartutako produktua, plastifikatzaile bezala erabiltzeagatik izan zen, izan ere, soja-aleen lantzea kontuan eduki baitzen.

Elkarketari, hau da, lehengaien erauzketa fasearen eta filmen manufaktura fasearen elkartzeari, eta bizi amaierako faseari dagozkien inpaktu balioak **3.5 taula**n argi ezberdinduta agertzen dira. Modu honetan, ingurumen-kategoria guztietan konposta ikuspegiak emandako onurak behar bezala ikusi daitezke. Konpostak hondakin biodegradagarriak lur-produktu erabilgarri bilakatzen zuenez, sorturiko karbono dioxidoak ez zuen berotegi-efektuko gasen hazkundean eragin, jadanik

karbonoaren ziklo biologikoaren parte zelako (Song et al., 2009). Gainera, lurra egokitzeko sortu zen konpostaren produkzioaren eta honi elkarturiko emisioen saihesteak, ingurumen-inpaktuan efektu positiboa eragin zuen.

3.5 taula Arrain gelatinazko filmen bizi amaiera faseko balio normalizatuak.

Inpaktu kategoria	Elkarketa	Bizi amaiera	Guztizkoa
Erregai fosilak	4,17583 E-05	-1,44962 E-07	4,16133 E-05
Mineralak	4,54575 E-07	-3,11713 E-09	4,51458 E-07
Lurraren erabilera	9,90902 E-06	-4,49753 E-09	9,90452 E-06
Azidotasuna/eutrofizazioa	1,60126 E-06	-8,53697 E-08	1,51589 E-06
Ekotoxikotasuna	7,04678 E-07	-2,80816 E-09	7,01870 E-07
Ozono-geruza	2,11478 E-09	-6,95414 E-12	2,10782 E-09
Erradiazioa	2,54337 E-07	-3,69787 E-10	2,53968 E-07
Klima-aldaketa	4,46968 E-06	-2,76574 E-07	4,19311 E-06
Ez-organiko arnasgarriak	2,00957 E-05	-2,18191 E-07	1,98775 E-05
Organiko arnasgarriak	1,13861 E-08	-2,85968 E-10	1,11001 E-08
Kartzinogenoak	1,85121 E-06	-2,54244 E-09	1,84866 E-06

Aurretik azaldutako emaitzek berriki egindako ingurumen analisiekin bat egin zuten. Izan ere, lan horietan erauzketa eta manufaktura prozesuetako energia kontsumoak filmen ingurumen-inpaktuen eragile nagusienak zirela ondorioztatu zen (Günkaya eta Banar, 2016). Nahiz eta biopolimeroak beraien izaera berriztagarri eta biodegradagarriarengatik materia ekologikotzat hartzen diren, erauzketaren eta produkzioaren jarduerek ingurumen-kargak sortu ditzakete, almidoia (Günkaya eta Banar, 2016), kitosanoa (Leceta et al., 2013) eta agarra (Leceta et al., 2014) bezalako polisakaridoetan oinarritutako filmetan ikusi zen bezala. Aipatzekoa da biopolimeroekin egindako ingurumen analisi gehienak aurretik aipaturiko polisakarido horietan (Leceta et al., 2014; Günkaya eta Banar, 2016; Leceta et al., 2013) edo azido polilaktikoa bezalako poliesterretan burutu zirela (Benetto et al., 2015). Aldiz, proteinetan oinarritutako filmen inguruan (Deng et al., 2013; Garrido et al., 2014) edo aurkeztutako lanean egin zen bezala sehaskatik-hilobirako fase ezberdineko ingurumen analisiak burutu dituzten ikerketa oso gutxi daude. Emaitza hauek, ingurumenarekiko jasangarriagoak diren eta propietate funtzional onak dituzten materialak lortzeko filmen garapenerako fase ezberdinen hobekuntzarako harturiko erabakiak sostengatzeko lan

honen garrantzia azpimarratu zuten. Hala ere, nabarmentzekoa da laborategi-mailatik industria-mailara pasatzean hobekuntza batzuk espero direla.

3.3 Ondorioak

Lan honetan, arrain gelatinazko film homogeneoak, gardenak eta koloregabeak prestatu ziren, soluzioaren pH-a kontuan hartu gabe. Gainera, filmek UV argiarekiko erresistentzia handia erakutsi zuten, paketatutako produktua argiak eragindako oxidazio erreakzioetatik babestuz eta beraz, produktuaren kalitatea luzeago mantenduz. Hala ere, soluzioaren pH-ak gelatinaren egituran eragin zuela ikusi zen. Zehazki, pH basikoan prestaturiko filmak 50 MPa-etako trakzio erresistentziak erakutsi zituzten. Arrain gelatinazko filmen propietate funtzional on hauek eta bizi amaierako konpostaren ikuspegiaren efektu positiboek, material ez-biodegradagarri eta ez-berriztagarrien kontsumo handia murrizteko paketatze aplikazioetan film hauek aukerabide moduan erabiltzearen garrantzia azpimarratzen dute.

4 Saretze erreakzioaren kontrola

4.1 Laburpena

Aurreko kapituluetan, gelatinazko filmek propietate funtzional egokiak erakutsi dituzte, hala nola, filma eratzeko gaitasuna, propietate optiko onak eta biodegradagarritasuna; ezaugarri hauek, filmak elikadura-industrian eta industria farmazeutikoan erabiltzea sustatzen dute (Bhutani et al., 2016; Garrido et al., 2013; Li et al., 2015a). Hala ere, gelatinaren berezko hidrofilotasunagatik, proteina honetan oinarritutako filmek hauskortasun handia eta urarekiko sentikortasuna erakusten dute, hauen erabilera aplikazio batzuetan mugatuz. Propietate funtzional hauen hobekuntza proteinaren saretze bidez lortu daiteke (Etxabide et al., 2015b). Gelatinaren saretze kimikoa propietate kimiko eta fisiko hobeak dituen materialak lortzeko bide eraginkorra izan daiteke. Azetilazioa, deamidazioa eta proteinen propietate funtzionalak hobetzeko eskuragarri dauden beste metodo kimikoekin aldaratuz, Maillard erreakzioa beroarekin handizki bizkortzen den erreakzioa da. Nahiz eta literaturako lan gehienak glikazio konjugatuen propietate biologikoetan kontzentratu diren, Maillard erreakzioa proteinen beste propietate funtzionalak hobetzeko etorkizun handiko metodoa izan daiteke.

Maillard erreakzioaren proportzioa faktore batzuen menpekoa da, hala nola, tenperatura, denbora, proteina:karbohidrato ratioa eta pH-a (Lin et al., 2012). Kapitulu honen helburua bi pH-tan (berezko pH-a eta pH azidoa) prestatutako eta berotutako (HT) laktosadun filmen karakterizazioa egitea izan zen, laktosa kantitatearen eta soluzioaren pH-aren eragina filmen propietate fisiko-kimikoetan, mekanikoetan, hesi-propietateetan, eta morfologian aztertzeko.

4.2 Emaitzak eta eztabaida

4.2.1 Propietate fisiko-kimikoak eta hesi-propietateak

Berokuntzagatik laktosadun filmetan ematen den kolore aldaketa Maillard erreakzioaren adierazletzat hartu daiteke. Filmen kolorea CIELAB kolore eskala erabiliz neurtu zen eta L*, a* eta b* parametroak kolore aldaketaren (ΔE*) balioa

kalkulatzeko erabili ziren. Laktosaren gehikuntzak L* eta a* balioen gutxitzea eragin zuen (erakutsi gabeko datuak) eta aldi berean b* balioaren handitzea eragin zuen (**4.1a irudia**). Aldaketa hau berezko pH-an nabariagoa izan zen pH azidoan baino. Hau, ez-protonatutako amina taldeen eta espezie erreaktibotzat hartutako azukrearen kateen forma irekien edukia pH-arekin handitu zelako izan zitekeen (Yayalayan, Ismail, eta Mandeville, 1993). Hortaz, ΔE* gehituriko laktosarekin eta erabilitako pH-arekin aldatu zen (**4.1b irudia**).

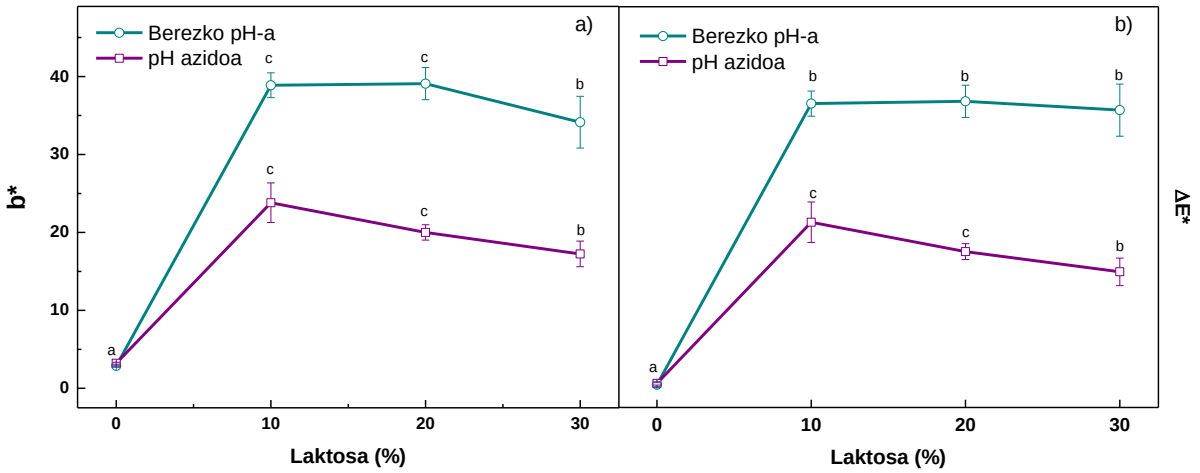

4.1 irudia Arrain gelatinazko HT filmen a) b* balioak eta b) ΔE* balioak, pH eta laktosa kantitatearen funtziopean. Lerro berean letra bera duten bi balio ez dira esanguratsuki (P > 0,05) desberdinak, Tukey-ren froga anizkoitzaren arabera.

ΔE* parametroak laktosa kantitateak eta pH-ak nabarmenki (P < 0,05) Maillard erreakzioaren mailan eragin zutela adierazi zuen. Morales eta Van Boekel-ek (1997) kolorea Maillard erreakzioaren azkeneko etapan sortzen dela ikusi zuten eta asegabeko nitrogenodun polimero eta kopolimero marroien eratzeagatik karakterizatu zen. Berezko pH-an prestaturiko filmek, ΔE* balio handiagoak erakutsi zituztenez, pH handiagoa duen ingurunean Maillard erreakzioa hedatuagoa zegoela ondorioztatu zen. Aipatzekoa da halaber, pH azidoan prestaturiko % 10 laktosadun filmetan ΔE*-ren balio handienak ikusi zirela, baldintza azidoetan erreakzioaren hedatzea laktosa

kantitate baxuetan azkarragoa izan zela adieraziz. Hau, pH baxuan laktosaren forma ziklikoen kantitate handiak oztopo esterikoak eragin zitzakeelako izan zitekeen.

UV argiaren xurgatzearen neurketa Maillard erreakzioaren hedatzea aztertzeko beste metodo bat da. Berotutako gelatinazko film guztiek UV argiarekiko xurgatze ahalmen handia erakutsi zuten (**4.2 irudia**), arrain gelatinan dauden lotura peptidiko (200-250 nm) eta ohizko aminoazido aromatikoengatik, hala nola, tirosina eta fenilalanina bezalako kromoforoengatik (250-300 nm) (Zhao et al., 2013).

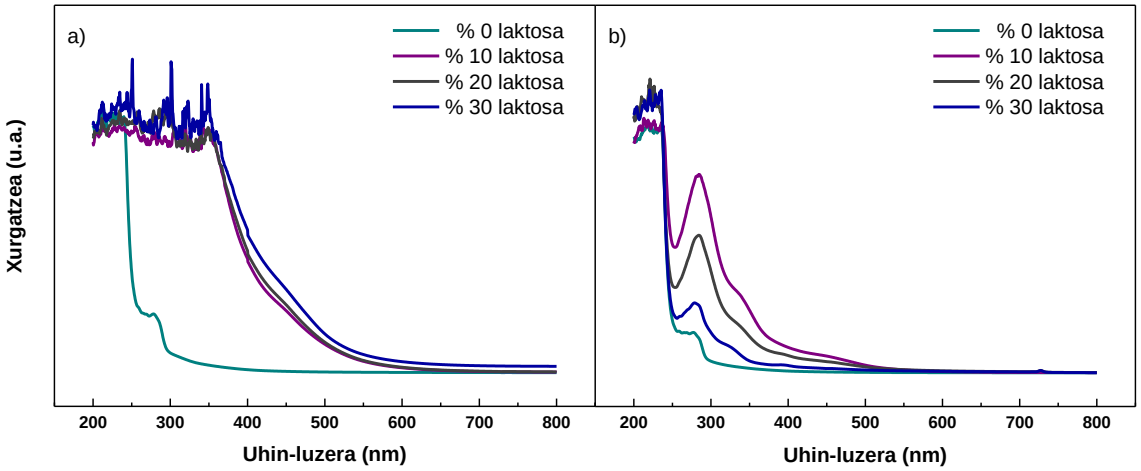

4.2 irudia a) Berezko pH-ko eta b) pH azidoko arrain gelatinazko HT filmen UV-vis espektroak, laktosa kantitatearen funtziopean.

Berezko pH-an prestaturiko filmetan (**4.2a irudia**), 420 nm-tik gora neurtutako xurgatzeek saretze erreakzioa azkeneko etapara iritsi zela erakutsi zuten, melanoidina izeneko konposatu marroi eta ez disolbagarriak sortu zirela adieraziz (Li et al., 2015b). Hala ere, pH azidoan prestatutako filmetan (**4.2b irudia**), 420 nm-an lorturiko xurgatze baxuek saretzearen hedatzea baxuagoa izan zela erakutsi zuten. 300 nm inguruko xurgatze banda, pentosidina glikazio produktuaren xurgatzearekin elkartu zen, saretzearen hedapenaren adierazletzat hartu zitekeen konposatu disolbagarria (Etxabide et al., 2015b). pH azidoan prestatutako filmen kasuan, erreakzioa

pentosidina eratu zenean gelditu zen eta berezko pH-ko filmetan aldiz, erreakzioa melanoidina konposatuen eraketa arte hedatu zen.

Aurretik aipatu moduan, erreakzioaren baldintzek Maillard erreakzio produktuen (MRP) eraketan izugarrizko eragina daukate. Van Boekel-en (1998) arabera, Amadori produktuaren bi deskonposizio bide daude; 1-deoxiosona izenekoa, pH altuetan gertatzen dena, eta 3-deoxiosona deritzona, pH baxuetan ematen dena (**4.1 eskema**). Bi bideek deoxiosona konposatuak eratzen dituzte, geroko erreakzioetan parte hartzen duten bitarteko erreaktiboak direnak. Maillard erreakzioaren azkeneko etapak nitrogenodun polimero marroien eraketa bideratzen du.

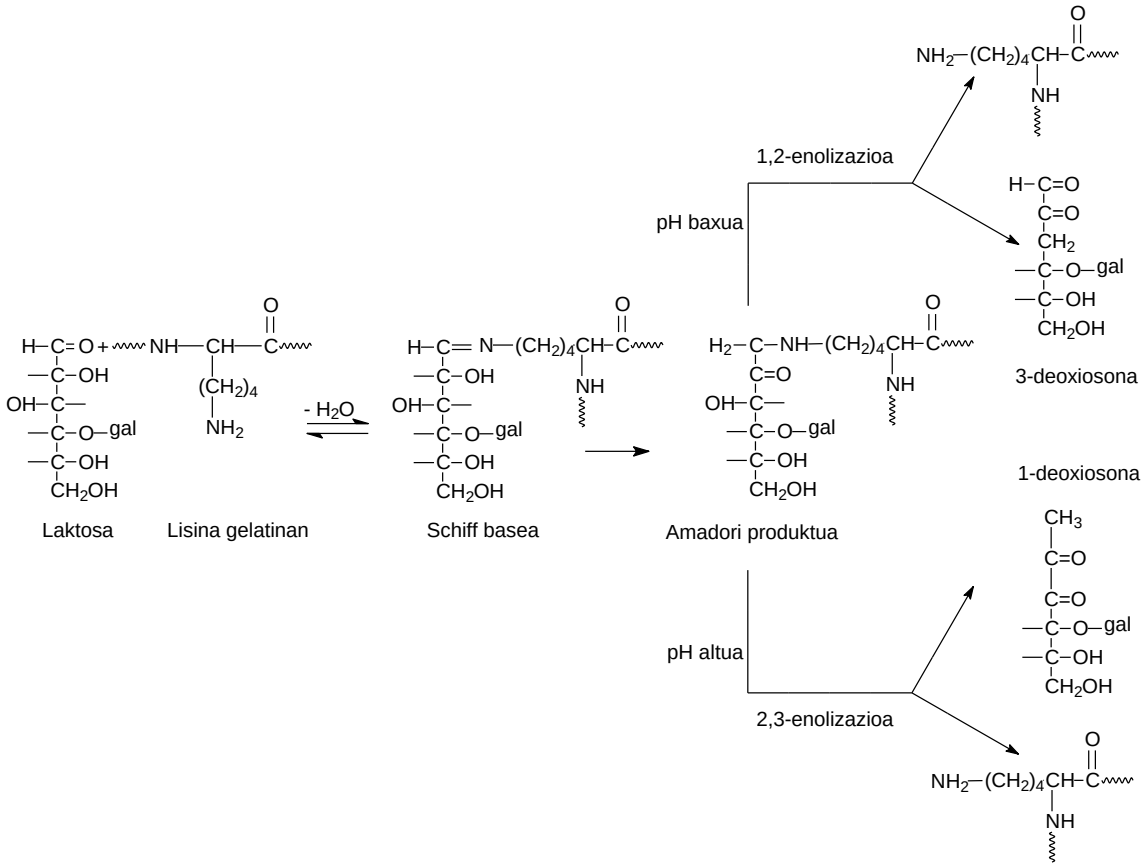

4.1 eskema Maillard erreakzioaren lehenengo etapa eta Maillard erreakzioaren etapa aurreratuan Amadori produktuaren deskonposaketa bideak pH baldintza ezberdinetan (gal=galaktosa).

Aurretik aipatu moduan, saretze erreakzioaren hedapena Maillard erreakzioan eratutako produktuen bitartez aztertu daiteke. Horien artean, pentosidina Amadori konposatuaren eraketaren ondotik sortzen den lehenengo produktu fluoreszente egonkorra da eta beraz, Maillard erreakzioaren hedapenaren adierazle kimiko moduan erabili daiteke (Labuza eta Basier, 1992). Hortaz, erreakzioaren hedapena aztertzeko, 335 nm-an (pentosidinari elkartutakoa) kitzikatutako gelatinazko filmen emisio espektroak neurtu ziren. **4.3 irudia**n ikus daitekeen moduan, pentosidinari elkartutako emisio banda 410 nm-an agertu zen, beste lan batzuekin bat etorriz (Bhat et al., 2014; Morales eta Van Boekel, 1997).

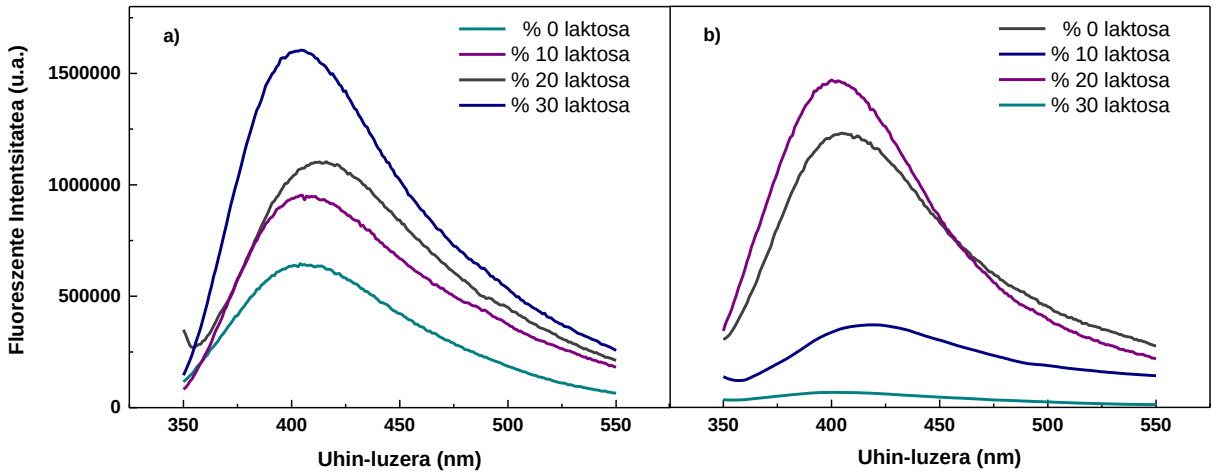

4.3 irudia a) Berezko pH-ko eta b) pH azidoko arrain gelatinazko HT filmen fluoreszentzia emisio espektroak, laktosa kantitatearen funtziopean.

Berezko pH-an (**4.3a irudia**), banden intentsitateak laktosa kantitatearen igoerarekin handitu ziren, pentosidinaren eraketa eta beraz, erreakzioaren hedapena azukre kantitatearekin handitzen zela adieraziz. Laktosa gabeko filmetan ere emisio banda ikusi zen eta honek, gelatinazko amina taldeekin erreakzionatu zezaketen gelatina lehengaian egon zitezkeen azukre hondarren presentzia adierazten zuen (Duconseille et al., 2015). Beste aldetik, pH azidoan prestaturiko filmen emisio espektroek (**4.3b irudia**) laktosa kantitatearen handitzearekin banden intentsitatea

jaisten zela erakutsi zuten, kolorearen analisian lortutako emaitzekin bat etorriz. Izan ere, kolore ezberdintasun handiena % 10-eko laktosadun filmetan ikusi baitzen.

Glikazioak pentosidina konposatu disolbagarriaren eraketa arte aurrera egin zuenez, pH azidoan sorturiko filmak guztiz disolbagarriak ziren. Hala ere, berezko pH-an prestaturiko filmen disolbagarritasuna laktosaren gehikuntzarekin nabarmenki ($P < 0,05$) gutxitu zen (**4.1 taula**).

4.1 taula pH azidoan eta berezko pH-an prestatutako arrain gelatinazko HT filmen propietate fisiko-kimikoak eta hesi-propietateak.

Laktosa (%)	TSM (%) Berezko pH-a	WCA (º) Berezko pH-a	WCA (º) pH azidoa
0	$75,0 \pm 5,4^{a}$	85 ± 1^{b}	83 ± 3^{b}
10	$57,3 \pm 9,8^{b}$	101 ± 2^{d}	99 ± 1^{c}
20	$26,1 \pm 0,5^{c}$	101 ± 1^{d}	101 ± 1^{d}
30	$31,8 \pm 0,9^{c}$	100 ± 2^{d}	109 ± 1^{f}

[a-f] Zutabe berean letra bera duten bi balio ez dira esanguratsuki ($P > 0,05$) desberdinak, Tukey-ren froga anizkoitzaren arabera.

Emaitza hauek, kolorearen neurketekin eta UV argiaren espektroekin bat egin zuten, laktosa edukiaren handitzearekin kolorazio handiagoa eta UV argiarekiko xurgatze hobea lortu zelako, hurrenez hurren. Honek, melanoidina konposatu disolbaezinen eraketarainoko glikazioaren hedapen handiagoa adierazi zuen. Emaitza hauek, pH-aren igoerarekin saretze erreakzioa gehiago hedatu zela erakutsi zuten (Wihodo eta Moraru, 2013). Gainera, % 20 laktosadun filmetan disolbagarritasun balio txikienak % 26 ingurura iritsi ziren. Hala ere, laktosaren balioa % 30era igotzerakoan, ez ziren TSM balioak txikitu; honek, saretze erreakzio maximoa eta disolbagarritasun minimoa lortzeko laktosa kantitate zehatz bat zegoela iradoki zuen. Harrezkero, laktosa kantitate handiagoek ez zuten saretze erreakzioa gehiago sustatuko. Emaitza hauek, pH-ak eta laktosa kantitateak saretzearen hedapenean eragin zutela adierazi zuten. Konposatu aktiboen askapenerako gelatinazko filmen erabilera kontuan hartuz, lorturiko emaitzek pH-a eta laktosa edukia kontrolatuz filmen disolbagarritasuna eta beraz, elikagaien paketatzerako film aktiboetatik edota apositu farmazeutikoak diren

filmetatik konposatu aktiboen askatzea kontrolatu zitekeela iradoki zuten (Santoro, Tatara eta Mikos, 2014).

Filmen gainazalen izaera hidrofiloa edo hidrofoboa determinatzeko, urarekiko kontaktu angelua (WCA) neurtu zen. **4.1 taula**n ikus daitekeen bezala, bi pH-en kasuan laktosaren gehikuntzak WCA-ren balioen handitzea eragin zuen. Berezko pH-an prestaturiko filmek WCA-ren balio berdintsuak ($P > 0,05$) erakutsi zituzten, laktosa kantitatea kontuan hartu gabe. Hala ere, pH azidoan prestatutako filmen WCA-ren balioak laktosa edukiarekin handitu ($P < 0,05$) ziren, saretzearen hedapenaren funtziopean zeuden taldeen gainazaleranzko orientazio ezberdinengatik. WCA-ren balio baxuek (< 90º) bustitze ahalmen handia edo izaera hidrofiloa adierazten dutenez eta aldiz, WCA-ren balio altuek (> 90º) bustitze ahalmen txikia edo izaera hidrofoboa adierazten dutenez (Yuan eta Lee, 2013), laktosadun filmek izaera hidrofoboa erakutsi zutela ondorioztatu zen.

4.2.2 Propietate mekanikoak

Propietate mekanikoak aztertu ziren eta trakzio erresistentzia (TS) eta haustura elongazioa (EB) neurtu ziren (**4.2 taula**).

4.2 taula Berezko pH-an eta pH azidoan prestatutako arrain gelatinazko HT filmen propietate mekanikoak.

Laktosa (%)	TS (MPa) Berezko pH-a	TS (MPa) pH azidoa	EB (%) Berezko pH-a	EB (%) pH azidoa
0	51 ± 1^{c}	49 ± 2^{c}	$3,3 \pm 0,1^{ab}$	$2,5 \pm 0,2^{a}$
10	62 ± 2^{d}	43 ± 3^{c}	$3,1 \pm 0,7^{ab}$	$2,2 \pm 0,3^{a}$
20	54 ± 4^{cd}	30 ± 1^{ab}	$2,8 \pm 0,6^{ab}$	$3,3 \pm 0,6^{ab}$
30	54 ± 3^{cd}	28 ± 2^{ab}	$3,3 \pm 0,5^{ab}$	$3,6 \pm 0,8^{ab}$

[a-d] Zutabe berean letra bera duten bi balio ez dira esanguratsuki ($P > 0,05$) desberdinak, Tukey-ren froga anizkoitzaren arabera.

pH azidoan prestatutako filmetan, laktosaren gehitzearekin TS balioak txikitu ($P < 0,05$) eta EB balioak handitu ($P < 0,05$) ziren. Emaitza hauekin, pH honetan emandako saretze erreakzioaren hedapen txikiarekin erreakzionatu gabeko laktosak plastifikatzaile moduan jokatu zuela azaldu zitekeen (Bhat eta Karim, 2014). Aldiz,

berezko pH-an prestaturiko filmetan, laktosaren gehikuntza bidez emandako saretzeak ez zituen EB balioak nabarmenki aldatu ($P > 0,05$) baina TS balioak handitu zituen ($P < 0,05$), 50 MPa-etako balioak lortuz.

4.2.3 Egitura-karakterizazioa

Gelatinazko filmen bigarren egitura amida I eta II profilen egokitze kurben bidez aztertu daiteke (Dave et al., 2000). **4.4 irudia**n ikusi daitekeen moduan, gelatinaren xurgatze banda nagusiak 1630 cm^{-1}-eko C=O loturaren luzatzearekin (amida I), 1530 cm^{-1}-eko N-H loturaren tolestearekin (amida II) eta 1230 cm^{-1}-eko C-N loturaren luzatzearekin (amida III) erlazionatu ziren (Etxabide et al., 2015a). Laktosari elkartutako xurgatze banda nagusiak 1180 eta 953 cm^{-1} artean kotatu ziren; 979 eta 987 cm^{-1}-eko bandak C-C loturaren bibrazioari egokitu zitzaizkion, eta 1034 cm^{-1}-eko banda CH_2-OH taldearen C-O loturaren bibrazioekin erlazionatu zen (Wang et al., 2013). Azkenik, glizerolaren banda nagusiak, 850, 940 eta 1000 cm^{-1}-eko C-C loturen eta 1050 eta 1100 cm^{-1}-eko C-O loturen bibrazioekin erlazionatu ziren (Basu et al., 2011).

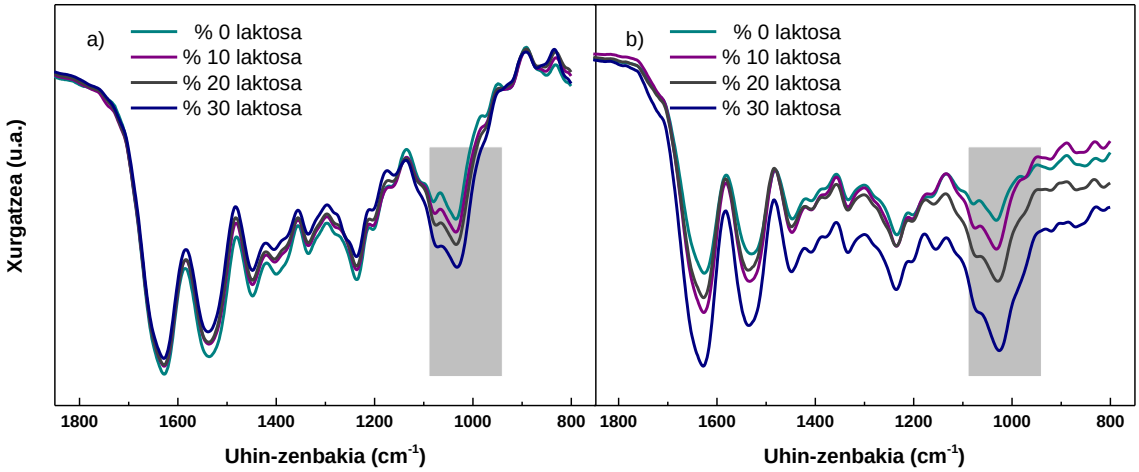

4.4 irudia a) Berezko pH-an eta b) pH azidoan prestaturiko arrain gelatinazko HT filmen FTIR espektroak, laktosa kantitatearen funtziopean.

4.4a irudian ikus daitekeen moduan eta pH azidoan prestatutako filmekin alderatuz gero (**4.4b irudia**), berezko pH-an prestaturiko filmetan laktosa kantitatea handitu zen heinean, 1100-1000 cm^{-1}-eko tartean kokaturiko bi bandek banda zabalago bat sortu zutela ikusi zen.

Aurretik aipatu moduan, aldaketa hauek pH-ak Maillard erreakzioaren hedapenean duen eraginarekin erlazionatuta egon zitezkeen. Gainera, **4.3 taula**n ikusten den bezala, amida II bandaren posizioan ere laktosa kantitateak eta pH-ak eragin zuten. Aipatzekoa da, laktosaren gehikuntzarekin amida I bandaren posizioa ez zela aldatu, amida II banda uhin-luzera txikiagoetara pittin bat mugitu zen bitartean, pH-a kontuan hartu gabe.

4.3 taula Amida I eta II banden posizioak laktosa kantitatearen eta pH-aren funtziopean.

	pH azidoa			Berezko pH-a		
Laktosa (%)	**Amida I (cm^{-1})**	**Amida II (cm^{-1})**	**Amida I/II**	**Amida I (cm^{-1})**	**Amida II (cm^{-1})**	**Amida I/II**
0	1631	1528	1,99	1632	1529	1,82
10	1631	1531	2,03	1632	1534	1,89
20	1632	1535	2,09	1632	1536	1,94
30	1632	1537	2,18	1632	1538	2,04

Gelatinaren egituran emandako aldaketak analisi kuantitatibo batekin erlazionatzeko, amida I-ari eta II-ari esleitutako bandak egokitze-kurba prozesu bidez sakonago aztertu ziren. Alde batetik, gelatinaren amida I profilak bi konposatu nagusi zituen, β-xafla (1630-1615 cm^{-1} eta 1700-1680 cm^{-1}) eta α-helize (1650 cm^{-1}) egiturei elkartuak egon zitezkeenak. Beste aldetik, amida II profilak lau konposatu nagusi zituen, β-xafla (1500 cm^{-1}), zorizko kiribil (1509-1523 cm^{-1}), α-helize (1540-1556 cm^{-1}) eta β-bira (1565 cm^{-1}) egiturei elkartuak egon zitezkeenak (Hu et al., 2010; Lefevre eta Subirade, 2000).

4.4 taulan ikusi daitekeen moduan, α-helize egiturak ehunekorik handiena erakutsi zuen. pH azidoan prestatutako filmen kasuan, laktosaren gehikuntzarengatik

gelatinaren bigarren egituran emandako aldaketak ez ziren nabariak izan, disolbagarritasun analisian lortutako emaitzekin bat etorriz. Hau, pH baxuan ematen den proteinaren desnaturalizazio baxuagatik saretze erreakziorako talde erreaktibo gutxiago egotearekin erlazionatu zitekeen. Hala ere, berezko pH-an prestaturiko filmetan laktosa kantitatea handitu heinean, β-xaflaren azalera pittin bat handitu eta α-helizearen azalera pixka bat txikitu ziren. Emaitza hauek, aurretik erakutsitako **4.1 taula**ko disolbagarritasunaren aldaketekin bat zetozen.

4.4 taula Amida I-aren egokitze-kurbaren azalera (%), laktosa kantitatearen eta pH-aren funtziopean.

Amida I	**pH azidoa**			**Berezko pH-a**		
Laktosa (%)	**β-xafla 1622 cm^{-1}**	**α-helizea 1650 cm^{-1}**	**β-xafla 1685 cm^{-1}**	**β-xafla 1622 cm^{-1}**	**α-helizea 1650 cm^{-1}**	**β-xafla 1685 cm^{-1}**
0	37,75	60,01	2,24	44,95	48,43	6,62
10	37,27	59,87	2,86	45,46	47,47	7,07
20	36,93	60,49	2,58	45,45	47,51	7,04
30	38,44	58,81	2,75	45,16	47,05	7,79

Amida II bandari dagokionez (**4.5 taula**), pH azidoan prestaturiko filmetan laktosa kantitatea handitu zenean, β-xafla eta α-helize egiturak txikitu ziren eta β-bira nahiz zorizko kiribil egiturak ordea handitu ziren. Hala ere, pH-aren handitzeak β-xaflaren azalera txikitzea eta α-helizearen egitura handitzea eragin zituen, β-bira nahiz zorizko kiribil egiturak ia-ia aldatu ez ziren bitartean.

4.5 taula Amida II-aren egokitze-kurbaren azalera (%), laktosa kantitatearen eta pH-aren funtziopean

Amida II	**pH azidoa**				**Berezko pH-a**			
Laktosa (%)	**β-xafla**	**Zorizko kiribila**	**α-helizea**	**β-bira**	**β-xafla**	**Zorizko kiribila**	**α-helizea**	**β-bira**
0	5,05	34,52	55,31	5,12	6,19	32,24	54,34	7,23
10	4,89	36,21	52,68	6,22	5,39	31,95	55,83	6,83
20	3,64	37,86	51,51	6,99	4,01	31,58	57,13	7,28
30	1,75	40,15	50,76	7,34	3,73	31,32	57,09	7,86

Proteinen egitura sekundarioko aldaketak kateen arteko interakzioekin hertsiki erlazionatuta daudenez, badirudi pH azidoan emandako Maillard erreakzioaren

hedapen txikiak kateen mugimendua sustatu zuela, ziur asko hidrogeno zubizko bezalako lotura fisikoengatik, proteinaren bigarren egituran aldaketak eraginez. Berezko pH-an prestatutako filmetan ordea, saretze erreakzioaren hedapena handiagoa zenez, kateen mugimendua mugatua zegoen eta beraz, bigarren egiturako aldaketak ez ziren nabarmenak izan.

Berotutako gelatinazko filmen egitura-aldaketak sakonago aztertzeko, XRD analisia burutu zen (**4.5 irudia**). Eredu guztiek bi difrakzio banda erakutsi zituzten, 21º-etako banda, gelatinaren kristalinitatearekin erlazionatu zena eta 7,4º-tako banda, kolageno natiboaren helize hirukoitzaren hondarrari egokitu zitzaiona (Schmidt, Giacomelli, eta Soldi, 2005).

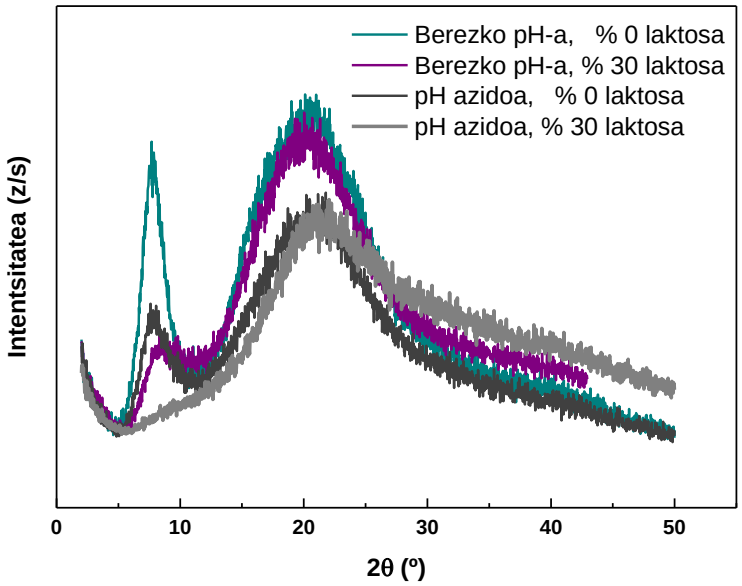

4.5 irudia Arrain gelatinazko HT filmen XRD ereduak, laktosa kantitatearen eta pH-aren funtziopean.

Proteinaren hirugarren egituran pH-aren eragina aztertzerakoan, emaitzek, proteinaren kateetako molekulen arteko interakzioengatik pH azidoan kolageno natiboaren helize hirukoitzaren birtolestea eta gelatinaren egitura kristalinoaren antolaketa oztopatua egon zitekeela erakutsi zuten. Laktosaren gehikuntzari

dagokionez, aurretik aipatu moduan, geroz eta pH baxuagoa izan orduan eta gelatinaren desnaturalizazio baxuagoa eman zen eta beraz saretze maila txikiagoa lortu zen. Horregatik, filmean erreakzionatu gabeko laktosa kantitate handiagoa soberan geratu zen eta honek, helize hirukoitzaren birtolestea eta gelatinaren egitura kristalinoaren berrantolaketa oztopatu zitzakeen.

Saretze erreakzioaren eragina filmen egitura-aldaketetan sakonki aztertzeko, SEM analisia burutu zen eta filmen zeharkako sekzioen irudiak laktosa kantitatearen funtziopean **4.6 irudia**n erakusten dira.

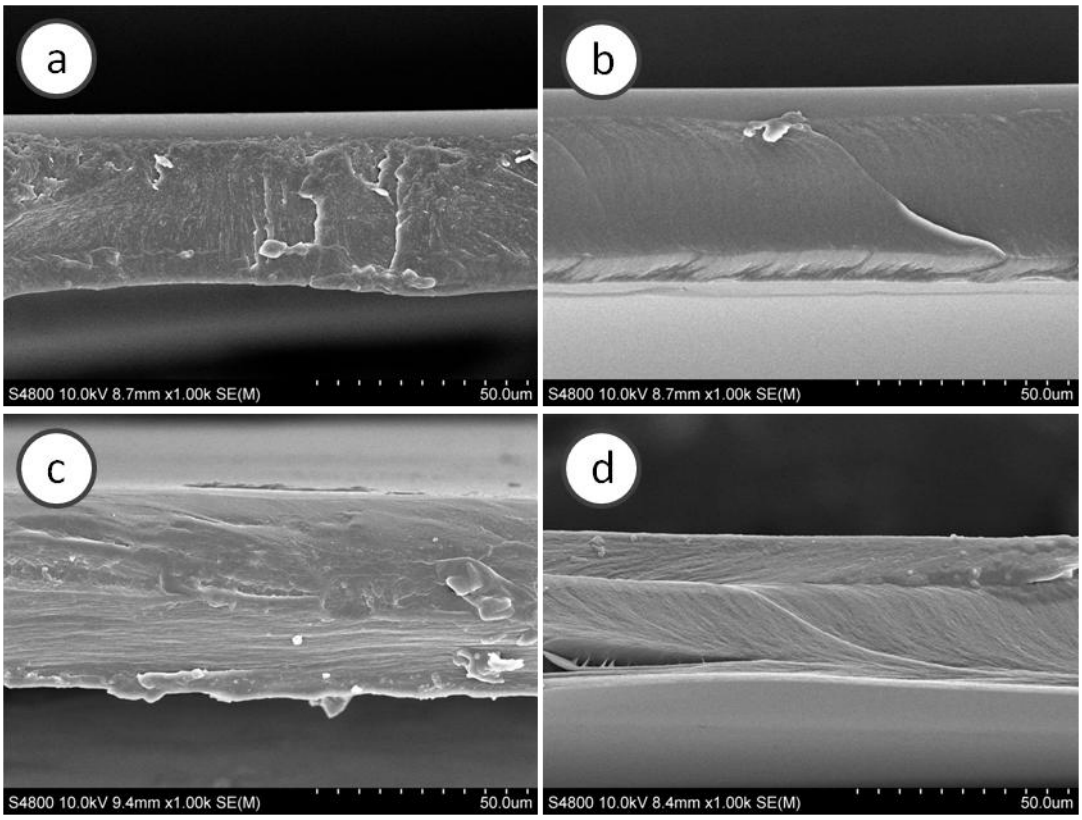

4.6 irudia pH azidoan prestatutako a) % 0 eta b) % 30 laktosadun arrain gelatinazko HT filmen eta berezko pH-an prestatutako c) % 0 eta % 30 laktosadun arrain gelatinazko HT filmen zeharkako sekzioko SEM-ren irudiak.

Zeharkako sekzioko SEM-ren irudiek laktosa gabeko gelatinazko filmek gainazal latza zutela erakutsi zuten eta hau, saretu gabeko laginetan geratutako kolageno zuntzengatik izan zen (Wang et al., 2015), XRD analisian erakutsi zen moduan. Hala ere, laktosa gehitu zenean helize hirukoitzaren kantitatea gutxitu zenez,

zuntz egitura ez zen hain nabaria izan (Liu et al., 2016), **4.5 irudia**n ikusi zen moduan. Ondorioz, behin erreakzioa eman zenean (**4.6b irudia** eta **4.6d irudia**), zeharkako sekzioko SEM-ren irudiek egituraren aldaketa nabaria erakutsi zuten. Izan ere, % 30 laktosadun filmetan erdigune leunagoa eta homogeneoagoa ikusi zen. Porositatearen analisiek, 0,01 eta 0,001 µm bitarteko erradiodun poro oso fineko egitura erakutsi zuten, % 8tik % 12ra bitarteko poro irekiekin.

4.3 Ondorioak

Egokitutako propietate funtzionalak lortzeko, gelatina eta laktosaren arteko saretze erreakzioaren hedapena filma eratzeko baldintzen bidez kontrolatu daiteke. pH azidoan, pentosidina eratzerakoan erreakzioaren inhibizioa eman zen, UV-vis espektroskopia bidez ikusi zen bezala, saretzearen hedapena txikiagoa izanik eta ondorioz, guztiz disolbagarriak ziren filmak lortu ziren. Emaitza hauek, film hauen erabilera dosifikazio solidoetan nabarmentzen dute. Izan ere, film polimeriko finez (10-100 µm) geruzatutako pastillak egin ohi dira sendagaiaren askatze-abiadura aldatzeko eta honen egonkortasuna fluxu gastrikoetan hobetzeko. Bestalde, saretze erreakzioak pH handiagoan aurrera egin zuen, kateen mugimendu txikiagoko, urarekiko erresistentzia nahiz UV-vis babes handiagoko, eta 50 MP baino trakzio erresistentzia balio handiagoko filmak lortuz. Azken film hauek, konposatu aktiboa denbora luzeagoetan askatua izateko etengabeko askatze sistemetan erabili daitezke, hala nola, paketatze aktiboetan. Kasu guztietan, lan honetan prestatutako laktosa bidez eraldatutako filmak homogeneoak, gardenak, hidrofoboak eta pororik gabekoak izan ziren.

5 Saretze bidezko gelatinazko filmen hobekuntza

5.1 Laburpena

Maillard erreakzioa, saretzea emateko bidea izan daiteke baina 4. kapituluan erakutsi den bezala, faktore asko daude nabarmenki saretzearen eraketan eragiten dutenak. Horien artean, tenperaturak, berokuntza denborak, eta pH-ak ezinbesteko papera jokatzen dutela uste da. Van Boekel-en (1998) arabera, Maillard erreakzioaren abiadura baldintza basikoetan nabarmenki handitzen da eta orduan, faktore honek nabariki Maillard erreakzioaren garapenean eta filmen propietate funtzionaletan eragiten du. Beraz, kapitulu honen helburua laktosa kantitate ezberdineko gelatinazko filmak baldintza basikoan prestatzea izan zen, propietate optikoengan, mekanikoengan eta hesi-propietateengan laktosa bidezko saretzearen eragina hasierako konposizioaren arabera aztertzeko, eta FTIR eta UV espektroskopia eta disolbagarritasun azterketa bidez ikusitako aldaketak neurtutako propietateekin erlazionatzeko.

5.2 Emaitzak eta eztabaida

5.2.1 Propietate fisiko-kimikoak

Filmek beraien osotasuna mantentzeko duten gaitasuna aztertzeko, hezetasun edukiaren (MC) eta disolbaturiko masa totalaren (TSM) balioak ezagutzea ezinbestekoa da. **5.1 taula**n ikusten den bezala, % 10 laktosa gehitu zenean, MC-ren balioek ezberdintasun hutsala ($P > 0,05$) erakutsi zuten, laktosa kantitate handiagoko filmek handitze esanguratsua ($P < 0,05$) erakutsi zuten bitartean. Disolbagarritasunari dagokionez, aipatzekoa da NH filmak guztiz disolbagarriak zirela, Maillard erreakzioa sustatzeko tenperaturaren eragina erakutsiz, aurreko lan batean azaldu zen moduan (Guerrero et al., 2012). HT filmen kasuan, laktosa gehitzerakoan TSM-ren balioen gutxitze nabaria ($P < 0,05$) ikusi zen. Literaturan, saretutako gelatinazko molekuletatik agregatuak sortzen dituzten pisu molekular handiko konposatuak eratu daitezkeela azaldu da (Chiou et al., 2006; Muyonga, Cole, eta Duodu, 2004). Filmaren disolbagarritasuna saretze mailaren handitzearekin txikitu zenez, ikusitako portaera

Maillard erreakzio bidez emandako gelatina eta laktosaren arteko erreakzio kimikoarengatik izan zitekeela ondorioztatu zen. % 20 laktosa gehitu zenean, TSM % 12ko balio minimora iritsi zen, laktosa eduki handiagoak erreakzioa gehiago bultzatzen ez zuela adierazteaz gain, balio horrek nagusiki glizerolari zegokiola iradoki zuen, glizerolak hidrogeno zubizko interakzio bidez gelatinarekin elkar eragiten duelako (Guerrero et al., 2011b).

5.1 taula Ez beroturiko (NH) eta beroturiko (HT) arrain gelatinazko filmen lodieraren, hezetasun edukiaren (MC) eta disolbaturiko masa totalaren (MTS) balioak, laktosa kantitatearen funtziopean. ([I]Edozein laktosa kontzentraziotan, NH eta HT filmen lodierak berdinak ziren; [II]HT filmen hezetasun edukia 0 da (erakutsi gabeko datuak); [III]NH filmak guztiz disolbagarriak ziren).

Laktosa (%)	Lodiera[I] (mm)	MC[II] (%)	TSM[III](%)
	NH/HT	NH	HT
0	0,043 ± 0,002[a]	10,669 ± 1,229[a]	77,384 ± 6,334[b]
10	0,044 ± 0,002[a]	10,189 ± 3,506[a]	16,063 ± 2,376[a]
20	0,054 ± 0,005[b]	14,497 ± 0,642[ab]	12,989 ± 4,013[a]
30	0,069 ± 0,003[c]	16,426 ± 2,005[b]	12,846 ± 3,262[a]

[a-c] Zutabe berean letra bera duten bi balio ez dira esanguratsuki (P > 0,05) desberdinak, Tukey-ren froga anizkoitzaren arabera.

Gainazaleko ezaugarriak aztertzeko, distira neurketak egin ziren eta emaitzak **5.2 taula**n aurkeztu dira. Laktosarik gabeko filmetan izan ezik, NH filmek HT filmek baino distira handiagoa eta beraz, gainazal leunagoa erakutsi zuten. Hau, gelatina eta glizerolaren arteko interakzioetan tenperaturak eragin zuelako izan zitekeen, gainazal leunagoa erakutsiz. Laktosadun filmei dagokionez, azukre amorfo higroskopikoek hezetasuna xurgatu dezakete, plastifikatzaile moduan jokatuz eta azukreei kristalizatzen utziz (Sormoli, Das, eta Landgrish, 2013). NH filmen kasuan aldiz, laktosak ez zuen gelatinarekin erreakzionatu, TSM-ren emaitzetan ondorioztatu zen moduan. Hortaz, laktosak hezetasuna xurgatu zezakeen, laktosa kantitatearen handitzearekin MC-ren balioek gora egin zutelako, eta kristalizatu zitekeen, filmen distira handituz ($P < 0,05$). Gainazal kristalinoek distira balio handiak erakusten dituztenez (Rindlav-Westling et al., 1998), NH filmek distira handiagoa erakutsi zuten.

HT filmei dagokionez, laktosaren eta gelatinaren arteko erreakzioak kristalen nukleazioa eta hazkuntza eragotzi zituen, distira balioen txikitzea ($P < 0,05$) eraginez.

5.2 taula Ez berotutako (NH) eta berotutako (HT) arrain gelatinazko filmen distira balioak, laktosa kantitatearen funtziopean.

Laktosa (%)	$Distira_{60^o}$ (DU)	
	NH	HT
0	$119,75 \pm 6,90^{c}$	$142,50 \pm 1,73^{d}$
10	$141,75 \pm 2,99^{b}$	$118,25 \pm 1,71^{c}$
20	$148,25 \pm 1,26^{b}$	$70,76 \pm 1,61^{b}$
30	$156,75 \pm 0,96^{a}$	$55,15 \pm 2,29^{a}$

$^{a-d}$ Zutabe berean letra bera duten bi balio ez dira esanguratsuki ($P > 0,05$) desberdinak, Tukey-ren froga anizkoitzaren arabera.

Kolorea ere garrantzitsua da, produktuaren itxuran eta beraz, kontsumitzailearen onargarritasunean zuzenean eragiten duelako (Monedero et al., 2009). **5.1 irudia**n erakusten den moduan, film guztiak homogeneoak eta gardenak ziren. HT filmen kasuan, kolorea laktosaren gehikuntzarekin aldatu zen, horixka bihurtuz.

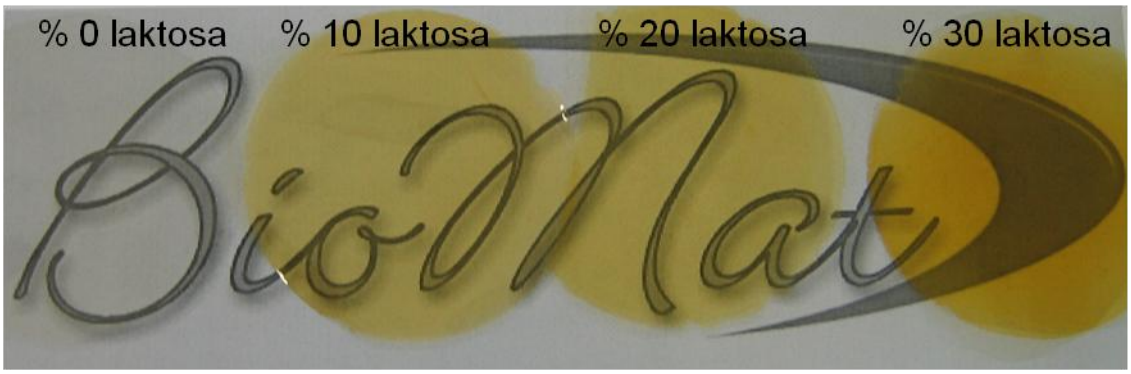

5.1 irudia Gardentasuna eta kolore ezberdintasuna berotutako (HT) arrain gelatinazko filmetan, laktosa kantitatearen funtziopean.

Kolore horixkaren garapen hau tenperatura altuetan arrain gelatinaren eta laktosaren artean emandako Maillard erreakzioarekin erlazionatu zen, eta L*, a* eta b* parametroen bidez kuantifikatu zen, **5.3 taula**n erakusten den moduan. NH filmetan, L*, a* eta b* balioek ez zuten aldaketa esanguratsurik ($P > 0,05$) erakutsi, laktosa

kantitatea kontuan hartu gabe. Hala ere, HT filmen kasuan, laktosaren gehikuntzak filmen iluntzeari egokitu zitzaion L* balioen gutxitzea ($P < 0,05$) eragin zuen eta hau, Maillard erreakzioaren etapa aurreratuan eratutako zenbait konposatuengatik izan zen. Gainera, a* eta b* balioak laktosa kantitatearekin nabarmenki ($P < 0,05$) handitu ziren, kolore hori iluna erakutsiz. Hortaz, HT filmetan kolore aldaketa totala (ΔE*) laktosa edukiarekin batera handitu zen, NH filmen erreferentziapean. Kolore aldaketak, laktosak nabarmenki saretze erreakzioaren mailan eragin zuela adierazi zuen, laktosa edukia handietan karbonilo talde kantitate gehiagoren presentziak ΔE*-ren balioen handitzean eragin zuelako.

5.3 taula Ez berotutako (NH) eta berotutako (HT) arrain gelatinazko filmen L*, a*, b* eta ΔE* balioak, laktosa kantitatearen funtziopean. HT filmen kolore aldaketa NH filmak erreferentziatzat hartuz neurtu zen.

Filma	Laktosa (%)	L*	a*	b*	ΔE*
NH	0	96,19 ± 0,25^{a}	-0,10 ± 0,03^{a}	3,01 ± 0,10^{a}	
	10	95,88 ± 0,11^{a}	-0,24 ± 0,04^{a}	3,17 ± 0,09^{a}	
	20	96,03 ± 0,07^{a}	-0,31 ± 0,02^{a}	3,34 ± 0,09^{a}	
	30	95,71 ± 0,29^{a}	- 0,43 ± 0,05^{a}	3,62 ± 0,13^{a}	
HT	0	96,12 ± 0,49^{a}	-0,81 ± 0,06^{a}	2,99 ± 0,06^{a}	0,71 ± 0,05^{a}
	10	85,66 ± 0,69^{b}	2,73 ± 0,11^{b}	36,92 ± 0,40^{b}	34,38 ± 0,41^{b}
	20	76,84 ± 0,53^{c}	14,01 ± 0,81^{c}	39,86 ± 0,48^{c}	37,33 ± 0,46^{c}
	30	47,85 ± 2,86^{d}	34,69 ± 1,71^{d}	70,99 ± 1,45^{d}	69,13 ± 1,59^{d}

$^{a-d}$ Zutabe berean letra bera duten bi balio ez dira esanguratsuki ($P > 0,05$) desberdinak, Tukey-ren froga anizkoitzaren arabera.

Maillard erreakzioak eragindako aldaketa kimikoak FTIR espektroan zenbait aldaketa uztea espero zenez, analisi hau proteinaren eta azukrearen arteko elkarrekintzak aztertzeko erabili zen eta espektroak **5.2 irudia**n erakusten dira. Ikusi daitekeen moduan, 1100-1000 cm^{-1}-eko tartean kokaturiko bi bandak banda bakar bilakatu ziren eta banda hauen intentsitatea laktosa ehunekoaren handitzearekin gehiagotu zela ikusi zen.

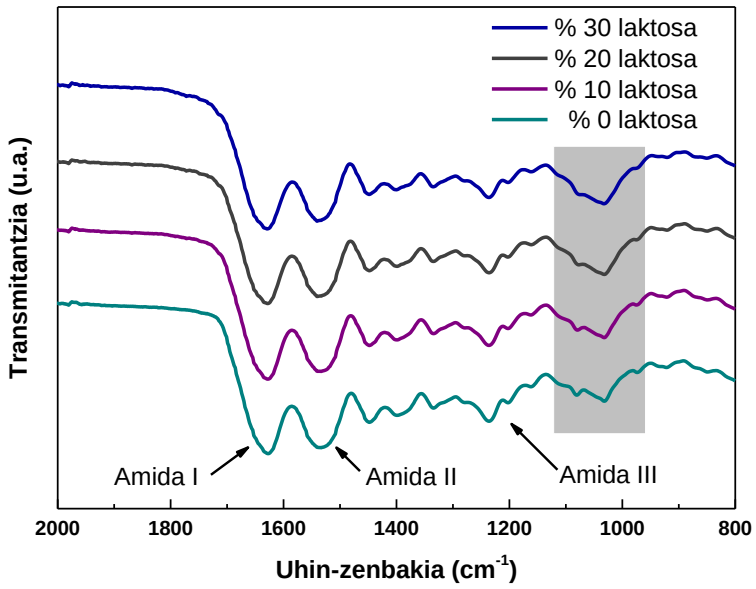

5.2 irudia Arrain gelatinazko HT filmen FTIR espektroak, laktosa edukiaren funtziopean.

Laktosa edukiaren eragina sakonkiago aztertzeko, amida I-ari egokitutako banda Maillard erreakzioagatik gelatinaren egituran emandako aldaketen analisi kuantitatiboa egiteko erabili zen. Amida I-ari dagokion banda proteinaren bigarren egituraren menpekoa denez, banda honek kate polipeptidikoaren talde polarrek hidrogeno zubizko loturen bidez sor ditzaketen interakzioei buruzko informazioa eskaini dezake.

Argi eta garbi, proteinaren destolestea, berezko proteinaren 1650 cm^{-1}-eko banda nagusiko, α-helize/nahaspilatua egiturari esleitua, eta 1630-1615 cm^{-1} eta 1700-1680 cm^{-1} eremuetako banden, β-xaflei egokitutakoa (Hu et al., 2010; Lefevre eta Subirade, 2000), intentsitateen aldaketekin karakterizatu zen, **5.3 irudia**n erakusten den moduan.

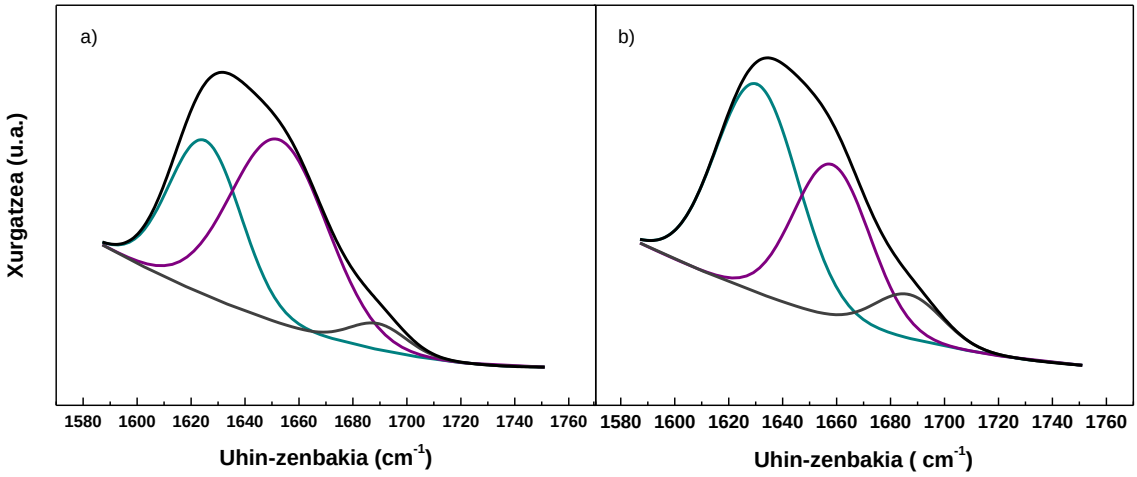

5.3 irudia Amida I bandaren egokitze kurbaren espektroa a) ez berotutako (NH) eta b) berotutako (HT) % 20 laktosadun filmentzat.

Egokitze kurba bidez zehaztutako egitura bakoitza kontsideratu zen eta egindako analisi kuantitatiboa **5.4 taula**n erakusten da.

5.4 taula Ez berotutako (NH) eta berotutako (HT) arrain gelatinazko filmen amida I bandaren egokitze kurbaren emaitzen ehunekoak (%), laktosa edukiaren funtziopean.

Laktosa (%)	NH filmen amida I-aren azalera (%)			HT filmen amida I-aren azalera (%)		
	1625 cm^{-1}	1652 cm^{-1}	1689 cm^{-1}	1625 cm^{-1}	1652 cm^{-1}	1689 cm^{-1}
0	41,65	53,07	5,28	51,10	39,70	9,20
10	36,03	59,48	4,49	50,24	40,15	9,62
20	36,66	58,43	4,91	53,87	36,77	9,36
30	35,38	59,68	4,93	52,18	38,49	9,33

NH filmen kasuan, laktosaren gehikuntzak, honen eta gelatinaren arteko hidrogeno zubizko loturak eragin zitzakeen, proteinen kateen molekularteko interakzioak ahulduz eta α-helizearen (1652 cm^{-1}) handitzea nahiz β-xaflaren (1625 eta 1689 cm^{-1}) txikitzea eraginez. HT filmei dagokienez, β-xafla antiparalelo egituraren molekularteko eraketarengatik 1689 eta 1625 cm^{-1} banden intentsitatea handitu zen (Lefevre, Subirade, eta Pezolet, 2005) eta ondorioz, 1652 cm^{-1}-eko α-helize/nahaspilatuaren banda txikitu zen. Hedatutako β-xafla antiparaleloak agregatutako proteinetan sarritan aurkitzen dira, bereziki beroagatik desnaturalizatutako proteinetan (Susi et al., 1967). Beraz, emaitza hauek agregazioa

eman zela eta agregatu hauek neurri batean β-xaflez osatuta zeudela adierazi zuten (Quinn et al., 2003), Maillard erreakzioaren eragina gelatinaren egituran erakutsiz.

5.2.2 Hesi-propietateak

Argiarekiko babesa materialen funtsezko betekizuna da, argiak oxidazio erreakzioak eta narriadura eragin ditzakeelako (Duncan eta Chang, 2012). **5.4 irudia**n ikus daitekeen moduan, gelatinazko film guztiek UV argiarekiko babes handia erakutsi zuten 200-250 nm bitartean. Balio-tarte honetako xurgatze altua proteinetan dauden lotura peptidikoekin erlazionatu zen (Hong et al., 2014). 250-300 nm bitarteko xurgatzea berriz, kromoforoen presentziari elkartu zitzaion, arrain gelatinan ohikoak diren tirosina eta fenilalanina bezalako aminoazido aromatikoei esaterako. Proteinen alboko talde batzuek, hala nola lisinaren amino taldeek, Maillard erreakzioan parte hartzen dute, aminoazido aromatikoen proportzio erlatiboa eta UV argiaren xurgatzea 250-300 nm-ko tartean handituz.

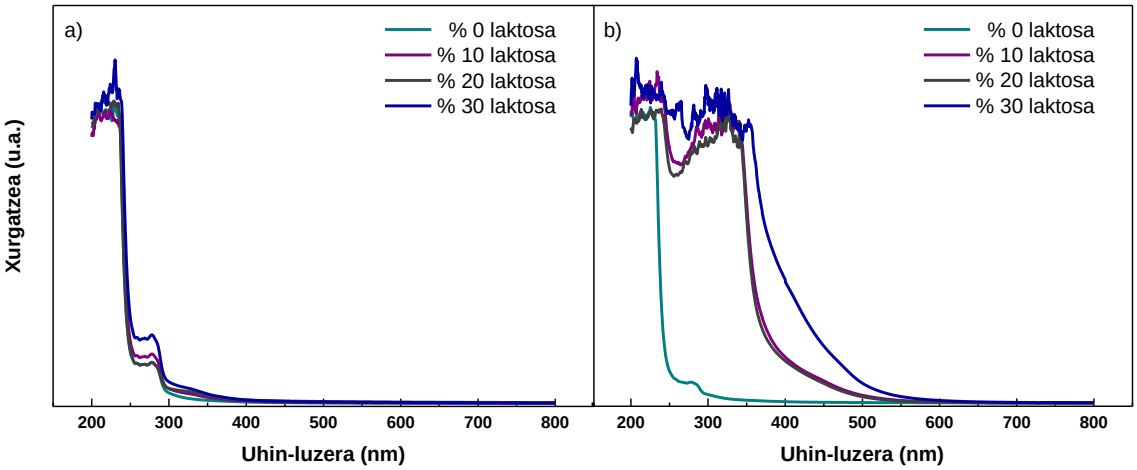

5.4 irudia a) Ez berotutako (NH) eta b) berotutako (HT) arrain gelatinazko filmen UV-vis espektroak, laktosa edukiaren funtziopean.

Gainera, **5.4b irudia**n erakusten den modan, HT filmetan 300-400 nm tartean UV ereduaren handitzea ikusi zen. Balio-tarte horietako xurgatze altuak gelatina eta laktosaren arteko erreakzioan sorturiko egitura konjugatuen presentziarekin erlazionatu

zitekeen. Glikazioaren presentzia saretzea neurtzeko maiz erabiltzen denez, 300-400 nm bitarteko xurgatze altua laktosa eta gelatinaren arteko saretze erreakzioaren adierazle izan zitekeen, goian ikusitako propietate fisiko-kimikoen aldaketetan bezala. FTIR-en emaitzen arabera, laktosa kantitatearen handitzearekin α-helize/nahaspilatuaren egituratik β-xaflaranzko saretzea garatu zen, ingurune hidrofoboetako aldarapen elektrostatikoek β-xaflen eraketa bideratu zutela adieraziz. Aipatzekoa da, UV-vis tarteko xurgatze maila altu hau aplikazio askotarako egokia den filmaren ezaugarria dela.

UV hesi-propietateez gain, filmak hezetasun ertaineko edo altuko baldintzetan erabiliak izateko asmoa dagoenean, hauek urarekiko propietate erresistenteak erakustea ezinbestekoa da. Urarekiko erresistentzia urarekiko kontaktu angelua (WCA) neurtuz aztertu daiteke, honek filmaren gainazalean ur tantaren azkeneko egoera adierazten duelako eta beraz, gainazalaren bustitze ahalmena definitzen du. Gainazalaren bustitze ahalmenean laktosaren eta tenperaturaren eragina aztertzeko, WCA balioak neurtu ziren eta hauek **5.5 taula**n erakusten dira.

5.5 taula Ez berotutako (NH) eta berotutako (HT) arrain gelatinazko filmen uraren kontaktu-angeluaren (WCA) eta ur lurrunaren iragazkortasunaren (WVP) balioak, laktosa edukiaren funtziopean.

Filma	Laktosa (%)	WCA (°)	WVP 10^{12} (g cm^{-1} s^{-1} Pa^{-1})
NH	0	88,61 ± 3,36^{a}	1,81 ± 0,16^{ab}
	10	107,53 ± 1,17^{b}	1,66 ± 0,11^{a}
	20	117,65 ± 0,96^{c}	2,00 ± 0,29^{ab}
	30	114,41 ± 2,41^{c}	2,15 ± 0,11^{b}
HT	0	91,13 ± 1,58^{a}	1,90 ± 0,18^{ab}
	10	104,99 ± 2,32^{b}	1,69 ± 0,09^{a}
	20	113,13 ± 0,37^{c}	1,82 ± 0,06^{ab}
	30	112,42 ± 2,35^{c}	2,18 ± 0,09^{b}

$^{a-c}$ Zutabe berean letra bera duten bi balio ez dira esanguratsuki ($P > 0,05$) desberdinak, Tukey-ren froga anizkoitzaren arabera.

Laktosa gehitu zenean, NH eta HT filmen WCA-ren balioak handitu ($P < 0,05$) ziren. NH filmen kasuan, aldaketa hau gelatina eta laktosaren arteko hidrogeno

zubizko interakzioekin erlazionatzeaz gain, filmaren gainazalerantz bideratutako talde hidrofoboen agerketarekin ere lotu zitekeen (Jayasundera et al., 2009), FTIR bidez lotura hauek gelatinaren egituran aldaketak eragin zituztela erakutsi zen bezala. HT filmetan berriz, gelatina eta laktosaren arteko Maillard erreakzioaren saretzeak, talde polarren edukia txikitu zuen eta honek filmen izaera hidrofoboa sendotzea eragin zuen. Hala ere, tenperaturaren eraginpean aldaketa hutsalak ($P > 0,05$) ikusi ziren konposizio berdineko laginetan, talde ez-polarrak gainazalerantz zuzentzeko joera zutela adieraziz eta hortaz, film guztiek 90º baino WCA-ren balio handiagoak erakutsi zituzten, filmak hidrofoboak zirela kontsideratuz (Karbowiak et al., 2006). Gainera, ur lurrunarekiko iragazkortasunaren (WVP) balioak neurtu ziren eta hauek **5.5 taula**n aurkeztu dira. Ikusi daitekeen moduan, film guztien WVP-en balioak antzekoak ziren eta ez laktosak ezta tenperaturak ere ez zituzten WVP-ren balioetan aldaketa nabariak eragin ($P > 0,05$). WVP bi pausutako prozesua denez, hau da, ur lurrunaren sortzioa eta ur lurrunaren difusioa, WCA-ren balioen handitzea proteinaren egitura aldaketekin orekatu zela zirudien, FTIR analisi bidez ikusi zen bezala, difusioren urratsarentzat mesedegarri izanik.

5.2.3 Propietate mekanikoak

Filmak erabiltzerakoan beraien osotasuna mantendu dezaten, orokorrean sendotasun eta malgutasun mekanikoak beharrezkoak dira. **5.6 taula**n arrain gelatinan oinarritutako filmen propietate mekanikoak erakusten dira. Ikusi daitekeen moduan, trakzio erresistentzien (TS) eta haustura elongazioen (EB) balioek, laktosa gehitzerakoan edota filmak berotzerakoan ez zuten aldaketa nabarmenik ($P > 0,05$) erakutsi. TS-ren balioak, 50 MPa ingurukoak, behi gelatinan oinarritutako filmen balioak baino handiagoak ziren (Nur Hanani, Roos, eta Kerry, 2012; Nur Hanani et al., 2012; Mu et al., 2012). Plastifikatzailearen gehikuntzak, normalean, EB-ren balioak handitzen ditu baina aldiz, TS-ren balioen txikitzea eragiten du (Haq, Hasnain, eta

Azam, 2014); lan honetan erabili zen glizerolaren eduki txikiak lorturiko TS-ren balio handiak azaldu zitzakeen.

5.6 taula Ez berotutako (NH) eta berotutako (HT) arrain gelatinazko filmen trakzio erresistentziaren (TS) eta haustura elongazioaren (EB) balioak, laktosa edukiaren funtziopean.

Filma	Laktosa (%)	TS (MPa)	EB (%)
NT	0	52,39 ± 3,16[a]	2,88 ± 0,68[a]
	10	54,19 ± 6,19[a]	2,57 ± 0,35[a]
	20	52,14 ± 4,95[a]	2,31 ± 0,37[a]
	30	54,28 ± 4,41[a]	2,56 ± 0,35[a]
HT	0	50,63 ± 4,01[a]	2,82 ± 0,68[a]
	10	45,40 ± 5,06[a]	2,54 ± 0,32[a]
	20	44,48 ± 2,78[a]	2,94 ± 0,21[a]
	30	43,76 ± 7,53[a]	2,12 ± 0,42[a]

[a] Zutabe berean letra bera duten bi balio ez dira esanguratsuki (P > 0,05) desberdinak, Tukey-ren froga anizkoitzaren arabera.

5.3 Ondorioak

Laktosaren gehikuntzak proteinaren egituran aldaketak sortu zituen, filmen izaera hidrofoboa hobetzeaz gain, hauen disolbagarritasuna nabarmenki txikituz. Gainera, berokuntzak, Maillard erreakzio ez-entzimatikoaren bidez, azukrearen eta proteinaren arteko glikazioa sustatu zuen. Erreakzio honek, proteinaren α-helizetik β-xaflarako egitura aldatu zuen eta Maillard erreakzioko konposatuen eraketarengatik filmetan kolore horixka garatu zen. Gainera, Maillard erreakzioko produktuek UV argia xurgatu zuten, filmak janaria ontziratzeko egokiak zirela iradokiz. Izan ere ahalmen honekin, filmak elikagaien oxidazioa saihesteko eta hauen iraungitzea luzatzeko gaitasuna zutela erakutsi zuten. Film guztiek gardentasuna eta trakzio erresistentzia balio altuak mantendu zituzten, 50 MPa ingurukoak. Kapitulu honek, Maillard erreakzioa arrain gelatinazko filmen propietate funtzionalak hobetzeko aukera bideragarria dela erakusten du. Gainontzeko propietate funtzionalei kalterik egin gabe ur lurrunaren iragazkortasuna hobetzeko, Maillard erreakzioaren urratsak eta

glikazioan zehar sortutako produktuen azterketarako ikerketa gehiago egitea beharrezkoa da.

6 Maillard erreakzioaren garapena

6.1 Laburpena

Aurreko kapituluan erakutsi den bezala, gelatinaren egitura eta propietate fisikoak Maillard erreakzioaren bidez aldatu daitezke. Gainera, Maillard erreakzioan eragiten duten faktoreen kontrolak, elikagai, medikutza eta industria bezalako aplikazio zehatzetarako gelatinaren propietateak egokitzea ahalbidetzen du. Nahiz eta arrain gelatina ugaztunetatik eratorritako gelatinak ordezkatzeko nabarmenki ikertua izaten ari den, UV-vis bidezko Maillard erreakzioaren aurrerapena, fluoreszentzia bidezko glikazio aurreratuko amaierako produktuen (AGE-ren) eraketa, eta FTIR bidezko proteinaren bigarren egituraren analisia, berokuntza denboran zehar eta pH basikoan, ez dira literaturan aurretik azaldu.

Testuinguru honetan, kapitulu honen helburua Maillard erreakzioaren urratsetan eta glikazio erreakzioan zehar eratutako produktuen analisian zentratu da, saretutako gelatinazko filmen morfologian eta jarduera fisikoan laktosa kantitatearen eta berokuntza denboraren eragina aztertzearekin batera, teknikoki balio handiko produktuak garatzeko konposizio egokiena aukeratzeko.

6.2 Emaitzak eta eztabaida

Berokuntza tratamendua, industrian asko erabiltzen den prozesatze metodoa da. Honi dagokionez, proteina eta lan honetan erabilitako laktosa bezalako azukre erreduktoreen artean gertatzen den erreakzio kimiko nagusienetarikoa Maillard izenez ezaguna den arretze-prozesu ez-entzimatikoa da. Konplexutasun handia eta aldaera ugari erakusten dituzten Maillard erreakzioko produktuen (MRP-en) analisiak, ikerkuntza arlo ezberdinetako ikerlarien interesa piztu du eta hori da ikerketa honen xede nagusia.

6.2.1 Saretzearen eragina gelatinaren egitura sekundarioan

Aurreko kapituluan azaldu bezala, filmen FTIR espektro-banda garrantzitsuenak proteinaren lotura peptidikoekin erlazionatutakoak ziren (**5.2 irudia**): C=O loturaren

luzatzea 1630 cm^{-1}-ean (amida I), N-H loturaren tolestea 1530 cm^{-1}-ean (amida II) eta C-N loturaren luzatzea 1230 cm^{-1}-ean (amida III). Kapitulu honetan, α-helize/nahaspilatua eta β-xafla konformazioen bidez berokuntza denbora ezberdinetan gelatinaren bigarren egiturako aldaketak FTIR espektroskopiaz amida I banda (1600-1700 cm^{-1}) aztertuz egin zen (**6.1 irudia**).

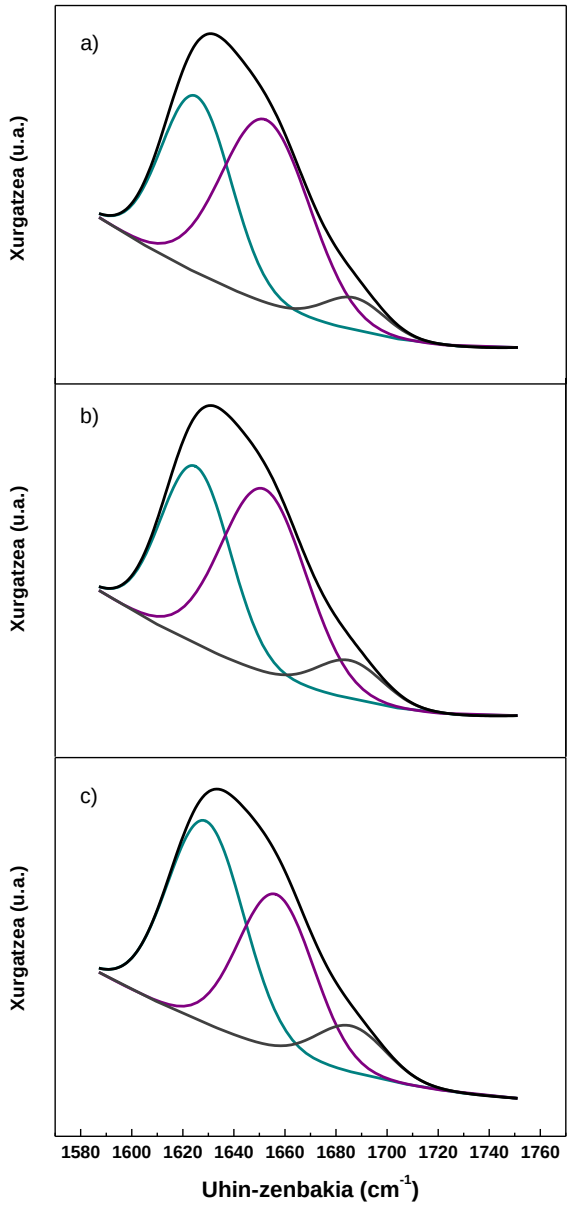

6.1 irudia % 30 laktosadun arrain gelatinazko filmen amida I bandaren egokitze kurbaren espektroak, berokuntza denboraren funtziopean: a) 0 minutu, b) 150 minutu eta c) 1440 minutu.

Laktosadun gelatinazko filmen egitura sekundarioa nagusiki α-helize/nahaspilatua (1650 cm^{-1}) eta β-xafla antiparalelo (1630-1615 cm^{-1} eta 1700-1680 cm^{-1}) konformazioez osatuta dago (Guerrero et al., 2014); azken konformazioa agregatutako proteinetan aurkitzen da oro har, batik bat berokuntza bidez desnaturalizatutako proteinetan (Susi, Timasheff, eta Stevens, 1967). Laktosa kantitateari dagokionez, % 10, % 20 (aurkeztu gabeko datuak) eta % 30 (**6.1 irudia**) laktosadun filmetan antzeko portaera ikusi zen. **6.1a irudia**n ikusi daitekeen moduan, berokuntza aurretik egiturarik nagusiena α-helizea izan zen. Hala ere, filmak 150 minutuz berotu ondoren, β-xafla egitura nagusiena izatera pasatu zen (**6.1b irudia**) eta egitura hau 1440 minutuz (24 h) filmak berotu ondoren mantendu zen, **6.1 irudia**n erakusten den bezala. Azterketa honek, laktosa eduki ezberdinekin eta berokuntza denbora ezberdinetan saretutako filmetan α-helizetik β-xaflarako aldaketa bat egon zela adierazi zuen. FTIR espektroen analisi kuantitatibo bat egiteko, **6.1 taula**n amida I bandaren ehunekoak erakusten dira.

6.1 taula Amida I bandaren egokitze kurbaren emaitzen ehunekoak, laktosa edukiaren eta berokuntza denboraren funtziopean.

		Amida I-aren azalera		
Laktosa (%)	**Denbora (min)**	**1625 cm^{-1}**	**1651 cm^{-1}**	**1688 cm^{-1}**
10	0	35,34	59,09	5,57
	90	38,54	52,23	9,23
	150	39,87	50,21	9,92
	210	42,21	47,74	10,05
	270	50,43	39,26	10,31
	1440	50,24	40,15	9,62
20	0	35,12	59,73	5,15
	90	37,12	57,11	5,77
	150	41,32	50,14	8,54
	210	51,23	39,38	9,39
	270	52,12	38,12	9,76
	1440	53,87	36,77	9,36
30	0	34,89	60,09	5,02
	90	40,23	52,89	6,88
	150	49,54	41,23	9,23
	210	50,12	40,23	9,65
	270	50,97	39,14	9,89
	1440	52,18	38,49	9,33

6.1 taulan ikusi daitekeen moduan, α-helizetik β-xaflarako aldaketak ia konstante mantendu zireneko berokuntza denborak, laktosa edukiaren igoerarekin txikitu ziren, % 10, 20 eta 30 laktosadun filmentzako konformazio-aldaketarako berokuntza denborak 270, 210 eta 150 minutu izanik, hurrenez hurren. Portaera honek, arrain gelatinazko filmen egitura sekundarioan laktosa edukiak eta berokuntza denborak duten eragina nabarmendu zuen.

Disolbaturiko masa totalaren (TSM) balioak, α-helizetik β-xaflarako aldaketak ia konstante mantendu ziren berokuntza denboretan neurtu ziren eta balio horiek, berokuntza aurretik (0 min) eta 1440 minutuz (24 h) filmak berotu ondorengo TSM-ren balioekin alderatzeko, guztiak **6.2 taula**n erakusten dira. Ikusi daitekeen moduan, filmen disolbagarritasun balioak % 33raino nabarmenki behera egin zuten % 10, 20 eta 30 laktosadun filmak 270, 210, eta 150 minutuz berotu zirenean, hurrenez hurren. Balio hauek, saretze erreakzioak laktosa eduki handiko filmen disolbagarritasuna azkarrago txikitu zuela adierazi zuten. Beraz, berokuntza eta laktosaren gehikuntza bidez eragindako saretze erreakzioa arrain gelatinazko filmen disolbagarritasuna kontrolatzeko bide eraginkorra izan zitekeen, filmak aplikazio farmazeutikoetan eta elikadura aplikazioetan askapen sistema moduan erabiltzeko propietate funtzionalez hornituak izan zirelako.

6.2 taula Arrain gelatinazko filmen disolbaturiko masa totalaren (TSM) balioak, laktosa kantitatearen funtziopean.

Laktosa (%)	Denbora (min)	TSM (%)
10	0	100^{a}
	270	$31,0 \pm 0,7^{b}$
	1440	$16,0 \pm 2,4^{c}$
20	0	100^{a}
	210	$33,1 \pm 1,1^{b}$
	1440	$13,0 \pm 4,0^{d}$
30	0	100^{a}
	150	$33,1 \pm 0,9^{b}$
	1440	$12,8 \pm 3,3^{d}$

$^{a-d}$ Zutabe berean letra bera duten bi balio ez dira esanguratsuki ($P > 0,05$) desberdinak, Tukey-ren froga anizkoitzaren arabera.

6.2.2 Pentosidinaren eraketa

Saretze erreakzioaren eragina laktosa edukiaren eta berokuntza denboraren funtziopean aztertzeko, UV-vis espektroskopia erabili zen eta espektroak **6.2 irudia**n agertzen dira. **6.2 irudia**n ikusi daitekeen moduan, berotu gabeko arrain gelatinazko filmek UV argiarekiko xurgatze ahalmen handia erakutsi zuten, gelatinan dauden lotura peptidiko (200-250 nm) eta ohizko kromoforoengatik, hala nola, tirosina eta fenilalanina (250-300 nm) (Samira, Thuan-Chew, eta Azhar, 2014; Hong et al., 2014). Berokuntza ondotik, lehenengo urratsean eratutako MRP-ak 220 nm-an emandako xurgatze igoeraren bidez aztertu ziren, karbonilo taldeen presentziari egokitu zitzaiona, eta 280 nm-tako xurgatzea aldiz, heterozikloetatik eratorritako produktuei esleitu zitzaien.

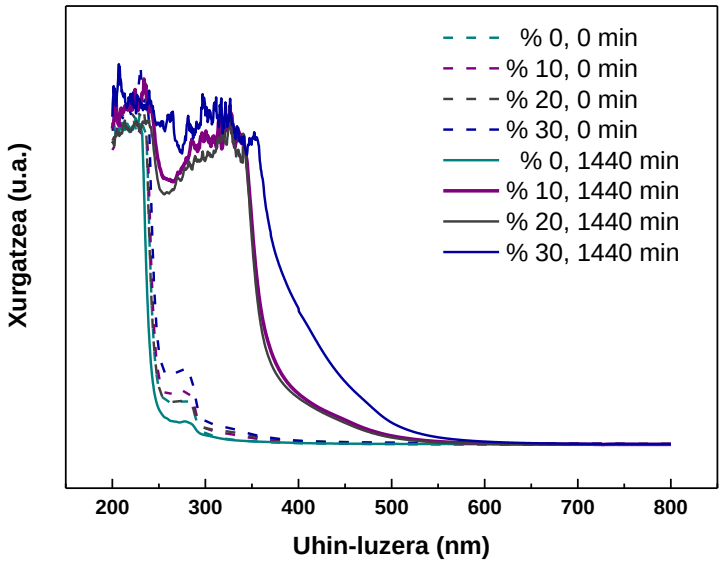

6.2 irudia Arrain gelatinazko filmen UV-vis espektroak laktosa edukiaren funtziopean, berokuntza aurretik (0 min) eta filmak 1440 minutuz (24 h) berotu ondoren.

Lehenengo urratsean, laktosak (aldehido moduan kate zabalduaren forman) beste aminoazidoak baino erreaktiboagoa den gelatinari lotutako lisina amino taldearekin Schiff basea eratzen du. Schiff basearen eraketa Maillard erreakzioaren

erdibideko urratsa da, Amadori produktua bezala ezaguna den Amadoriren berrantolaketagatik laktulosil-lisinean azkar eraldatzen delako (**6.1 eskema**).

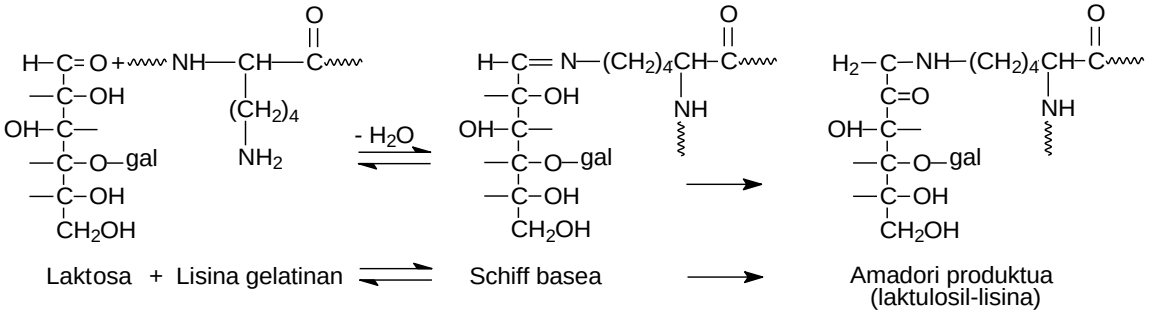

6.1 eskema Maillard erreakzioaren lehenengo etapa (gal = galaktosa).

Erreakzioak aurrera jarratu heinean, premelanoidina izenez ezagunak diren konposatu disolbagarri konplexuagoak eratzen dira eta ondorioz, 280 nm-tako xurgatze balioak etengabe handitzen dira eta 325 nm-an xurgatze banda berria agertzen da (Cuzzoni et al., 1988; Wijewickreme, Kitts, eta Durance, 1997). MRP-en eraketari erreakzioaren baldintzek izugarri eragiten diote. Van Boekel-en arabera (1998), Amadori produktuaren degradazioa baldintza basikoetan azkarragoa da eta Maillard erreakzioak kolore arrexka garatzen du, 420 nm-tako xurgatze bidez neurtu daitekeena. Arrexka konposatuen kimikari buruz gutxi ezagutzen den arren, jakina da baldintza alkalinoetako disakaridoen kasuan Amadori produktuaren degradazioa 4-deoxiosona bidea dela (**6.2 eskema**).

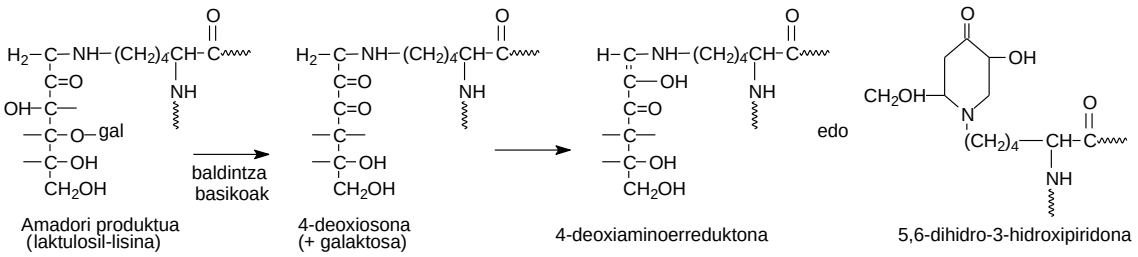

6.2 eskema Baldintza basikoetan Amadori produktuaren degradazioa Maillard erreakzioaren etapa aurreratuan (gal=galaktosa).

Eratutako bi produktuak 4-deoxiaminoerreduktona eta 5,6-dihidro-3-hidroxipiridona dira (Martins, Jongen, eta Van Boekel, 2001). Aurretik erakutsitako konposatuak oso erreaktiboak dira eta geroko erreakzioetan parte hartzen dute. Maillard erreakzioaren etapa aurreratuan, erreakzio ugarik parte hartzen dute; ziklazioak, deshidratazioak, retroaldolizazioak, isomerizazioak, eta gainerako kondentsazio erreakzioak, esaterako. Hala ere, beraien izaera erreaktiboagatik eratutako produktu motak eta hauen kantitateak determinatzea zaila da. Maillard erreakzioaren azken etapak nitrogenodun polimero arrexken eraketa bideratzen du, eraturiko AGE-tako bat pentosidina izanik, hau da, argininari lotutako lisina (**6.3 irudia**).

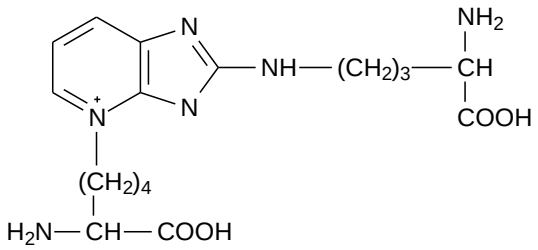

6.3 eskema Maillard erreakzioaren etapa aurreratuan sorturiko pentosidina.

Erreakzioaren hedatzea jarraitzeko helburuarekin, **6.3 irudia**k % 30 laktosadun arrain gelatinazko filmen UV-vis espektroak berokuntza denboraren funtziopean erakusten ditu. Espektroek, 480 minutura arte, 325 nm-tako xurgatze bandaren handitze jarrai bat aurkeztu zuten eta ondoren, denbora luzeagoetan, xurgatze balioak mantendu zirela ikusi zen. Jokaera honek, berokuntza eta laktosaren gehikuntza bidez gertatutako saretzeagatik arrain gelatinazko filmen UV argiarekiko babesaren hobekuntza adierazten zuen. Berokuntzak, Amadori produktuaren eraketa areagotu zuen eta ondoren, AGE-ren eraketa (Deyl et al., 1997; Morales eta Van Boekel, 1997). AGE fluoreszenteak, hala nola kroslina, pentosidina eta besperlisina, eta fluoreszentzia gabeko ez-saretutako AGE-ak, argirimidina, imidazolona eta pirralina esaterako, eratu daitezke (Van Boekel, 1998; Nguyen, 2006).

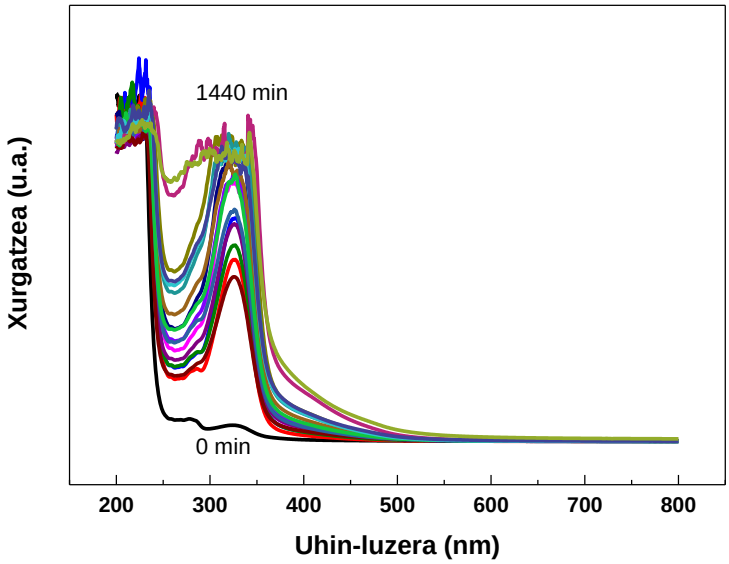

6.3 irudia % 30 laktosadun arrain gelatinazko filmen UV-vis espektroak, beroketa denboraren funtziopean. Neurketak, 480 minuturaino 30 minuturo, eta azkenik 1140 minutuan egin ziren.

Konposatu fluoreszenteen artean, pentosidina, erreakzioaren trazabilitatea jarraitzeko gehien erabiltzen den markatzaileetako bat da. Amadori konposatuaren eraketaren ondoren pentosidina lehenengo eratutako produktu egonkor fluoroforoa izan zela ziurtatzeko, fluoreszentzia analisia burutu zen. Arrain gelatinazko filmen fluoreszentzia espektroak **6.4 irudia**n erakusten dira. Alde batetik, 335 nm-an kitzikatutako % 30 laktosadun filmen emisio espektroak **6.4a irudia**n erakusten dira. Ikusi daitekeen moduan, emisio banda 410 nm-an agertu zen. Emaitza hauek beste lan batzuekin bat egin zuten (Morales eta Van Boekel, 1997; Bhat et al., 2014), pentosidinak, 335/408 nm-an kitzikapen/emisio uhin-luzerak erakutsi zituelako. Gainera, berokuntza denborarekin banda azpiko azalera zabaldu zen, pentosidina kantitate handiagoen eraketa eman zela adieraziz. Bestaldetik, 120 minutuz berotutako arrain gelatinazko filmen fluoreszentzia espektroak laktosaren funtziopean **6.4 irudia**n agertzen dira. Ikusi daitekeen moduan, laktosaren edukia handitu zenean, bandak uhin-luzera txikiagoetara mugitu ziren eta intentsitate balio handiagoak lortu ziren,

Maillard erreakzioa eta pentosidinaren eraketa laktosa eduki handiagoarekin azkarragoak zirela iradokiz, UV-vis emaitzekin bat etorriz. Gainera, emaitza hauek FTIR bidez ikusitako α-helizetik β-xaflarako aldaketa azkarrarekin eta TSM-ren neurketa bidez ikusitako disolbagarritasunaren gutxitze azkarrarekin bat zetozen.

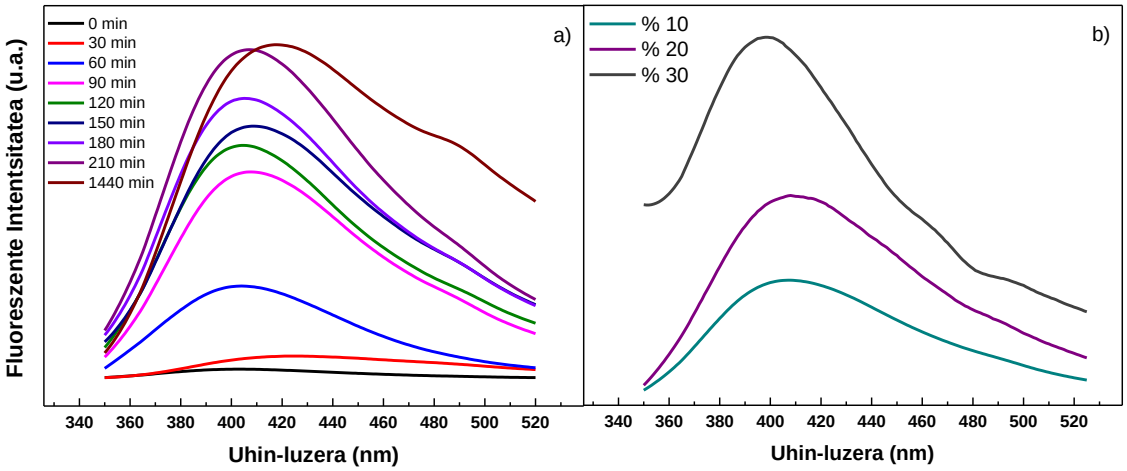

6.4 irudia a) Beroketa denboraren funtziopean % 30 laktosadun eta b) laktosa edukiaren funtziopean 120 minutuz berotutako arrain gelatinazko filmen fluoreszentzia espektroak.

6.2.3 Maillard errreakzioaren zinetika

Berokuntza ondotik laktosadun filmetan gertatzen den kolore aldaketa Maillard erreakzioaren adierazletzat hartu daiteke (Nursten, 1986). **6.5 irudia**n, % 30 laktosadun filmen irudia agertzen da, berokuntza denboraren funtziopean.

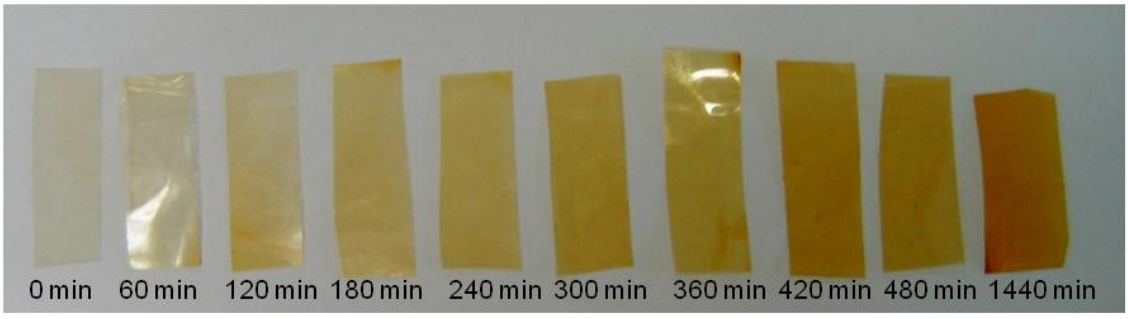

6.5 irudia % 30 laktosadun arrain gelatinazko filmen kolore aldaketa berokuntza denboraren funtziopean.

Film guztiak gardenak eta homogeneoak ziren, baina kolore aldaketa berokuntza denboraren luzatzearekin nabariagoa izan zen, filmek denbora luzeagotan kolore hori iluna garatu zutelako. Filmen kolorea CIELAB eskala erabiliz neurtu zen, eta L*, a* eta b* parametroak arrexka indizea (BI) kalkulatzeko erabili ziren. L* eta a* balioek (erakutsi gabeko datuak) ez zuten aldaketa esanguratsurik ($P > 0,05$) erakutsi, filmak 480 minutuz berotu ondoren. b* balioa aldiz, laktosa edukiaren handitzearekin eta berokuntza denboraren luzatzearekin nabarmenki ($P < 0,05$) igo zen (**6.3 taula**).

6.3 taula Arrain gelatinazko filmen b* balioak, laktosa kantitatearen eta berokuntza denboraren funtziopean.

Laktosa (%)	b*					
	30 min	60 min	150 min	210 min	270 min	480 min
10	8,5 ± 0,5^{a}	10,2 ± 0,3^{a}	13,8 ± 0,1^{b}	18,5 ± 0,2^{c}	24,8 ± 2,6^{d}	33,8 ± 0,2^{f}
20	8,6 ± 0,3^{a}	10,2 ± 0,4^{a}	17,8 ± 1,4^{c}	24,7 ± 2,3^{d}	30,2 ± 0,7^{e}	36,5 ± 0,4^{f}
30	9,3 ± 0,1^{a}	14,0 ± 1,4^{b}	26,7 ± 1,2^{d}	31,6 ± 1,3^{e}	36,5 ± 0,4^{f}	46,1 ± 1,2^{g}

$^{a-g}$ Zutabe berean letra bera duten bi balio ez dira esanguratsuki ($P > 0,05$) desberdinak, Tukey-ren froga anizkoitzaren arabera.

BI-ren balioengan laktosa edukiaren eragina berokuntza denboraren funtziopean **6.6 irudia**n erakusten da. Ikusi daitekeen moduan, BI-k lehenengo mailako zinetika erakutsi zuen, beste egile batzuk aipatu zuten moduan (Isleroglu et al., 2012; Jiménez et al., 2012; Gupta et al., 2011).

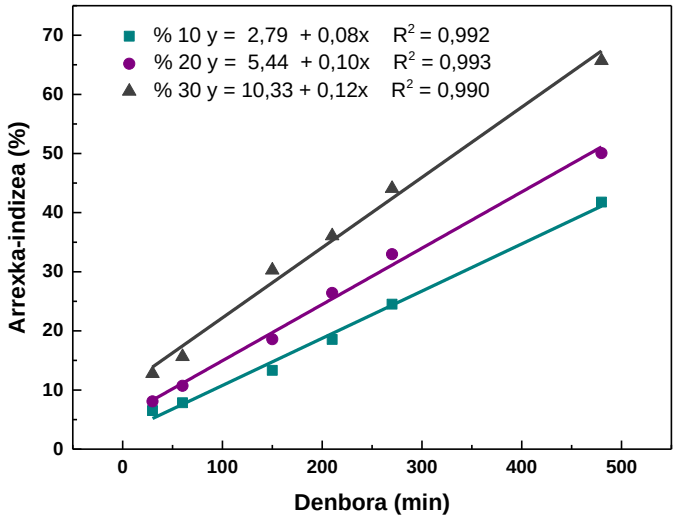

6.6 irudia Arrain gelatinazko filmen arrexka indizea (BI), laktosa edukiaren eta berokuntza denboraren funtziopean.

BI-ren balioak berokuntza denborarekin handitu ziren, laktosa eduki handiagoetan balio handiagoak erakutsiz. Honetaz gain, laktosa eduki handiko filmen zuzenen malda handiagoa zen, sistema horietan koloreztatutako melanoidinen eraketa azkarragoa zela adieraziz, aurretik UV-vis espektroskopian ikusitakoarekin bat etorriz.

Bestaldetik, pentosidinaren eraketaren zinetika, berokuntza denboraren eta laktosa edukiaren funtziopean, UV xurgatzea 335 nm-an neurtuz aztertu daiteke. **6.7 irudia**n ikusi daitekeen moduan, pentosidinaren eraketak bigarren mailako zinetika erakutsi zuen. Film guztietan, UV xurgatzea balio konstanteetaraino igo zen, laktosa edukia kontuan hartu gabe. Hala era, pentosidina eraketaren proportzioa txikiagoa zen laktosa eduki txikiagoa zuten filmetan. Pentosidinaren eraketa filmak 480, 420 eta 180 minutuz berotu ostean egonkortzera iritsi zen, % 10, 20 eta 30 laktosadun filmetan, hurrenez hurren.

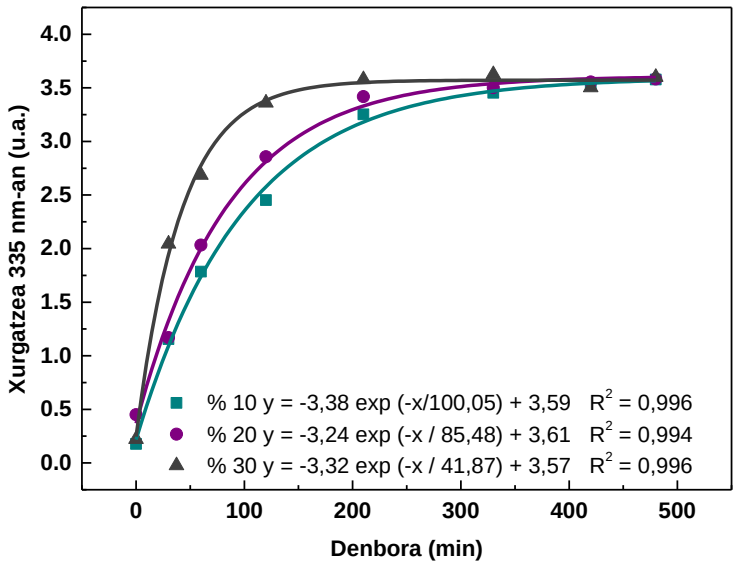

6.7 irudia Arrain gelatinazko filmen UV argiaren xurgatzea 335 nm-an, laktosa edukiaren eta berokuntza denboraren funtziopean.

6.2.4 Saretzearen eragina nanoegituran

X-izpien difrakzioa (XRD) proteinen egitura zehazteko teknika arrunta da eta hortaz, arrain gelatinazko filmen difrakzio bandak laktosa edukiaren eta berokuntza denboraren funtziopean **6.8 irudia**n erakusten dira. Lagin guztiek bi difrakzio banda erakutsi zituzten, 21º-etako banda, gelatinaren kristalinitatearekin erlazionatu zena, eta 7,4º-tako banda, kolageno natiboaren helize hirukoitzaren hondarrari egokitu zitzaiona (Chen, Wang, eta Jiang, 2012; Guerrero et al., 2012). Laktosaren edukia igo zenean, gelatinaren kristalinitatea igo zen, laktosaren eta gelatinaren artean sorturiko lotura kobalente berriek egitura ordenatuagoa sortu zutela adieraziz. Hala ere, helize hirukoitzaren hondarraren edukia filmen berokuntzagatik txikitu zen. Hau, kolageno natiboaren helize hirukoitzaren hondarraren berrantolaketa oztopatu zuten Maillard erreakzioan eratutako gliko-konjugatuek, eta saretzeak proteinaren kateen arteko interakzio molekularrak txikitu zituztelako izan zen (Carvalho eta Grosso, 2004; Liu eta Zhong, 2012).

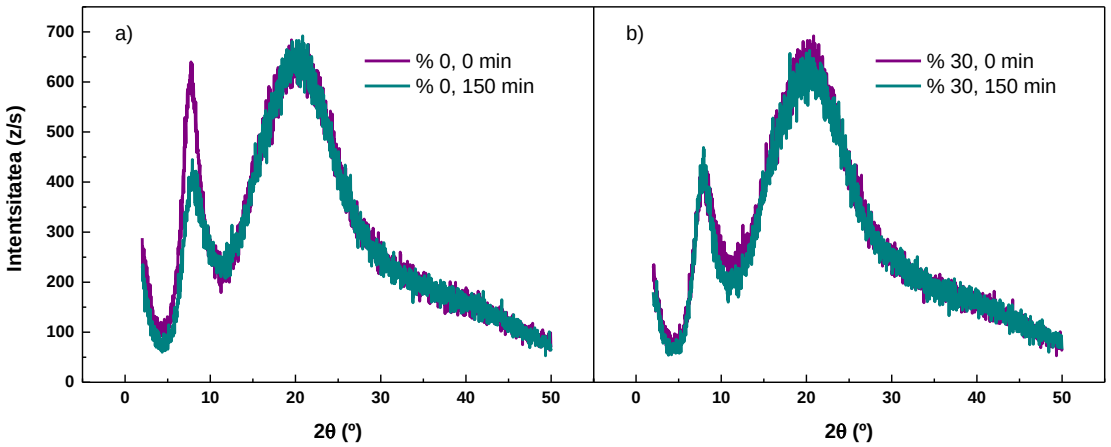

6.8 irudia a) Laktosarik gabeko eta b) % 30 laktosadun arrain gelatinazko filmen XRD ereduak, berokuntza aurretik (0 min) eta berokuntza ondoren (150 min).

Arrain gelatinazko filmen nano-egitura sakonkiago aztertzeko, indar atomikozko mikroskopioaz (AFM) neurketak egin ziren eta lorturiko altuera eta fase irudiak **6.9 irudia**n erakusten dira.

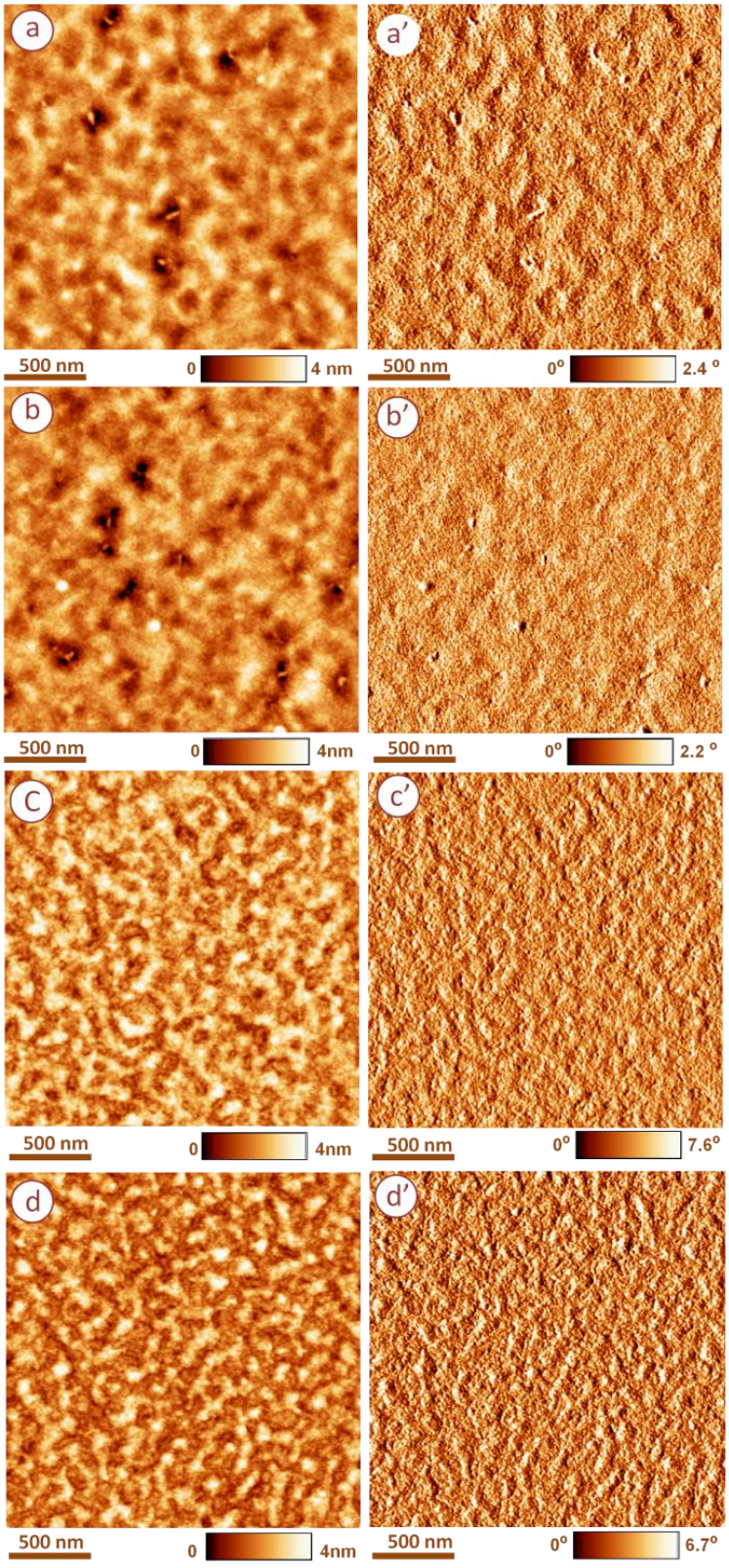

6.9 irudia a) Berokuntza aurretik (0min) eta b) berokuntza ondoren (150 min) laktosa gabeko, eta c) berokuntza aurretik (0min) eta d) berokuntza ondoren (150 min) % 30 laktosadun arrain gelatinazko filmen AFM irudiak. Altuera irudiak (a, b, c, d) eta fase irudiak (a', b', c', d').

Laktosa gabeko filmen **6.9a** eta **6.9b irudi**etan ikusten den moduan, gelatinak zuntz egitura erakutsi zuen, beste egile batzuek ikusi zuten moduan (Yang et al., 2007; Wang, Yang, eta Regenstein, 2008). Emaitza hau, XRD bidez ikusitako kolagenoaren helize hirukoitzaren hondarrean emandako aldaketekin bat zetorren. Laktosaren gehikuntzak gelatinaren nano-egitura aldatu zuen, **6.9c irudia**n ikusi daitekeen moduan. Laktosaren presentziaren ondorioz, irudietan ez zen zuntzik ikusi, XRD-n erakutsitako zuntzei egokitutako seinalearen murrizte nabariarekin bat etorriz. Gainera, laktosarik gabeko filmetako zuntzak inguratzen zituen matrizea egituratuagoa bihurtu zen, eta honek, gelatina eta laktosaren artean gertatutako Maillard erreakzioan agregazioak sortu zirela iradoki zuen. Ondoko berokuntzak, oraindik bereizgarriagoak ziren ezaugarriak sortu zituen (**6.9d irudia**), betiere, Maillard erreakzioa areago hedatua zegoenean. Laburbilduz, AFM-ko irudiek, gelatinaren nano-egitura laktosaren gehitzearekin eta berokuntzaren eraginarekin nabariki aldatu zela nabarmendu zuten, egituratuagoa eta ordenatuagoa zen matrizea sortuz, aurretik erakutsitako disolbagarritasunaren balio baxuekin bat etorriz. Beraz, AFM analisia, beste neurketa batzuekin, hala nola, ikerketa honetan burututako disolbagarritasun eta XRD analisiekin ikusitako aldaketa fisiko-kimikoak egiaztatzeko erabili zitekeela ondorioztatu zen.

6.2.5 GTA, GP edo laktosa bidez saretutako filmen konparazio-analisia

Gelatinan dagoen lisinaren amina taldearekin ematen den saretze erreakzioaren mekanismoa, erabilitako saretze erreaktiboaren menpekoa da. GTA saretze erreaktibo sintetikoa da, medikuntzako ikerketetan asko erabiltzen dena. GTA-ren karbonilo taldearen eta gelatinaren lisina amino taldearen arteko erreakzioak, horitze prozesuarekin batera, Schiff basea eratzen du (**6.10a irudia**), (Farris, Song, eta Huang, 2010). GTA-k zitotoxikotasun altua erakusten duenez, GP, saretze erreaktibo naturala, alternatiba moduan erabili daiteke. Jakina da, GP-k proteinetako lisina amino taldeekin erreakzionatzen duela, pigmentu urdinak eratuz (Ali Poursamar et al., 2016;

Sung et al., 1999). Nahiz eta oraindik erreakzio honen mekanismoa ez den guztiz ulertzen, GP-k egitura hemiazetalean, dialdehido baten egituraren baliokide bihurtzen dela uste da. Nahiz eta GP-k zitotoxikotasuna balio baxuak aurkeztu dituen, saretze erreaktiboaren kostu altuarengatik eskuragarri dauden datu gutxi erakusten dira literaturan (Panzavolta et al., 2011). Beraz, lan honetan, saretzea sustatzeko beste saretze erreaktibo natural bat erabili zen, hau da, laktosa. Berokuntzak, laktosaren presentzian, proteinaren barrualdean interakzioak aldatu ditzake eta honekin proteinaren konformazioa, glikazio ez-entzimatikoa bideratuz (**6.10c irudia**), kapitulu honetan aurretik erakutsi den bezala (Etxabide et al., 2015a). Filmen kolorea erabilitako saretze erreakzioaren arabera aldatu zen, film horixkak sortuz, laktosa edota GTA erabili zenean eta film urdinak lortuz, GP gehitu zenean. Filmen koloreak saretzearen adierazletzat hartu ziren.

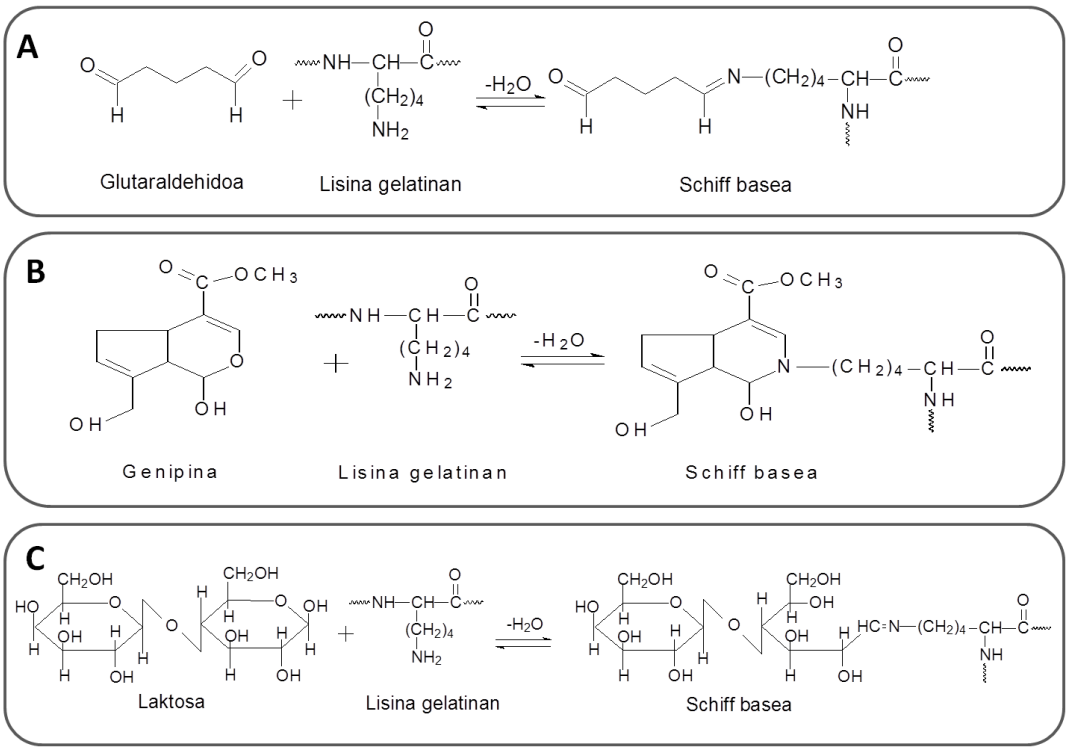

6.10 irudia Gelatina eta (a) GTA-ren, (b) GP-ren, eta (c) laktosaren arteko saretze erreakzioa.

Filmen egonkortasun hidrolitikoa saretze-mailaren zeharkako neurketa denez, filmak PBS soluzioan 3 egunez 25 ºC-an murgildu ziren. **6.11 irudia**n ikusi daitekeen moduan, filmen egonkortasuna saretze erreaktibo motaren eta buffer soluzioaren tenperaturaren funtziopean zegoen. Filmak PBS-an 25 ºC-an murgildu ostean, GP eta GTA erreaktiboekin saretutako filmek laktosarekin saretutako filmek baino soluzio urtarra xurgatzeko gaitasun handiagoa erakutsi zuten (**6.11a-b irudia**k). Jokaera honek, laktosa saretze erreaktibo moduan erabili zenean, saretze-maila handiagoa lortu zela adierazi zuen eta, beraz, film hauen soluzio urtarra xurgatzeko gaitasuna txikiagoa zen (Saarai et al., 2013). GP edo GTA bidez saretutako filmen likidoa xurgatzeko gaitasun handiak, filmak itsaskorrak eta hauskorrak izatea eragin zuen, maneiatzeko ahulegiak izanik. Aldiz, laktosarekin saretutako filmek ez zuten maneiatzeko arazorik erakutsi.

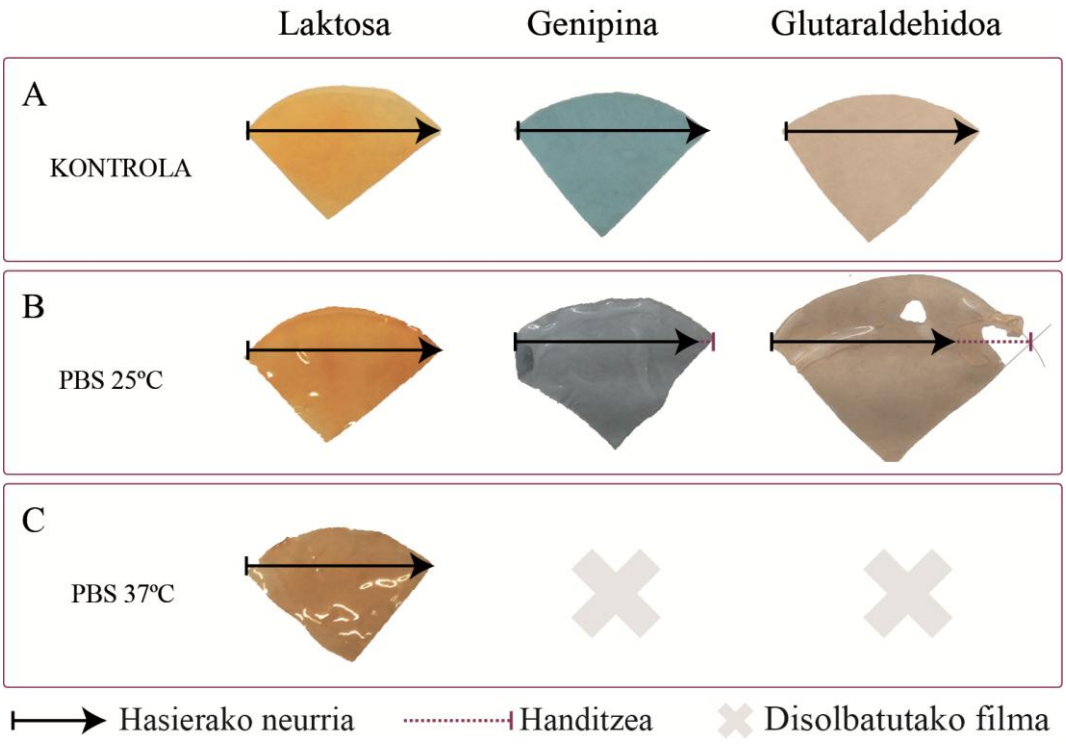

6.11 irudia Laktosa, GP eta GTA erreaktiboen bidez saretutako arrain gelatinazko filmen itxura, filmak (a) PBS bufferrean murgildu aurretik, eta PBS bufferrean (b) 25 ºC-an eta (c) 37 ºC-an filmak 3 egunez murgildu ostean.

PBS soluzioaren tenperatura 37 ºC-ra igo zenean, GP eta GTA erreaktiboekin saretutako filmak guztiz disolbagarriak bilakatu ziren, horiek 24 eta 20 orduz murgilduta egon ostean, hurrenez hurren (**6.11 irudia**). Hala ere, tenperaturaren igoerak ez zuen laktosarekin saretutako filmen osotasun fisikoan eragin. Gainera, laktosarekin erreakzionatutako filmek, beraien hasierako itxura mantendu zuten eta ez zuten maneiatzeko arazorik erakutsi. Emaitza hauek, laktosak GP eta GTA baino saretze maila handiagoa lortu zuela adierazten dute. Hau guztia kontuan edukiz, laktosarekin saretutako filmak, ondoren burututako azterketa biologikoak egiteko aukeratuak izan ziren. Bereziki, film hauek biobateragarritasun bikaina erakutsi zuten, ISO 10993-5:2009 medikuntzako gailuen azterketa biologikorako arauaren arabera, eta filmaren gainazalak itsatsitako, hedatutako eta ugaldutako zelulen kopuru handiak erakutsi zituen (aurkeztu gabeko datuak). Datu hauek kontuan edukiz, laktosarekin saretutako gelatinazko filmak zauriak sendatzeko ehun-ingeniaritzaren aplikazioetan erabiltzeko etorkizun handiko hautagaitzat hartu ziren.

6.3 Ondorioak

Maillard erreakzioa sustatzeko eta propietate funtzionalak hobetzeko asmoz, berokuntza denbora ezberdinetan, laktosarekin saretutako arrain gelatinazko film eraldatuak prestatu ziren. Filmen disolbagarritasuna laktosaren edukia eta berokuntza denbora bidez kontrolatu zitekeela frogatu zen, sendagaien askapen-sistema bezalako medikuntzako aplikazioetan nahiz film bioaktibo moduan elikagaien babeserako aplikazioetan erabiltzeko propietate onuragarria zena. Honetaz gain, lehenengo mailako zinetika erakutsi zuen konposatu koloredunen eraketa, erreakzioaren hedapenaren adierazle gisa erabili zitekeen. Honi dagokionez, konposatu fluoreszenteen eraketa, bigarren mailako zinetika erakusten zuena, erreakzioaren hedapena jarraitzeko adierazle gisa ere kontsideratu zen. Modu interesgarrian, erreakzioaren zinetikak, saretze erreakzioaren hedapena kontrolatzeko ezagutza eman

zuen, baita erreakzio ez-entzimatikoan eratutako nano-egiturarekin zuzenki erlazionatutako propietate funtzionalena ere.

Azkeneko hiru kapituluetako emaitzak kontuan hartuz, aipatzekoa da, pH basikoan prestatutako % 20 laktosadun HT filmek disolbagarritasun balio txikienak erakutsi zituztela, laktosaren gehikuntza handiagoak erreakzioa gehiago ez zuela sustatuko iradokiz. Gainera, film hauek WCA-ren balio altuak, UV argiarekiko hesi-propietate bikainak eta 50 MPa inguruko trakzio erresistentzia balioak erakutsi zituzten. Hortaz, formulazioa hau aurrerago egin ziren analisietarako egokiena zela kontsideratu zen.

7 Gelatinazko filmen aktibitate antioxidatzailea

7.1 Laburpena

Gaur egun konposatu sintetikoen osasun arriskuetan sorturiko kezkengatik, naturalki sortutako bioaktiboak kontsumitzaileen eta enpresen artean nahiago dira. Testuinguru honetan, landareak, polifenolikoak bezalako balio handiko antioxidatzaileen iturri dira, aplikazioa farmazeutikoetan, medikuntzan eta elikagaietan erabiltzen direnak (Bandyopadhyay, Ghosh, eta Ghosh, 2012; Freile-Pelegrín eta Robledo, 2014; Gómez-Guillén et al., 2009; Ozdal, Capanoglu, eta Altay, 2013; Rao eta Ravishankar, 2002). Landareetatik eratorritako konposatu antioxidatzaileen artean, tetrahidrokurkumina (THC), kurkuminaren (*Curcuma longa* L.) metabolito hidrogenatua, elikagai-, farmazia- eta kosmetikoen industrietan geroz eta interes handiagoa pizten ari da, izan ere, kurkumina, bitamina E-a eta α-tokoferola baino antioxidatzaile ahalmen hobea erakutsi duelako (Mehanny et al., 2016; Priyadarsini, 2014; Venkatesen et al., 2003). Honetaz gain, kurkumina ez bezala, THC koloregabea eta zaporegabea da (Portes, Gardrat, eta Castellan, 2007). THC-ren antioxidatzaile ahalmenaz gain (Somporn et al., 2007), konposatu honek diabetesaren (Murugan eta Pari, 2006), minbiziaren (Plyduang et al., 2014), eta hanturaren (Murakami et al., 2008) kontrako aktibitateak erakutsi ditu. Hortaz, filma eratzeko soluzioan THC sartzea, kontsumitzaileen osasunarentzat onuragarria izan daitekeen film aktiboen garapena sustatzeko bidea izan daiteke.

Aurreko kapituluetan, laktosadun gelatinazko filmen karakterizazioa burutu zen, eta laktosa eta gelatinaren arteko saretze erreakzioa aztertu zen. Konposatu fenolikoen eraketa eman zenez eta konposatu hauek antioxidatzaile aktibitatea zutela uste zenez, lan honen helburua, % 20 laktosarekin saretutako gelatinazko filmen ahalmen antioxidatzailea aztertzea izan zen. Gainera, gelatinazko filmetan THC bezalako antioxidatzaile organikoa gehitu zen, filmen ahalmen antioxidatzailearen hobekuntza eta THC gehituriko filmen gainazalen propietateak aztertzeko.

7.2 Emaitzak eta eztabaida

Prestaturiko filmak hauexek ziren: G filmak (laktosarik gabeko gelatinazko filmak), G-THC filmak (laktosarik gabeko baina THC duten filmak), GL filmak (laktosadun gelatinazko filmak), eta GL-THC filmak (laktosadun eta THC-dun gelatinazko filmak). Lehenik eta behin, filmen lodiera neurtu zen eta film guztientzako lorturiko lodieraren batezbesteko balioa 54 ± 5 μm izan zen.

7.2.1 Filmen karakterizazioa

Filmen kolorea L*, a* eta b* balioen bidez kuantifikatu zen, **7.1 taula**n erakusten den bezala. Laktosaren gehitzeak, L* balioaren txikitzea eragin zuen, filmen iluntzeari egokitu zitzaiona. Izan ere, GL-THC filmek kolore hori iluna erakutsi zuten, a* eta b* balioek erakutsi zuten moduan. Balio hauek, laktosaren gehikuntzarekin gora egin zuten. Laktosaren gehikuntzak eta ondorengo berokuntzak filmen kolorea aldatu zuten, kolore horixka garatuz eta argitasuna murriztuz. Iluntze eta horizkatze hau, laktosa eta gelatinaren arteko saretze erreakzioarekin erlazionatu zen. Ondorioz, GL-THC filmen kolore aldaketa totalaren (ΔE*) balioak handitu ziren, G-THC filmekin alderatuz gero.

7.1 taula THC-dun arrain gelatinazko filmen L*, a*, b* eta ΔE* balioak.

Filma	L*	a*	b*	ΔE*	Distira$_{60^\circ}$ (DU)
G-THC	93,79 ± 0,29	-0,42 ± 0,02	13,54 ± 0,79		35 ± 1
GL-THC	83,06 ± 1,41	3,43 ± 1,25	58,74 ± 3,49	46,59 ± 3,80	25 ± 2

7.1 taulan THC-dun filmen distira balioak erakusten dira. Ikusi daitekeen moduan, GL-THC filmek G-THC filmek baino distira txikiagoa eta beraz, gainazal latzagoa erakutsi zuten. Gainazaleko aldaketa hau, filma eratzeko soluzioen konposatuen artean egondako interakzio bidez azaldu zitekeen.

Interakzio horiek aztertzeko asmoz, FTIR analisia burutu zen eta espektroak **7.1 irudia**n erakusten dira. THC-ren banda ezaugarriak 1598 cm^{-1}-ean (bentzeno eraztunaren C-C loturaren luzapena), 1511 cm^{-1}-ean (C-O loturaren luzapena), eta 1425 cm^{-1}-ean (C-H planoko loturaren tolestea) kokatuta zeuden (Souguir et al., 2013).

Laktosa gabeko filmetan, amida II-ari (N-H loturaren tolestea ,1530 cm^{-1}-ean) dagokion bandaren sorbalda maiztasun altuagotan ikusi zen, **7.1a irudia**n agertzen den moduan. Hau, THC-ren hidroxilo taldeen eta gelatinan dauden prolinaren eta hidroxiprolinaren amino taldeen arteko hidrogeno zubizko loturei egotzi zitzaien (Rao et al., 2015). Hala ere, laktosadun filmetan (**7.1 irudia**), 1100-1000 cm^{-1} tarteko bandek (C-O loturei dagozkiena) banda bakarra eratzeko joera erakutsi zuten, gelatina eta laktosaren arteko erreakzio kimikoa zegoela adieraziz, aurreko lanetan ikusi zen moduan (Etxabide et al., 2015a; Etxabide et al., 2015b). Laktosadun film hauetan, ez zen aurretik aipaturiko amida II bandaren sorbalda ikusi, gelatina eta laktosaren arteko erreakzio kimikoak THC eta gelatinaren arteko hidrogeno zubizko loturen eraketa eragotzi zuela adieraziz.

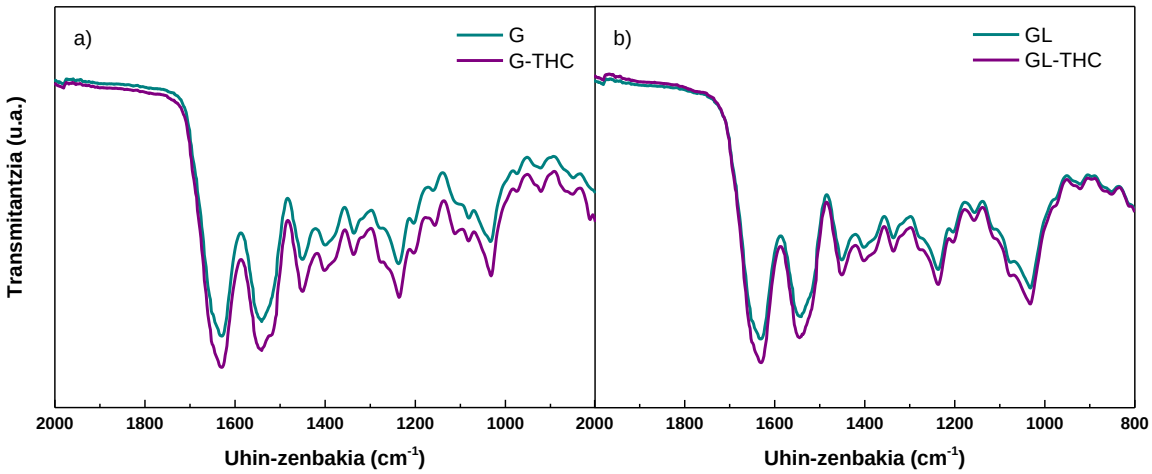

7.1 irudia a) G eta G-THC eta b) GL eta GL-THC arrain gelatinazko filmen FTIR espektroak.

Interakzioak filmen gainazalean eragindako aldaketak XPS bidez aztertu ziren eta emaitzak **7.2 irudia**n erakusten dira. Ikusi daitekeen moduan, C 1s (284,6 eV), N 1s (398,8 eV) eta O 1s (532,0 eV) bandak identifikatu ziren.

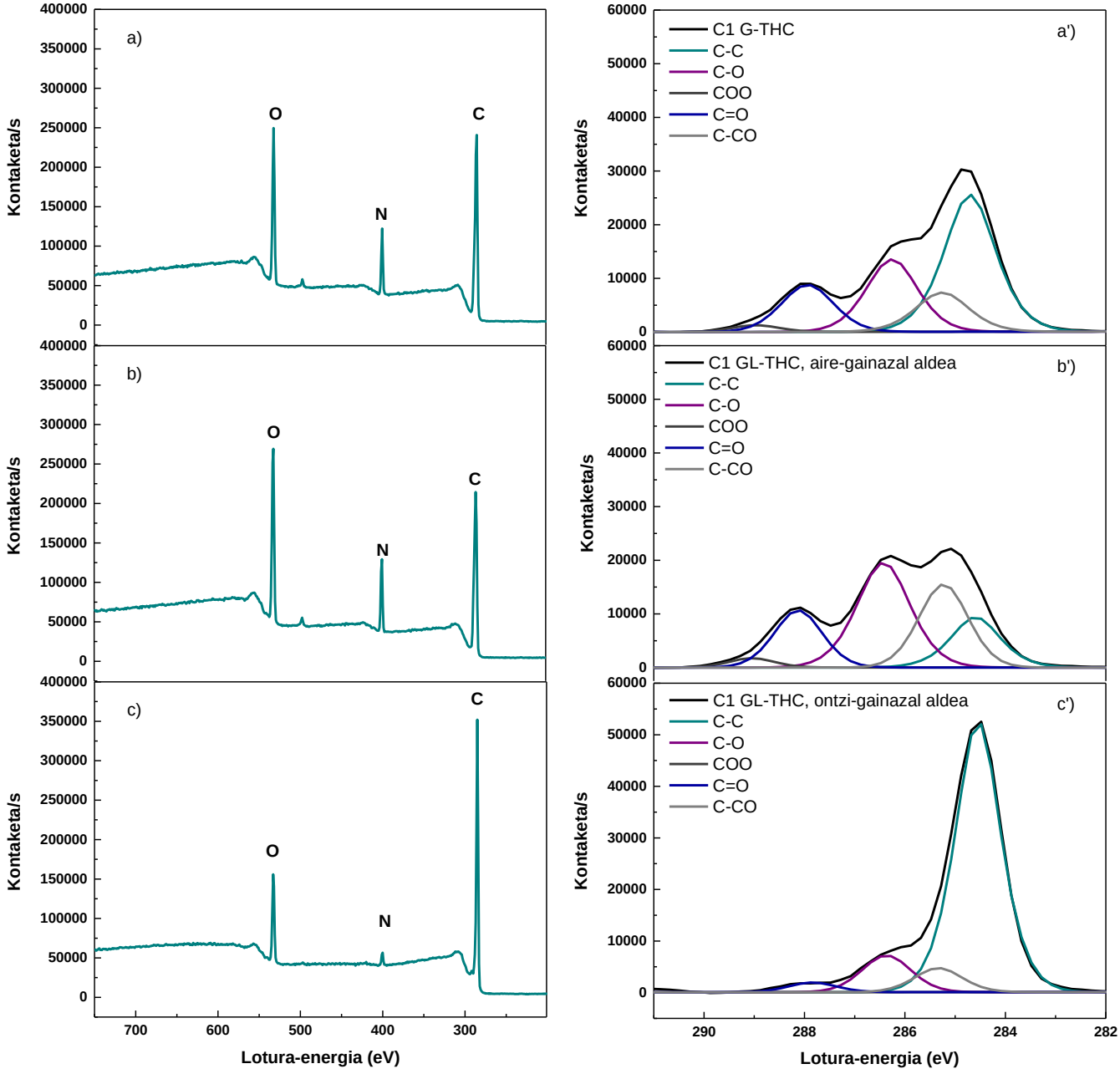

7.2 irudia Arrain gelatinazko a) G-THC filmen (aire-gainazal eta ontzi-gainazal aldeak), b) GL-THC filmen aire-gainazal aldearen, eta c) GL-THC filmen ontzi-gainazal aldearen XPS espektroak, eta a') G-THC filmen (aire-gainazal eta ontzi-gainazal aldeak), b') GL-THC filmen aire-gainazal aldearen, eta c') GL-THC filmen ontzi-gainazal aldearen C 1s bereizgarriaren XPS-a.

Laktosaren faltagatik, eta beraz, saretze erreakziorik ez zegoenez, G-THC filmen bi aldeen artean ez zen ezberdintasun nabaririk ikusi (**7.2a irudia**). Hala ere, aipatzekoa da GL-THC filmen aire-gainazal (**7.2b irudia**) eta ontzi-gainazal

(**7.2c irudia**) aldeen artean aldaketak egon zirela. Izan ere, N 1s fotoelektroi banda, matrize organikoen nitrogenoaren ohiko banda, GL-THC filmen ontzi-gainazal aldean ia guztiz desagertu zen. Banda honen desagertzea, proteinaren konformazioa aldatu zezakeen gelatinaren talde nitrogenatuen eta laktosaren karbonilo taldeen arteko erreakzio kimikoarekin erlazionatuta egon zitekeen, gainazalaren egituran aldaketak eragin zitzakeena, distiraren emaitzetan ikusi zen moduan. Gainazalen arteko ezberdintasun hau, THC-k uretan disolbagarritasun txikia erakusten duenez, filma eratzeko prozesuan zehar filmaren aire-gainazal aldean THC-ren pilaketa gertatu zelako izan zitekeen. Ondorioz, aire-gainazal aldean THC-ren pilaketak gelatina eta laktosaren arteko erreakzio kimikoa oztopatu zezakeen. Hala ere, erreakzio kimiko hau gertatu zenean, C 1s bandaren handitzea eta O 1s bandaren txikitzea ikusi zen. Azterketa sakonagoa egiteko, C-ri esleitutako banda egokitu egin zen. C 1s banda, C-C (284,60 eV), C-C=O (285,28 eV), C-O (286,28 eV), C=O (287,88 eV) eta O-C=O (288,88 eV) loturei egokitutako bandetan deskonposatu zen, **7.2a', 7.2b',** eta **7.2c' irudi**etan ikusi daitekeen moduan. 284,60 eV-tan agertutako banda nagusia, gelatinaren karbono alifatikoen albo-taldeei zegokien, 285,9 eV-tako banda proteinaren egituraren NH–CHR–CO karbonoari zegokion, eta 287,7 eV-tako banda aldiz, –CO–NH– karbono peptidikoei zegokien (Deligianni et al., 2001; Guerrero et al., 2014). GL-THC filmen bi gainazalak alderatzerakoan, ontzi-gainazal aldea nagusiki C-C loturez osatuta dagoela ikus zitekeen, C-CO, C-O, C=O eta COO loturei esleitutako bandak txikitu zirelako. Hau guztia, gelatina eta laktosaren arteko erreakzio kimikoan pisu molekular altuko nitrogenodun konposatuen eraketari lotu zitzaion (Etxabide et al., 2015b).

Nahiz eta G-THC eta GL-THC filmen XPS espektroak antzekoak izan (**7.2a** eta **7.2b irudiak**), aipatzekoa da laktosaren presentziagatik egokitutako C-ren espektroek (**7.2a'** eta **7.2b' irudiak**) beraien artean ezberdintasunak erakutsi zituztela. Ezberdintasun hauek sakonkiago aztertzeko, mikroskopia optikoa erabili zen

(**7.3 irudia**). Alde batetik, laktosarik gabeko filmetan (**7.3a irudia**), hau da, erreakzio kimikorik egon ez zen filmetan, THC-rekin hidrogeno zubizko loturak eratzeko amino talde eskuragarri gehiago zeuden (FTIR-ko emaitzetan ikusi den bezala, **7.1a irudia**). Ondorioz, aglomeratuen tamaina handiagoa zen eta honek gainazal leunagoa erakutsi zuen, distiraren balio altuek nabarmendu zuten bezala (**7.1 taula**). Bestaldetik, gelatina eta laktosaren arteko erreakzio kimikoak, THC-rekin hidrogeno zubizko loturak eratzeko amino talde eskuragarri gutxiago utzi zituen eta beraz, aglomeratuen kopurua handitu egin zen, hauen tamaina txikitu zen bitartean (**7.3b irudia**), gainazal latza erakutsiz eta distira balioak txikituz (**7.1 taula**).

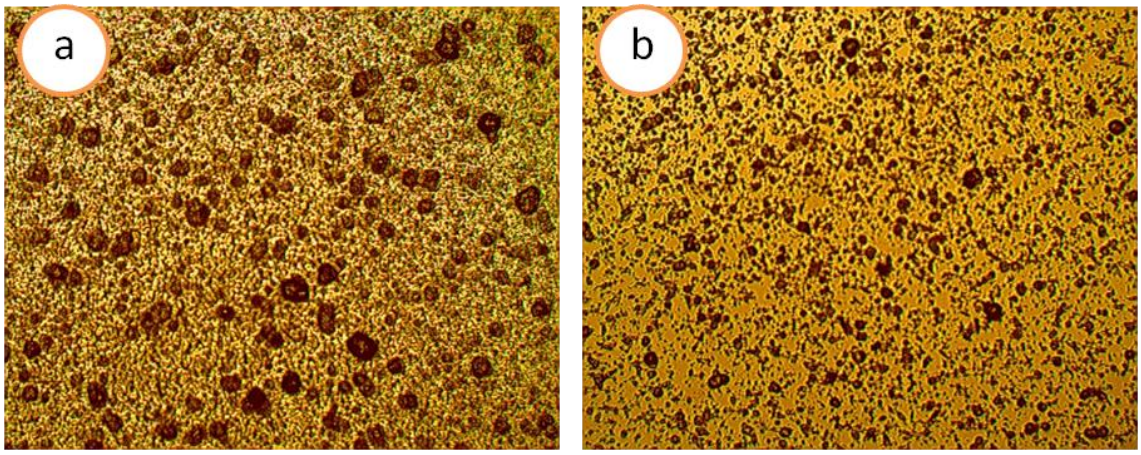

7.3 irudia a) G-THC eta b) GL-THC arrain gelatinazko filmen aire-gainazaleko mikrografia optikoa. 40X handiketa.

7.3.2 Aktibitate antioxidatzailea

Lehenik eta behin, THC-ren egonkortasuna filma prestatzeko baldintzetan aztertu zen. Horretarako, pH basikoan zegoen urarekin bustitako THC hautsa izoztu eta liofilizatu zen (THC*). THC*-ren egonkortasun termikoa ikerketa honetan erabilitako baldintzetan (105 ºC, 24 ordu) aztertu zen. Konposatuaren masa galera aipaturiko baldintzetan aztertzeko TGA erabili zen, eta ez zen ezberdintasun esanguratsurik ikusi konposatuaren masa galeran (% 0,4ko masa galera, erakutsi gabeko datuak). Masa galera hau, laginetik guztiz kendu ez zen uraren lurrunketarena izan zitekeen. Gainera, THC eta THC*-ren disoluzioak (209,5 µM) MeOH-n prestatu ziren eta beraien

propietate antioxidatzaileak DPPH entsegu bidez aztertu ziren. Nahiz eta THC*-k (86 ± 2) THC-k (90 ± 2) baino inhibizio balio baxuagoak erakutsi zituen, antioxidatzaile aktibitatean ez zen ezberdintasun nabaririk egon.

Behin filma prestatzeko baldintzapean THC-ren egonkortasuna egiaztatu zela, THC gabeko (G eta GL filmak) eta THC-dun (G-THC eta GL-THC filmak) arrain gelatinazko filmetatik askaturiko konposatu antioxidatzaileen azterketa burutu zen, UV-vis espektroskopiaren bidez (**7.4 irudia**).

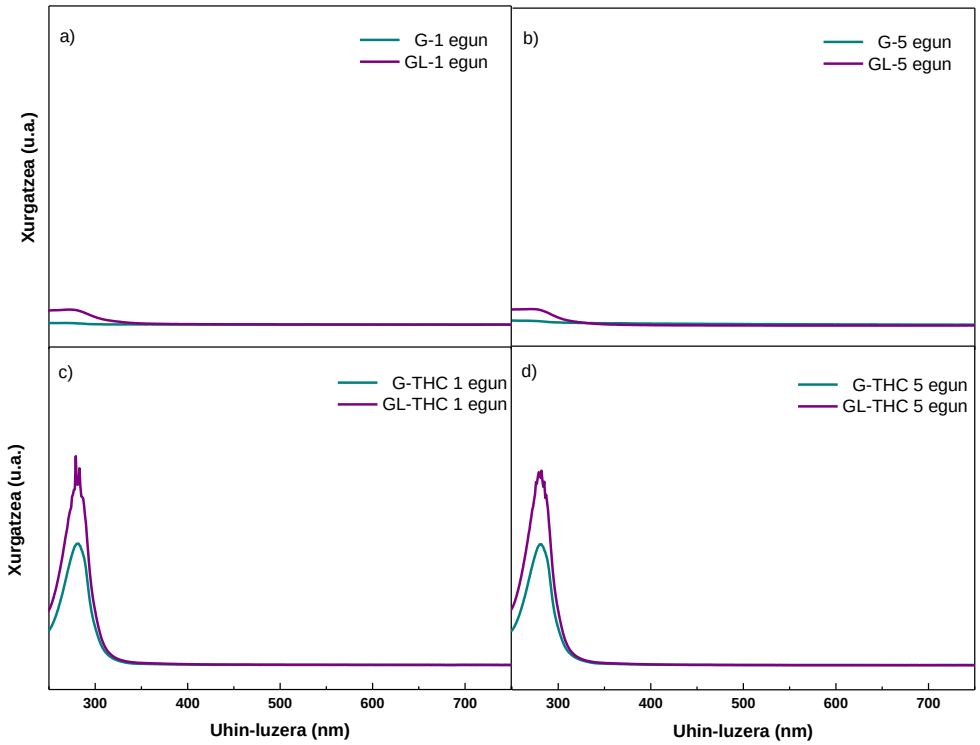

7.4 irudia G eta GL arrain gelatinazko filmak a) 1 egunez eta b) 5 egunez murgilduta egon osteko, eta G-THC eta GL-THC arrain gelatinazko filmak c) 1 egunez eta b) 5 egunez murgilduta egon osteko UV-vis xurgatzeak.

7.4a eta **7.4b irudi**etan erakusten den moduan, GL filmetan 280 nm inguruan argiaren xurgatzearen handitze arin bat ikusi zen, G filmekin alderatzerakoan. Handitze txiki hau, gelatina eta laktosaren arteko erreakzio kimikoan sortutako konposatu fenolikoen askatzearekin lotuta egon zitekeen (Monti et al., 2000; Monti et al., 1999). Aipatzekoa da, denboran zehar ez zela xurgatzearen handitzerik ikusi (**7.4b irudia**),

filmen murgilketaren lehenengo egunetik aurrera askapen gehiago ez zela egon adieraziz. THC filma eratzeko soluzioan gehitu zenean (G-THC eta GL-THC), argiaren xurgatzearen handitze nabarmena ikusi zen (**7.4c** eta **7.4d irudiak**), filmetik THC askatu zela adieraziz. Izan ere, 280 nm-tako xurgatze maximoko banda THC-ri zegokion (Portes et al., 2009). THC gabeko filmen emaitzen antzera, GL-THC filmetan xurgatze handiagoak ikusi ziren G-THC filmekin alderatuz.

Emaitza hauek **7.2 taula**n erakusten diren masa galeren balioekin bat datoz. Ikusi daitekeen bezala, laktosadun filmen balioak (GL eta GL-THC) bi bider handiagoak ziren, THC-ren gehikuntza kontuan hartu gabe. Handitze hau, gelatinaren eta laktosaren arteko erreakzioaren lehen urratsean sortzen diren eta disolbagarriak diren produktuengatik izan zitekeen, baina baita erreakzionatu gabeko laktosarengatik ere, aurreko lan batean ikusi zen bezala (Etxabide et al., 2015b).

7.2 taula THC gabeko (G eta GL filmak) eta THC-dun (G-THC eta GL-THC) arrain gelatinazko filmen masa galeraren, azido galikoaren baliokidearen (GAE), inhibizioaren (I) eta butilhidroxitoluenoaren baliokidearen (BHTE) balioak.

Filma	Masa galera (%)	GAE (mg/L)	I (%)	BHTE (mg/L)
G	$7,93 \pm 0,39^{a}$	$12,8 \pm 1,1^{a}$	-	-
GL	$14,15 \pm 0,42^{b}$	$14,4 \pm 0,8^{a}$	$27,2 \pm 1,4^{a}$	$5,6 \pm 0,5^{a}$
G-THC	$8,20 \pm 0,01^{a}$	$29,7 \pm 1,4^{b}$	$84,5 \pm 1,5^{b}$	$198,0 \pm 1,1^{b}$
GL-THC	$15,14 \pm 0,02^{c}$	$43,2 \pm 2,3^{c}$	$88,5 \pm 0,3^{c}$	$425,7 \pm 17,1^{c}$

[a-c] Zutabe berean letra bera duten bi balio ez dira esanguratsuki ($P > 0,05$) desberdinak, Tukey-ren froga anizkoitzaren arabera.

7.2 taulan ere, G filmek beste egile batzuek (Wu et al., 2013) aurkeztutako fenolikoen guztizko edukiaren balio antzekoak zituztela, eta GL filmek G filmekiko ezberdintasun nabarmenik ($P > 0,05$) erakusten ez zutela ikusten da, gelatinaren eta laktosaren arteko erreakzio kimikoaren ondotik askaturiko konposatu disolbagarria nagusiki erreakzionatu gabeko laktosa izan zitekeela adieraziz. THC-ren gehikuntzak, GAE-ren balioen handitzea eragin zuen, bereziki laktosarekin prestaturiko filmetan, sorturiko mikroegiturak THC-ren askatzea erraztu zezakeelako. DPPH erradikalak ezabatzeko aktibitateari zegokionez, G filmetan ez zen antioxidatzaile aktibitaterik

ikusi, GL filmek % 27ko inhibizioa erakutsi zuten bitartean. Emaitza hauek, gelatina eta laktosaren arteko erreakzio kimikoan antioxidatzaile aktibitatedun konposatu berrien eraketa gertatu zela adierazi zuten (Serpen et al., 2007). THC-ren gehikuntzak gelatinazko filmen propietate antioxidatzaileak nabarmenki handitu zituen. Gainera, GL-THC filmetan G-THC filmetan baino aktibitate antioxidatzaile handiagoa ikusi zen.

7.3 Ondorioak

THC konposatua duen gelatinazko filmetan, gelatina eta laktosaren arteko erreakzio kimikoak filmen egituran eragin zuen, distira gutxiagoko eta laztasun handiagoko filmak eratu zirelako. Disoluzio metodoaz prestaturiko filmen XPS azterketak, filmen bi aldeen arteko aldaketak erakutsi zituen, aire-gainazal aldean THC-ren aglomerazioari esleitu zitzaizkionak. Film hauen aktibitate antioxidatzaileari zegokionez, laktosadun gelatinazko filmek antioxidatzaile ahalmena erakutsi zuten, gelatinaren amino taldeen eta laktosaren karbonilo taldeen artean emandako erreakzio kimikoan sortu ziren konposatu fenolikoengatik. Hala ere, garaturiko filmen soluzioan THC konposatua gehitu zenean, hauen ahalmen antioxidatzailea izugarri handitu zen. Ondorioz, THC konposatua zuten gelatinazko filmek elikagaien babesa eta kalitatea hobetzeko ahalmena zeukatela erakutsi zuten, elikagaien ontziratze ekologikoen garapenari lagunduz. Gainera, 6. kapituluan erakutsi ziren laktosarekin saretutako gelatinazko filmen ehun-ingeniaritza aplikazioetarako propietateak kontsideratuz, kurkumaren deribatua zen konposatuaren gehitzeak, filmaren sendatze eragina nabarmenki hobetu zezakeen, honek erakutsitako osasun onurengatik.

8 Gelatinazko biokonpositeen ekoizpena

8.1 Laburpena

Behin filmak prozesatu eta karakterizatu zirela, eta biokonpositeak prestatzeko helburuarekin, plastikoen industrian erabilitako zenbait fabrikatze metodo erabili ziren. Gelatinaren urtze-puntua abantailatzat hartuz, gelatina estrusio bidez prozesatu zen. Estrusioa erabilera askotakoa, oso eraginkorra eta etengabeko fabrikazio teknologia da, estruitutako materialetan eraldaketa fisiko eta kimikoak eragiten dituzten prozesu termomekaniko eta termokimiko ugari barne dituena (Hernández-Izquierdo eta Krochta, 2009; Fakhouri et al., 2013). Nahiz eta estrusioa ondo finkatutako industria teknika izan, ez da proteinekin asko erabili. Hala ere, soja proteinarekin (Guerrero, Kerry, eta de la Caba, 2014), serum proteinarekin (Nor Afizah eta Rizvi, 2014), eta ilar proteinarekin egin berri diren estrusioan fokatutako lanek, estrusioa proteinak prozesatzeko metodo egokia dela iradokitzen dute. Honek, proteinaren merkatu bideragarritasuna sustatu dezake.

Kapitulu honen berritasuna, arrain gelatinazko biokonpositeak ekoizteko estrusio eta injekzio prozesatze metodoak erabiltzean oinarritu zen. Gainera, biokonpositeen berokuntza bidez emandako erreakzio kimiko ez-entzimatikoa sustatzeko, formulazioan laktosa eduki ezberdinak gehitu ziren. Disolbagarritasuna, handitzea eta propietate mekanikoak bezalako propietate funtzionalak analizatu ziren eta hauek, ekorketa diferentzialeko kalorimetria (DSC), X-izpien difrakzioa (XRD), ekorketazko elektroi-mikroskopioa (SEM) eta Fourierren transformatuaren espektroskopia infragorria (FTIR) bidez ikusitako egitura aldaketekin erlazionatu ziren.

8.2 Emaitzak eta eztabaida

Batera biratzen duten torloju bikoitzeko estrusio-makina gelatinazko xaflak sortzeko erabili zen, bigarren kapituluan azaldu den bezala. Estrusio bidez lortutako xaflen (**8.1a irudia**) lodiera eta zabalera 1,06 ± 0,19 mm eta 3,79 ± 0,33 mm ziren, hurrenez hurren. Ondoren, xafla hauek moztu, injektatu eta lortutako biokonpositeak

105 ºC-an 270 minutuz berotu ziren (**8.1b irudia**), aurreko ikerketa lan baten arabera (Etxabide et al., 2015b).

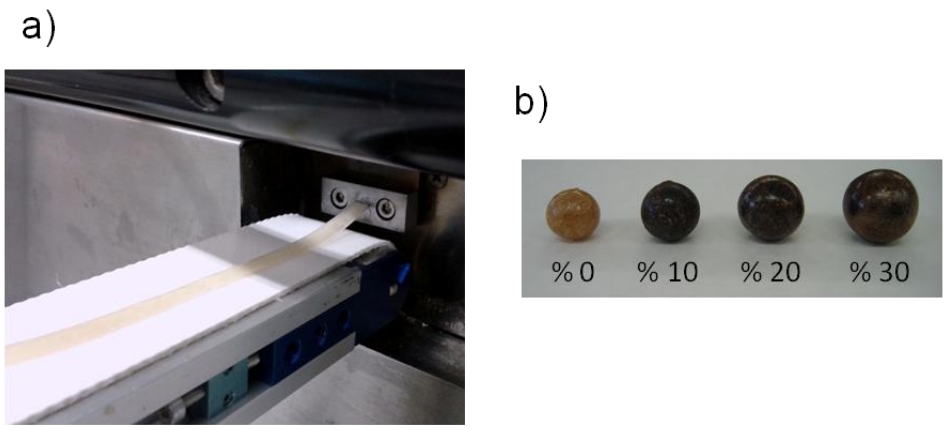

8.1 irudia a) Arrain gelatinazko xaflen estrusio bidezko etengabeko produkzioa eta b) injekzio bidez lorturiko arrain gelatinazko biokonpositeak 105 ºC-an 270 minutuz berotu ostean.

8.3.1 Propietate termikoak

Arrain gelatinazko biokonpositeen TGA-ren eta DTG-ren termogramak laktosa edukiaren funtziopean **8.2a** eta **8.2b irudi**etan erakusten dira, hurrenez hurren. Ikusi daitekeen moduan, biokonposite guztiek jarrera berdintsua zuten, denek antzeko hiru masa galeren etapa erakutsi zituztelako. 100 ºC-tarainoko lehenengo etapa, libre zegoen eta xurgatu zen urarekin erlazionatu zen. Bigarren etapa, 190-260 ºC-ko eremuan agertutako sorbalda, nagusiki pisu molekular baxuko proteinaren frakzioekin, plastifikatzailearekin eta helize hirukoitzaren konformazioan zuzenki egiturari lotutako urarekin lotu zen (Wetzel et al., 1987). Bigarren etapa hau, glizerolaren irakite puntua (182 ºC) baino tenperatura altuagoetan agertu zen, gelatina eta laktosaren artean hidrogeno zubizko loturak bezalako interakzioen presentzia iradokiz (Guerrero et al., 2011a). Gainera, laktosaren edukia igo zenean, 250 ºC-ko sorbalda desagertu zen, seguruenik glizerolaren askatzea oztopatu zezaketen pisu molekular handiko erreakzio produktuak eratu zirelako (Pastoriza eta Rufián-Henares, 2014). Azkenik, 310 ºC-an

hirugarren etapa ikusi zen eta hau tamaina handiko edo ongi elkartutako gelatina frakzioekin erlazionatu zen (Biscarat et al., 2015).

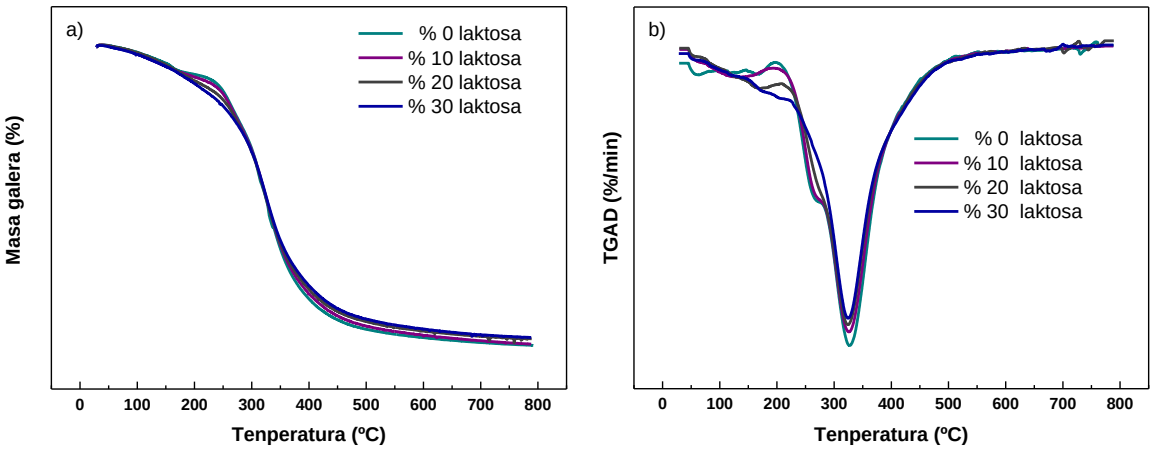

8.2 irudia Arrain gelatinazko biokonpositeen TGA-ren emaitzak a) masa galera kurba moduan eta b) kurben deribatu moduan, laktosa edukiaren funtziopean.

Gainera, DSC burutu zen eta termogramak **8.3 irudia**n erakusten dira. Ikusi daitekeen bezala, laktosarik gabeko biokonpositeek bi banda endotermiko aurkeztu zituzten: 69 ºC-an banda txiki bat, zorizko kiribil eremuarekin erlazionatu zena, eta 160 ºC-an urtze banda zabala, gelatinaren kristalizazio tenperaturarekin lotu zena (Coppola, Djabourov, eta Ferrad, 2008). Izan ere, gelatina, hidrolisi partzial bidez lortzen den desnaturalizatutako kolagenoa da eta prozesu horretan helize-hirukoitzeko egitura puskatu egiten da, zorizko kiribil egitura osatuz. Hala ere, kolagenoa gai da 35-40 ºC azpitik bere berezko egitura berreskuratzeko eta fenomeno hori, kiribiletik helizerako transformazioa bezala ezagutzen da (Ghoshal, Stapf, eta Mattea, 2014). Laktosa gehitu zenean, gelatinaren urtze bandaren txikitze esanguratsu bat gertatu zen, laktosa edukia kontuan hartu gabe. Honek, laktosaren eta berokuntzaren eraginagatik arrain gelatinaren saretzea adierazi zuen. Honetaz gain, 137 ºC-an laktosaren kristaltze-tenperaturari zegokion banda txikia ikusi zen, batez ere % 30 laktosadun biokonpositeetan, erreakzionatu gabeko laktosaren presentzia iradokiz (Islam eta Langrish, 2010).

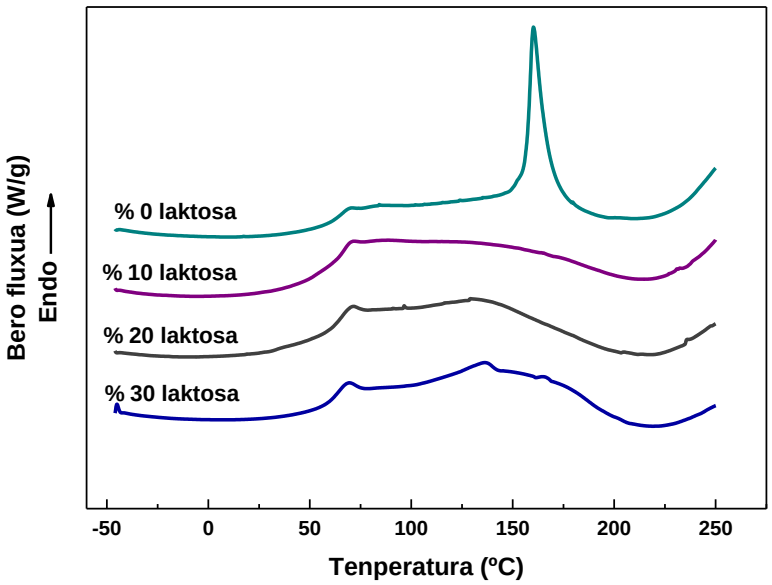

8.3 irudia Arrain gelatinazko biokonpositeen DSC termogramak, laktosa edukiaren funtziopean.

8.3.2 Propietate mekanikoak

Beirazko egoeratik goma-antzeko egoerarainoko trantsizioa DMA bidez aztertu zen eta beirazko trantsizio tenperatura (T_g), biltegiratze modulua (E') eta galera faktorea (tan δ) neurtu ziren. % 10 laktosadun biokonpositeentzat, **8.4 irudia**n erakusten den moduan, lehenengo T_g (T_{g1}) -100 eta -55 ºC artean ikusi zen, hidrogeno zubizko lotura fisikoen bidez gelatinari lotutako glizerol konposatuari zegokiona. Honek, gelatina eta glizerolaren artean erreakzio kimikorik ez zegoela iradoki zuen (Mathew eta Dufresne, 2002). 45 ºC-tarainoko tenperaturaren igoerak E'-ren mailakako txikitzea eragin zuen, kiribiletik helizerako transformazioagatik (Bigi, Panzavolta, eta Rubini, 2004) eta aldiz, E'-ren gainbehera bizkorra eta tan δ-ren banda estua 45-75 ºC-an ikusi ziren, arrain gelatinaren beirazko trantsizio tenperaturarekin (T_{g2}) lotu zirenak (Ghanbarzadeh eta Oromiehi, 2009), aurretik DSC-an 69 ºC-an ikusi moduan. 70 eta 100 ºC-ko tartean, goma-antzeko egonkortasuna ikusi zen.

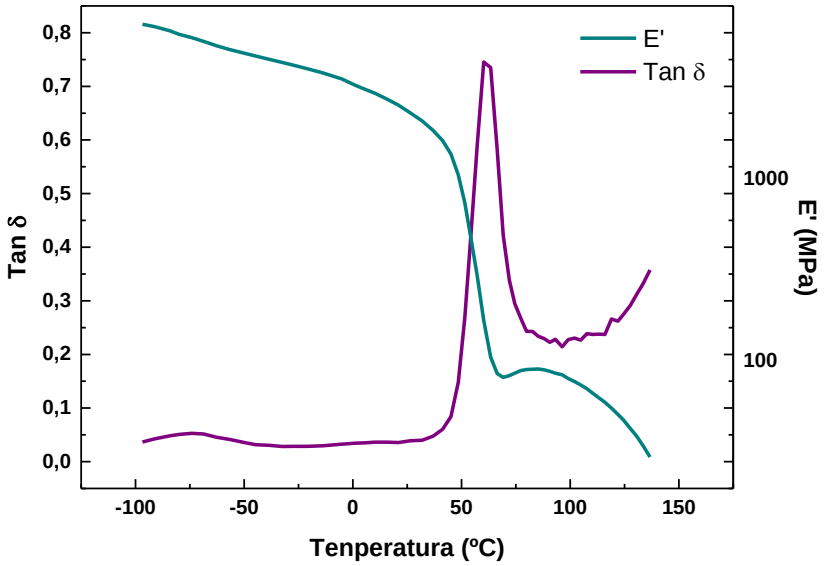

8.4 irudia % 10 laktosadun arrain gelatinazko biokonpositeen biltegiratze moduluaren (E') eta galera faktorearen (tan δ) balioak.

Lan honetan burutu zen bezala, tenperatura tarte hau laktosa bidez eraldatutako arrain gelatinazko materialak prozesatu nahi direnean erabili daiteke. Laktosa eduki handiagoko biokonpositeetan antzeko grafikoak lortu ziren, eta T_g balioak laktosa edukiaren funtziopean, **8.1 taula**n erakusten dira. Laktosaren edukia handitu zen heinean, T_g balioak txikitu egin ziren eta hau, seguru aski, erreakzionatu gabeko laktosaren efektu plastifikatzailearengatik izan zen (Suyatma, Tighzert, eta Copinet, 2005). Erreakzionatu gabeko laktosak, bere izaera higroskopikoagatik, ingurumenetik hezetasuna xurgatu zezakeen, kristalak eratuz, DSC-an ikusi zen bezala. Honela, bolumen librea handiagoa izan zitekeen, kateen mugimendua handituz eta T_g txikituz.

8.1 taula Glizerolaren (T_{g1}) eta gelatinaren (T_{g2}) beirazko trantsizio tenperaturak, laktosa edukiaren funtziopean

Laktosa (%)	T_{g1} (ºC)	T_{g2} (ºC)
0	-71,1	69,0
10	-74,1	66,4
20	-71,7	60,6
30	-72,9	58,3

Arrain gelatinazko biokonpositeen propietate mekanikoak aztertzeko, trakzio saiakuntza burutu zen eta tentsio-deformazio kurbak aztertu ziren, laktosa edukiaren funtziopean. Nahiz eta hausturan trakzio erresistentzia balioen artean ezberdintasun esanguratsurik (P > 0,05) ez egon, laktosa edukia kontuan hartu gabe, laktosa gehitzerakoan erantzun mekanikoan aldaketa nabaria ikusi zen (**8.5 irudia**). Laktosa gabeko biokonpositearen portaera plastikoa, gelatina eta glizerolaren arteko hidrogeno zubizko interakzio fisikoei egokitu zitzaien, deformazioa jasaten ari zen material zurrun batean geratuz, biokonpositearen egitura porotsuarekin bat eginez (Gibson eta Ashby, 1999), behean erakusten den bezala. Laktosa bidez eraldatutako biokonpositeen tentsio-deformazio kurba hiru eremu ezberdinez osatuta zegoen: eremu lineal elastikoa, egonkorra zen eremu zurruna eta saretze kimikoak eragindako biokonpositearen dentsitatearen txikitzeari elkartutako tentsioaren igoera linealaren azken eremua.

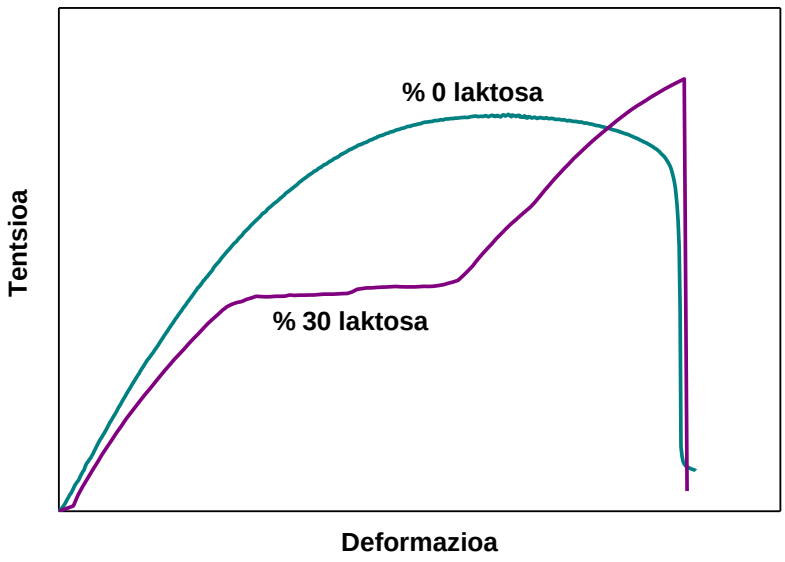

8.5 irudia Laktosadun arrain gelatinazko biokonpositeen tentsio-deformazio kurbak.

Tentsio-deformazio portaeraz gain, Young modulua (E), trakzio erresistentzia (TS) eta haustura elongazioa (EB) neurtu ziren eta balioak **8.2 taula**n erakusten dira. Laktosa gehitu zenean, E balioak txikitu ziren ($P < 0,05$), azukre kantitatea kontuan hartu gabe. DSC-ko emaitzek erakutsi zuten bezala, laktosaren gehikuntzak saretzea sustatu zuen, proteina kateen molekularteko interakzioak gutxituz eta kolagenoaren berezko helize hirukoitzaren berrantolaketa oztopatuz (Zaman eta Beg, 2015). Beraz, arrain gelatinazko biokonpositeen zurruntasuna txikitu zen, DMA-ko emaitzekin bat eginez. Trakzio erresistentziari zegokionez, laktosaren gehikuntzak balio hauetan ez zuen eragin esanguratsurik ($P > 0,05$) izan, eta 20 MPa inguruko balioetan mantendu ziren. Haustura elongazioari dagokionez berriz, laktosa gehitzerakoan balio hauek % 5 arte igo ziren eta hau, seguruenik erreakzionatu gabeko laktosaren plastifikatzaile izaeragatik izan zen, DMA bidez erakutsi zen moduan.

8.2 taula Arrain gelatinazko biokonpositeen propietate mekanikoak, laktosa edukiaren funtziopean.

Laktosa (%)	E (MPa)	TS (MPa)	EB (%)
0	1396 ± 120^{a}	20 ± 2^{a}	$1,9 \pm 0,1^{a}$
10	906 ± 107^{b}	22 ± 1^{a}	$5,6 \pm 0,4^{b}$
20	857 ± 70^{b}	20 ± 3^{a}	$5,4 \pm 1,1^{b}$
30	925 ± 147^{b}	18 ± 2^{a}	$4,8 \pm 0,2^{b}$

[a-b] Zutabe berean letra bera duten bi balio ez dira esanguratsuki ($P > 0,05$) desberdinak Tukey-ren froga anizkoitzaren arabera.

8.3.3 Biokonpositeen egitura

Biokonpositeen propietateetan laktosa edukiaren eragina azaltzeko, hauen egitura ezagutzea funtsezkoa da eta beraz, arrain gelatinazko biokonpositeen kristalinitatea eta morfologia aztertzeko, XRD eta SEM analisiak burutu ziren. **8.6 irudia**n ikusi daitekeen bezala, difraktogramek bi difrakzio banda erakutsi zituzten: 21º-etako banda, gelatinaren kristalinitatearekin erlazionatu zena, eta 7,4º-tako banda, kolageno natiboaren helize hirukoitzaren hondarrari egokitu zitzaiona (Bigi, Panzavolta, eta Rubini, 2004). Laktosaren edukia handitu zenean, gelatinaren kristalinitatea handitu zen, honen eta laktosaren artean sortutako lotura kobalenteen eraketarengatik egitura ordenamendu handiagoa eman zela adieraziz (Etxabide et al., 2015b). Horretaz gain,

erreakzionatu gabeko laktosak hezetasuna xurgatu zezakeen, ondoren kristalizatuz, laktosa edukiaren handitzearekin DSC-ko 137 ºC-ko kristalinitatearen bandaren igoerarekin bat etorriz. Aldiz, helize hirukoitzaren hondarra txikitu zen, saretzearengatik proteinaren kateen molekularteko interakzioen txikitzeak helize hirukoitzaren hondarraren berrantolaketa ekidin zuelako. Emaitza hauek, trakzio erresistentzia bidez neurturiko Young moduluaren txikitzearekin bat zetozen.

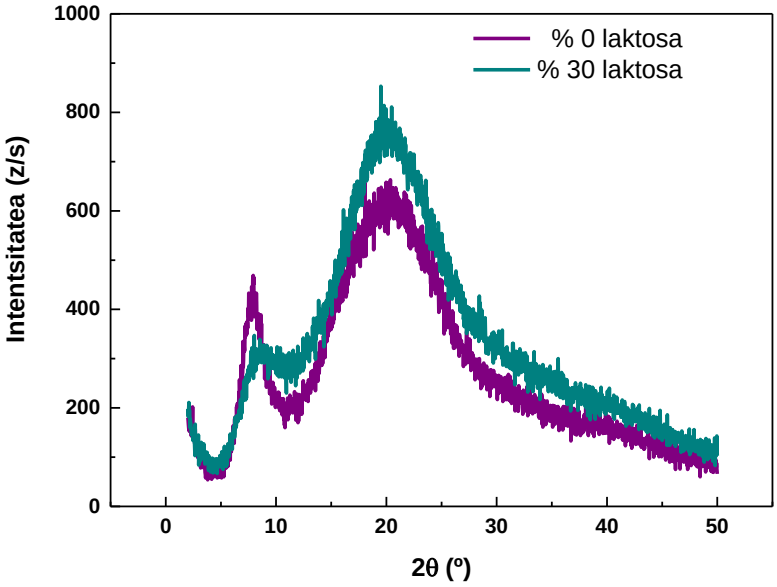

8.6 irudia % 0 eta % 30 laktosadun arrain gelatinazko biokonpositeen XRD emaitzak.

Arrain gelatinazko biokonpositeen egituraren analisi sakonagoa egiteko, materialen haustura gainazalen SEM mikrografiak aztertu ziren (**8.7 irudia**).

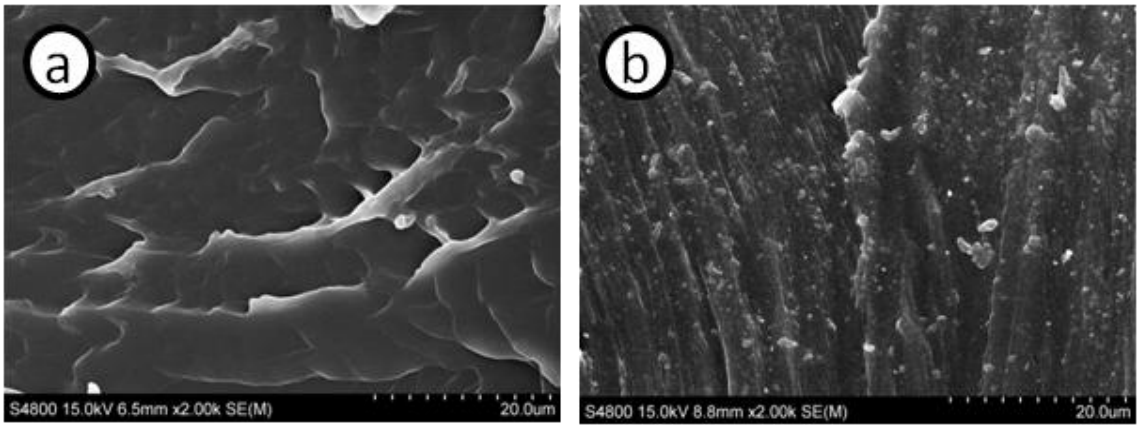

8.7 irudia a) % 0 laktosadun eta b) % 30 laktosadun arrain gelatinazko biokonpositeen SEM irudiak.

Biokonpositeen egitura ezkata itxurako egituratik (**8.7a irudia**) zuntz itxurako egiturara (**8.7b irudia**) aldatu zen. Azken honetan, laktosa gehitu zenean, erreakzionatu gabeko laktosa kristalak zuntzen inguruan ikusi ziren, XRD bidez ikusitako egitura ordenatuago batekin bat etorriz.

8.3.4 Biokonpositeen handitzea

Handitze-azterketa burutu zen eta murgilketa aurretik eta ondoren ateratako laginen irudiak **8.8 irudia**n erakusten dira. Ikusi daitekeen moduan, laktosadun laginek kolore arrexka erakutsi zuten, melanoidinak izenez ezagunak diren arrexka koloreko pigmentu disolbaezinen eraketagatik (Jiang eta Brodkorb, 2012). Aipatzekoa da, biokonposite guztiek beraien egitura oso-osorik mantendu zutela, hauek uretan 4320 minutuz (3 egun) murgilduta egon ostean. Hala ere, laktosadun laginen ura xurgatzeko gaitasuna txikiagoa zen laktosarik gabeko biokonpositeetan baino, erreakzioak likidoak xurgatzeko ahalmenean eragiten zuela iradokiz. Laktosa gehitu zenean, saretzea handitu zen eta beraz, likidoaren difusioa laginean zehar txikitu zen (Saarai et al., 2013).

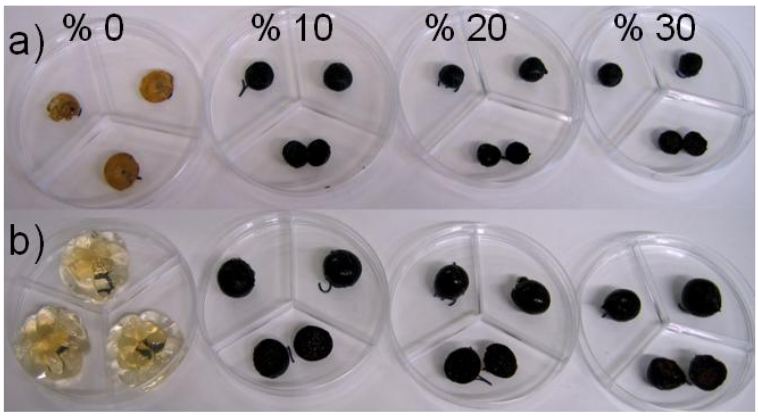

8.8 irudia Arrain gelatinazko biokonpositeak laktosa edukiaren arabera, a) murgilketa aurretik eta b) 4320 minutuz murgilduta egon ostean.

Honetaz gain, handitze-zinetika aztertu zen eta emaitzak **8.9a** eta **8.9b irudi**etan erakusten dira. Laginek, 4320 minututaraino bigarren mailako zinetika aurkeztu zuten (**8.9a irudia**), 480 minututaraino lehenengo mailako zinetika erakusten

zuten bitartean (**8.9b irudia**). Alde batetik, laktosarik gabeko laginak 480 minutu ostean % 230, eta 4320 minutu ostean % 1500 handitu ziren, handitze lineala denboran zehar erakutsiz. Bestaldetik, laktosaren gehikuntzak handitzea esanguratsuki txikitu zuen, 480 minutuan % 150-eko balioak eta 4320 minuturaino, saretze kimikoarengatik, % 250 inguruko balio konstanteak erakutsiz. Hala ere, laktosa edukiaren handitzearekin, handitze-balioak pittin bat igo ziren eta hau erreakzionatu gabeko laktosaren izaera higroskopikoagatik izan zen. Behaketa hauek, DSC eta DMA bidez lortutako emaitzekin bat egin zuten.

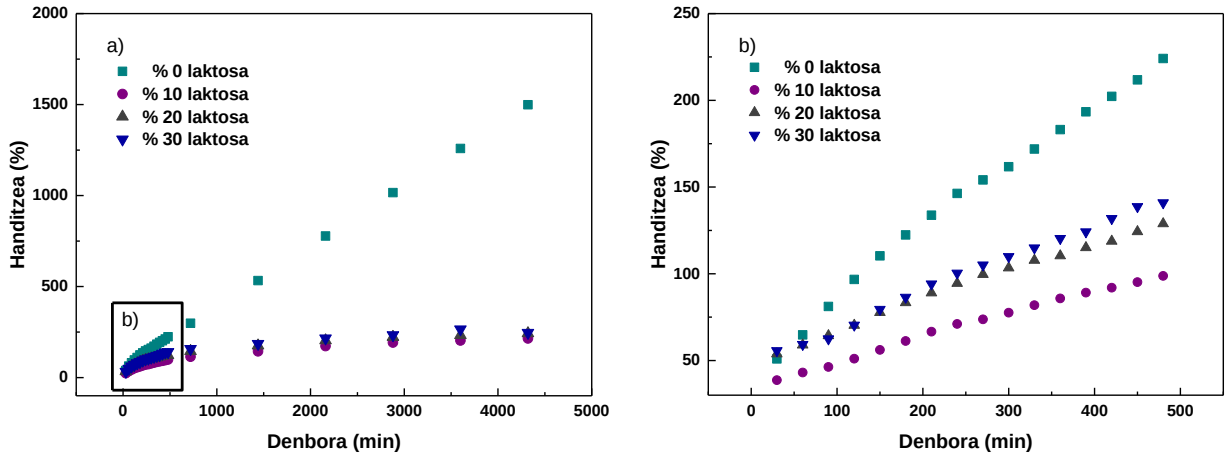

8.9 irudia a) 4320 minututaraino (3 egun) eta b) 480 minututaraino (8 ordu) arrain gelatinazko biokonpositeen handitze-balioak, laktosa edukiaren arabera.

Saretze eta handitze-prozesuetan masa eta bolumen aldaketak gertatu zirenez, dentsitatearen eta porositatearen balioak kalkulatu ziren eta hauek **8.3 taula**n azaltzen dira. Ikusi daitekeen moduan, kontrol-biokonpositeek (berotu gabeko biokonpositeek) eta laktosarik gabeko berotutako biokonpositeek antzeko dentsitateak ($P > 0,05$) erakutsi zituzten, giro tenperaturan uraren dentsitatea (0,997 g/mL) baino balio altuagoak aurkeztuz. Hala ere, laktosa edukia igotzerakoan, berokuntza ondotik dentsitatearen txikitze esanguratsua ($P < 0,05$) ikusi zen eta dentsitatearen balioak uraren dentsitatearenak baino txikiagoak ziren. Portaera hau, glizerolaren eta erreakzionatu gabeko laktosaren lekutzeagatik izan zitekeen edota saretze

kimikoagatik gelatinaren egituran eragindako bolumen handitzearen ondorioz gerta zitekeen (Learner et al., 2008).

8.3 taula Arrain gelatinazko biokonpositeen dentsitate eta porositate balioak, laktosa edukiaren funtziopean.

Laktosa (%)	$\rho_{kontrola}$ (g/mL)	ρ_x (g/mL)	Porositatea (%)
0	1,34 ± 0,06[a]	1,20 ± 0,04[a]	---
10	1,33 ± 0,04[a]	0,87 ± 0,01[b]	36,54 ± 1,53[d]
20	1,29 ± 0,12[a]	0,58 ± 0,01[c]	53,83 ± 4,43[e]
30	1,32 ± 0,09[a]	0,41 ± 0,03[c]	68,78 ± 0,45[f]

[a-f] Zutabe berean letra bera duten bi balio ez dira esanguratsuki (P > 0,05), desberdinak Tukey-ren froga anizkoitzaren arabera.

Porositatearen balioak handitu zirenez, arrain gelatinazko biokonpositeen egitura aldaketa azaltzeko SEM analisia burutu zen. Ikusi daitekeen moduan, laktosarik gabeko laginetan hutsune batzuk zituen gainazal homogeneoak eta leunak lortu ziren (**8.10a irudia**). Aldiz, % 30 laktosa gehitu zenean, egitura oso porotsua ikusi zen (**8.10b irudia**). Portaera hau, handitze-prozesuan zehar glizerolaren eta erreakzionatu gabeko laktosaren lekutzearekin bat zetorren, laktosa kantitate handiagoko laginetan poro gehiago ikusi zirelako. Dentsitate baxuko egitura porotsu hauek konposatu aktiboak garraiatzeko interesgarriak izan zitezkeen.

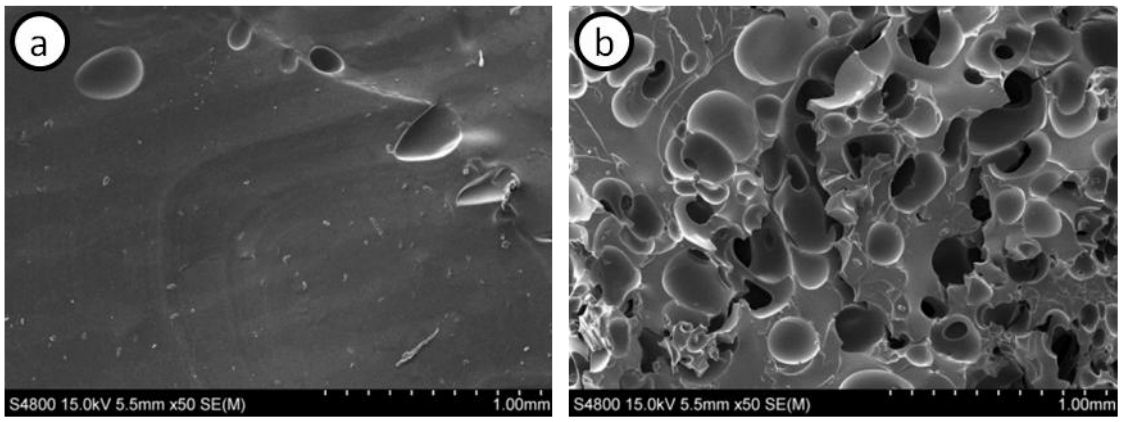

8.10 irudia a) % 0 eta b) % 30 laktosadun arrain gelatinazko filmen SEM irudiak, 4320 minutuz PBS-n murgilduta egon ostean.

Handitze-prozesuan zehar pisu molekular baxuko konposatuen lekutzea aztertzeko, arrain gelatinazko biokonpositeak FTIR espektroskopia bidez aztertu ziren.

Murgilketa aurretik eta 4320 minutuz murgilduta egon osteko biokonpositeen FTIR espektroak **8.11 irudia**n erakusten dira. Ikusi daitekeen bezala, laktosarik gabeko filmetan glizerolaren banda bereizgarria desagertu zen, plastifikatzailearen lekutzea eta glizerolaren eta gelatinaren arteko interakzioak nagusiki hidrogeno zubizko loturak zirela iradokiz (Guerrero et al., 2011b). Bestaldetik, erreakzionatu gabeko laktosaren lekutzeagatik, **8.11b irudia**n laktosa banden intentsitateen txikitze nabaria ikusi zen.

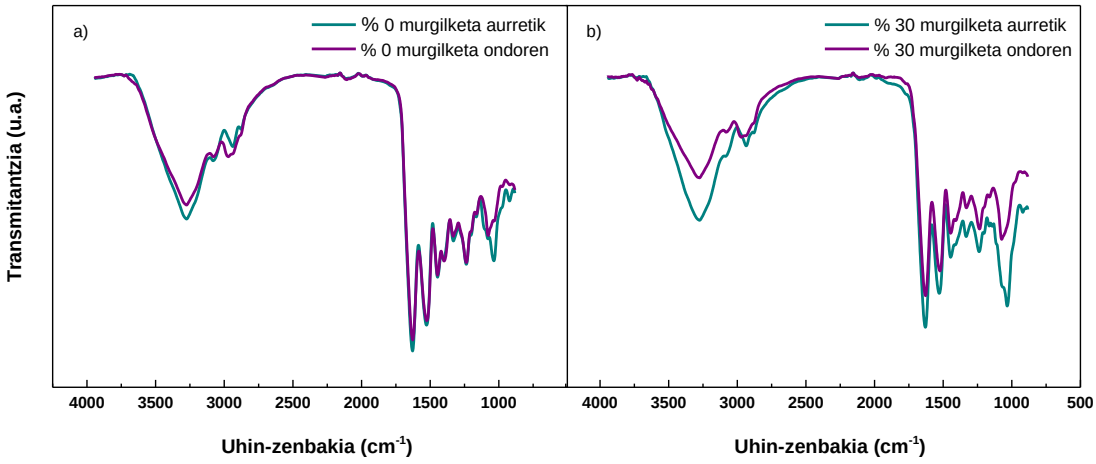

8.11 irudia a) % 0 laktosadun eta b) % 30 laktosadun arrain gelatinazko biokonpositeen FTIR espektroak, PBS-n murgildu aurretik eta ondoren.

8.3 Ondorioak

Gelatinazko pelletak estrusio bidez lortu ziren eta ondoren hauek injektatu egin ziren, gelatinan oinarritutako biokonpositeak ekoizteko. Saretze kimikoa, laktosaren gehikuntzarekin eta berotzearekin sustatu zen erreakzio ez-entzimatikoaren eraginez gertatu zen. Saretze honek, SEM bidez ikusitako egitura porotsuaren eraketarengatik, gelatinazko biokonpositeen disolbagarritasuna, handitzea eta dentsitatea txikitu zituen. Gainera, laktosa edukiaren handitzeak kristalinitatearen handitzea eragin zuen, DSC bidez ikusi zena, eta helize hirukoitza egitura txikiarazi zuen, XRD emaitzekin ziurtatu zena, trakzio analisi bidez ikusitako modulu elastikoaren txikitzearekin bat etorriz. Azkenik, laktosaren gehikuntzarekin gertatutako haustura elongazioaren handitzeak eta beirazko trantsizio tenperaturaren txikitzeak, prestatutako biokonpositeetan

erreakzionatu gabeko laktosak plastifikatzaile moduan jokatu zezakeela erakutsi zuten. Emaitza hauek, erreakzio ez-entzimatiko bidez saretutako gelatinek, hobetutako propietateak dituzten biokonpositeak garatzeko hurbilketa berri bat eman zutela adierazi zuten.

9 Ondorio orokorrak

Kapitulu honetan, tesian zehar aurkeztutako ikerlan guztien ondorio orokorrak azaltzen dira:

- UV argiarekiko erresistentzia eta trakzio erresistentzia handiko arrain gelatinazko film homogeneoak eta gardenak prestatu ziren. Propietate funtzional hauek elikagaien paketatze aplikazioetan elikagaien iraungitzea luzatzeko film hauen gaitasuna nabarmendu zuten.
- Zaborren kudeaketa errazteaz gain, material ez-biodegradagarrien kontsumoa gutxiagotzeko bizi amaierako fasean konpostaren ingurumen-inpaktu positiboek filmak epe motzeko paketatze aplikazioetan erabiltzea sustatu zuten.
- Laktosaren gehikuntzak gelatinaren egituran eragin zuen, bereziki berokuntza ostean Maillard erreakzioa sustatu zelako. Aplikazio zehatzetarako eskakizunen arabera erreakzioaren hedapena soluzioaren pH-aren bidez kontrolatu zitekeen.
- pH azidoan, saretze erreakzioaren hedapena txikiagoa izan zen, guztiz disolbagarriak ziren filmak lortuz. Hauek, fluxu gastrikoekin kontaktuan dauden film aktibo moduan erabili zitezkeen.
- pH basikoan, saretze erreakzioaren hedapena handia izan zen, urarekiko erresistentzia handiko UV argiarekiko babes-filmak lortuz eta beraz, paketatze aplikazioetarako film egokiak prestatu ziren. Horretaz gain, biokonpatibilitate eta zelulen ugalketarako propietate bikainek, filmek aplikazio farmazeutikoetan, hala nola, zaurien sendaketan erabiltzeko propietate egokiak erakutsi zituzten.
- Laktosadun gelatinazko filmek antioxidatzaile ahalmena erakutsi zuten, Maillard erreakzioan sortutako konposatu fenolikoengatik.
- Filma eratzeko soluzioetan THC konposatua gehitzeak, prestatutako filmen ahalmen antioxidatzailea nabarmenki handitu zuen, paketatze aktiboan elikagaien kalitatea hobetzeko film hauen gaitasuna erakutsiz.

- Gelatinazko xaflak eta biokonpositeak lortzeko, estrusio eta injekzio parametroak optimizatu ziren. Egitura porotsuaren eraketak biokonpositeen disolbagarritasuna, handitzea eta dentsitatea txikitu zituen.
- Formulazioak eta prozesatze baldintzak optimizatu ziren, industri-mailan gaur egun eskuragarri dauden teknika bidez gelatinazko materialak ekoizteko.

10 Erreferentziak

Ahmad, M., Benjakul, S., Prodpran, T., eta Agustini, T.W. (2012). Physico-mechanical and antimicrobial properties of gelatin film from the skin of unicorn leatherjacket incorporated with essential oils. *Food Hydrocolloids*, 28, 189-199.

Ali Poursamar, S., Lehner, A.N., Azami, M., Ebrahimi-Barough, S., Samadikuchaksaraei, A., eta Antunes, A.P.M. (2016). The effects of crosslinkers on physical, mechanical, and cytotoxic properties of gelatin sponge prepared *via in-situ* gas foaming method as a tissue engineering scaffold. *Mater Sci Eng*, 63, 1-9.

Ali, J., Md, S., Baboota, S., eta Sahni, J.K. (2012). Polymeric nanoparticles, magnetic nanoparticles and quantum dots: current future perspectives. In *Patenting nanomedicines*. Souto, E.B. (Ed.). Berlin, Springer-Verlag, pp. 107-110.

Anbinder, P.S., Peruzzo, P.J., Martino, M.N., eta Amalvy, J.I. (2015). Effect of antioxidant active films on the oxidation of soybean oil monitored by Fourier infrared spectroscopy. *J Food Eng*, 151, 43-50.

Arfat, Y.A., Benjakul, S., Vongkamjan, K., Sumpavapol, P., eta Yarnpakdee, S. (2015). Shelf-life extension of refrigerated sea bass slices wrapped with fish protein isolate/fish skin gelatin-ZnO nanocomposite film incorporated with basil leaf essential oil. *J Food Sci Technol*, 52, 6182-6193.

Arrieta, M.P., Fortunati, E., Dominici, F., Rayón, E., López, J., eta Kenny, J.M. (2014). PLA-PHB/cellulose based films: mechanical, barrier and disintegration properties. *Polym Degrad Stab*, 107, 139-149.

ASTM D1708-93(1993). Standard test method for tensile properties of plastics by use of microtensile specimens. In *Annual Book of ASTM Standards*. Philadelphia: American Society for Testing Materials.

ASTM D523-14 (2014). Standard test method for specular gloss. In *Annual Book of ASTM Standards*. Philadelphia: American Society for Testing Materials.

ASTM D570-98 (1998). Standard test method for water absorption of plastics. In *Annual Book of ASTM Standards*. Philadelphia: American Society for Testing Materials.

ASTM E96-00 (2000). Standard test methods for water vapour transmission of material. In *Annual Book of ASTM Standards.* Philadelphia: American Society for Testing Materials.

Atarés, L. eta Chiralt, A. (2016). Essential oils as additives in biodegradable films and coatings for active food packaging. *Trends Food Sci Technol*, 48, 51-62.

Bandyopadhyay, P., Ghosh, A.K., eta Ghosh, C. (2012). Recent developments on polyphenol-protein interactions: effects on tea and coffee taste, antioxidant properties and the digestive system. *Food Funct*, 3, 592-605.

Bare, J.C., Hofstetter, P., Pennington, D.W., eta Udo de Haes, H.A. (2000). Midpoints versus endpoints: the sacrifices and benefits. *Int J Life Cycle Assess*, 5, 319-326.

Basu, S., Shivhare, U.S., Singh, T.V., eta Beniwal, V.S. (2011). Rheological, texture and spectral characteristics of sorbitol substituted mango jam. *J Food Eng*, 105, 503-512.

Benbettaïeb, N., Assifaoui, A., Karbowiak, T., Debeaufort, F., eta Chambin, O. (2016a). Controlled release of tryrosol and ferulic acid encapsulated in chitosan-gelatin films after electron beam irradiation. *Radiat Phys Chem*, 118, 81-86.

Benbettaïeb, N., Chambin, O., Assifaoui, A., Al-Assaf, S., Karbowiak, T., eta Debeaufort, F. (2016b). Release of coumarin incorporated into chitosan-gelatin irradiated films. *Food Hydrocolloids*, 56, 266-276.

Benbettaïeb, N., Chambin, O., Karbowiak, T., eta Debeaufort, F. (2016c). Release behavior of quercetin from chitosan-fish gelatin edible films influenced by electron beam irradiation. *Food Control*, 66, 315-319.

Benetto, E., Jury, C., Igos, E., Carton, J., Hild, P., Vergne, C., eta Di Martino, J. (2015). Using atmospheric plasma to design multilayer film from polylactic acid and thermoplastic starch: a screening life cycle assessment. *J Cleaner Prod*, 87, 953-960.

Benjakul, S., Kittiphattanabawon, P., eta Regenstein, J.M. (2012). Fish gelatin. In *Food Biochemistry and Food*. Simpson, B.K., Nollet, L.M.L., eta Toldrae, F. (Eds). John Wiley eta Sons Inc, Ames, IA, USA, pp. 388-405.

Bergo, P. eta Sobral, P.J.A. (2007). Effects of plasticizer on physical properties of pigskin gelatin films. *Food Hydrocolloids*, 12, 1285-1289.

Bhat, R. eta Karim, A.A. (2014). Towards producing novel fish gelatin films by combination treatments of ultraviolet radiation and sugars (ribose and lactose) as cross-linking agents. *J Food Sci Technol*, 51, 1329-1333.

Bhat, S.A., Sohail, A., Siddiqui, A.A., eta Bano, B. (2014). Effect of non-enzymatic glycation on cystatin: a spectroscopy study. *J Fluoresc*, 24, 1107-1117.

Bhutani, U., Laha, A., Mitra, K., eta Majumdar, S. (2016). Sodium alginate and gelatin hydrogels: viscosity effect on hydrophobic drug release. *Mater Lett*, 164, 76-79.

Bigi, A., Panzavolta, S., eta Rubini, K. (2004). Relationship between triple-helix content and mechanical properties of gelatin films. *Biomaterials*, 25, 5675-5680.

Biscarat, J., Charmette, C., Sanchez, J., eta Pochat-Bohatier, C. (2015). Preparation of dense gelatin membranes by combining temperature induced gelation and dry-casting. *J Membr Sci*, 473, 45-53.

Bitencourt, C.M., Fávaro-Trindade, C.S., Sobral, P.J.A., eta Carvalho, R.A. (2014). Gelatin-based films additivated with curcuma ethanol extract: antioxidant activity and physical properties of films. *Food Hydrocolloids*, 40, 145-152.

Bolumar, T., Andersen, M.L., eta Orlien, V. (2011). Antioxidant active packaging for chicken meat processed by high pressure treatment. *Food Chem*, 129, 1406-1412.

Boulekbache-Makhlouf, L., Slimani, S., eta Madani, K. (2013). Total phenolic content, antioxidant and antibacterial activities of fruits of *Eucalyptus globulus* cultivated in Algeria. *Ind Crops Prod*, 41, 85-89.

Bower, C.K., Avena-Bustillos, R.J., Olsen, C.W., Mchugh, T.H., eta Bechtel, P.J. (2006). Characterization of fish-skin gelatin gels and films containing the antimicrobial enzyme lysozyme. *J Food Sci*, 71, 141-145.

Bravin, B., Pressini, D., eta Sensidoni, A. (2006). Development and application of polysaccharide-lipid edible coating to extend shelf-life of dry bakery products. *J Food Eng*, 76, 280-290.

Calderón, L.A., Iglesias, L., Laca, A., Herrero, M., eta Díaz, M. (2010). The utility of life cycle assessment in the ready meal food industry. *Resour Conserv Recycl*, 54, 1196-1207.

Carlsen, M.H., Halvorsen, B.L., Holte, K., Bøhn, S.K., Dragland, S., Sampson, L., Willey, C., Senoo, H., Umezono, Y., Sanada, C., Barikmo, I., Berhe, N., Willett, W.C., Phillips, K.M., Jacobs, D.R., eta Blomhoff, R. (2010). The total antioxidant content of more than 3100 foods, beverages, spices, herbs and supplements used worldwide. *Nutr J*, 9, 1-11.

Carvalho, R.A. eta Grosso, C.R.F. (2004). Characterization of gelatin based films modified with transglutaminase, glyoxal and formaldehyde. *Food Hydrocolloids*, 18, 717-726.

Chen, Z., Wang, L., eta Jiang, H. (2012). The effect of procyanidine crosslinking on the properties of the electrospun gelatin membranes. *Biofabrication*, 4, 1-11.

Chiou, B., Avena-Bustillos, R.J., Bechtel, P.J., Jafri, H., Narayan, R., Imam, S.H., Glenn, G.M., eta Orts, W.J. (2008). Cold water fish gelatin films: Effects of cross-linking on thermal, mechanical, barrier, and biodegradation properties. *Eur Polym J*, 44, 3748-3753.

Chiou, B.S., Avena-Bustillos, R.J., Shey, J., Yee, E., Bechtel, P.J., eta Imam, S.H. (2006). Rheological and mechanical properties of cross-linked fish gelatins. *Polymer*, 47, 6379-6386.

Coppola, M., Djabourov, M., eta Ferrand, M. (2008). Phase diagram of gelatin plasticized by water and glycerol. *Macromol Symp*, 273, 56-65.

Costa, D.C., Costa, H.S., Albuquerque, T.G., Ramos, F., Castilho, M.C., eta Sanches-Silva, A. (2015). Advances in phenolic compounds analysis of aromatic plants and their potential applications. *Trends Food Sci Technol*, 45, 336-354.

Crizel, T.M., Costa, T.M.H., Rios, A.O., eta Flôres, S.H. (2016). Valorization of food-grade industrial waste in the obtaining active biodegradable films for packaging. *Ind Crops Prod*, 87, 218-228.

Cuq, B., Gontard, N., Cuq, J.L., eta Guilbert, S. (1996). Functional properties of myofibrillar protein-based biopackaging as affected by film thickness. *J Food Sci*, 61, 580-584.

Cuzzoni, M.T., Stoppini, G., Gazzani, G., eta Mazza, P. (1988). Influence of water activity and reaction temperature of ribose-lysine and glucose-lysine Maillard systems on mutagenicity, absorbance and content of furfurals. *Food Chem Toxicol*, 26, 815-822.

Da Silva, B.V., Barreira, J.C.M., eta Oliveira, M.B.P.P. (2016). Natural phytochemicals and probiotics as bioactive ingredients for functional foods: extraction, biochemistry and protected-delivery technologies. *Trends Food Sci Technol*, 50, 144-158.

Da Silva, G.P., Mack, M., eta Contiero, J. (2009). Glycerol: a promising and abundant carbon source for industrial microbiology. *Biotechnol Adv*, 1, 30-39.

Deligianni, D.D., Katsala, N., Ladas, S., Sotiropoulou, D., Amedee, J., eta Missirlis, Y.F. (2001). Effect of surface roughness of the titanium alloy Ti-6Al-4V on human bone marrow cell response and on protein adsorption. *Biomaterials*, 22, 1241-1251.

Deng, Y., Achten, W.M.J., Van Acker, K., eta Duflou, J.R. (2013). Life cycle assessment of wheat gluten powder and derived packaging film. *Biofuels Bioprod Biorefin*, 7, 429-458.

Deyl, Z., Mikšík, I., Zicha, J., eta Jelínková, D. (1997). Reversed-phase chromatography of pentosidine-containing CNBr peptides from collagen. *Anal Chim Acta*, 352, 257-270.

Díaz-Visurraga, J., Meléndrez, M.F., García, A., Paulraj, M., eta Cárdenas, G. (2010). Semitransparent chitosan-TiO_2 nanotubes composite film for food package applications. J *Appl Polym Sci*, 116, 3503-3515.

Djilani, A. eta Dicko, A. (2012). The therapeutic benefits of essential oils. INTECH.

Duconseille, A., Astruc, T., Quintana, N., Meersman, F., eta Sante-Lhoutellier, V. (2015). Gelatin structure and composition linked to hard capsule dissolution: A review. *Food Hydrocolloids*, 43, 360-376.

Duncan, S.E. eta Chang, H.H. (2012). Implications of light energy on food quality and packaging selection. In *Advances in Food and Nutrition Research.* Taylor, S. (Ed.). Elsevier, San Diego, pp. 25-73.

El Asbahani, A., Milada, K., Badri, W., Sala, M., Addi, E.H.A., Casabianca, H., El Mousadik, A., Hartmann, D., Jilale, A., Renaud, F.N.R., eta Elaissari, A. (2015). Essential oils: From extraction to encapsulation. *Int J Pharm*, 483, 220-243.

Embuscado, M.E. (2015). Spices and herbs: natural sources of antioxidants - a mini review. *J Funct Foods*, 18, 811-819.

Etxabide, A., Guerrero, P., eta de la Caba, K. (2016). A novel approach to manufacture porous biocomposites using extrusion and injection moulding. *Eur Polym J*, 82, 324-333.

Etxabide, A., Leceta, I., Cabezudo, S., Guerrero, P., eta de la Caba, K. (2016a). Sustainable fish gelatin films: from food processing waste to compost. *ACS Sustainable Chem Eng*, 4, 4626-4634.

Etxabide, A., Uranga, J., Guerrero, P., eta de la Caba, K. (2015a). Improvement of barrier properties of fish gelatin films promoted by gelatin glycation with lactose at high temperatures. *LWT-Food Sci Technol*, 63, 315-321.

Etxabide, A., Uranga, J., Guerrero, P., eta de la Caba, K. (2016). Development of active gelatin films by means of valorisation of food processing waste: a review. *Food Hydrocolloids*, 68, 192-198.

Etxabide, A., Urdanpilleta, M., Guerrero, P., eta de la Caba, K. (2015b). Effects of cross-linking in nanostructure and physicochemical properties of fish gelatin for bio-applications. *React Funct Polym*, 94, 55-62.

Fabian, H. eta Mäntele, W. (2002). Infrared spectroscopy of proteins. In *Handbook of Vibrational Spectroscopy*. Chalmer, J.M. eta Griffiths, P.R. (Eds.). John Wiley eta Sons, Chichester, UK, pp. 3399-3426.

Fakhouri, F.M., Costa, D., Yamashita, F., Martelli, S.M., Jesus, R.C., Alganer, K., Collares-Queiroz, F., eta Innocentini-Mei, L.H. (2013). Comparative study of processing methods for starch/gelatin films. *Carbohydr Polym*, 20, 681-689.

Farris, S., Song, J., eta Huang, Q. (2010). Alternative reaction mechanism for the cross-linking of gelatin with glutaraldehyde. *J Agric Food Chem*, 58, 998-1003.

Freile-Pelegrín, Y. eta Robledo, D. (2014). Bioactive phenolic compounds from algae. In *Bioactive compounds from marine foods: plant and animal sources*. Hernández-Ledesma, B. eta Herrero, M. (Eds.) John Wiley eta Sons, Ltd., Chichester, UK, pp. 131-152.

Garrido, T., Etxabide, A., Leceta, I., Cabezudo, S., de la Caba, K., eta Guerrero, P. (2014). Valorization of soya by-products for sustainable packaging. *J Cleaner Prod*, 64, 228-233.

Garrido, T., Etxabide, A., Peñalba, M., de la Caba, K., eta Guerrero, P. (2013). Preparation and characterization of soy protein thin films: processing-properties correlation. *Mater Lett*, 105, 110-112.

Ghanbarzadeh, B. eta Oromiehi, A.R. (2009). Thermal and mechanical behavior of laminated protein films. *J Food Eng*, 90, 517-524.

Ghoshal, S., Stapf, S., eta Mattea, C. (2014). Protein renaturation in the gelatin film formation process. *Appl Magn Reson*, 45, 145-154.

Gibson, L.J. eta Ashby, M.F. (1999). Cellular solids: structure and properties. Cambridge University Press, Cambridge.

Giménez, B., Gómez-Guillén, M.C., López-Caballero, M.E., Gómez-Estaca, J., eta Montero, P. (2012). Role of sepiolite in the release of active compounds from gelatin-egg white films. *Food Hydrocolloids*, 27, 475-486.

Giménez, B., López de Lacey, A., Pérez-Santín, E., López-Caballero, M.E., eta Montero, P. (2013). Release of active compounds from agar and agar-gelatin films with green tea extract. *Food Hydrocolloids*, 30, 264-271.

Gómez-Estaca, J., Giménez, B., Gómez-Guillén, C., eta Montero, P. (2010a). Influence of frozen storage on aptitude of sardine and dolphinfish for cold-smoking process. *LWT-Food Sci Technol*, 43, 1246-1252.

Gómez-Estaca, J., Gómez-Guillén, M.C., Fernández-Martin, F., eta Montero, P. (2011). Effect of gelatin origin, bovine-hide and tuna-skin, on the properties of compound gelatin-chitosan films. *Food Hydrocolloids*, 25, 1461-1469.

Gómez-Estaca, J., López de Lacey, A., López-Caballero, M.E., Gómez-Guillén, M.C., eta Montero, P. (2010b). Biodegradable gelatin-chitosan films incorporated with essential oils as antimicrobial agents for fish preservation. *Food Microbiol*, 27, 889-896.

Gómez-Guillén, M.C., Giménez, B., López-Caballero, M.E., eta Montero, M.P. (2011). Functional and bioactive properties of collagen and gelatin from alternative sources: a review. *Food Hydrocolloids*, 25, 1813-1827.

Gómez-Guillén, M.C., Pérez-Mateos, M., Gómez-Estaca, J., López-Caballero, E., Giménez, B., eta Montero, P. (2009). Fish gelatin: a renewable material for developing active biodegradable films. *Trends Food Sci Technol*, 20, 3-16.

Gómez-Guillén, M.C., Turnay, J., Fernandez-Diaz, M.D., Ulmo, N., Lizarbe, M.A., eta Montero, P. (2002). Structural and physical properties of gelatin extracted from different marine species: a comparative study. *Food Hydrocolloids*, 16, 25-34.

Guadipati, V. (2013). Fish gelatin: a versatile ingredient for the food and pharmaceutical industries. In *Marine Proteins and Peptides-Biological activities and applications*. Kim, S.K. (Ed.). John Wiley eta Sons, Ltd, West Sussex, UK, Chapter 13.

Guerrero, P., Beatty, E., Kerry, J.P., eta de la Caba, K. (2012). Extrusion of soy protein with gelatin and sugars at low moisture content. *J Food Eng*, 110, 53-59.

Guerrero, P., Etxabide, A., Leceta, I., Peñalba, M., eta de la Caba, K. (2014). Extraction of agar from *Gelidium sesquipedale* (*Rodhopyta*) and surface characterization of agar based films. *Carbohydr Polym*, 99, 491-489.

Guerrero, P, Kerry, J.P., eta de la Caba, K. (2014). FTIR characterization of protein-polysaccharide interactions in extruded blends. *Carbohyd Polym*, 111, 598-605.

Guerrero, P., Nur Hanani, Z.A., Perry, J.P., eta de la Caba, K. (2011a). Characterization of soy protein-based films prepared with acids and oils by compression. *J Food Eng*, 107, 41-49.

Guerrero, P., Stefani, P.M., Ruseckaite, R., eta de la Caba, K. (2011b). Functional properties of films based on soy protein isolate and gelatin processed by compression molding. *J Food Eng*, 105, 65-72.

Günkaya, Z. eta Banar, M. (2016). An environmental comparison of biocomposite film based on orange peel-derived pectin jelly-corn starch and LDPE film: LCA and biodegradability. *Int J Life Cycle Asses*, 21, 465-475.

Gupta, R.K., Kumar, P., Sharma, A., eta Patil, R.T. (2011). Color kinetics of aonla shreds with amalgamated blanching during drying. *Int J Food Prop*, 14, 1232-1240.

Haddar, A., Sellimi, S., Ghannouchi, R., Alvarez, O.M., Nasri, M., eta Bougatef, A. (2012). Functional, antioxidant and film-forming properties of tuna-skin gelatin with a brown algae extract. *Int J Biol Macromol*, 51, 477-483.

Hammann, F. eta Schmid, M. (2014). Determination and quantification of molecular interactions in protein films: a review. *Materials*, 7, 7975-7996.

Haq, M.A., Hasnain, A., eta Azam, M. (2014). Characterization of edible gum cordia film: effects of plasticizers. *LWT-Food Sci Technol*, 55, 163-169.

Hernández-Izquierdo, V.M. eta Krochta, J.M. (2009). Thermal transitions and heat-sealing of glycerol-plasticized whey protein films. *Packag Technol Sci*, 22, 255-260.

Hong, P.K., Gottardi, D., Ndagijimana, M., eta Betti, M. (2014). Glycation and transglutaminase mediated glycosylation of fish gelatin peptides with glucosamine enhance bioactivity. *Food Chem*, 142, 285-293.

Hoque, S. (2011). Improvement of properties of edible film based on gelatin from cuttlefish (*Sepia pharaonis*) skin. PhD. Dissertation, Prince of Songkla University.

Hoque, S., Benjakul, S., eta Prodpran, T. (2011). Properties of film from cuttlefish (*Sepia pharaonis*) skin gelatin incorporated with cinnamon, clove and star anise extracts. *Food Hydrocolloids*, 25, 1085-1097.

Hu, X., Lu, Q., Sun, L., Cebe, P., Wang, X., Zhang, X., eta Kaplan, D.L. (2010). Biomaterials from ultrasonication-induced silk fibroin-hyaluronic acid hydrogels. *Biomacromolecules*, 11, 3178-3188.

Iahnke, A.O.S., Costa, T.M.H., Rios, A.O., eta Flôres, S.H. (2015). Residues of minimally processed carrot and gelatin capsules: potential materials for packaging films. *Ind Crops Prod*, 76, 1071-1078.

Ingrao, C., Lo Giudice, A., Bacenetti, J., Khaneghah, A.M., Sant'Ana, A.S., Rana, R., eta Siracusa, V. (2015). Foamy polystyrene trays for fresh-meat packaging: life-cycle inventory data collection and environmental impact assessment. *Food Res Int*, 76, 418-426.

Islam, M.I.U. eta Langrish, T.A.G. (2010). An investigation into lactose crystallization under high temperature conditions during spray drying. *Food Res Int*, 43, 46-56.

Isleroglu, H., Kemerli, T., Sakin-Yilmazer, M., Guven, G., Ozdestan, O., Uren, A., eta Kaymak-Ertekin, F. (2012). Effect of steam baking on acrylamide formation and browning kinetics of cookies. *J Food Sci*, 77, 257-263.

ISO 10993-5 (2009). Biological evaluation of medical devices - Part 5: Tests for in vitro cytotoxicity.

ISO 14040 (2006). Environmental Management - Life Cycle Assessment - Principals and Framework.

Iturriaga, L., Olabarrieta, I., eta de Marañón, I.M. (2012). Antimicrobial assays of natural extracts and their inhibitory effect against *Listeria innocua* and fish spoilage bacteria, after incorporation into biopolymer edible films. *Int J Food Microbiol*, 158, 58-64.

Jayasundera, M., Adhikari, B., Aldred, P., eta Ghandi, A. (2009). Surface modification of spray dried food and emulsion powders with surface-active proteins: a review. *J Food Eng*, 93, 266-277.

Jiang, Z. eta Brodkorb, A. (2012). Structure and antioxidant activity of Maillard reaction products from α-lactalbumin and β-lactoglobulin with ribose in an aqueous model system. *Food Chem*, 133, 960-968.

Jiménez, N., Bohuon, P., Donier, M., Bonazzi, C., Pérez, A.M., eta Vaillant, F. (2012). Effect of water activity on anthocyanin degradation and browning kinetics at high temperatures (100-140 ºC). *Food Res Int*, 47, 106-115.

Kadam, S.U., Pankaj, S.K., Tiwari, B.K., Cullen, P.J., eta O'Donnell, C.P. (2015). Development of biopolymer-based gelatin and casein films incorporating brown seaweed *Ascophyllum nodosum* extract. *Food Packing and Shelf Life*, 6, 68-74.

Kaewprachu, P. eta Rawdkuen, S. (2016). Application of active edible films as food packaging for food preservation and extending shelf life. In *Microbes in food and health*. Garg, N., Abdel-Aziz, S.M., eta Aeron, A. (Eds.). Springer-Verlag, Berlin, Germany, pp. 185-205.

Kaewprachu, P., Osako, K., Benjakul, S., eta Rawdkuen, S. (2015). Quality attributes of minced pork wrapped with catechin-lysozyme incorporated gelatin film. *Food Packaging and Shelf Life*, 3, 88-96.

Karbowiak, T., Debeaufort, F., Champion, D., eta Voilley, A. (2006). Wetting properties at surface of iota-carrageenan-based edible films. *J Colloid Interface Sci*, 294, 400-410.

Karim, A.A. eta Bhat, R. (2008). Gelatin alternatives for the food industry: recent development challenges and prospects. *Trends Food Sci Tehcnol*, 19, 644-656.

Karnjanapratum, S., O'Callaghan, Y.C., Benjakul, S., eta O'Brien, N.M. (2016). *In vitro* cellular bioactivities of Maillard reaction products from sugar-gelatin hydrolysate of unicorn leatherjacket skin system. *Funct Foods*, 23, 87-94.

Kavoosi, G., Rahmatallahi, A., Dadfar, S.M.M., eta Purfard, A.M. (2014). Effects of essential oil on the water binding capacity, physico-mechanical properties, antioxidant and antibacterial activity of gelatin films. *LWT-Food Sci Technol*, 57, 556-561.

Keyf, F. eta Etikan, I. (2004). Evaluation of gloss changes of two denture acrylic resin materials in four different beverages. *Dent Mater*, 20, 244-251.

Kijchavengkul, T. eta Auras, R. (2008). Compostability of polymers. *Polym Int*, 57, 793-804.

Kim, J.S. eta Lee, Y.S. (2009). Antioxidant activity of Maillard reaction products derived from aqueous gluose/glycine, diglycine, and triglycine model systems as a function of heating time. *Food Chem*, 116, 272-232.

Kittiphattanabawon, P., Benjakul, S., Visessanguan, W., Nagai, T., eta Tanaka, M. (2015). Characterization of acid soluble collagen from skin and bone of bigeye snapper (*Priacanthus tayenus*). *Food Chem*, 89, 363-372.

Kowalcyzk, D. eta Biendl, M. (2016). Physicochemical and antioxidant properties of biopolymer/candelilla wax emulsion films containing hop extract - A comparative study. *Food Hydrocolloids*, 60, 384-392.

Kowalczyk, D. (2016). Biopolymer/candelilla wax emulsion films as carriers of ascorbic acid - A comparative study. *Food Hydrocolloids*, 52, 543-553.

Krochta, J.M. (2002). Proteins as raw materials for films and coatings: definitions, current status, and opportunities. In *Protein-based films and coatings*. Gennadios, A. (Ed.). CRC Press, Taylor eta Francis Group, New York, pp. 1-42.

Kunte, L., Gennadios, A., Cuppett, S., Hanna, M., eta Weller, C. (1997). Cast films from soy protein isolates and fractions. *Cereal Chem*, 72, 115-118.

Labuza, T. P. eta Baiser, W. M. (1992). The kinetics of nonenzymatic browning. In *Physical chemistry of foods*. Schwartzberg, H. G. eta Hartel, R. W. (Eds.). Marcel Dekker, New York, USA, pp. 595-649

Lacroix, M. eta Vu, K.D. (2014). Edible coating and film materials: proteins. In *Innovations in Food Packaging*. Han, J.H. (Ed). Academic Press, San Diego CA, USA, pp. 277-294.

Learner, T.J.S., Smithen, P., Krueger, J.W., eta Schilling, M.R. (Eds.) (2008). Modern Paints Uncovered. Getty Publications, Los Angeles (US).

Leceta, I., Etxabide, A., Cabezudo, S., de la Caba, K., eta Guerrero, P. (2014). Bio-based films prepared with by-products and wastes: environmental assessment. *J Cleaner Prod*, 64, 218-227.

Leceta, I., Guerrero, P., Cabezudo, S., eta de la Caba, K. (2013). Environmental assessment of chitosan-based films. *J Cleaner Prod*, 41, 312-318.

Lefevre, T. eta Subirade, M. (2000). Molecular differences in the formation and structure of fine-stranded and particulate β-lactoglobulin gels. *Biopolymers*, 54, 578-586.

Lefevre, T., Subirade, M., eta Pezolet, M. (2005). Molecular description of the formation and structure of plasticized globular protein films. *Biomacromolecules*, 6, 3209-3219.

Li, W., Gao, H., Mu, H., Chen, H., Fang, X., Zhou, Y., eta Tao, F. (2015b). Three different active aldehydes induce the production of oxidation advanced lipoxidation end products upon incubation with bovine serum albumin. *Eur J Lipid Sci Technol*, 117, 1432-1443.

Li, Y., Li, C., Mujeeb, A., Jin, Z., eta Ge, Z. (2015a). Optimization and characterization of chemically modified polymer microspheres and their effect on cell behavior. *Mater Lett*, 154, 68-72.

Lin, C.S.K., Pfaltzgraff, L.A., Herrero-Davila, L., Mubofu, E.B., Abderrahim, S., Clark, J.H., Koutines, A., Kopsahelis, N., Stamatelatou, K., Dickson, F., Thankappan, S., Mohamed, Z., Brocklesby, R., eta Luque, R. (2013). Food waste as a valuable resource for the production of chemicals, materials and fuels. Current situation and global perspective. *Energy Environ Sci*, 6, 426-464.

Lin, L.H., Chen, K.M., Liu, H.J., Chu, H.W., Kuo, T.C., Hwang, M.C., eta Wang, C.F. (2012). Preparation and surface activities of modified gelatin-conjugates. *Colloids Surf A: Physicochem Eng Aspects*, 408, 97-103.

Liu, F., Avena-Bustillos, R.J., Chiou, B.S., Li, Y., Ma, Y., Williams, T.G., Wood, D.F., McHugh, T.H., eta Zhong, F. (2017). Controlled-release of tea polyphenol from gelatin

films incorporated with different ratios of free/nanoencapsulated polyphenols into fatty food simulants. *Food Hydrocolloids*, 62, 212-221.

Liu, F., Majeed, H., Antoniou, J., Liu, Y., Ma, J., eta Zhong, F. (2016). Tailoring physical properties of transglutaminase-modified gelatin films by varying drying temperature. *Food Hydrocolloids*, 58, 20-28.

Liu, G. eta Zhong, Q. (2012). Glycation of whey protein to provide steric hindrance against thermal aggregation. *J Agric Food Chem*, 60, 9754-9762.

López-Rubio, A., Lagarón, J.M., eta Ocio, M.J. (2008). Active polymer packaging of non-meat food products. In *Smart packaging technologies*. Kerry, J. eta Butler, P. (Eds.). John Wiley eta Sons Ltd, Chichester, England, pp. 19-30.

Ma, W., Tang, C.H., Yin, S.W., Yang, X.Q., eta Qi, J.R. (2013). Genipin-crosslinked gelatin films as controlled releasing carriers of lysozyme. *Food Res Inter*, 51, 321-324.

Martínez-Ruvalcaba, A., Becerra-Bracamontes, F., Sánchez-Díaz, J.C., eta González-Álvarez, A. (2009). Polyacrylamide-gelatin polymeric networks: effect of pH and gelatin concentration on the swelling kinetics and mechanical properties. *Polym Bull*, 62, 539-548.

Martins, I.M., Barreiro, M.F., Coelho, M., eta Rodrigues, A.E. (2014). Microencapsulation of essential oils with biodegradable polymeric carriers for cosmetic applications. *Chem Eng J*, 245, 191-200.

Martins, S.I.F.S., Jongen, W.M.F., eta Van Boekel, M.A.J.S. (2001). A review of Maillard reactions in food and implications to kinetic modeling. *Trends Food Sci Tech*, 11, 364-373.

Mathew, A.P. eta Dufresne, A. (2002). Plasticized waxy maize starch: effect of polyols and relative humidity on material properties. *Biomacromolecules*, 3, 1101-1108.

Mehanny, M., Hathout, R.M., Geneidi, A.S., eta Mansour, S. (2016). Exploring the use of nanocarrier systems to deliver the magical molecule; Curcumin and its derivatives. *J Controlled Release*, 225, 1-30.

Mikšovská, J. eta Larsen, R.W. (2007). Photothermal studies of pH induced unfolding of proteins. In *Protein structures: methods in protein structure and stability analysis*. Uversky, V.N. eta Permyakov, E.A. (Eds.). Nova Science Publishers, New York, USA, pp.159-187.

Molyneux, P. (2004). The use of the stable free radical diphenlpicrylhydrazyl (DPPH) for estimating antioxidant activity. *Songklanakarin J Sci Technol*, 26, 211-219.

Monedero, F.M., Fabra, M.J., Talens, P., eta Chiralt, A. (2009). Effect of oleic acid-beeswax mixtures on mechanical, optical and water barrier properties of soy protein isolate based films. *J Food Eng*, 91, 509-515.

Monti, S.M., Borreilli, R.C., Ritieni, A., eta Fogliano, V. (2000). A comparison of color formation and Maillard reaction products of a lactose-lysine and lactose-N(alpha)-acetyllysine model system. *J Agric Food Chem*, 48, 1041-1046.

Monti, S.M., Ritieni, A., Graziani, G., Randazzo, G., Mannina, L., Segre, A.L., eta Fogliano, V. (1999). LC/MS analysis and antioxidative efficiency of Maillard reaction products from a lactose-lysine model system. *J Agric Food Chem*, 47, 1506-1513.

Morales, F.J. eta Van Boekel, M.A.J.S. (1997). A study on advanced Maillard reaction in heated casein/sugar solutions: fluorescence accumulation. *Int Dairy J*, 7, 675-683.

Mu, C., Guo, J., Li, X., Lin, W., eta Li, D. (2012). Preparation and properties of dialdehyde carboxymethyl cellulose crosslinked gelatin edible films. *Food Hydrocolloids*, 27, 22-29.

Murakami, Y., Ishii, H., Takada, H., Tanaka, S., Machino, M., Ito, S., eta Fujisawa, S. (2008). Comparative anti-inflamatory activities of curcumin and tetrahydrocurcumin based on the phenolic O-H bond dissociation enthalpy, ionization potential and quantum chemical descriptor. *Anticancer Res*, 28, 699-707.

Murugan, P. eta Pari, L. (2006). Antioxidant effect of tetrahydrocurcumin in streptozotocin-nicotinamide induced diabetic rats. *Life Sci*, 79, 1720-1728.

Muyonga, J.H., Cole, C.G.B., eta Duodu, K.G. (2004). Extraction and physico chemical characterisation of Nile perch (*Lates niloticus*) skin and bone gelatin. *Food Hydrocolloids*, 18, 581-592.

Nagaranjan, M., Benjakul, S., eta Prodpran, T. (2015). Effects of bio-nanocomposite films from tilapia and squid skin gelatins incorporated with ethanolic extract from coconut husk on storage stability of mackerel meat powder. *Food Packaging and Shelf Life*, 6, 42-52.

Nakamatsu, J., Torres, F.G., Troncoso, O.P., Min-Lin, Y., eta Boccaccini, A.R. (2006). Processing and characterization of porous structures from chitosan and starch for tissue engineering scaffolds. *Biomacromolecules*, 7, 3345-3355.

Nguyen, C.V. (2006). Toxicity of the AGEs generated from the Maillard reaction: on the relationship of food-AGEs and biological-AGEs. *Mol Nutr Food*, 50, 1140-1149.

Nollet, L.M.L. eta Toldrá, F. (Eds.) (2015). Handbook of food analysis (3rd edition-Volume I). CRC-Press, Taylor & Francis group, Boca Ratón, Florida, USA, pp. 695-716.

Nor Afizah, M. eta Rizvi, S.S.H. (2014). Functional properties of whey protein concentrate texturized at acidic pH: effect of extrusion temperature. *LWT-Food Sci Technol*, 57, 290-298.

Núñez-Flores, R., Giménez, B., Fernández-Martín, F., López-Caballero, M.E., Montero, M.P., eta Gómez-Guillén, M.C. (2012). Role of lignosulphonate in properties of fish gelatin films. *Food Hydrocolloids*, 27, 60-71.

Núñez-Flores, R., Giménez, B., Fernández-Martín, F., López-Caballero, M.E., Montero, M.P., eta Gómez-Guillén, M.C. (2013). Physical and functional characterization of active fish gelatin films incorporated with lignin. *Food Hydrocolloids*, 30, 163-172.

Nur Hanani, Z.A., McNamara, J., Roos, Y.H., eta Kerry, J.P. (2013). Effect of plasticizer content on the functional properties of extruded gelatin-based composites. *Food Hydrocolloids*, 31, 264-269.

Nur Hanani, Z.A., Roos, Y.H., eta Kerry, J.P. (2012). Use of beef, pork and fish gelatin sources in the manufacturing of films and assessment of their composition and mechanical properties. *Food Hydrocolloids*, 29, 144-151.

Nur Hanani, Z.A., Ross, Y.H., eta Kerry, J.P. (2014). Use and applications of gelatin as potential biodegradable packaging materials for food products. *Int J Biol Macromol*, 71, 94-102.

Nursten, H.E. (Ed.) (1986). Concentration and Drying of Foods. Elsevier, London eta New York.

Olivas, G.I., Mattinson, D.S., eta Barbosa-Cánovas, G.V. (2007). Alginate coatings for preservation of minimally processed “gala” apples. *Postharvest Biol Technol*, 45, 89-96.

Osen, R., Toelstede, S., Wild, F., Eisner, P., eta Schweiggert-Weisz, U. (2014). High moisture extrusion cooking of pea protein isolates: raw material characteristics, extruder responses, and texture properties. *J Food Eng*, 127, 67-74.

Oussalah, M., Caillet, S., Saucier, L., eta Lacroix, M. (2007). Inhibitory effects of selected plant essential oils on the growth of four pathogenic bacteria: *E. coli* O157:H7, *Salmonella typhimurium*, *Staphylococcus aureus* and *Listeria monocytogenes*. *Food Control*, 18, 414-420.

Ozdal, T., Capanoglu, E., eta Altay, F. (2013). A review on protein-phenolic interactions and associated changes. *Food Res Int*, 51, 954-970.

Palou, E., López-Malo, A., Barbosa-Cánovas, G.V., Welti-Chanes, J., eta Swanson, B.G.J. (1999). Polyphenoloxidase activity and color of blanched and high hydrostatic pressure treated banana puree. *Food Sci*, 64, 42-45.

Panzavolta, S., Gioffrè, M., Focarete, M.L., Gualandi, C., Foroni, L., eta Bigi, A. (2011). Electrospun gelatin nanofibers: optimization of genipin cross-linking to preserve fiber morphology after exposure to water. *Acta Biomater*, *7*, 1702-1709.

Pastoriza, S. eta Rufián-Henares, J.A. (2014). Contribution of melanoidins to the antioxidant capacity of the Spanish diet. *Food Chem*, 164, 438-445.

Perez-Espitia, P.J., Ferreira Soares, N.F.F., Coimbra, J.S.R., Andrade, N.J., Cruz, R.S., eta Medeiros, E.A.A. (2012). Bioactive peptides: synthesis, properties, and applications in the packaging and preservation of food. *Comp Rev Food Sci Food Safe*, 11, 187-204.

PlasticsEurope (2016). Plastics-the facts 2016. Brussels: PlasticsEurope.

Plyduang, T., Lomlim, L., Yuenyongsawad, S., eta Wiwattanapatapee, R. (2014). Carboxymethylcellulose-tetrahydrocurcumin conjugates for colon-specific delivery of a novel anti-cancer agent, 4-amino tetrahydrocurcumin. *Eur J Pharm Biopharm*, 88, 351-360.

Portes, E., Gardrat, C., eta Castellan, A. (2007). A comparative study on the antioxidant properties of tetrahydrocurcuminoids and curcuminoids. *Tetrahedron*, 63, 9092-9099.

Portes, E., Gardrat, C., Castellan, A., eta Coma, V. (2009). Environmentally friendly films based on chitosan and tetrahydrocurcumoid derivative exhibiting antibacterial and antioxidative properties. *Carbohydr Polym*, 76, 578-584.

Prakash Maran, J., Sivakumar, V., Thirugnanasambandham, K., eta Sridhar, R. (2014). Degradation behavior of biocomposites based on cassava starch buried under indoor soil conditions. *Carbohyd Polym*, 101, 20-28.

Priyadarsini, K.I. (2014). The chemistry of curcumin: from extraction to therapeutic agent. *Mol*, 19, 20091-20112.

Quinn, G., Monahan, F. J., O'Sullivan, M., eta Langares, A. (2003). Role of covalent and noncovalent interactions in the formation of films from unheated whey protein solutions following pH adjustment. *J Food Sci*, 68, 2284-2288.

Rahman, M.S. (Ed.) (2007). Handbook of Food Preservation (2nd edition). CRC Press, Taylor eta Francis Group, New York, USA.

Rao, K.M., Rao, K.S.V.K., Ramanjaneyulu, G., eta Ha, C.S. (2015). Curcumin encapsulated pH sensitive gelatin based interpenetrating polymeric network nanogels for anti cancer drug delivery. *Int J Pharm*, 478, 788-795.

Rao, S.R. eta Ravishankar, G.A. (2002). Plant cell cultures: chemical factories of secondary metabolites. *Biotechnol Advances*, 20, 101-153.

Ravindran, R. eta Jaiswal, A. (2016). Exploitation of food industry waste for high-value products. *Trends Biotechnol*, 34, 58-69.

Rawdkuen, S., Suthiluk, P., Kamhangwong, D., eta Benjakul, S. (2012). Mechanical, physico-chemical, and antimicrobial properties of gelatin-based film incorporated with catechin-lysozyme. *Chem Central J*, 6, 131-140.

Reddy, N. eta Yang, Y. (2013). Thermoplastic films from plant proteins. *J Appl Polym Sci*, 130, 729-736.

Rindlav-Westling, A., Standing, M., Hermansson, A.M., eta Gatenholm, P. (1998). Structure, mechanical and barrier properties of amylase and amylopectin films. *Carbohydr Polym*, 36, 217-224.

Roberston, G.L. (Ed.) (2013). Food Packaging. Principles and Practice (3rd edition). CRC Press, Taylor eta Francis Group, LLC, New York, USA, Chapter 1.

Saarai, A., Kasparkova, V., Sedlacek, T., eta Saha, P. (2013). On the development and characterisation of crosslinked sodium alginate/gelatin hydrogels. *J Mech Behav Biomed Mater*, 18, 152-166.

Samira, S., Thuan-Chew, T.C., eta Azhar, M.E. (2014). Effect of ribose-induced Maillard reaction on physical and mechanical properties of bovine gelatin films prepared by oven drying. *Int Food Res J*, 2, 269-276.

Sanches-Silva, A., Costa, D., Albuquerque, T.G., Buonocore, G.G., Ramos, F., Castilho, M.C., Machado, A.V., eta Costa, H.S. (2014). Trends in the use of natural antioxidants in active food packaging: a review. *Food Addit Contam, Part A*, 31, 374-395.

Santoro, M., Tatara, A.M., eta Mikos, A.G. (2014). Gelatin carriers for drug and cell delivery in tissue engineering. *J. Control. Release,* 190, 210-218.

Schmidt, V., Giacomelli, C., eta Soldi, V. (2005). Thermal stability of films formed by soy protein isolate-sodium dodecyl sulfate. *Polym Degrad Stab*, 87, 25-31.

Serpen, A., Capuano, E., Fogliano, V., eta Gokmen, V. (2007). A new procedure to measure the antioxidant activity of insoluble food components. *J Agric Food Chem*, 55, 7676-7681.

Shakila, R.J., Jeevithan, E., Arumugam, V., eta Jeyasekaran, G. (2015). Suitability of antimicrobial grouper bone gelatin films as edible coatings for vacuum-packaged fish steaks. *J Aquat Food Prod Technol*, 25, 724-734.

Silva, N.H.C.S., Vilela, C., Marrucho, I.M., Freire, C.S.R., Neto, C.P., eta Silvestre, A.J.D. (2014). Protein-based materials: from sources to innovative sustainable materials for biomedical applications. *J Mater Chem B*, 2, 3715-3740.

Singh, S., Lee, M.H., Park, I., Shin, Y., eta Lee, Y.S. (2016). Antimicrobial seafood packaging: a review. *J Food Sci Technol*, 53, 2505-2518.

Somporn, P., Phisalaphong, C., Nakornchai, S., Unchern, S., eta Morales, N.P. (2007). Comparative antioxidant activities of curcumin and its demethoxy and hydrogenated derivatives. *Biol Pharm Bull*, 20, 74-78.

Song, A.Y., Oh, Y.A., Roh, S.H., Kim, J.H., eta Min, S.C. (2016). Cold oxygen plasma treatments for the improvement of the physicochemical and biodegradable properties of polylactic acid films for food packaging. *J Food Sci*, 81, 86-96.

Song, J.H., Murphy, R.J., Narayan, R., eta Davies, G.B.H. (2009). Biodegradable and compostable alternatives to conventional plastics. *Philos Trans R Soc B*, 364, 2127-2139.

Sormoli, M.E., Das, D., eta Landgrish, T. (2013). Crystallization behavior of lactose/sucrose mixtures during water-induced crystallization. *J Food Eng*, 116, 873-880.

Souguir, H., Salaün, F., Douillet, P., Vroman, I., eta Chatterjee, S. (2013). Nanoencapsulation of curcumin in polyurethane and polyurea shells by an emulsion diffusion method. *Chem Eng J*, 221, 133-145.

Sung, H., Huang, D., Chang, W., Huang, R., eta Hsu, J. (1999). Evaluation of gelatin hydrogel crosslinked with various crosslinking agents as bioadhesives: *in vitro* study. *J Biomed Mater Res*, 46, 520-530.

Susi, H., Serge, N., Timasheff, S.N., eta Stevens, L. (1967). Infrared spectra and protein conformations in aqueous solutions: I. The amide I band in H_2O and D_2O solutions. *J Biol Chem*, 242, 5460-5466.

Suyatma, N.E., Tighzert, L., eta Copinet, A. (2005). Effects of hydrophilic plasticizers on mechanical, thermal, and surface properties of chitosan films. *J Agric Food Chem*, 53, 3950-3957.

Tayel, A.A., El-Tras, W.F., Moussa, S., El-Baz, A.F., Mahrous, H., Salem, M.F., eta Brimer, L. (2011). Antibacterial action of zinc oxide nanoparticles against foodborne pathogens. *J Food Safe*, 3, 211-218.

Tian, F., Decker, E.A., eta Goddard, J.M. (2013). Controlling lipid oxidation of food by active packaging technologies. *Food Funct*, 4, 669-680.

Tongnuanchan, P., Benjakul, S., eta Prodpran, T. (2012). Properties and antioxidant activity of fish skin gelatin film incorporated with citrus essential oils. *Food Chem*, 134, 1571-1579.

Tongnuanchan, P., Benjakul, S., eta Prodpran, T. (2013). Physico-chemical properties, morphology and antioxidant activity of film from fish skin gelatin incorporated with root essential oils. *J Food Eng*, 117, 350-360.

Tovar, L., Salafranca, J., Sanchez, C., eta Nerin, C. (2005). Migration studies to assess the safety in use of a new antioxidant active packaging. *J Agric Food Chem*, 53, 5270-5275.

UNE-EN 13432:2001 (2001). Requirements for packaging recoverable through composting and biodegradation. Test scheme and evaluation criteria for the final acceptance of packaging.

Uranga, J., Leceta, I., Etxabide, A., Guerrero, P., eta de la Caba, K. (2016). Cross-linking of fish gelatin films to develop sustainable films with enhanced properties. *Eur Polym J*, 78, 82-90.

Van Boekel, M.A.J.S. (1998). Effect of heating on Maillard reactions in milk. *Food Chem*, 62, 403-414.

Venkatesen, P., Unnikrishnan, M.K., Kumar, M.S., eta Rao, M.N.A. (2003). Effect of curcumin analogues on oxidation of haemoglobin and lysis of erythrocytes. *Curr Sci*, 84, 74-78.

Wang, S., Marcone, M.S., Barbut, S., eta Lim, L.T. (2012). Formation of dietary biopolymers-based packaging material with bioactive plant extracts. *Food Res Int*, 49, 80-91.

Wang, W.Q., Bao, Y.H., eta Chen, Y. (2013). Characteristics and antioxidant activity of water-soluble Maillard reaction products from interactions in a whey protein isolate and sugars system. *Food Chem*, 139, 355-361.

Wang, Y., Liu, A., Ye, R., Wang, W., eta Li, X. (2015). Transglutaminase-induced crosslinking of gelatin-calcium carbonate composite films. *Food Chem*, 166, 414-422.

Wang, Y., Yang, H., eta Regenstein, J.M. (2008). Characterization of fish gelatin at nanoscale using atomic force microscopy. *Food Biophysics*, 3, 269-272.

Wardhani, D.H., Fuciños, P., Vázquez, J.A., eta Pandiella, S.S. (2013). Inhibition kinetics of lipid oxidation of model foods by using antioxidant extract of fermented soybeans. *Food Chem*, 139, 837-844.

Wetzel, R., Buder, E., Hermel, H., eta Hüttner, A. (1987). Conformations of different gelatins in solutions and in films. An analysis of circular dichroism (CD) measurements. *Colloid Polym Sci*, 265, 1036-1045.

Wihodo, M. eta Moraru, C.I. (2013). Physical and chemical methods used to enhance the structure and mechanical properties of protein films: a review. *J Food Eng*, 114, 292-302.

Wijewickreme, A.N., Kitts, D.D., eta Durance, T.D. (1997). Reaction conditions influence the elementary composition and metal chelating affinity of nondialyzable model Maillard reaction products. *J Agric Food Chem*, 45, 4577-4583.

Wu, J., Chen, S., Ge, S., Miao, J., Li, J., eta Zhang, L.Q. (2013). Preparation, properties and antioxidant activity of an active film from silver carp (*Hypophthalmichthys molitrix*) skin gelatin incorporated with green tea extract. *Food Hydrocolloids*, 32, 42-51.

Wu, J., Liu, H., Ge, S., Wang, S., Qin, Z., Chen, L., Zheng, Q., Liu, Q., eta Zhang, Q. (2015). The preparation, characterization, antimicrobial stability, and *in vitro* release evaluation of fish gelatin films incorporated with cinnamon essential oil nanoliposomes. *Food Hydrocolloids*, 43, 427-435.

Xie, Y., He, Y., Irwin, P.L., Jin, T., eta Shi, X. (2011). Antibacterial activity and mechanism of action of zinc oxide nanoparticles against *Campylobacter jejuni*. *Appl Environ Microbiol*, 77, 2325-2331.

Yang, H., Wang, Y., Zhou, P., Regenstein, J.M., eta Rouse, B. (2007). Nanostructural characterization of catfish skin gelatin using atomic force microscopy. *J Food Sci*, 72, 430-440.

Yates, M.R. eta Barlow, C.Y. (2013). Life cycle assessments of biodegradable, commercial biopolymers - A critical review. *Resour, Conser Recycl*, 78, 54-66.

Yayalayan, V.A., Ismail, A.A., eta Mandeville, S. (1993). Quantitative determination of the effect of pH and temperature on the keto form of D-fructose by FTIR spectroscopy. *Carbohydr Res,* 248, 355-360.

Yu, X., Zhao, M., Hu, J., Zeng, S., eta Bai, X. (2012). Correspondence analysis of antioxidant activity and UV-Vis absorbance of Maillard reaction products as related to reactants. *LWT-Food Sci Technol*, 46, 1-9.

Yuan, Y. eta Lee, T.R. (2013). Contact angle and wetting properties. In *Surface Science Techniques*. Bracco, G. eta Holst, B. (Eds.). Spinger-Verlag, Berlin, Germany, pp. 3-33.

Zaman, H.U. eta Beg, M.D.H. (2015). Improvement of physico-mechanical, thermomechanical, thermal and degradation properties of PCL/gelatin biocomposites: effect of gamma radiation. *Radiat Phys Chem*, 109, 73-82.

Zhao, S., Yao, J., Fei, X., Shao, Z., eta Chen, X. (2013). An antimicrobial film by embedding in situ synthesized silver nanoparticles in soy protein isolate. *Mater Lett*, 95, 142-144.


Cross-linking
Gelatin
Maillard reaction
Lactose
Cross-linking
Maillard
Gelatin

BioMat

eman ta zabal zazu

Universidad del País Vasco

Euskal Herriko Unibertsitatea

Control of crosslinking to tailor the properties of protein films and biocomposites

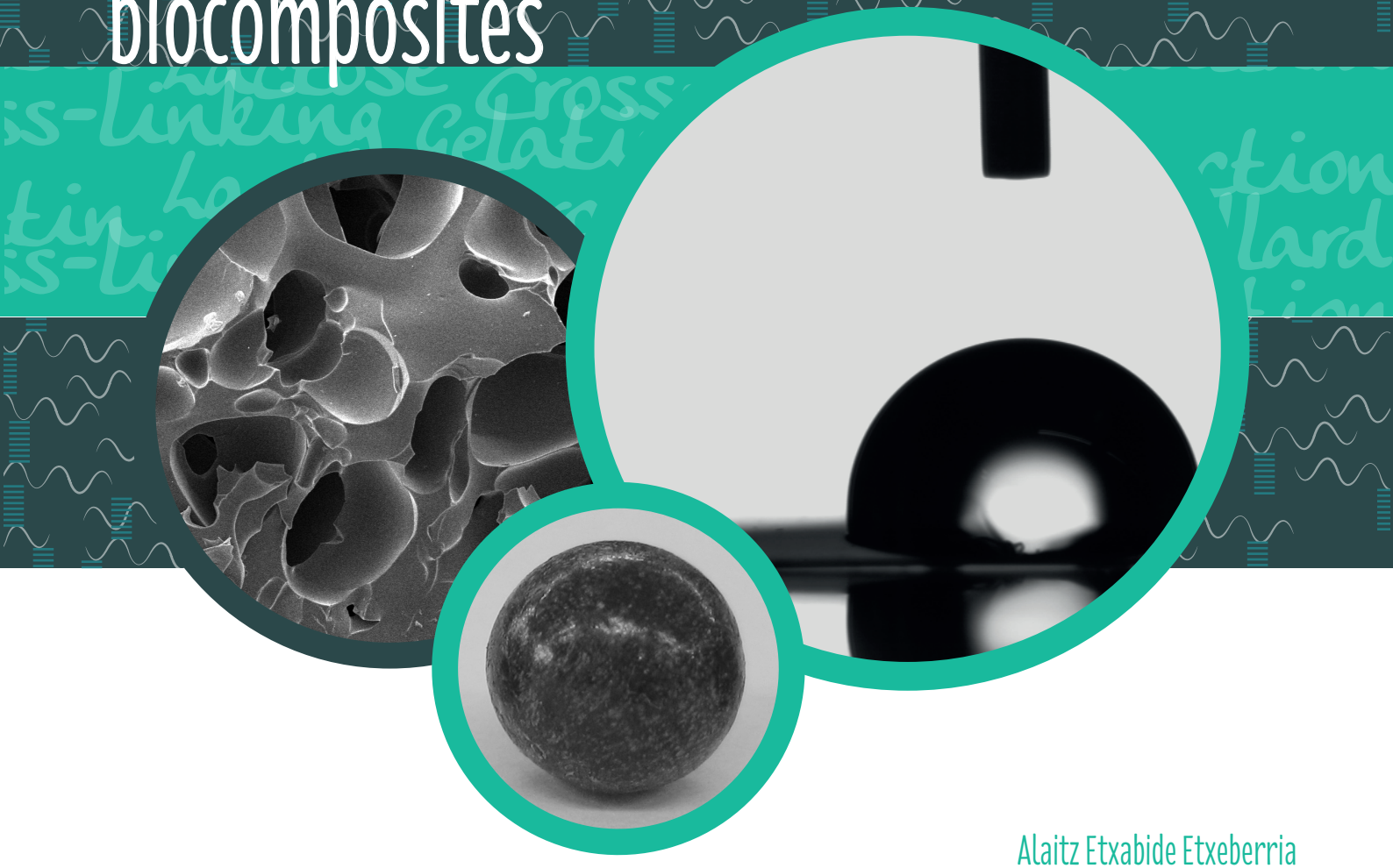

Alaitz Etxabide Etxeberria

Department of Chemical & Environmental Engineering

Donostia-San Sebastián, 2017

Control of crosslinking to tailor the properties of protein films and biocomposites

Alaitz Etxabide Etxeberria

Supervisors: Koro de la Caba and Pedro Guerrero

Department of Chemical and Environmental Engineering

Donostia-San Sebastián, 2017

Universidad del País Vasco

Euskal Herriko Unibertsitatea

Control of crosslinking to tailor the properties of protein films and biocomposites

Alaitz Etxabide Etxeberria

Department of Chemical and Environmental Engineering

Donostia-San Sebastián, 2017

Esker onak / Agradecimientos/ Remerciements/ Acknowledgements

Bizitzako bertze fase berri bati hasiera eman dion hiru urte t`erdiko etapa honen amaierara iristeko nire ondoan egon diren pertsona guztiei eskerrak eman nahi dizkiet.

Comenzar agradeciendo a Koro de la Caba y Pedro Guerrero, directores de mi tesis-doctoral. Gracias por ofrecerme esta oportunidad de dar los primeros pasos en la investigación junto a vosotros. Un placer haberos conocido y haber compartido con vosotros ese tiempo durante los proyectos fin de grado y máster. Gracias también por la confianza depositada en mí a la hora de iniciar esta tesis doctoral dentro del grupo BIOMAT. La orientación, el seguimiento y la supervisión continua junto con el apoyo recibido a lo largo de estos años han sido esenciales para mi desarrollo profesional como personal. Gracias, de nuevo por establecer en mí unos principios de trabajo sólidos e imprescindibles.

Bertzetik, doktorego-tesi honetan jardunean, nire ondoan egon diren hasieran lankide ziren eta orain lagun direnei, beraien laguntza eta pazientzia eskertu nahi dizkiet. Aldi berean, etxekoek emandako babesa eta bereziki niganako erakutsitako konfiantza eskertu nahiko nituzke, beraiek gabe lan honen bidea aldapatsuagoa izango litzateke eta. Orain arte aipatu ez ditudan lagun minak eta kuadrillakoak ere, eskerrak aunitz hor egoteagatik. Ahaztu gabe, Jose Emilio Txoperenari “Txoltxan” tesiaren euskarazko bertsioan emandako laguntza eskertu nahiko nizuke.

Je tiens à remercier infiniment Madame Véronique Coma et Monsieur Christian Gardrat pour m’avoir dirigée pendant mon séjour scientifique dans le Laboratoire de Chimie des Polymères Organiques (LCPO), à l’Université Bordeaux 1 (France). Leurs enseignements et conseils m’ont été d’une grande aide. I would also like to thank Dr. Piergiorgio Gentile and Dr. Ana Maria Ferreira-Duarte for giving me the chance to carry out scientific stay in the School of Mechanical and Systems Engineering at Newcastle

University (UK). Their good humor and wide knowledge were important and helpful for going on advancing in my investigation.

Azkenik, Euskal Herriko Unibertsitateak (UVP/EHU, PIF13/008 kontratua) eta Biomat ikerketa taldeak (UPV/EHU, GIU15/03) emandako diru-laguntza eskertzearekin batera, Gipuzkoako Foru Aldundia, UPV/EHU-ko Ikerkuntzarako Zerbitzu Orokorra (SGIker) eta NanoBioCell nahiz Enedi ikerketa taldeak eskertu nahiko nituzke.

Summary

Plastics have transformed everyday life and have brought many societal benefits. However, some concerns about their usage and disposal have promoted the development of alternative materials to address a more sustainable use of resources in accordance with the circular economy concepts. With this regard, gelatin is a renewable and biodegradable material with some advantages like availability, low cost, film forming ability and sensory acceptability. In this context, the overall objective of this study was to develop and characterize gelatin-based materials as a function of formulations composition and processing methods and conditions for different purposes, such as packaging and pharmaceutical applications, among others.

This work consists of 10 chapters. Chapter 1 is an overview of the recent improvements made on active films, highlighting the importance of using industrial wastes or by-products as raw materials for new products and applications. The materials and methods employed to carry out this research work are described in chapter 2. After that, in chapter 3, the effect of processing conditions on functional properties and environmental impacts of gelatin films are analysed in order to identify not only the benefits achieved but also those aspects that need further improvement.

Taking into account that the hydrophilic nature of gelatin is responsible for the high brittleness and water sensitivity of films, the improvement of those functional properties is analysed by means of crosslinking with lactose, which leads to the occurrence of Maillard reaction. The effect of lactose content, heating, and solution pH on Maillard reaction and, therefore, on film properties is analysed in chapters 4 and 5. Considering the results obtained in those chapters, a monitoring of the Maillard reaction at basic pH as a function of heating time is performed in chapter 6. Since antioxidant compounds can be formed during Maillard reaction, the antioxidant capacity of crosslinked gelatin films is analysed in chapter 7, as well as the improvement of the

antioxidant properties by the incorporation of a curcumin derivative into film forming solutions. After a thorough study of films, the properties of lactose-crosslinked gelatin biocomposites manufactured by extrusion and injection are studied in chapter 8. Finally, the general conclusions of this research work are summarized in chapter 9, and the references cited along the text are listed in chapter 10.

Objectives

The overall objective of this study was to develop gelatin-based materials with enhanced functional properties by means of modifying formulations composition and processing methods and conditions.

The specific objectives of this thesis were:

- Provide an overview of the recent improvements on active films.
- Study the effect of processing conditions on the functional properties of gelatin films.
- Assess the environmental impacts of gelatin films from extraction to disposal.
- Analyse the effect of lactose content, heating time, and solution pH on crosslinking reaction and functional properties of gelatin films.
- Analyse the antioxidant capacity of crosslinked gelatin films.
- Optimize extrusion and injection parameters to manufacture gelatin biocomposites.

Index

1 Introduction

1.1 Gelatins as raw materials for active packaging

The market for plastics in Europe has increased exponentially to an estimated annual production of 58 million tonnes in 2015 (PlasticsEurope, 2016), of which approximately 39.9% are demanded for packaging industry. Packaging has become a necessary and essential commodity in our daily life. It performs functions such as containment, protection, convenience and communication, ensuring the quality and safety of food products (Roberston, 2013). Synthetic plastics present excellent properties for this use; however, their durability is causing evident waste-disposal problems, since these materials are not biodegradable and are not totally recyclable.

In recent years biodegradable polymers obtained from renewable resources, such as agro-industrial and marine wastes and by-products, have been considered as sustainable alternatives to petroleum-derived polymers (Leceta et al., 2014). Besides, consumers' concerns related to health, nutritional value and food safety (migration of potentially toxic compounds from packaging to food) have increased the interest in substituting synthetic components by natural substances (Bravin, Peressini, & Sensidoni, 2006; López-Rubio, Lagarón, & Ocio, 2008). Hence, the use of biopolymers and natural additives for food protection may be advantageous in terms of environmental sustainability and consumer acceptability. Biodegradable and edible materials derived from plants and animals, such as proteins, polysaccharides and lipids, have shown a potential ability to be used as edible films in contact with food (Nur Hanani, Roos, & Kerry, 2014; Wang et al., 2012).

Among biopolymers, proteins offer valuable characteristics for the production of food packaging due to their abundance, film forming ability, transparency and excellent barrier properties against O_2, CO_2 and lipids (Krochta, 2002; Lacroix & Vu, 2014). In addition, proteins are heteropolymers that contain a great variety of functional groups and so, the properties of protein-based materials can be tailored by means of enzymatic, chemical and/or physical modifications to obtain the desirable final

properties required for specific applications (Hammann & Schmid, 2014). Moreover, it is worth noting that protein-based films can function as excellent vehicles for incorporating a wide variety of additives such as nutrients, antioxidants, antimicrobials, antifungal and flavours (Guadipati, 2013).

In the specific field of proteins' research, the interest in gelatin-based materials has increased in the last years (Gómez-Guillén et al., 2011). Gelatin is an animal protein, obtained by hydrolysis of collagen, present in bones, skins and connective tissues of land and marine animals. Among gelatins, fish gelatin has attracted much attention as an alternative of mammalian gelatins because of socio-cultural reasons (Benjakul, Kittiphattanabawon, & Regenstein, 2012). The abundance, availability and low cost of gelatin facilitate its use in a wide variety of applications. Gelatins are tasteless food grade materials with excellent biocompatibility, biodegradability, and non-toxicity (Ali et al., 2012), so they possess a great potential as edible films (Bergo & Sobral, 2007; Karim & Bhat, 2008). Besides, they can be used as carriers of bioactives. In this context, the purpose of this chapter is to provide an overview of the recent improvements made on gelatin-based films used as active packaging to prevent or retard food deterioration and extend food shelf-life.

One of the major deterioration reactions in foods is the chemical reaction of lipids, particularly polyunsaturated fatty acids, with oxygen. In addition to lipid oxidation, food products are highly prone to microbial deterioration since they are rich in nutrients (Kaewpprachu & Rawdkuen, 2016). These degradation processes occur during different stages of the food production chain, such as packaging and storage, and they bring to the development of rancidity. Lipid oxidation and microbial growth lead to food quality deterioration, including texture, appearance and colour changes, off-odours, off-flavours, nutrition losses and formation of oxidized polymers and potentially toxic compounds (Anbinder et al., 2015; Tian, Decker, & Goddard, 2013). Therefore, the spoilage causes a reduction of food shelf-life and this causes consumer dissatisfaction

and complaints, affecting product acceptability and sales. Consequently, important amounts of food products are lost due to consumers' rejection, causing negative economic and environmental impacts (Lin et al., 2013; Wardhani et al., 2013).

Different preservation methods have been used in order to extend food shelf-life and preserve foods from spoilage: freezing, drying, modified atmosphere packaging (MAP), vacuum packaging and addition of active compounds, among others (Rahman, 2007). The direct addition of active compounds into foodstuff reduces lipid oxidation and microbial growth, but presents short preservation times (Costa et al., 2015; Bolumar, Andersen, & Orlien, 2011). Moreover, there are many foodstuffs that cannot be preserved by the direct addition of active compounds, since they are fresh or raw food products in which the addition of other substances is not permitted (Tovar et al., 2005). These issues have driven researches towards active packaging to address the demands from food industry and consumers needs (Roberston, 2013; Sanches-Silva et al., 2014). The incorporation of antioxidants and antimicrobials into film formulations is a promising approach to successfully inhibit lipid oxidation and microbial growth and so, to prevent food rancidity.

1.2 Antioxidant compounds for gelatin films

Potential health hazards of many synthetic antioxidants, such as butylated hydroxytoluene (BHT), butylated hydroxyanisole (BHA), tert-butylhydroquinone (TBHQ) and propyl gallate (PG), require searching for safer alternatives in food packaging (Boulekbache-Makhlouf, Slimani, & Madani, 2013). Therefore, the need for using natural antioxidants has expanded rapidly and natural substances have been investigated as sources to obtain these natural and active compounds (**Table 1.1**). In particular, phenolic compounds, which show a wide structural and chemical variety, are considered the most important group of natural antioxidants, with excellent biological properties, such as anti-inflammatory, antimicrobial, anticancer and antimutagenic activities. These compounds are derived from different sources (**Table 1.2**), such as

fruits, herbs, species, vegetables, legumes, nuts, seeds, grains and cereals (Carlsen et al., 2010; Costa et al., 2015; Nollet & Toldrá, 2015).

Table 1.1 Natural antioxidants added to bovine, porcine, and fish gelatin to develop active films.

Gelatin source	Antioxidant	Reference
Bovine gelatin	*Ascophyllum nodosum* brown seaweed extract	Kadam et al., 2015
	Carrot residue fibre	Iahnke et al., 2015
	Zatoria multiflora	Kavoosi et al., 2014
	Eucalyptus wood lignosulphonates	Núñez-Flores et al., 2012
Porcine gelatin	Ascorbic acid	Kowalzyk, 2016
	Ethanol hop extract	Kowalczyk & Biendl, 2016
	Curcuma ethanol extract	Bitencourt et al., 2014
Fish gelatin	Coumarin, ferulic acid, tyrosol, quercetin	Benbettaïeb et al., 2016c
	Coconut husk ethanolic extract	Nagaranjan et al., 2015
	Cinnamon essential oil	Wu et al., 2015
	Green tea extract	Wu et al., 2013
	Sulphur-free water insoluble lignin	Núñez-Flores et al., 2013
	Ginger, turmeric, plai	Tongnuanchan et al., 2013
	Bergamot, lemon, lime	Tongnuanchan et al., 2012
	Clove essential oil	Giménez et al., 2012
	C. barbata seaweed extract	Haddar et al., 2012
	Cinnamon, clove, star anise extract	Hoque et al., 2011

Among active substances, essential oils have been widely used for pharmaceutical applications due to their antifungal and antiseptic properties against a variety of microorganisms (Djilani & Dicko, 2012). Additionally, some essential oils are used for food preservation due to their potential antioxidant activity. Citrus essential oils from diverse sources, such as bergamot, lemon and lime, have been incorporated into fish skin gelatin film formulations (Tongnuanchan, Benjakul, & Prodpran, 2012). In addition to the improvement of barrier properties against water vapour and light, it was observed that bergamot essential oil showed the highest 2,2-diphenyl-1-picrylhydrazil (DPPH) free radical scavenging capacity. Essential oils from roots, such as ginger, turmeric and plai, have been also incorporated into fish skin gelatin films (Tougnuanchan, Benjakul, & Prodpran, 2013). Results showed that plai essential oil exhibited the highest DPPH radical scavenging activity. Besides the antioxidant activity, the addition of essential oils into film forming solutions increased the film flexibility and improved water vapour permeability.

Table 1.2 Natural sources of phenolic compounds.

Source	Extracted phenolic compounds	Reference
Galangal, ginger & cinnamon spices	Ferulic, chlorogenic, protocatechuic, p-coumaric acids, galangin, rutin, quercetin, naringin	Lu et al., 2011
Lamiaceae spice	2,5- and 2,4-dihydroxybenzoic acid, rosmarinic acid, origanoside	Zhang et al., 2014
Cork oak tree	Gallic, protocatechuic, caffeic, vanillic, ellagic, chlorogenic acids, vanillin, methyl-gallate, syringledhyde	Touati et al., 2015
Artichoke bracts, stems & leaves	Caffeoylquinic acids, apigenin, luteolin	Sihem et al., 2015
Rosaceae flower	Hydroquinone, 4-hydroxybenzaldehyde, cynanoneside A, arbutin, gastrodin, apigenin	He et al., 2015
Potato peels	Chlorogenic, ferulic, gallic, caffeic, protocatechuic, syringic, coumaric, gentisic, salicylic, vanillic, p-hydroxy benzoic acids, hydroxycinnamic	Singh et al., 2011; Farvin et al., 2012; Amado et al., 2014
Pomegranate peels	Ellagitan acid and its derivatives, ellagitannin acid, punicalagin	Masci et al., 2016; Gullon et al., 2016
Tomato peels & seeds	Cinnamic, phloretic, p-coumaric, ferulic, caffeic, sinapic, chlorogenic, p-OH benzoic, vanillic, syringic, chrysin, epicatechin, naringenin, catechin, quercetin, reveratrol, rosmarinic, rutin acids	Ćetković et al., 2012; Kalogeropoulos et al., 2012
Grape pomace	Anthocyanins, flavonols, flavanols, hydroxycinnamic acids, hydroxybenzoic acids, stilbenes.	Bosso et al., 2016; Lingua et al., 2016; Jara-Palacios et al., 2015; Melo et al., 2015
Olive pomace & wastewater	Hydroxytyrosol, oleuropein, protocatechuic acid, tyrosol, verbascoside, isoverbascoide caffeic acid, vanillin, apigenin, luteolin, rutin, apigein, decarboxymethyl elenolic acid	Lozano-Sánchez et al., 2011; Cardinali et al., 2012; Ramos et al., 2013; Araújo et al., 2015
Garlic husk	Ferulic, gallic, hydroxybenzoic, caffeic, *p*-coumaric, di-ferulic, chlorogenic, coumaroylquinic acids, caffeic acid-O-glucoside, coumaric acid-O-glucoside, caffeoylputrescine	Kallel et al., 2014
Rice bran & husk	Gallic, protocatechuic, vanillic, chorogenic, caffeic, *p*-coumaric, ferulic, sinapic, gentisic, *p*-hydroxybenzoic, syringic, vanillin acids	Wanyo et al., 2014; Pourali et al., 2010

In addition to the type of essential oil, its concentration affects the antioxidant capacity. When *Zatoria multiflora* essential oil was incorporated into bovine gelatin film forming solutions at different concentrations, the antioxidant activity of the films increased from 2.6 ± 0.11 to 5.5 ± 0.51 mg ascorbic acid equivalent/g film when the essential oil concentration increased from 2 to 8%, (Kavoosi et al., 2014). The antioxidant activity of this essential oil was related to the presence of nitric oxide and malondialdehyde. Furthermore, the films presented antimicrobial activity, showing more effectiveness against Gram-positive bacteria (*Staphylococcus aureus, Bacillus subtilis*) than against Gram-negative bacteria (*Pseudomonas aeruginosa, Escherichia coli*).

Atarés & Chiralt (2016) reviewed the effect of essential oil addition on the structural, physical and bioactive properties of edible/biodegradable films and coatings for food packaging. Essential oils were mainly incorporated into films and coatings by emulsification, a potential tool in food technology to reduce additive losses by volatilization, and improve the contact between the active compound and the polymer matrix. They concluded that improvement of antioxidant and/or antimicrobial properties of edible films and coatings by means of essential oil addition could extend the shelf life and add value to foodstuffs.

Besides essential oils, crude extracts of herbs and species are good retardants of lipid oxidation due to their high content of phenolic compounds and so, they are used as antioxidant agents in polymer matrices (Embuscado, 2015). Bitencourt et al. (2014) assessed the antioxidant capacity of curcuma ethanol extract on pig skin gelatin films and found that this was proportional to the concentration of the extract added. When 2% of the extract was added, DPPH radical scavenging assay indicated an increase of the antioxidant activity from 1.8% up to 79.2%. This antioxidant activity was related to the presence of curcumin and other phenolic compounds in the extract. In addition to the antioxidant effect, the incorporation of curcuma ethanol extract improved tensile strength and barrier properties against water vapour and light. Other extracts like green

tea extract also promoted improvements in mechanical and barrier properties of silver carp skin gelatin films (Wu et al., 2013). Regarding the antioxidant capacity of the extract, results showed that the addition of 0.7% of green tea extract significantly increased the total phenolic content up to 39.05 mg galic acid equivalent/g film and the DPPH radical scavenging activity up to 31.4%. However, the antioxidant activity decreased during storage time, reaching values of 22% in DPPH radical scavenging activity after 180 days of storage. In order to keep films active in applications for longer periods of time, Kowalczyk & Biendl (2016) analysed the release of ethanol hop extract from pig gelatin films. Results showed that it was possible to deliver the extract over an extended period of time due to the swelling-controlled release from gelatin films. Similar results were found when incorporating ascorbic acid (vitamin C) into pig gelatin film forming solutions (Kowalczyk, 2016). Vitamins, phlorotannins, laminarins, sulphated polysaccharides, carotenoids and minerals present in seaweeds can also be used as bioactives. Haddar et al., 2012 observed that the antioxidant activity of fish gelatin films was significantly enhanced when adding *C. barbata* seaweed extract due to the phenolic and flavonoids compounds present in this extract. The addition of other seaweed extracts, such as *Ascophyllum nodosum* extract, also promoted antioxidant activity when it was incorporated into bovine gelatin films (Kadam et al., 2015).

1.3 Antimicrobial compounds for gelatin films

Microbial activity is also a cause of deterioration in many foods and it is responsible for reducing the quality and safety in food products (Rawdkuen et al., 2012). The direct addition of antimicrobials into food products during food processing can be used to control microbial growth and extend food shelf-life (Singh et al., 2016). However, the incorporation of those antimicrobial compounds into food packaging is attracting more and more attention. Natural antimicrobials have been incorporated into gelatin films, including essential oils, extracts of herbs, plants and species, peptides, and chitosan (**Table 1.3**).

In addition to antioxidant activity, essential oils have shown antimicrobial effect when being incorporated into gelatin film forming solutions to prepare active films. In particular, fish gelatin films with lemongrass oil showed inhibitory effect against Gram-positive bacteria (*S. aureus*, *Listeria monocytogenes*) and Gram-negative bacteria (*E. coli*, *Salmonella typhimurium*), while the films prepared with bergamot essential oil only inhibited Gram-positive bacteria (Ahmad et al., 2012). The antimicrobial activity of essential oils is attributed to terpenes, which could disrupt cell wall of bacteria and penetrate into the cell, leading to denaturation of proteins, destruction of cell membrane and cell death. Taking the above into consideration, the antimicrobial activity of essential oils would be lower against Gram-negative bacteria due to the presence of an additional external membrane surrounding the cell wall of these bacteria, restricting the diffusion of hydrophobic compounds through the membrane and reducing the effect of the antimicrobial compounds (Oussalah et al., 2007).

Bioactive peptides, such as lysozyme, can also be incorporated into gelatin films for food preservation. Their antimicrobial activity is associated with the hydrolysis of peptidoglycan layers in the cell wall of bacteria (Perez-Espitia et al., 2012). Lysozyme-incorporated fish gelatin films did not inhibit the growth of *E. coli* due to the fact that lysozyme cannot penetrate the lipopolysaccharide layer of Gram-negative bacteria (Bower et al., 2006). However, gelatin films with lysozyme, even at very low concentrations (0.001%), were effective against Gram-positive bacteria (*Bacillus subtilis*, *Streptoccocus cremoris*). When combining lysozyme with catechin in fish gelatin film forming solutions, the resulting films exhibited antimicrobial activity against both Gram-positive and Gram-negative bacteria, although the highest inhibition was found for Gram-positive bacteria (*S. aureus*, *Listeria innocua*) and yeast (*Saccharomyces cerevisiae*), while the lowest inhibition corresponded to Gram-negative bacteria (*E. coli*) (Rawdkuen et al., 2012). The effect of catechin-lysozyme incorporated into bovine gelatin films on the growth of yeasts and moulds was

assessed in minced pork (Kaewprachu et al., 2015). Results showed that meat samples wrapped in gelatin films exhibited lower counts in yeasts and moulds than commercial films, such as polyvinyl chloride (PVC) films.

The incorporation of chitosan into gelatin film forming solutions also resulted in active films against relevant food poisoning microorganism like *S. aureus* (Gómez-Estaca et al., 2011). These authors observed that mixing gelatin and chitosan was a means to improve water and mechanical resistance of gelatin films, but also to provide gelatin films with antimicrobial activity. Gelatin has been also mixed with other polysaccharides, such as agar, in addition to the incorporation of green tea extract (Giménez et al., 2013). When the release of active compounds was analysed, results revealed that the antimicrobial effect of green tea extract was maintained when the extract was incorporated into the film forming solutions, since the resulting films inhibited the growth of *Vibrio parahaemolyticus, Photobacterium phosphoreum*, *Shewanella putrefaciens,* and *Pseudomonas fluorescens* bacteria. Other extracts from species and fruits, such as the water soluble extracts of rosemary, oregano and citrus fruits were also evaluated in order to measure their antimicrobial activity against Gram-positive (*L. innocua*) and Gram-negative (*P. fluorescens*, *Aeromonas hydrophila/caviae*) bacteria. *L. innocua* was sensitive to all the extracts, whilst *P. fluorescens* was the most resistant (Iturriaga, Olabarrieta, & de Marañón, 2012).

Table 1.3 Antimicrobials added to bovine, porcine, and fish gelatin to develop active films.

Gelatin source	Antimicrobial	Microorganisms	Test	Reference
Bovine gelatin	Rosemary, oregano & citrus extracts	*L. innocua, P. fluorescens, A. hydrophila/caviae*	*In vitro*	Iturriaga et al., 2012
	Clove, lavender, rosemary & thyme essential oils	*L. acidophilus, L. Monocytogenes*	In food (dolphinfish)	Gómez-Estaca et al., 2010b
	Catechin-lysozyme	Lactic acid bacteria, yeasts and moulds	In food (minced pork)	Kaewprachu et al., 2015
	Chitosan	*S. aureus*	*In vitro*	Gómez-Estaca et al., 2011
Porcine gelatin	Oregano & rosemary essential oils	*Enterobacteriaceae*	In food (sardines)	Gómez-Estaca et al., 2010a
Fish gelatin	Green tea extract	*V. parahaemolyticus, P. phosphoreum, S. putrefaciens, P. fluorescens*	*In vitro*	Giménez et al., 2013
	Lemongrass essential oil	*S. aureus, L. monocytogenes, E. coli, S. typhimurium*	*In vitro*	Ahmad et al., 2012
	Clove & pepper essential oils	*S. aureus, A. hydrophila, L. monocytogenes*	In food (fish steaks)	Shakila et al., 2015
	Basil leaf essential oil & ZnO nanoparticles	*Pseudomonas, S. putrefaciens, Enterobacteriaceae*	In food (sea bass)	Arfat et al., 2015
	Lysozyme	*E. coli, B. subtilis, S. Cremoris*	*In vitro*	Bower et al., 2006
	Catechin-lysozyme	*E. coli, S. aureus, L. innocua, S. cerevisiae*	*In vitro*	Rawdkuen et al., 2012

Among antimicrobial agents, inorganic compounds, such as some metal oxides, are Generally Regarded as Safe (GRAS) and, additionally, they are stable at those high temperatures and pressures used during both food processing and packaging. With this regard, the mechanism of action of ZnO nanoparticles was assessed and results suggested that nanoparticles disrupted the cell membrane and caused oxidative stress (Xie et al., 2011). Specifically, Zn^{2+} ions could penetrate through the cell wall, react with the cell components and so, affect the cell viability. Furthermore, ZnO nanoparticles could generate hydrogen peroxide, a well-known oxidising agent, damaging the cell membrane (Tayel et al., 2011). When ZnO nanoparticle-incorporated gelatin films were used to wrap sea bass, its shelf-life extended from 4 to 12 days (Arfat et al., 2015).

1.4 Controlled-release of active compounds from gelatin films

The release rate of active compounds can be evaluated by using diffusion migration studies. On the one hand, the evaluation *in vitro* can be performed through the total immersion of the film in food-simulating solvents, liquids that emulate the behaviour of real food, such as aqueous simulants or fatty simulants. On the other hand, the active packaging can be directly used with the foodstuff to assess the release of the active compound. In both cases, after the migration trials, the food simulant or the foodstuff must be analysed to determine the efficacy of the active compound and quantify the amount released.

Different approaches, such as the active compound encapsulation, the biopolymer crosslinking or nanofillers' addition, can be carried out in order to prepare active packaging with the controlled release of the active compound. Liposomes, polymeric particles or lipid nanoparticles are delivery vehicles used to encapsulate and isolate an active compound (solid or liquid) from the surrounding environment until its release is triggered. These protected delivery techniques provide protection to active agents from the oxidation induced by heat, light and moisture, avoid/retard the

evaporation of volatile compounds, and facilitate material handling during processing and storage, in addition to the control of the release rate of the active compound (Martins et al., 2014; El Asbahani et al., 2015).

Encapsulation of active ingredients is usually carried out by emulsification and spray-drying, or by coacervation and solvent evaporation (Da Silva, Barreira, & Oliveira, 2016). Wu et al. (2015) prepared gelatin films with cinnamon essential oil and compared the release rate when the essential oil was directly incorporated into the film forming solution or though the encapsulation in nanoparticles. It was found that the essential oil release decreased from 98% after 99.5 h to 87% after the same period of time when the active compound was encapsulated.

Besides encapsulation, crosslinking induced by irradiation can also be used to control the release of active compounds. Benbettaïeb et al. (2016b) found that the effective diffusion coefficient of active compounds, such as coumarin or tyrosol, in aqueous medium decreased after electron beam irradiation (60 kGy) of chitosan-fish gelatin films due to the steric hindrance caused by the network crosslinking induced by irradiation. Similar results were observed in an ethanol simulant for chitosan-fish gelatin films when using quercetin as active compound (Benbettaïeb et al., 2016a), showing that irradiation delayed the release of quercetin from the films due to the new interactions promoted as a consequence of the structure changes induced by the irradiation process.

Changes in gelatin network can also be promoted by the incorporation of nanoclays. Giménez et al. (2012) prepared fish gelatin films containing clove essential oil as an active compound and evaluated the role of sepiolite nanoclay to control the release of the essential oil in water at different time-intervals. As eugenol is the major component of clove essential oil, the release of eugenol from gelatin films and gelatin-sepiolite films in water was monitored. Films containing sepiolite showed a gradual

release of eugenol, while gelatin films reached the maximum release of eugenol in 45 min.

1.5 Future trends and opportunities from a global perspective

Special attention has been recently paid to the compounds isolated from food wastes generated in food processing industries. Actually, the large amounts of food waste (peels, husks, whole pomace) are raising serious management problems from the economic and environmental point of view. In order to overcome this situation, industrial ecology concepts, such as cradle to cradle and circular economy, have been developed with the aim of using industrial wastes as raw materials for new products and applications.

Some studies have been recently carried out in order to prepare gelatin films with waste generated in linseed oil encapsulation and carrot processing industries, specifically, gelatin capsule residue and carrot residue fibre (Iahnke et al., 2015). These gelatin films prepared with 8.5% of carrot residue were used to package sunflower oil and it was found that the presence of carotenoids in carrots protected sunflower oil from oxidation. Crizel et al. (2016) also used gelatin from capsule waste to prepare films with active compounds obtained from the processing of blueberry juice. Blueberry pomace dietary fibre was incorporated into film forming solutions and fish gelatin films prepared with different concentration of fibre were used to package sunflower oil. The antioxidant activity was assessed over 35 days of storage and it was observed that the films with a fibre concentration of 0.15 g/mL presented higher antioxidant activity. In particular, these gelatin films exhibited a constant and stable peroxide value over time.

Legislation on waste management highlights the valorisation of food industry waste (Ravindran & Jaiswal, 2016). Therefore, the use of industrial waste as a raw material for the development of active packaging is economical and environmentally

appealing. Using waste for value added production comes within the spirit of the circular economy to address the possibilities of the conversion of renewable biological resources into economically viable products (**Figure 1.1**). With this regard, in addition to the source of raw materials, the manufacturing processes also play a key role. Although extrusion is a well-established industrial technique, it has not been widely used for gelatins. However, some recent works focused on the extrusion of bovine (Nur Hanani et al., 2013) and fish gelatin (Etxabide, Guerrero, & de la Caba, 2016) suggest the possibility of this manufacture process as a suitable processing method for gelatins. Furthermore, due to its relative low melting point, gelatin can be processed by extrusion at lower temperatures than commodities, which could increase not only its commercial feasibility but also the process sustainability. Considering that thermoplastic extrusion is a versatile, highly efficient, and continuous manufacturing technology, together with the high availability of gelatin from food processing waste, the use of this technique could allow scaling up production and would greatly increase the application of gelatin films as food packaging.

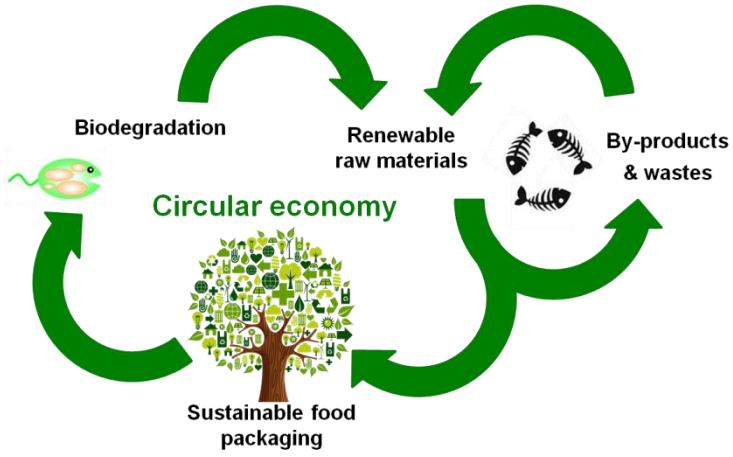

Figure 1.1 Valorisation of food processing waste and by-products towards circular economy.

Finally, the assessment of biodegradability is a key step in order to increase the commercial potential of food packaging nowadays. Although some recent works have

been published in relation to the biodegradability of food packaging based on biopolyesters (Arrieta et al., 2014; Song et al., 2016), few studies have been carried out for gelatin films (Etxabide et al, 2016a; Uranga et al., 2016). Therefore, the analysis of the end of life of this type of new active films is expected to be one of the objectives to be addressed in future works related to this interdisciplinary research area of food packaging.

In sum, in relation to the three abovementioned stages involved in circular economy (extraction, production, and disposal treatment), in future works many efforts will be focused on the improvement of those three processes with the aim of increasing yields and reducing chemicals in order to reduce both product prices and environmental impacts, enabling the development of competitive and sustainable food packaging.

2 Materials and methods

2.1 Materials and reagents

Commercial fish gelatin (type A, 200 bloom, 11.06% moisture, and 0.147% ash) was kindly supplied by Weishardt International (Liptovsky Mikulas, Slovakia). Glycerol and lactose were purchased from Panreac Química S.A. (Barcelona, Spain) and were used as plasticizer and crosslinker, respectively. Glutaraldehyde (GTA, 25% w/v in water), provided by Panreac Química S.A. (Barcelona, Spain), and genipin (GP, ≥ 98% HPLC purity), provided by Sigma-Aldrich (Madrid, Spain) were also used as crosslinkers for film preparation. Tetrahydrocurcumin (THC) was gifted by Sabinsa Corporation (New Jersey, USA) and was used as antioxidant. 2,2-diphenyl-1-picryl hydrazyl (DPPH), Folin Ciocalteu reagent and gallic acid were purchased from Sigma-Aldrich (Saint-Louis, USA). Sodium carbonate (Na_2CO_3) was gained from Merck (Fontenary Sous Bois, France) and 2,6-di-tert-butyl-4-methylphenol (BHT) was supplied by Sigma-Aldrich (Saint-Louis, USA). Methanol (MeOH) was analytical grade and the water was distilled.

2.2 Film and biocomposite preparation

2.2.1 Film preparation

Gelatin films with different lactose contents (10, 20 and 30 wt % on gelatin dry basis) were prepared by casting. Firstly, 5 g of gelatin and the amount of lactose required for each formulation were dissolved in 100 mL of distilled water for 30 min at 80 ºC under continuous stirring. After that, 10 wt % glycerol (on gelatin dry basis) was added to the solution, the pH was adjusted to 2.0 with 1 N HCl (named acid pH) or to 10.0 with 1 N NaOH (named basic pH), and the blend was maintained at 80 ºC for other 30 min under stirring. Films were also prepared without modifying the solution pH (5.4), named native pH. Afterwards, 17 mL of film forming solutions were poured into each Petri dish and left drying for 48 h at room temperature to obtain non-heated (NH) films. Additionally, some of the films peeled from the Petri dishes were heated at 105 ºC for 24 h to obtain heat-treated (HT) films.

Films were also prepared with GTA or GP as crosslinkers. For that, gelatin films (50 μm thickness) were prepared as described above. Briefly, 5 g of gelatin were dissolved in 100 mL of distilled water for 30 min at 80 ºC under continuous stirring. After that, 10 wt % glycerol (on gelatin dry basis) was added to the solution and the pH was adjusted to 10.0 with NaOH (1 N). Then, the crosslinker (lactose, GP or GTA) was added to the solution, which was kept stirring for 5 min at 37 ºC. Based on previous studies, 20 wt % lactose (Etxabide et al., 2015b), 0.75 wt % GTA (Chiou et al., 2008), or 0.25 wt % GP (Ma et al., 2013), all of them based on dry gelatin, were added to the solution as optimum crosslinker concentrations. Finally, 17 mL of film forming solution were poured into each Petri dish and left drying at room temperature for 48 h. In the event of films prepared with lactose, they were peeled from the Petri dishes and heated at 105 ºC for 24 h to obtain crosslinked gelatin films.

In the case of the films prepared with THC, 5 g of gelatin and 20 wt % lactose (on gelatin dry basis) were dissolved in 100 mL of distilled water for 30 min at 80 °C under continuous stirring, as explained above. After that, a mixture of 10 wt % glycerol and 5 wt % THC (on gelatin dry basis) was added to the solution and the pH was adjusted to 10 with NaOH (1 N). Then, the solution was placed in an ultrasonic device (Elmasonic S 30 (H), Singen, Germany) at room temperature for 5 min. Finally, the film forming solution was maintained at 80 ºC for 30 min under stirring, 17 mL of it were poured into each Petri dish, and kept at room temperature during 48 h to evaporate water and form the film. Films were peeled from the Petri dishes and were heated at 105 °C for 24 h to obtain G films (gelatin films without lactose), G-THC films (gelatin films with THC but without lactose), GL films (gelatin films with lactose), and GL-THC films (gelatin films with lactose and THC).

All films were conditioned in a controlled bio-chamber at 25 °C and 50% relative humidity for 48 h before testing. Thickness was measured to the nearest 0.001 mm with a hand-held QuantuMike digimatic micrometer (Mitutoyo Spain). A minimum of

three measurements at different positions were taken on each sample and average values and deviations were shown.

2.2.2 Biocomposite preparation

A co-rotating conical twin screw extruder, micro compounder Thermo Haake MiniLab II model (Thermo Fisher Scientific), was used to produce gelatin sheets. Extruder feed was prepared by mixing 40 g gelatin, 10 wt % glycerol (on gelatin dry basis) and different lactose contents (10, 20 and 30 wt % on gelatin dry basis) in distilled water (50 wt % on gelatin dry basis) adjusted to pH 10.0 with 1 N NaOH. The mixture was manually mixed until getting a homogeneous mixture. Afterwards, the extruder was fed at 1.6 g/min, barrel temperature was fixed at 90 ºC, screw speed was set at 70 rpm, and the torque values ranged from 25 to 30 N·cm.

After cooling sheets, gelatin samples were cut into small squares and pellets were subsequently injected. An injector, Thermo Haake MiniJet II model (Thermo Fisher Scientific), was used to obtain fish gelatin biocomposites. Different injection moulds were used, depending on the properties analysed, spherical moulds or bone-shaped moulds. Injected biocomposites were heated at 105 ºC for 270 min. Heating time was selected according to the work carried out by Etxabide et al. (2015b), which showed that at least 270 min at 105 ºC were required to promote changes in the secondary structure of fish gelatin by the addition of 10 wt % lactose. Finally, all samples were conditioned in the bio-chamber at 25 ºC and 50% relative humidity for 48 h before testing.

2.3 Physicochemical characterization

2.3.1 Moisture content (MC) and total soluble matter (TSM)

Three specimens of each film were weighted (m_w) and subsequently dried in an air-circulating oven at 105 ºC for 24 h. After this time, the films were reweighted (m_0) to determine MC values. MC was calculated as:

$$MC\ (\%) = \frac{m_w - m_0}{m_w} \times 100$$

Afterwards, dry samples were immersed in 30 mL distilled water in the presence of sodium azide (0.02 g/100 mL) in order to prevent microbial growth. Flaks were stored in an environmental chamber at 25 ºC for 24 h with occasional gentle stirring. After that, specimens were dried in an air-circulating oven at 105 ºC for 24 h and weighted (m_f). TSM was expressed as the percentage of film dry matter solubilised after 24 h immersion in distilled water (Cuq et al., 1996; Kunte et al., 1997):

$$TSM\ (\%) = \frac{m_0 - m_f}{m_0} \times 100$$

2.3.2 Swelling measurements

Swelling of biocomposites was calculated gravimetrically according to ASTM D570-98 (ASTM, 1998). Three specimens of each composition were weighted (W_0) and immersed in a phosphate-buffered saline (PBS) solution at pH 7.0. After that, samples were removed from the buffer solution at fixed times, wiped with a paper and reweighted (W_t). The process was repeated until getting constant values. Swelling (S) was calculated using the following equation (Martínez-Ruvalcaba et al., 2009):

$$S\ (\%) = \frac{(W_t - W_0)}{W_0} \times 100$$

A graph depicting swelling (S) against time (t) was plotted in order to determine the equilibrium swelling.

2.3.3 Fourier transform infrared (FTIR) spectroscopy

FTIR spectra were carried out in a Nicolet Nexus FTIR spectrometer using ATR Golden Gate (Thermo Scientific). A total of 32 scans were performed at 4 cm^{-1} resolution. Measurements were recorded between 4000 and 800 cm^{-1}. All spectra were smoothed using the Savitzky-Golay function. Second-derivative spectra of the amide

region were used at peak position guides for the curve fitting procedure, using OriginPro 9.1 software.

2.4 Optical properties

2.4.1 Gloss measurement

Gloss was measured at 60º incidence angle according to ASTM D-523-14 (ASTM, 2014) using a flat surface Multi Gloss 268 plus gloss meter (Konica Minolta). Measurements were taken ten times for each sample at 25 ºC.

2.4.2 Colour measurement

Colour was determined with the CR-400 Minolta Croma Meter colourimeter (Konica Minolta). Films specimens were placed on the surface of a white standard plate (calibration plate values L*= 97.39, a*= 0.03 and b*= 1.77) and colour parameters L*, a*, b* were measured using the CIELAB colour scale: L*= 0 (black) to L*= 100 (white), -a* (greenness) to +a* (redness), and –b* (blueness) to +b* (yellowness). Colour difference (ΔE*) for HT films as a function of lactose content was calculated referred to the NH films for the same lactose content as follows:

$$\Delta E^{*}=\sqrt{(\Delta L^{*})^{2}+(\Delta a^{*})^{2}+(\Delta b^{*})^{2}}$$

Since the browning index (BI) represents the purity of brown colour and it is an important parameter in non-enzymatic browning processes (Olivas et al., 2007; Palou et al., 1999), the BI value was calculated as follows:

$$BI\ (\%)=\frac{x-0.31}{0.172}\times 100$$

where,

$$x=\frac{(a^{*}+1.75L^{*})}{(5.645L^{*}+a^{*}-3.012b^{*})}$$

2.4.3 Light absorption

The V-630 UV-vis spectrophotometer (Jasco) was used to determine light barrier properties of films. Light absorption was measured at wavelengths from 200 to 800 nm. Three specimens were tested for each composition.

2.4.4 Fluorescence spectroscopy

Fluorescence emission measurements were performed with the spectrophotometer of Photon Technology International (PTI, Horiba ABX) with the controlled cuvette Holder TLC50 (Quantum North West) and the spectra were obtained using FeliX32 software. Gelatin films were excited at 335 nm and emission spectra were recorded from 360 to 650 nm at 105 ºC every 30 min.

2.5 Barrier properties

2.5.1 Water contact angle (WCA) determination

WCA measurements were performed using an OCA 20 contact angle system (DataPhysics Instruments). A 3 µL droplet of distilled water was placed on film surface to estimate the hydrophobic character and the image of the drop was carried out using SCA20 software. Five measurements were made for each composition at 25 ºC.

2.5.2 Water vapour permeability (WVP)

WVP measurements were carried out in a controlled humidity environment chamber PERME™ W3/0120 (Labthink Instruments Co. Ltd.). Each film was cut in samples of 7.4 cm diameter and a test area of 33 cm^2. Films were maintained at a temperature of 38 ºC and a relative humidity of 90%, according to ASTM E96-00 (ASTM, 2000), and WVP was determined gravimetrically until constant weight. Firstly, water vapour transmission rate (WVTR) was calculated as:

$$WVTR\left(\frac{g}{s \cdot cm^2}\right) = \frac{G}{t \times A}$$

where, G is the change in weight (g), t is time (s), and A is test area (cm^2).

Water vapour permeability (WVP) was determined as:

$$WVP\ \left(\frac{g}{s \cdot cm \cdot Pa}\right) = \frac{WVTR \times L}{\Delta P}$$

where, L is the thickness of the samples (cm) and ΔP is the partial pressure difference of water vapour across the film (Pa). Measurements were carried out in triplicate.

2.6 Mechanical properties

Tensile strength (TS) and elongation at break (EB) were measured for each film at least five times on an electromechanical Insight 10 testing system (MTS Systems) at 25 ºC, according to ASTM D1708-93 (ASTM, 1993). Samples were cut into strips of 4.75 mm × 22.25 mm.

2.7 Thermal characterization

2.7.1 Thermo-gravimetric analysis (TGA)

Thermo-gravimetric measurements were performed in a Mettler Toledo TGA SDTA 851 (Mettler Toledo S.A.E.). Tests were run from 25 ºC up to 800 °C at a heating rate of 10 ºC/min under inert atmosphere (10 mL N_2/min) to avoid thermo-oxidative reactions.

2.7.2 Differential scanning calorimetry (DSC)

DSC measurements were performed using a Mettler Toledo DSC 822, provided with a robotic-arm and with an electric intercooler as a refrigeration unit (Mettler Toledo S.A.E.). Samples (4.0 ± 0.1 mg) were hermetically encapsulated in aluminium pans to prevent mass losing during heating from -50 to 250 ºC at a rate of 10 °C/min under inert atmosphere (10 mL N_2/min).

2.7.3 Dynamic-mechanical analysis (DMA)

DMA measurements were carried out in tensile mode with an Eplexor 100N analyser (Gabo Qualimeter). Testing was conducted at a constant frequency of 1 Hz.

The strain amplitude was fixed at 0.05% and the temperature range was from -100 to 140 ºC at a heating rate of 2 ºC/min.

2.8 Surface and structural characterization

2.8.1 Scanning electron microscopy (SEM)

The morphology of fracture surfaces was visualized using a field emission scanning electron microscope Hitachi S-4800 (Hitachi High-Technologies Corporation) at an acceleration voltage of 15 kV. Samples were mounted on a metal stub with double-side adhesive tape and coated under vacuum with gold (JFC-1100) in an argon atmosphere prior to observation.

2.8.2 Atomic force microscopy (AFM)

The morphology of the samples was studied by AFM under ambient conditions. AFM images were obtained using a scanning probe microscope (Nanoscope IIIa Multimode™, Bruker). Tapping mode was employed in air using an integrated tip/cantilever at 200-400 kHz resonance frequency, 0.6-1.0 Hz scan rate and 20-80 N/m force constant. Regarding sample preparation, a small volume (10 µL) of film forming solution at 80 ºC was pipetted onto a piece of mica sheet (1.0 cm diameter) attached to a substrate (1.5 cm diameter) with double-adhesive tabs and conditioned at 80 ºC to avoid possible conglomeration of gelatin. After that, a high speed spin (2000 rpm) was employed during 120 s to get well expanded thin films. Finally, some of the films were heated at 105 ºC for 24 h to promote crosslinking and then, all films were kept in a controlled bio-chamber at 25 ºC and 50% relative humidity for 48 h before analysing their structure.

2.8.3 X-ray photoelectron spectroscopy (XPS)

A K-Alpha spectrometer (ThermoFisher Scientific) was used for the chemical surface analysis. The monochromatized AlKα source (hv = 1486.6 eV) was activated with a spot size of 200 µm in diameter. The full spectra (0-1350 eV) were obtained with

a constant pass energy of 200 eV, whilst high resolution spectra were obtained with a constant pass energy of 40 eV. Depth profiles (about 3-10 nm) were obtained through Ar^+ sputtering. Quantification and fitting of C 1s, N 1s and O 1s spectra were performed using the AVANTAGE software provided by ThermoFisher Scientific.

2.8.4 Optical microscopy

Optical microscopy was used to analyse the film surface and the optical micrographs with a magnification of 40X were captured with a digital microscope (Leica).

2.8.5 X-ray diffraction (XRD)

XRD analysis was performed with a diffraction unit (PANalytic Xpert PRO) operating at 40 kV and 40 mA. The radiation was generated from a Cu-Kα (λ = 1.5418 Å) source. The diffraction data were collected from 2θ values from 2.5º to 50º, where θ is the incidence angle of the X-ray beam on the sample.

2.8.6. Film porosity measurement

Porosity percentage of films was obtained by mercury intrusion porosimetry (MIP) using a mercury intrusion porosimeter (Autopore IV, Micromeritics Instrument). The obtained intrusion curve relates the mercury intrusion signal into volume of mercury intruded for each value of applied mercury pressure. The determination of porosity was based on the relationship between the applied mercury pressure (0.0036-228 MPa) and the pore size into which mercury intrudes. During the MIP test, the initial evacuation pressure was 50 µm Hg, for an evacuation time of 5 min. The mercury filling pressure was 0.53 psia and the equilibration time was 10 s.

2.8.7 Biocomposite density and porosity measurements

Density values were calculated for three spherical samples of each composition after swelling. The diameter (d) was measured three times for each sample by using a calliper (Mitutoyo Corporation, Japan), and the mass (m) was determined by using the

electronic balance ES 125 SM (Precisa Ldt.), reading to 5 decimals places. The density (ρ) of the samples was calculates as:

$$\rho\ \left(\frac{g}{cm^3}\right) = \frac{6m}{\pi d^3}$$

where, m is sample mass (g) and d is the sphere diameter (cm). Density values were measured for the biocomposites after heating at 105 ºC for 270 min (ρ_x) and for the non-heated biocomposites ($\rho_{control}$), used as control samples.

The porosity was calculated according to the following equation (Nakamatsu et al., 2006):

$$\text{Porosity}\ (\%) = \left(1 - \frac{\rho_x}{\rho_{control}}\right) \times 100$$

where, ρ_x and $\rho_{control}$ are the density values of the biocomposites with the same lactose content.

2.9 Antioxidant activity

2.9.1 Thermal stability of tetrahydrocurcumin (THC)

TGA was performed in a TGA-Q 500 (TA Instruments). Sample (10 mg) was placed in a platinum pan and tests were running at 105 ºC for 24 h under inert atmosphere (60 mL N_2/min) to avoid thermo-oxidation.

2.9.2 THC release and mass loss of films

The THC release was determined by immersion of films (1.5 cm x 2.0 cm) in MeOH (5 mL) at 25 ºC under stirring at 250 rpm for 5 days. Films were immersed into dark glass vessels to protect the antioxidant compound from light. UV-vis spectroscopy (Perkin-Elmer Lambda 18 spectrometer, Perkin-Elmer) was used to measure light absorption from 250 to 800 nm. The absorption spectra of the solutions were recorded

every 24 h up to 5 days. The experiments were repeated 3 times for the evaluation of each composition.

After 5 days of immersion, films were removed from the solution and dried for 1 day at room temperature. Then, films were conditioned in the controlled bio-chamber for 48 h and weighted. Three samples were used for each composition and the mass loss of each film was calculated with the following equation:

$$\text{Mass loss } (\%)=(1-\frac{W_5}{W_0})\times 100$$

where, W_0 is the weight of films before immersion and W_5 is the weight of films after 5 days of immersion.

2.9.3 Total phenolic content (TPC)

TPC values were determined by using the Folin-Ciocalteu assay. After film immersion for 5 days, 50 µL of the solution was transferred to a flask of 10 mL, where 500 µL of Folin-Ciocalteu reagent was added, and the mixture was vigorously shaken. Then, 1000 µL of 20% (w/v) Na_2CO_3 was added and the solution was shaken again. Finally, the flask volume was completed with distilled water and the solution was allowed to stand at room temperature in the dark for 2 h. After that, the absorbance against the reagent blank (MeOH) was determined at 760 nm by UV-vis spectroscopy. All tests were carried out in triplicate and TPC was expressed as mg gallic acid equivalent (GAE).

2.9.4 DPPH radical scavenging activity

DPPH radical scavenging activity was measured according to the method of Molyneux (2004). After film immersion for 5 days, 2 mL of solution was mixed with 2 mL of DPPH solution (150 µM). The mixture was vigorously shaken and then, allowed to stand at room temperature in the dark for 30 min. Free radical scavenging activity of test samples was compared to butylated hydroxytoluene (BHT) standard

solution which was used as reference. The inhibition values (I) were determined by the absorbance decrease at 517 nm as follows:

$$I\ (\%) = \frac{A_{control} - A_{sample}}{A_{control}} \times 100$$

where, $A_{control}$ is the absorbance of the MeOH solution and A_{sample} is the absorbance of the solution after film immersion for 5 days. All tests were carried out in triplicate.

2.10 Film disintegration

Indoor soil burial was carried out as a simulation test at laboratory scale in order to evaluate film disintegration (Prakash-Maran et al., 2014). Briefly, a series of Petri dishes were used as soil containers and natural microflora present in soil was used as the degrading medium. The initial microbial composition of a soil is known to be pH dependent. The initial soil pH was 7.3, determined by a mass/volume ratio of 1:5 (1 g soil/5 mL distilled water). Gelatin films were cut into rectangular shape (2 cm x 3 cm) and then, the specimens were buried at the depth of 4 cm from the soil surface. The samples were incubated at room temperature and the soil humidity was 100% during the whole study (15 days). The disintegration of films was followed by FTIR spectroscopy.

2.11 Environmental assessment

Environmental assessment was performed according to ISO 14040 guidelines and recommendations (ISO 14040, 2006). Therefore, assessment was divided into four phases: goal and scope definition, life cycle inventory (LCI), life cycle impact assessment (LCIA) and results interpretation.

The aim of this analysis was to calculate the environmental load of fish gelatin films, identifying their environmental impacts in order to propose correcting measures when designing packaging films and thus, increase their commercial potential. As also shown in recent analyses for packaging films (Günkaya & Banar, 2016), the functional

unit selected was 1 m^2 (50 μm film thickness). In this work, a 'cradle to grave' perspective was considered, including three stages: raw material extraction, film manufacture and disposal.

The software used to carry out this analysis was SimaPro 7.3.3. LCI data for the extraction stage, which was not carried out in our labs, were obtained from literature in the case of fish gelatin (Karim & Bhat, 2009), and from Ecoinvent 2.2 database, available in SimaPro software, in the case of glycerol and the additives used in the extraction processes. As the manufacture of the films was performed in our labs, LCI data were collected based on this work. Finally, the data for the end of life stage was provided by Lapatx composting facility located in the Basque Country. Some assumptions were considered when performing the environmental assessment. The glycerol employed as a plasticizer was considered a by-product of the soy oil production destined for biodiesel. In the end of life stage, out of every 1 kg of film waste, 200 g were considered as compost, whereas the remaining organic matter was considered to be digested by microorganisms that take part in the biodegradation process. In addition, generated compost for soil improvement purposes was considered an avoided product.

Based on the inventory data, the final results were presented in the impact categories used in the Eco-indicator 99 methodology. This methodology groups the environmental impacts in three damage categories or end-points: human health, ecosystem quality and resources (Calderón et al., 2010). In this work, midpoint measurements were carried out since midpoints are considered to be links in the cause-effect chain of an impact category, in which characterization factors reflect the importance of the emissions (Bare et al., 2000). Human health category accounts for 6 midpoint impact categories: carcinogens, respiratory organics, respiratory inorganics, climate change, and ozone layer. These impact categories use DALY scale (Disability Adjusted Life Years). Ecosystem quality accounts for ecotoxicity,

acidification/eutrophication and land use. Ecotoxicity and land use are expressed in terms of Potentially Affected Fraction (PAF m^{-2} $year^{-1}$) and acidification/eutrophication is expressed as Potentially Disappeared Fraction (PDF m^{-2} $year^{-1}$). Additionally, resources category accounts for minerals and fossil fuels; both of them are expressed as MJ surplus energy. In order to consider the relative importance of the studied impact categories, normalized impact values were represented. Normalization was performed by determining the ratio of the category indicator result and that of a reference based on European level with updates of the most relevant emissions.

2.12 Statistical analysis

Data were subjected to one-way analysis of variant (ANOVA) by means of a SPSS computer program (SPSS Statistic 20.0). Post hoc multiple comparisons were determined by the Tukey's test with the level of significance set at $P < 0.05$.

3 Sustainable fish gelatin films

3.1 Summary

Concerns over the fossil fuels depletion and the environmental pollution caused by human activity lead to the development of novel products based on renewable materials with lower environmental charge in its whole life cycle (Yates & Barlow, 2013). As previously mentioned, the European plastic demand in 2015 reached 58 million tonnes, of which 39.9% were used in packaging applications, most of them for short term-applications. Furthermore, 25.8 million tonnes of consumed plastics ended up in the waste stream, of which 30.8% went to landfills because waste burial is still the first option in many EU countries (PlasticsEurope, 2016). Different kinds of plastics are used in extensive range of needs, being the synthetic polymers, such as polypropylene (PP), low density polyethylene (LDPE), high density polyethylene (HDPE) or polyvinyl chloride (PVC), the most common materials used in a wide variety of markets. In order to reduce the impact of petroleum-derived plastics, considerable attention is focused on bio-based films (Leceta et al., 2014), among them, those prepared with proteins from food processing wastes, such as gelatin (Reddy & Yang, 2013; Silva et al., 2014). The production of gelatin from fish wastes is a topic that has recently gained much attention. Since fish skins and bones contribute almost 30% of the total fish weight, the use of these fishery industry wastes can be considered a promising way for gelatin production (Gómez-Guillen et al., 2002). Furthermore, their valorisation could reduce the problems associated with waste management (Kittiphattanabawon et al., 2005), avoiding serious ecological problems and environmental pollution due to an inappropriate waste handling.

The goal of this chapter was to analyse the effect of preparation conditions on the functional properties of fish gelatin films, such as mechanical, optical and barrier properties. The changes observed in properties were related to the changes occurred in gelatin structure, analysed by spectroscopic and diffraction methods. Furthermore,

environmental impacts were measured in order to identify both the benefits and those aspects that need further improvement.

3.2 Results and discussion

Packaging technology must balance product protection with other issues such as appearance, consumer acceptability and social and environmental consciousness. Taking these aspects into consideration, characterization of optical, barrier and mechanical properties of fish gelatin films was carried out and related to the material structure to analyse the effect of solution pH (acid, native, and basic) on film properties.

3.2.1 Film characterization

A good protection from UV light could prevent the packaged product deterioration as a consequence of oxidation reactions caused by UV light (Díaz-Visurraga et al., 2010). As shown in **Figure 3.1**, fish gelatin films exhibited high UV light absorption due to the presence of peptide bonds (200-250 nm) and chromophores such as tyrosine and phenylalanine (250-300 nm), common aromatic amino acids found in fish gelatins (Samira, Thuan-Chew, & Azhar, 2014; Hong et al., 2014).

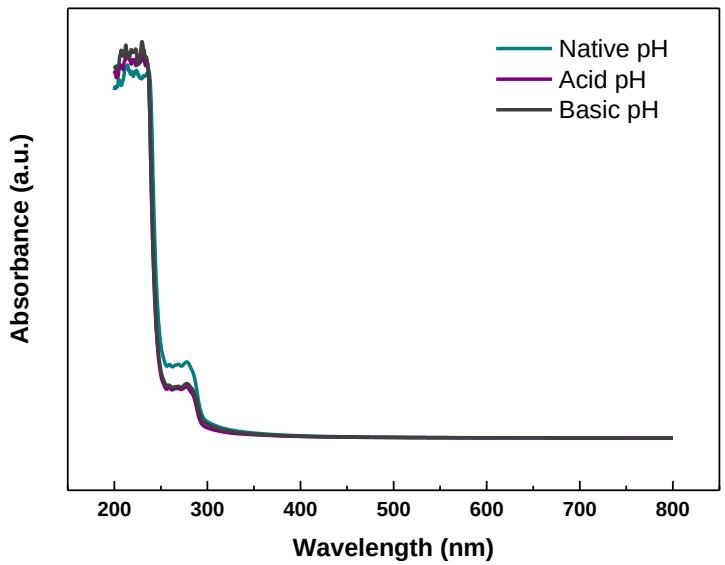

Figure 3.1 UV-vis spectra of fish gelatin films as a function of solution pH.

In addition to UV light resistance, other optical properties, such as transparency and colour, affect consumers' willingness to purchase and thus, those are properties that must be taken into consideration. As can be seen in **Figure 3.1**, films were transparent since there was not absorbance at 600 nm, irrespective of the solution pH used to prepare films. In the same manner, no significant ($P > 0.05$) change was observed for colour parameters, as shown in **Table 3.1**, where L*, a* and b* values are listed. Also in **Table 3.1**, gloss values are shown. Gloss is directly related to the surface roughness of films, so gloss values are lower when surface is rougher. Gloss values higher than 70 gloss units (GU), measured at an incidence angle of 60º, indicate glossy and smooth surfaces (Keyf & Etikan, 2004). When solution pH was modified, films showed higher gloss and thus, a smoother surface than native pH films, suggesting that pH modifies the film structure.

Table 3.1 Optical properties of fish gelatin films as a function of solution pH.

pH	L*	a*	b*	$Gloss_{60º}$ (GU)
Native	96.13 ± 0.53^{a}	-0.18 ± 0.09^{a}	2.86 ± 0.41^{a}	35.89 ± 2.85^{a}
Acid	96.14 ± 0.44^{a}	-0.18 ± 0.04^{a}	2.65 ± 0.10^{a}	152.00 ± 1.58^{c}
Basic	96.19 ± 0.25^{a}	-0.10 ± 0.03^{a}	3.01 ± 0.10^{a}	119.75 ± 6.90^{b}

[a-c]Two means followed by the same letter in the same column are not significantly ($P > 0.05$) different through the Tukey's multiple range test.

In addition to barrier properties against UV light, barrier properties against water were measured. The water contact angle (WCA) is a measure of the wettability of the surface and defines the hydrophilic or hydrophobic character of the material. Low WCA values, lower than 90º, correspond to high wettability or hydrophilicity, while high values, higher than 90º, correspond to low wettability or hydrophobicity (Yuan & Lee, 2013). The WCA values of fish gelatin films are shown in **Table 3.2**. As can be seen, higher WCA values were obtained when solution pH was modified. This fact could be explained by protein conformational changes that expose non-polar groups towards the surface.

Table 3.2 Water contact angle (WCA) and water vapour permeability (WVP) values for fish gelatin films as a function of solution pH.

pH	WCA (°)	WVP 10^{12} (g cm^{-1} s^{-1} Pa^{-1})
Native	76.85 ± 1.36[a]	1.48 ± 0.16[a]
Acid	91.35 ± 3.26[b]	1.52 ± 0.10[a]
Basic	88.61 ± 3.36[b]	1.81 ± 0.16[b]

[a-b]Two means followed by the same letter in the same column are not significantly (P > 0.05) different through the Tukey's multiple range test.

In order to control moisture transfer to and from the surrounding environment, films must show values of water vapour permeability suitable for their use. WVP values of fish gelatin films are shown in **Table 3.2**. As can be seen, WVP values increased (P < 0.05) at basic pH, probably due to a higher degree of protein denaturation and, thus, higher unfolding that facilitates permeation of water vapour molecules.

Finally, mechanical properties were measured since appropriate tensile strength and elongation at break are of great importance when handling materials in order to maintain their integrity. As can be seen in **Table 3.3**, the best mechanical properties were obtained when a basic pH was used to prepare films. TS values significantly (P < 0.05) increased when pH was modified and TS values higher than 50 MPa were obtained at basic pH. However, the elongation at break was not significantly (P > 0.05) affected by the solution pH.

Table 3.3 Tensile strength (TS) and elongation at break (EB) values for fish gelatin films as a function of solution pH.

pH	TS (MPa)	EB (%)
Native	36.52 ± 2.98[a]	1.79 ± 0.54[a]
Acid	43.02 ± 0.52[b]	2.31 ± 0.33[a]
Basic	52.39 ± 3.16[c]	2.88 ± 0.68[a]

[a-c]Two means followed by the same letter in the same column are not significantly (P > 0.05) different through the Tukey's multiple range test.

In order to relate the functional properties of fish gelatin films with the structure changes promoted by solution pH, XRD was carried out since it is a common technique

to determine the tertiary structure of proteins. The diffraction bands of fish gelatin films as a function of solution pH are shown in **Figure 3.2**.

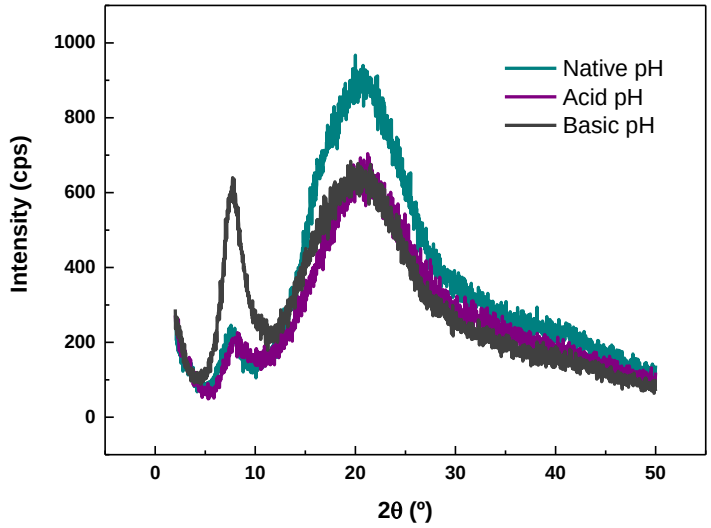

Figure 3.2 XRD patterns of fish gelatin films as a function of solution pH.

All patterns displayed two diffraction peaks, the peak at 21º, related to the crystallinity of gelatin, and the peak at 7.4º, corresponding to the residual triple helix from native collagen (Learner et al., 2008; Schmidt, Giacomelli, & Soldi, 2005). When solution pH was modified, lower crystallinity was observed, indicating that a less ordered structure was obtained as a consequence of a higher denaturation degree, which resulted in changes in the tertiary structure of gelatin (Mikšovská & Larsen, 2007). As the tertiary structure of proteins is governed by non-covalent interactions, such as hydrogen bonding, hydrophobic interactions, and charge attractions and repulsions, the change in solution pH could disrupt these non-covalent interactions, leading to the decrease in crystallinity observed in **Figure 3.2**. These results are in accordance with WVP values, which showed that a higher degree of denaturation facilitated water vapour permeation. Otherwise, the content of residual triple helix was lower at native and acid pHs than at basic conditions. Although gelatin is obtained by a partial hydrolysis of collagen, which breaks its triple helix structure and forms random

coils, gelatin is able to recover partially the native structure of collagen, phenomenon known as coil-to-helix transition (Ghoshal, Stapf, & Mattea, 2014). Results showed that the refolding of the typical collagen triple helix could be favoured at basic conditions during drying of fish gelatin films.

Infrared spectroscopy is also a valuable tool for the investigation of protein structure due to the sensitivity of the amide I vibration to the secondary structure of proteins (Fabian & Mäntele, 2002). Therefore, FTIR spectroscopy was used to study changes in the secondary structure of gelatin in terms of α-helix/unordered and β-sheet conformations by means of analysing the amide I band (1600-1700 cm^{-1}), associated with the vibration of the carbonyl group (C=O) of the peptide bond in proteins. The secondary structure of gelatin films consists mainly of α-helix/unordered conformations, associated with the band at 1650 cm^{-1}, and antiparallel β-sheet conformations, related to the bands at 1630-1615 cm^{-1} and 1700-1680 cm^{-1} (Guerrero, Kerry, & de la Caba, 2014; Susi, Timasheff, & Stevens, 1967), as shown in **Figure 3.3**.

The predominant structure was α-helix, irrespective of solution pH. However, films prepared at basic conditions showed higher area (**Table 3.4**) and, thus, higher quantity of α-helix structure than the films prepared at acidic conditions. Otherwise, an area with absorbance reduction in β-sheet structure (1700-1680 cm^{-1}) was seen when films were prepared at acidic conditions. Therefore, results showed that solution pH altered the secondary structure of fish gelatin films. In aqueous solutions, protein residues are charged, hence, protein mobility depends on pH. When the pH is far from the isoelectric point, the protein net charge changes towards positive or negative charges depending on solution pH. As same charges repel one another, this prevents protein from aggregating. Therefore, the internal interactions are altered, forcing protein structure to open up (denaturalization or unfolding) (Hoque, 2011). Due to these phenomena, the film structure changes and so do some functional properties of the films, as abovementioned.

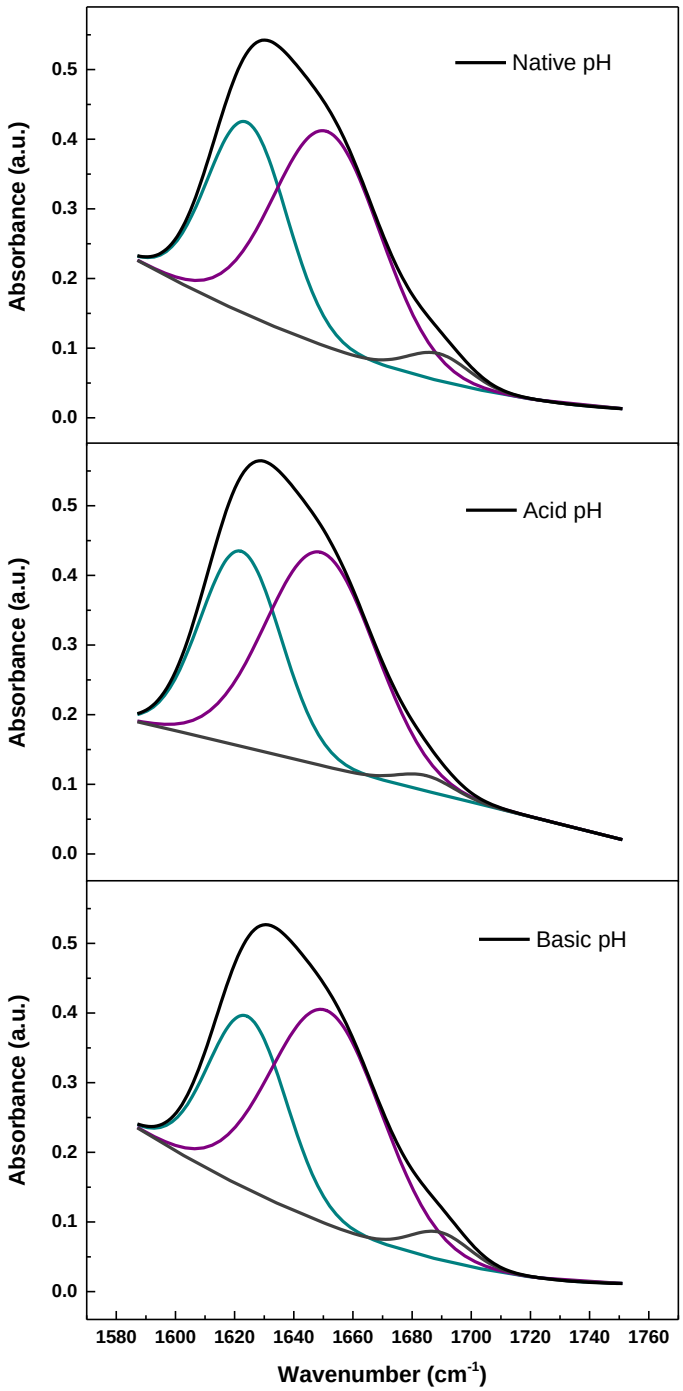

Figure 3.3 Curve fitting spectra of amide I for fish gelatin films as a function of solution pH.

Table 3.4 Resulting percentage of the curve fitting of amide I as a function of solution pH.

pH	β-sheet/random coil (1630-1615 cm^{-1})	α-helix (1650 cm^{-1})	β-sheet/random coil (1700-1680 cm^{-1})
Native	38.16	57.63	4.21
Acid	39.13	58.71	2.16
Basic	34.72	61.03	4.25

In addition to functional properties of gelatin films, their biodegradability is a relevant benefit in comparison with commercial non-biodegradable polymers, which cause problems and costs associated with their waste management after disposal. Since gelatin and glycerol are biodegradable compounds and no chemical reaction occurs between them, biodegradation test is not necessary to certify the film biodegradability (UNE-EN 13432, 2001). However, film disintegration tests were carried out by burying films into soil under controlled conditions to analyse the disintegration of gelatin films by FTIR spectra. There was no variation in the spectra of the films prepared at different pHs (data not shown). Therefore, as a higher unfolding and so, more available sites for interactions appeared at basic conditions, the disintegration tests were carried out with the films prepared at basic conditions and results are shown in **Figure 3.4**. The main absorption bands were located in the spectral range from 1630 to 800 cm^{-1}. Gelatin bands were related to C=O stretching at 1630 cm^{-1} (amide I), N-H bending at 1530 cm^{-1} (amide II) and C-N stretching at 1230 cm^{-1} (amide III) (Schmidt, Giacomelli, & Soldi, 2005). The main absorption bands of glycerol were related to the five bands corresponding to the vibrations of C-C bonds at 850, 940 and 1000 cm^{-1} and C-O bonds at 1050 and 1100 cm^{-1} (Basu et al., 2011). No shift of the characteristic bands was observed but decrease in intensities of amide I, II and III were shown during film disintegration. This fact indicates the cleavage of bonds, which is the principle of degradation. Besides, the decrease of absorption band intensity was more notable for amide II and III bands than for amide I band. Since biodegradation rate depends on the accessibility of the microorganisms to polymer chains, this process depends on the

flexibility of chains and on the amorphous regions of the protein, among others (Kijchavengkul & Auras, 2008).

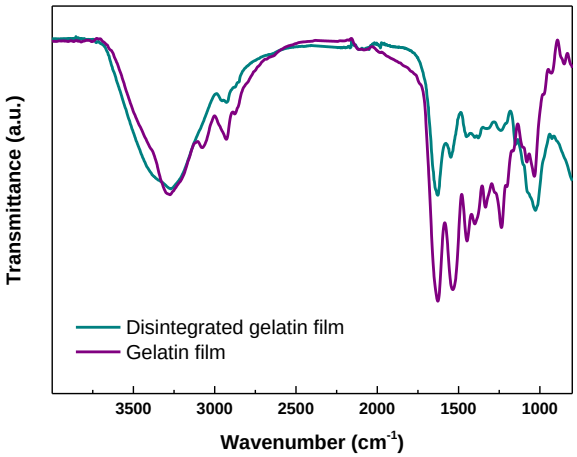

Figure 3.4 FTIR spectra of fish gelatin films before and after soil burial disintegration.

Results indicated that microorganisms mainly attacked the C-N stretching bond, following with N-H bending bond, and hardly acting on the C=O stretching bond. Therefore, the hydrolysable functional groups of amide III (C-N) and amide II (N-H) presented better accessibility than the amide I (C=O). These results are in accordance with the energy required to break the abovementioned bonds related to the amide group. Specifically, 305 kJ/mol, 390 kJ/mol and 799 kJ/mol are the bond energies for C-N, N-H, and C=O, respectively. Furthermore, it is worth noting that the band corresponding to glycerol barely changed due to the fact that microorganisms present in the soil did not attack the plasticizer. In fact, a number of microorganisms are able to grow on glycerol (Da Silva, Mack, & Contiero, 2009), so proliferation of microorganisms on the plasticizer could promote the disintegration of protein. As a consequence, there was a slight increase of the soil pH up to 7.9. This rise in pH may be caused by the ammonification of proteins from the film.

3.2.2 Environmental assessment

Concerning the environmental impacts of fish gelatin films, three main stages were assessed: material extraction, film manufacture, and end of life. A schematic diagram of the system boundaries is shown in **Figure 3.5**.

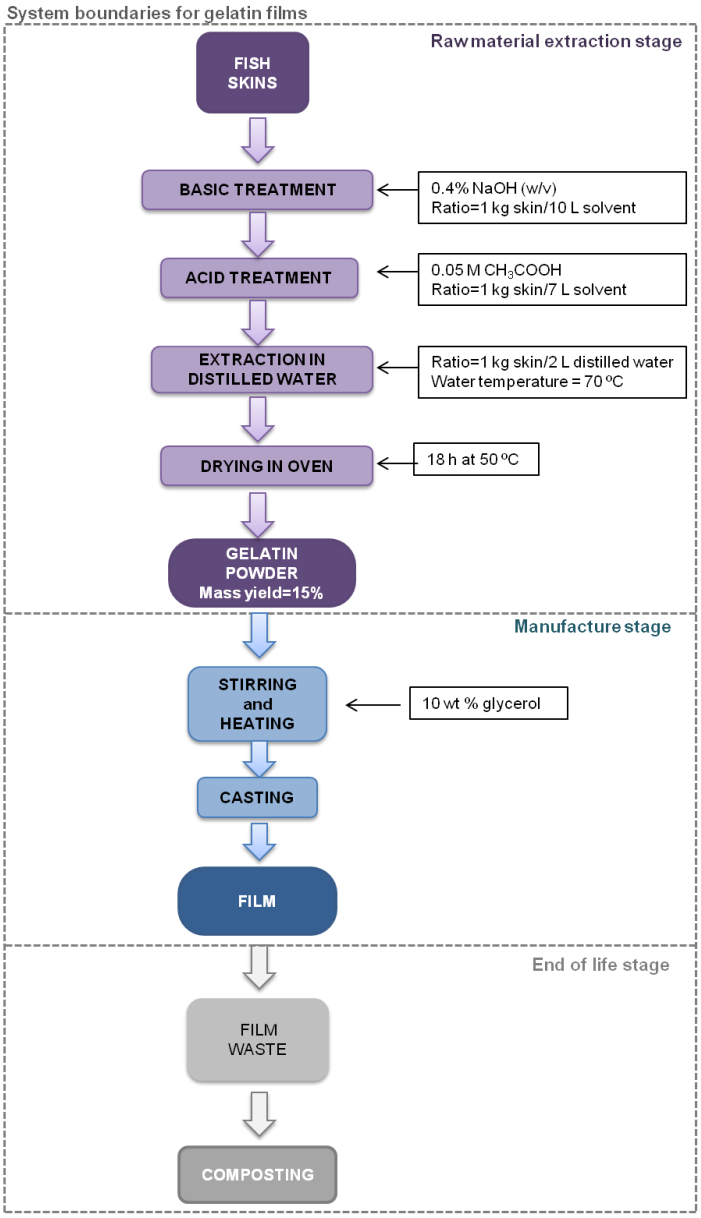

Figure 3.5 System boundaries for the environmental assessment of fish gelatin films.

The preparation of fish gelatin films is a way of adding value to the waste from fish processing industry. About 30% of such waste consists of skins and bones with high collagen content (Gómez-Guillén, 2002). The extraction method consists of a mild

swelling in sodium hydroxide and afterwards in acetic acid. Subsequently, gelatin extraction is carried out in distilled water at 70 ºC during 90 min and then, the sample is dried in an oven for 18 h at 50 ºC. Based on the average extraction yield of fish gelatins, the yield considered in this work was 15% (Karim & Bhat, 2009). This process was not carried out in our labs and data were taken from literature (Karim & Bhat, 2009). Furthermore, the production of the edible part of the fish was out of the system boundaries.

Concerning the manufacture of fish gelatin films, data were obtained from the process employed in our laboratories, described in the experimental section. In the film manufacture, the environmental load of the process from turning raw materials into films was considered, so the additives employed and the energy consumed during the process were taken into account. Since glycerol was considered as a by-product of soybean oil production to obtain biodiesel, the esterification process of soybean oil to methyl ester and glycerol in this oil production process was considered.

Finally, the disposal scenario was composting, a process based on the aerobic degradation of wastes. Out of every 1 kg of film waste, 200 g were considered as compost and residual organic matter was considered to be digested by microorganisms within the biodegradation process. It was considered that the composting facility is energetically self-sufficient and no electric consumption was taken into account. This process was not carried out in our labs and the abovementioned data were provided by the composting facility in the Basque Country. Furthermore, transportation was not considered in any stage of the assessment.

Eco-indicator 99 was the method used to assess the environmental impact of fish gelatin films. This methodology has been broadly employed in Europe due to the fact that it links results via midpoints or impact categories to endpoint or damage categories, providing the negative environmental effects due to the substances emitted

and resources used (Ingrao et al., 2015). According to the goal of this environmental assessment, the impact categories in relation to each of the three product stages are shown in **Figure 3.6**.

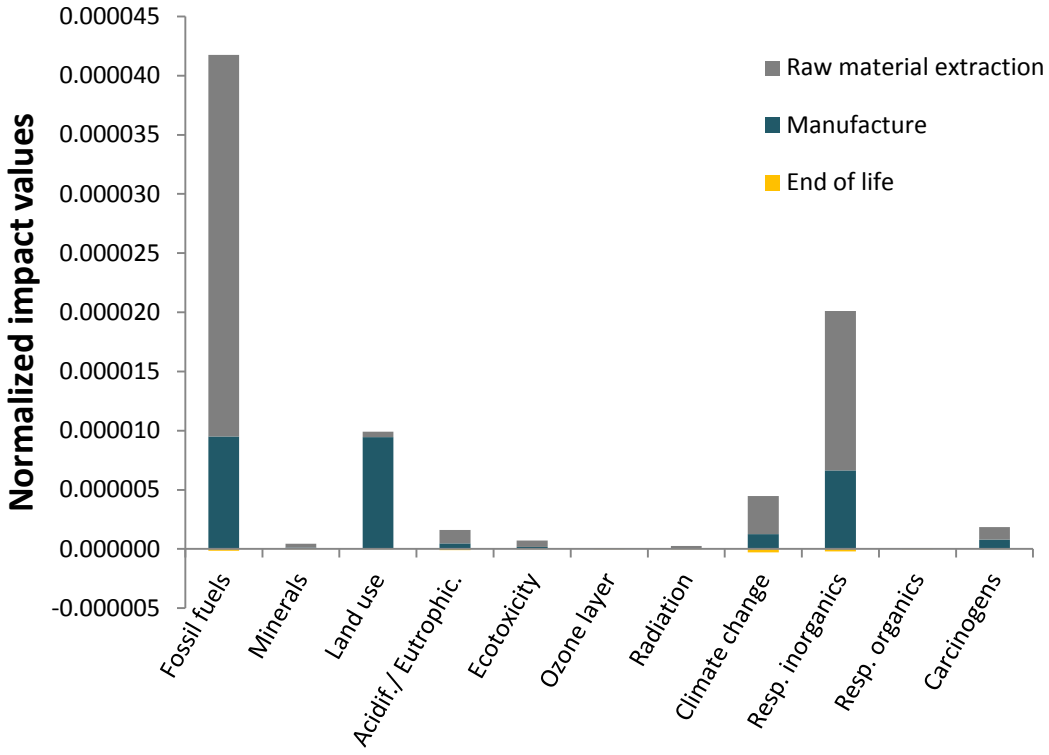

Figure 3.6 Environmental impact values normalized for fish gelatin films.

As can be seen, the raw material extraction was the most pollutant phase in the majority of the impact categories analysed. Specifically, fossil fuels and respiratory inorganics were the impact categories in which fish gelatin films caused higher environmental damage. The energy consumption during gelatin extraction was the main responsible for the environmental load in these categories.

In relation to the manufacture stage, the energy consumption together with the soya cultivation process to obtain glycerol were the main reasons for the environmental burden in fossil fuels, land use, and respiratory inorganics. With regard to land use, the environmental burden was due to the glycerol used as plasticizer since it is considered as a co-product from the production of soybean oil to obtain biodiesel and thus, cultivation of soybean was considered.

The environmental impact of the assembly, in which raw material extraction stage and manufacture stage were gathered, and the impact values related to the end of life phase are clearly differentiated in **Table 3.5**. By this way, the environmental benefit provided by composting scenario in all the environmental categories under analysis can be properly appreciated. Since composting transfers biodegradable waste into useful soil products, the carbon dioxide produced does not contribute to an increase in greenhouse gases because it is already part of the biological carbon cycle (Song et al., 2009). Moreover, avoiding the production of generated compost for soil conditioner and the associated emissions provides a positive effect on the environmental impact.

Table 3.5 Normalized results for the end of life stage of fish gelatin films.

Impact category	Assembly	End of life	Total
Fossil fuels	4.17583 E-05	-1.44962 E-07	4.16133 E-05
Minerals	4.54575 E-07	-3.11713 E-09	4.51458 E-07
Land use	9.90902 E-06	-4.49753 E-09	9.90452 E-06
Acidif/Eutrop.	1.60126 E-06	-8.53697 E-08	1.51589 E-06
Ecotoxicity	7.04678 E-07	-2.80816 E-09	7.01870 E-07
Ozone layer	2.11478 E-09	-6.95414 E-12	2.10782 E-09
Radiation	2.54337 E-07	-3.69787 E-10	2.53968 E-07
Climate change	4.46968 E-06	-2.76574 E-07	4.19311 E-06
Resp. inorganics	2.00957 E-05	-2.18191 E-07	1.98775 E-05
Resp. organics	1.13861 E-08	-2.85968 E-10	1.11001 E-08
Carcinogens	1.85121 E-06	-2.54244 E-09	1.84866 E-06

The results explained above agree with recent environmental assessments in which energy consumption for extraction and manufacturing processes were mainly responsible for the environmental impact of films (Günkaya & Banar, 2016). Although biopolymers are considered eco-friendly materials due to their renewable and biodegradable character, extraction and production practices can cause environmental burdens, as shown for some polysaccharide-based films such as starch (Günkaya & Banar, 2016), chitosan (Leceta et al., 2013), or agar (Leceta et al., 2014). It is worth noting that the majority of the environmental assessments related to biopolymers have been carried out with polysaccharides like the abovementioned (Leceta et al., 2014; Günkaya & Banar, 2016; Leceta et al., 2013) or biopolyesters like polylactic acid (PLA)

(Benetto et al., 2015) and very few studies have determined the environmental impacts for protein-based films (Deng et al., 2013; Garrido et al., 2014), or for different stages from cradle to grave, as the present work did. These results highlight the importance of this study to support decision making related to the improvements that must be incorporated into the different phases of the film development in order to achieve materials with good functional properties that are really environmentally more sustainable. However, it must be emphasized that some improvements could be expected when scaling up production from laboratory to large-scale facilities.

3.3 Conclusions

Homogeneous, colourless and transparent fish gelatin films were developed in this work, irrespective of solution pH. Furthermore, films showed high resistance against UV light, which could prevent the product packaged from oxidation reactions caused by light, maintaining its quality for longer periods of time. However, it was observed that solution pH affected gelatin structure. In particular, the films prepared at a basic pH showed high tensile strength with values higher than 50 MPa. These good functional properties of fish gelatin films and the positive environmental effect of composting as the end of life scenario highlight the potential use of these films as alternative materials for packaging applications in order to reduce the huge consumption of non-renewable and non-biodegradable materials.

4 Control of crosslinking reaction

4.1 Summary

In the previous chapter, gelatin films showed adequate functional properties, such as film forming ability, good optical properties, and biodegradability, features that promote their application in food and pharmaceutical industries (Bhutani et al., 2016; Garrido et al., 2013; Li et al., 2015a). However, due to their hydrophilic nature films based on gelatins show high brittleness and water sensitivity, which limit some applications. The improvement of those functional properties can be achieved by means of protein crosslinking (Etxabide et al., 2015b). Chemical crosslinking of gelatin can be an effective way to obtain a modified material which could provide improved chemical and physical properties. In contrast to acetylation, deamidation, and other chemical methods available to improve the functional properties of proteins, Maillard reaction is a reaction greatly accelerated by heat. Although most of the works in the literature have focused on the biological properties of glycation conjugates, Maillard reaction can be a promising approach to improve other functional properties of proteins.

The Maillard reaction rate depends upon many factors, such as temperature, time, protein:carbohydrate ratio, and pH (Lin et al., 2012). The aim of this chapter was to characterize heat-treated (HT) films prepared with lactose at two different pHs (native pH and acid pH) in order to analyse the effect of lactose content and solution pH on their physicochemical, barrier, mechanical, and morphological properties.

4.2 Results and discussion

4.2.1 Physicochemical and barrier properties

The colour change that takes place in the films with lactose after heating can be considered as an indicator of the Maillard reaction. Film colour was measured using CIELAB scale and L*, a* and b* parameters were used to calculate colour difference (ΔE*) values. The addition of lactose caused a decrease in L* and a* values (data not

shown) while b* values increased (**Figure 4.1a**). This change was more noticeable in films at native pH than at acid pH. This could be due to the fact that the amount of unprotonated amino groups and the open chain form of sugar, considered reactive species, increased with pH (Yayalayan, Ismail, & Mandeville, 1993). Therefore, total colour difference (ΔE*) changed with the lactose incorporation and the pH used (**Figure 4.1b**). ΔE* indicated that lactose content and pH significantly ($P < 0.05$) affected the degree of Maillard reaction. Morales and Van Boekel (1997) found that colour is produced in the final stage of Maillard reaction, which is characterized by the formation of unsaturated, brown nitrogenous polymers and copolymers. Since films prepared at native pH showed higher ΔE* values, it can be concluded that Maillard reaction was further extended at higher pH media. It is also worth noting that films prepared at acid pH with 10 wt % lactose showed the highest ΔE* value, indicating that the reaction extention in acid conditions might be faster at low lactose contents due to the fact that the higher amount of lactose in the cyclic form at low pH could cause higher steric hindrance.

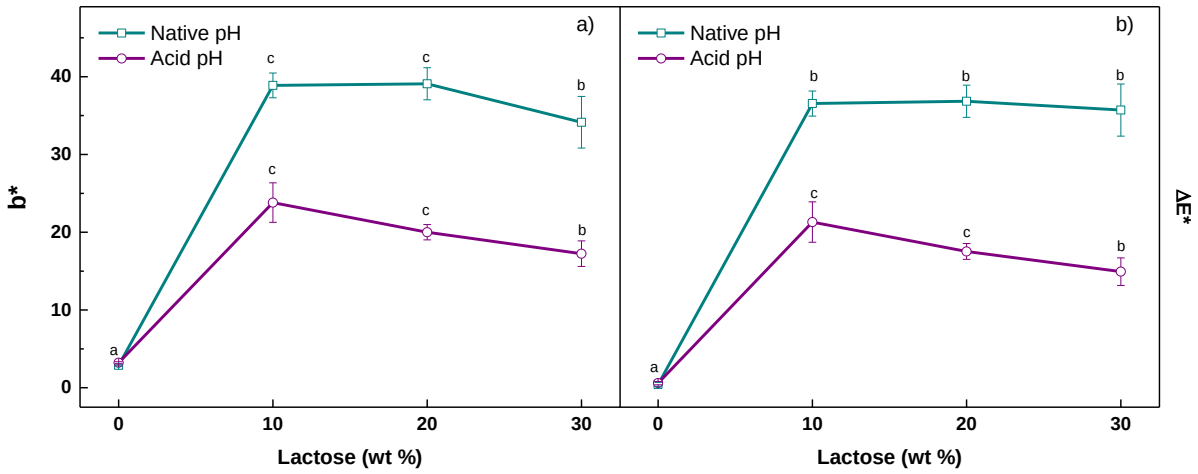

Figure 4.1 a) b* values and b) ΔE* values for HT fish gelatin films as a function of pH and lactose content. Two means followed by the same letter in the same line are not significantly ($P > 0.05$) different through the Tukey's multiple range test.

The measurement of UV light absorption of gelatin films is another method to assess the extension of Maillard reaction. All HT gelatin films exhibited high UV light absorption (**Figure 4.2**) due to the presence of peptide bonds (200-250 nm) and chromophores such as tyrosine and phenylalanine (250-300 nm), common aromatic amino acids found in proteins (Zhao et al., 2013). For the films prepared at native pH (**Figure 4.2a**), the increase in the absorption above 420 nm indicated that the crosslinking reaction reached the final stage, in which melanoidins, brown and non-soluble compounds, were formed (Li et al., 2015b). However, for the films prepared at acid pH (**Figure 4.2b**), lower absorbance values at 420 nm revealed a lower degree of crosslinking. The absorption peak around 300 nm was associated to the absorbance of the glycation product known as pentosidine, a soluble compound that can be considered as a chemical indicator of the crosslinking extent (Etxabide et al., 2015b). In the case of the films prepared at acid pH, glycation stopped when pentosidine was formed, while the reaction progressed up to the formation of melanoidins at native pH.

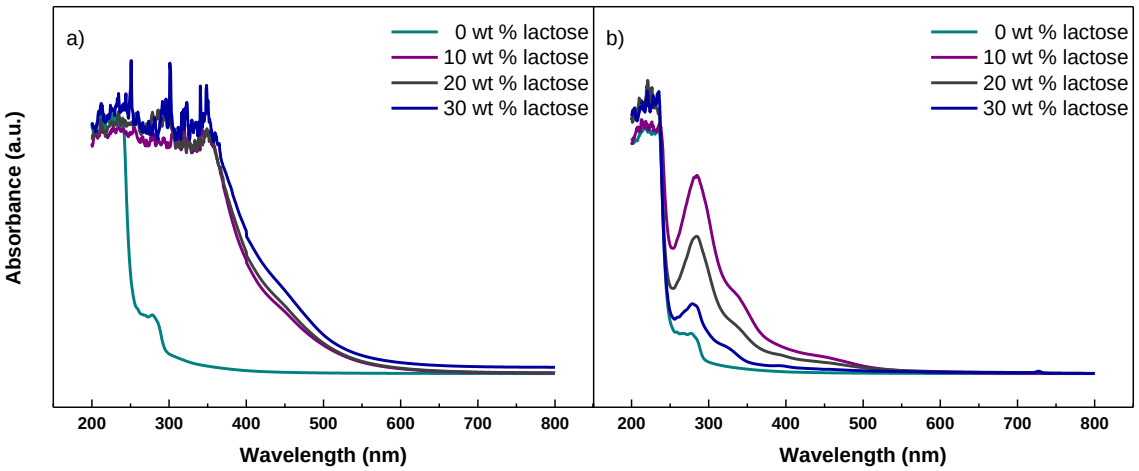

Figure 4.2 UV-vis spectra of the HT fish gelatin films prepared at a) native pH and b) acid pH, as a function of lactose content.

As abovementioned, the formation of MRPs is greatly influenced by the reaction conditions. According to Van Boekel (1998), there are two general Amadori product breakdown routes, namely the 1-deoxyosone pathway at high pHs and the 3-deoxyosone pathway at low pHs (**Scheme 4.1**). Each route gives deoxyosones, very

reactive intermediates that take part in further reactions, and the final stage of Maillard reaction leads to the formation of brown nitrogenous polymers.

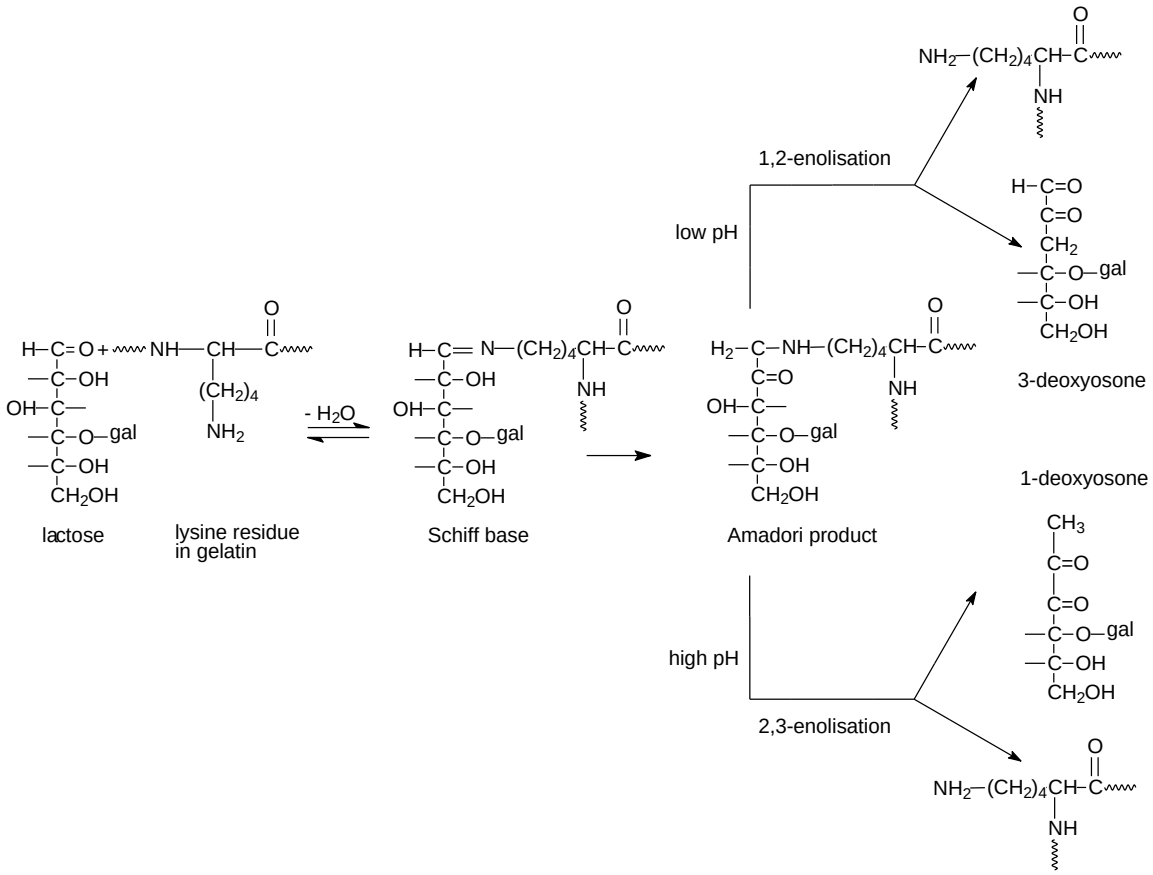

Scheme 4.1 The early stage of the Maillard reaction and the breakdown of the Amadori product in the advanced stage of Maillard reaction at different pH conditions (gal=galactose).

Among them, pentosidine is generated as the first stable fluorophore product after the formation of the Amadori compound and, thus, it can be used as a chemical indicator of the extension of Maillard reaction (Labuza and Basier, 1992). Therefore, the emission spectra of gelatin films excited at 335 nm (associated to pentosidine) was assessed to analyse the reaction extension. As can be seen in **Figure 4.3**, an emission peak corresponding to pentosidine appeared at 410 nm, in agreement with other works (Bhat et al., 2014; Morales & Van Boekel, 1997). At native pH (**Figure 4.3a**), the intensity of the bands increased as lactose content increased, indicating that the formation of pentosidine and, so, the reaction extension was higher when increasing lactose content. An emission peak also appeared in films without lactose, which could

indicate the presence of some residual sugar in the gelatin used as raw material, which could react with the amino groups in gelatin (Duconseille et al., 2015). On the other hand, the fluorescence emission spectra of the films prepared at acid pH (**Figure 4.3b**) showed that the band intensity decreased as lactose content increased, in accordance with colour results, which showed the maximum colour difference when lactose content was 10 wt %.

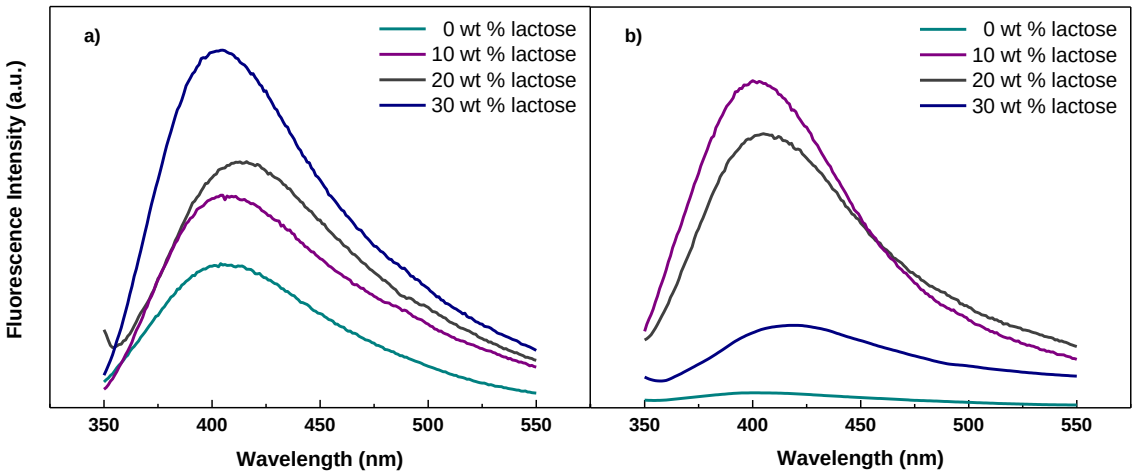

Figure 4.3 Fluorescence emission spectra of HT fish gelatin films prepared at a) native pH and b) acid pH as a function of lactose content.

Due to the fact that glycation progressed up to pentosidine formation, a soluble compound, films prepared at acid pH were totally soluble. However, lactose addition significantly ($P < 0.05$) reduced solubility for the films prepared at native pH (**Table 4.1**), in agreement with colour measurements and UV-vis spectra that showed a higher colouration as well as better UV light absorption, respectively, which means further extent of glycation with the formation of melanoidins, non-soluble compounds. These results revealed the promotion of crosslinking reaction when increasing pH (Wihodo & Moraru, 2013). Furthermore, solubility reached a minimum value around 26% for the films prepared with 20 wt % lactose. However, when increasing lactose content up to 30 wt %, TSM value did not decrease, indicating that there was a specific lactose

content at which the highest crosslinking and the lowest solubility was reached; thereafter, higher lactose content did not cause further crosslinking. These results indicated that pH and lactose content affected crosslinking extension. Considering the use of gelatin films for the release of active compounds, these results suggested that controlling pH and lactose concentration could modify film solubility and, subsequently, the active compound delivery in applications such as active films for food packaging (Liu et al., 2017) or film dressings for pharmaceutical applications (Santoro, Tatara & Mikos, 2014).

Table 4.1 Physicochemical and barrier properties for the HT fish gelatin films prepared at acid pH and native pH.

Lactose (wt %)	TSM (%) Native pH	WCA (º) Native pH	WCA (º) Acid pH
0	75.0 ± 5.4^{a}	85 ± 1^{b}	83 ± 3^{b}
10	57.3 ± 9.8^{b}	101 ± 2^{d}	99 ± 1^{c}
20	26.1 ± 0.5^{c}	101 ± 1^{d}	101 ± 1^{d}
30	31.8 ± 0.9^{c}	100 ± 2^{d}	109 ± 1^{f}

[a-f]Two means followed by the same letter in the same column are not significantly ($P > 0.05$) different through the Tukey's multiple range test.

In order to determine the hydrophilic or hydrophobic character of the film surface, water contact angle (WCA) was measured. As can be seen in **Table 4.1**, lactose addition increased WCA values for both pHs. The films prepared at native pH showed similar WCA values ($P > 0.05$), irrespective of lactose content. However, WCA values increased ($P < 0.05$) with lactose content for the films prepared at acid pH, due to the different orientation of the groups towards the surface as a function of the crosslinking extent. Since small WCA values (< 90°) correspond to high wettability or hydrophilic character, while large WCA values (> 90°) correspond to low wettability or hydrophobic character (Yuan & Lee, 2013), it can be concluded that all the films modified by lactose addition showed hydrophobic character.

4.2.2 Mechanical properties

Mechanical properties were analysed and tensile strength (TS) and elongation at break (EB) were determined (**Table 4.2**). For the films prepared at acid pH, TS decreased ($P < 0.05$) and EB increased ($P < 0.05$) as lactose content increased. These results could be explained by the lower crosslinking extent at this pH and the non-reacted lactose that acted as plasticizer (Bhat & Karim, 2014). In contrast, EB values did not significantly changed ($P > 0.05$) and TS values increased ($P < 0.05$) by lactose addition for the films prepared at the native pH due to the crosslinking reaction, reaching values higher than 50 MPa.

Table 4.2 Mechanical properties for the HT fish gelatin films prepared at acid pH and native pH.

Lactose (wt %)	TS (MPa) Native pH	TS (MPa) Acid pH	EB (%) Native pH	EB (%) Acid pH
0	51 ± 1^{c}	49 ± 2^{c}	3.3 ± 0.1^{ab}	2.5 ± 0.2^{a}
10	62 ± 2^{d}	43 ± 3^{c}	3.1 ± 0.7^{ab}	2.2 ± 0.3^{a}
20	54 ± 4^{cd}	30 ± 1^{ab}	2.8 ± 0.6^{ab}	3.3 ± 0.6^{ab}
30	54 ± 3^{cd}	28 ± 2^{ab}	3.3 ± 0.5^{ab}	3.6 ± 0.8^{ab}

$^{a-d}$Two means followed by the same letter in the same column are not significantly ($P > 0.05$) different through the Tukey's multiple range test.

4.2.3 Structural characterization

The secondary structure of gelatin films can be analysed by means of curve fitting of amide I and II profiles (Dave et al., 2000). As can be observed in **Figures 4.4**, the main absorption bands of gelatin were related to C=O stretching at 1630 cm^{-1} (amide I), N-H bending at 1530 cm^{-1} (amide II) and C-N stretching at 1230 cm^{-1} (amide III) (Etxabide et al., 2015a). The main absorption bands associated with lactose were located between 1180 and 953 cm^{-1}. The bands at 979 and 987 cm^{-1} were referred to vibration of C-C, and the band at 1034 cm^{-1} was associated with the vibration of C-O in CH_2-OH group (Wang et al., 2013). Finally, glycerol bands were related to the vibrations of C-C bonds at 850, 940 and 1000 cm^{-1} and C-O bonds at 1050 and 1100 cm^{-1} (Basu et al., 2011). As can be observed in **Figure 4.4a**, the two bands

situated in the range of 1100-1000 cm^{-1} joined into a broader band when increasing lactose content in the films prepared at native pH, in contrast to the films prepared at acid pH (**Figure 4.4b**).

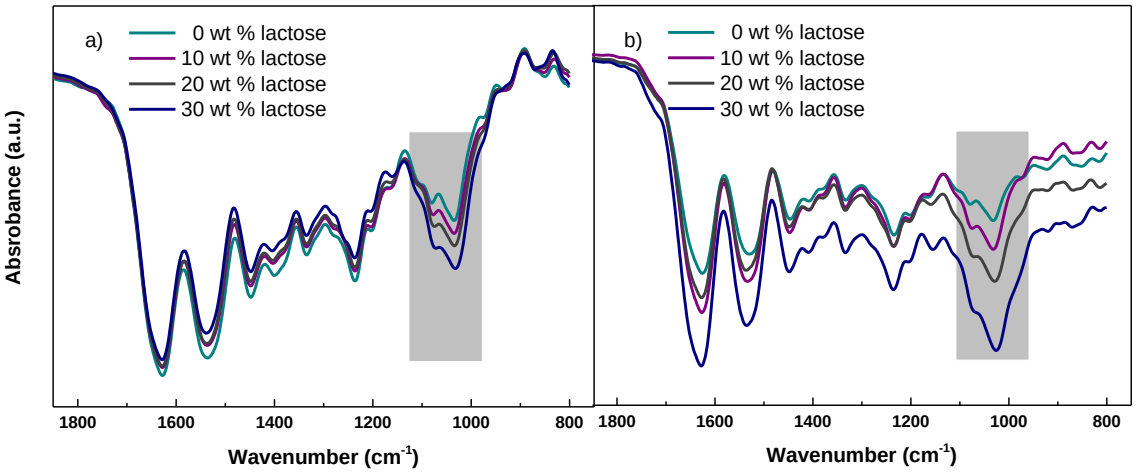

Figure 4.4 FTIR spectra of the HT fish gelatin films prepared at a) native pH and b) acid pH as a function of lactose content.

These changes could be related to the effect of pH on the extension of Maillard reaction, as explained above. Furthermore, the position of the amide II band was also affected by lactose content and pH, as shown in **Table 4.3**. It is worth noting that the position of amide I band did not change, while the position of amide II band slightly shifted to a lower wavenumber when adding lactose, irrespective of pH.

Table 4.3 Position of amide I and amide II bands as a function of lactose content and pH.

	Acid pH			Native pH		
Lactose (wt %)	**Amide I (cm^{-1})**	**Amide II (cm^{-1})**	**Amide I/II**	**Amide I (cm^{-1})**	**Amide II (cm^{-1})**	**Amide I/II**
0	1631	1528	1.99	1632	1529	1.82
10	1631	1531	2.03	1632	1534	1.89
20	1632	1535	2.09	1632	1536	1.94
30	1632	1537	2.18	1632	1538	2.04

The bands corresponding to amide I and amide II were further assessed by a curve-fitting process to carry out a quantitative analysis in relation to the changes produced in gelatin structure. On the one hand, the amide I profile of gelatin contains

two major components, which can be linked to β-sheets (1630-1615 cm^{-1} and 1700-1680 cm^{-1}) and α-helix (1650 cm^{-1}); on the other hand, the amide II profile contains four major components that can be linked to β-sheets (1500 cm^{-1}), random coil (1509-1523 cm^{-1}), α-helix (1540-1556 cm^{-1}) and β-turn (1565 cm^{-1}) (Hu et al., 2010; Lefevre and Subirade, 2000).

As can be observed in **Table 4.4**, the α-helix structure represented the highest percentage. In the case of the films prepared at acid pH, there was no significant change in the secondary structure of gelatin as a result of lactose addition, in agreement with solubility results. This could be related to a lower protein denaturation at low pH, providing less reactive sites for crosslinking. However, the area of β-sheets slightly increased and the area of α-helix slightly decreased when increasing lactose content for the films prepared at native pH. These results are in accordance with the solubility changes previously shown in **Table 4.1**.

Table 4.4 Area (%) of the curve fitting of amide I as a function of lactose content and pH.

Amide I	**Acid pH**			**Native pH**		
Lactose (wt %)	**β-sheet 1622 cm^{-1}**	**α-helix 1650 cm^{-1}**	**β-sheet 1685 cm^{-1}**	**β-sheet 1622 cm^{-1}**	**α-helix 1650 cm^{-1}**	**β-sheet 1685 cm^{-1}**
0	37.75	60.01	2.24	44.95	48.43	6.62
10	37.27	59.87	2.86	45.46	47.47	7.07
20	36.93	60.49	2.58	45.45	47.51	7.04
30	38.44	58.81	2.75	45.16	47.05	7.79

Regarding the amide II band (**Table 4.5**), when increasing lactose content, β-sheet and α-helix structures decreased, whereas β-turn and random coil structures increased for the films prepared at acid pH. However, increasing pH led to a decrease of the area of β-sheet and an increase of α-helix structures, while the areas corresponding to random coil and β-turn structures practically did not change. Since changes in the secondary structure of proteins are closely related to the interactions between chains, it seems that the lower extension of Maillard reaction at acid pH

allowed further chain movement resulted in more changes in the secondary structure, probably by physical interactions such as hydrogen bonding, while the films prepared at native pH, in which the crosslinking degree was higher, the chain movement was restricted and, thus, the changes in the secondary structure were not so noticeable.

Table 4.5 Area (%) of the curve fitting of amide II as a function of lactose content and pH.

Amide II	**Acid pH**				**Native pH**			
Lactose (wt %)	**β-sheet**	**Random coil**	**α-helix**	**β-turn**	**β-sheet**	**Random coil**	**α-helix**	**β-turn**
0	5.05	34.52	55.31	5.12	6.19	32.24	54.34	7.23
10	4.89	36.21	52.68	6.22	5.39	31.95	55.83	6.83
20	3.64	37.86	51.51	6.99	4.01	31.58	57.13	7.28
30	1.75	40.15	50.76	7.34	3.73	31.32	57.09	7.86

In order to further analyse the structural changes in HT gelatin films, XRD analysis was carried out (**Figure 4.5**). All patterns displayed two diffraction peaks, the peak at 21º, related to the crystallinity of gelatin, and the peak at 7.4º, corresponding to the residual triple helix from native collagen (Schmidt, Giacomelli, & Soldi, 2005). Analysing the effect of pH on the protein tertiary structure, results showed that the refolding of the typical collagen triple helix and the ordering of gelatin crystalline region could be hindered at acid pH due the intermolecular interactions among protein chains. Regarding lactose addition, the lower was the pH, the lesser was the denaturation of gelatin and a minor degree of crosslinking was obtained, as explained above. As a consequence, higher amount of unconsumed lactose remained in the films, which could be a hindrance to the triple helix rearrangement and to the reordering of the gelatin crystalline region.

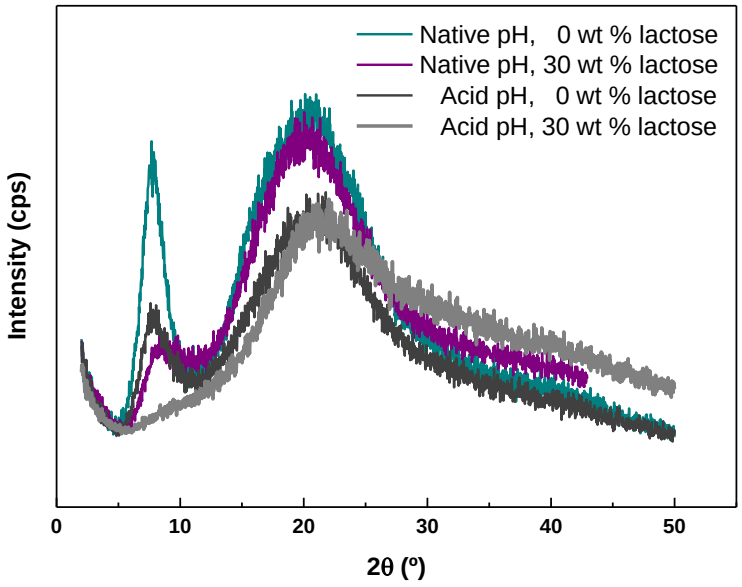

Figure 4.5 XRD patterns of the fish gelatin films as a function of lactose content and pH.

In order to further assess the effect of crosslinking on film structure, SEM analysis was carried out and the images of film cross-section as a function of lactose content are shown in **Figure 4.6**. SEM micrographs of the cross-section showed that gelatin films without lactose had a rough structure due to the remaining collagen fibrils in non-crosslinked samples (Wang et al., 2015), as shown by XRD analysis. However, when lactose was added, the fibrous structure became less obvious due to the decrease of the triple helix content (Liu et al., 2016), as shown in **Figure 4.5**. Consequently, the cross-sectional SEM images showed a notably structural change once the reaction was promoted (**Figures 4.6b** and **4.6d**). In fact, more homogeneous and smoother core was observed in films with 30 wt % lactose. Porosimetry analysis showed a structure consisting of a system of very fine pores with a radius between 0.01-0.001 μm and open porosity ratio ranged from 8 to 12%.

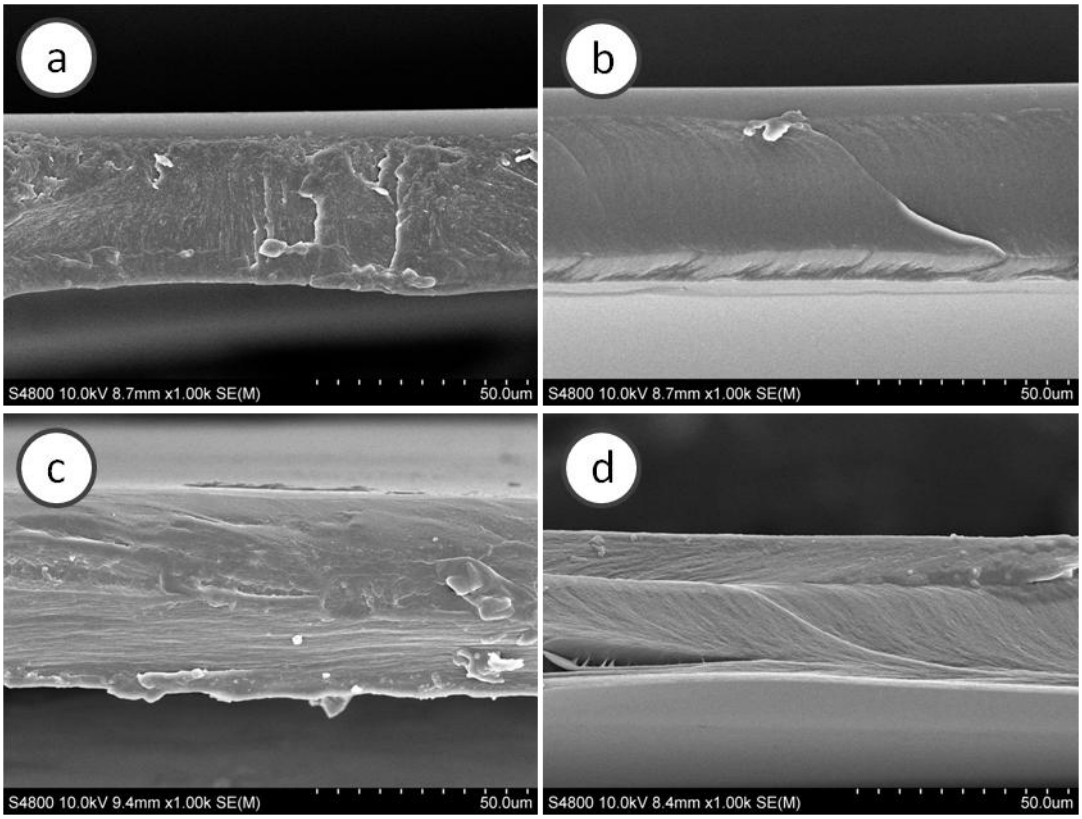

Figure 4.6 SEM cross-sectional images of the fish gelatin films prepared at acid pH with (a) 0 wt % and (b) 30 wt % lactose, and films prepared at native pH with (c) 0 wt % lactose and (d) 30 wt % lactose.

4.3 Conclusions

The extent of the crosslinking reaction between gelatin and lactose can be controlled by film preparation conditions in order to tailor functional properties. At acid pH, the extent of crosslinking was lower, as shown by UV-vis spectroscopy, indicating the inhibition of crosslinking when pentosidine was formed, resulting in totally soluble films. These results highlight the potential use of these films in solid dosage forms in which coating tablets with a thin polymeric film (10-100 µm) is commonly performed to modify drug release and enhance the stability of the drug within gastrointestinal fluids. In contrast, crosslinking reaction progressed at a higher pH, resulting in films with lower chain mobility, higher water resistance, high UV-vis protection and tensile strength higher than 50 MPa, which could be used as sustained release systems to allow active compounds to be delivered over more prolonged periods of time (e.g. active

packaging). In all cases, the lactose-modified films prepared in this work were homogeneous, transparent, hydrophobic and non porous structure was observed.

5 Improvement of gelatin properties by crosslinking

5.1 Summary

Maillard reaction is a potential route for crosslinking but, as shown in chapter 4, there are many factors that significantly affect crosslinks formation. Among them, temperature, time of heating and pH are believed to play crucial roles. According to Van Boekel (1998), Maillard reaction rate significantly increases at basic conditions and so, this factor notably influences the extension of Maillard reaction and the functional properties of films. Therefore, the aim of this chapter was to prepare gelatin films with different lactose contents at basic pH in order to evaluate the effect of lactose-induced glycation on optical, barrier and mechanical properties as a function of film composition, and to relate the properties measured to the changes observed by FTIR and UV spectroscopy as well as by solubility tests.

5.2 Results and discussion

5.2.1 Physicochemical properties

The knowledge of moisture content (MC) and total soluble matter (TSM) values is essential to assess the film ability of maintaining its integrity. As can be seen in **Table 5.1**, MC values showed no significant difference ($P > 0.05$) when 10 wt % lactose was added, while the films with higher lactose contents exhibited a significant increase ($P < 0.05$). Regarding film solubility, it is worth noting that NH films were totally soluble, demonstrating the effect of temperature to promote Maillard reaction, as reported in a previous work (Guerrero et al., 2012). In the case of HT films, a significant decrease ($P < 0.05$) of TSM values was observed when adding lactose. It has been reported that high molecular weight compounds may be formed by crosslinked gelatin molecules that form aggregates in gelatin films (Chiou et al., 2006; Muyonga, Cole, & Duodu, 2004). Since film solubility decreases when crosslinking degree increases, the behaviour observed could be due to the chemical reaction between gelatin and lactose through Maillard reaction. When 20 wt % lactose was added, TSM values reached a minimum value around 12%, indicating that further addition of lactose did not promote

further reaction and suggesting that this value mainly corresponded to glycerol, which interacts with gelatin through hydrogen bonding (Guerrero et al., 2011b).

Table 5.1 Film thickness, moisture content (MC) and total soluble matter (TSM) values for non-heated (NH) and heat-treated (HT) fish gelatin films as a function of lactose content. ([I] Thickness was the same for NH and HT films for any given lactose concentration; [II] Moisture content for HT films is 0 (data not shown); [III] All NH films were totally soluble).

Lactose (wt %)	Thickness[I] (mm)	MC[II] (%)	TSM[III](%)
	NH/HT	NH	HT
0	0.043 ± 0.002[a]	10.669 ± 1.229[a]	77.384 ± 6.334[b]
10	0.044 ± 0.002[a]	10.189 ± 3.506[a]	16.063 ± 2.376[a]
20	0.054 ± 0.005[b]	14.497 ± 0.642[ab]	12.989 ± 4.013[a]
30	0.069 ± 0.003[c]	16.426 ± 2.005[b]	12.846 ± 3.262[a]

[a-c]Two means followed by the same letter in the same column are not significantly ($P > 0.05$) different through the Tukey´s multiple range test.

In order to evaluate surface attributes, gloss measurements were carried out and the results are presented in **Table 5.2**. NH films showed higher gloss and thus, smoother surfaces than HT films, except for the films without lactose where gelatin-glycerol interactions can be influenced by the effect of temperature, leading to smoother surfaces. Regarding the films with lactose, amorphous hygroscopic sugars can absorb moisture, which acts as plasticizer and allows sugars to crystallize (Sormoli, Das, & Landgrish, 2013). In the case of NH films, lactose did not react with gelatin, as mentioned above in relation to TSM values; therefore, lactose can absorb moisture, as shown by rising MC values when increasing lactose content, and crystallize, increasing gloss ($P < 0.05$). Since crystalline surfaces are associated with higher gloss (Rindlav-Westling et al., 1998), NH films showed higher gloss values. Regarding HT films, the reaction of lactose with gelatin prevented crystal nucleation and growth, causing the decrease ($P < 0.05$) in gloss values.

Table 5.2 Gloss values for non-heated (NH) and heat-treated (HT) fish gelatin films as a function of lactose content.

Lactose (wt %)	$Gloss_{60°}$ (GU)	
	NH	HT
0	119.75 ± 6.90[c]	142.50 ± 1.73[d]
10	141.75 ± 2.99[b]	118.25 ± 1.71[c]
20	148.25 ± 1.26[b]	70.76 ± 1.61[b]
30	156.75 ± 0.96[a]	55.15 ± 2.29[a]

[a-d]Two means followed by the same letter in the same column are not significantly (P > 0.05) different through the Tukey´s multiple range test.

Colour is also relevant since directly influences product appearance and thus, consumer acceptability (Monedero et al., 2009). As shown in **Figure 5.1**, films were homogeneous and transparent, and colour changed with the addition of lactose for HT films, which turned yellowish.

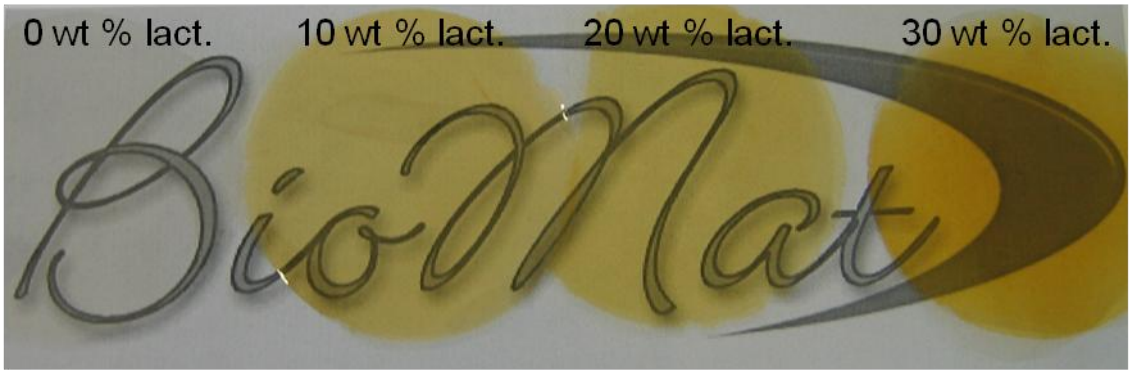

Figure 5.1 Transparency and colour difference of heat-treated (HT) fish gelatin films as a function of lactose content.

This colour development is related to the reaction between fish gelatin and lactose through Maillard reaction at high temperatures, and was quantified by the L*, a* and b* values shown in **Table 5.3**. L*, a* and b* values did not show significant change (P > 0.05), irrespective of lactose content for NH films. However, in the case of HT films, the addition of lactose caused a decrease (P < 0.05) in L* values attributed to the darkening of films as some compounds were formed during the advanced stage of Maillard reaction. Moreover, a* and b* values increased significantly (P < 0.05) with lactose content, showing dark yellowing. Therefore, total colour difference (ΔE*)

increased ($P < 0.05$) with lactose for HT films in reference to NH films. Colour difference indicated that lactose content affected significantly the degree of glycation, being higher for higher lactose contents due to the presence of a higher amount of carbonyl groups.

Table 5.3 L*, a*, b* and ΔE* values for non-heated (NH) and heat-treated (HT) fish gelatin films as a function of lactose content. Colour differences for HT films are referred to NH films.

Film	Lactose (wt %)	L*	a*	b*	ΔE*
NH	0	96.19 ± 0.25^{a}	-0.10 ± 0.03^{a}	3.01 ± 0.10^{a}	
	10	95.88 ± 0.11^{a}	-0.24 ± 0.04^{a}	3.17 ± 0.09^{a}	
	20	96.03 ± 0.07^{a}	-0.31 ± 0.02^{a}	3.34 ± 0.09^{a}	
	30	95.71 ± 0.29^{a}	- 0.43 ± 0.05^{a}	3.62 ± 0.13^{a}	
HT	0	96.12 ± 0.49^{a}	-0.81 ± 0.06^{a}	2.99 ± 0.06^{a}	0.71 ± 0.05^{a}
	10	85.66 ± 0.69^{b}	2.73 ± 0.11^{b}	36.92 ± 0.40^{b}	34.38 ± 0.41^{b}
	20	76.84 ± 0.53^{c}	14.01 ± 0.81^{c}	39.86 ± 0.48^{c}	37.33 ± 0.46^{c}
	30	47.85 ± 2.86^{d}	34.69 ± 1.71^{d}	70.99 ± 1.45^{d}	69.13 ± 1.59^{d}

$^{a-d}$Two means followed by the same letter in the same column are not significantly ($P > 0.05$) different through the Tukey´s multiple range test.

As the chemical changes accompanying the Maillard reaction were expected to lead to several changes in FTIR spectra, this analysis was carried out in order to evaluate protein-sugar interactions and spectra are shown in **Figure 5.2**. As can be observed, the two bands situated in the range of 1100-1000 cm^{-1} became one single band, and the intensity of the band was higher when increasing lactose percentage.

In order to further analyse the effect of lactose content, the band corresponding to amide I was used for the quantitative analysis of the changes produced in gelatin structure as a result of Maillard reaction. As the band corresponding to amide I depend on the secondary structure of the protein backbone, this band can provide an efficient mechanism of pairing polar groups of the polypeptide backbone by hydrogen bonds.

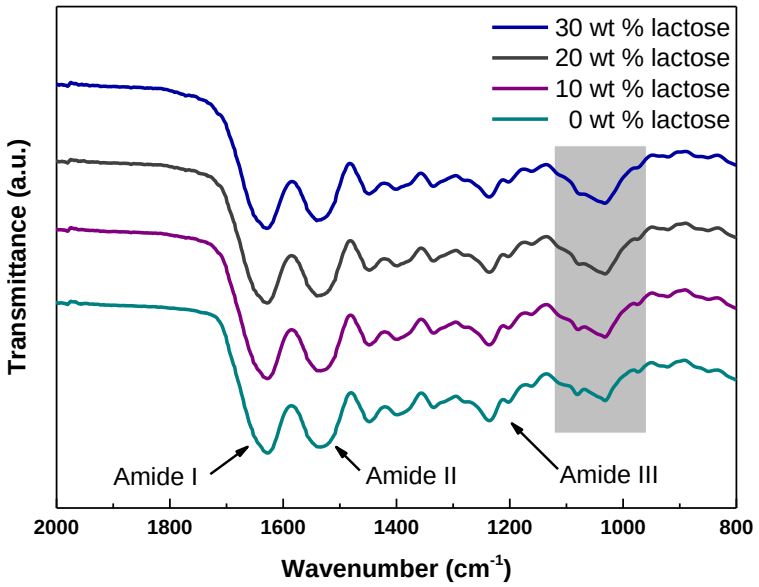

Figure 5.2 FTIR spectra of fish gelatin films as a function of lactose content for HT films.

Specifically, protein unfolding is characterized by changes in the intensity of the dominant band in the native protein at 1650 cm^{-1}, assigned to α-helix/unordered structures, and in the regions at 1630-1615 cm^{-1} and 1700-1680 cm^{-1}, assigned to β-sheets, (Hu et al., 2010; Lefevre & Subirade, 2000), as shown in **Figure 5.3**.

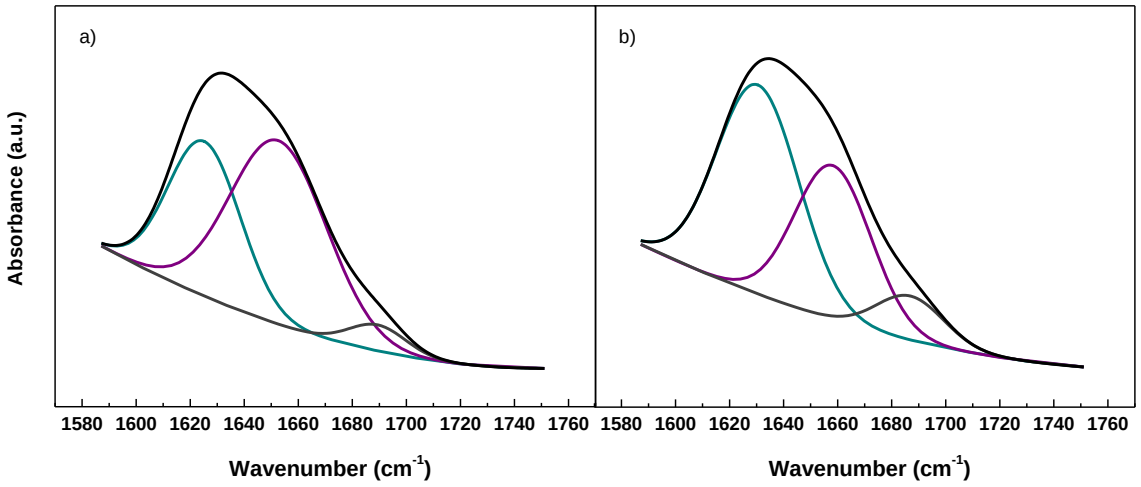

Figure 5.3 Curve fitting spectra of amide I for a) non-heated (NH) and b) heat-treated (HT) fish gelatin films containing 20 wt % lactose.

The individual components determined by curve fitting have been considered and the quantitative analysis is shown in **Table 5.4**. In the case of NH films, the addition of lactose could lead to the formation of hydrogen bonds between gelatin and lactose, weakening intermolecular interactions among protein chains and resulting in an increase of α-helix (1652 cm^{-1}) and a decrease of β-sheets (1625 and 1689 cm^{-1}). Regarding HT films, the intensity of the bands at 1689 and 1625 cm^{-1} increased due to the formation of intermolecular antiparallel β-sheets (Lefevre, Subirade, & Pezolet, 2005) and consequently, the band at 1652 cm^{-1}, associated to α-helix/unordered structures, decreased. Extended antiparallel β-sheets are commonly found in aggregated proteins, especially in heat-denatured proteins (Susi et al., 1967), so these results lead to the view that aggregation occurred and that the aggregates were partly composed of β-sheets. These findings indicate a progressive conversion of residual regular structures and unordered segments into intermolecular β-sheets (Quinn et al., 2003), showing the effect of Maillard reaction on gelatin structure.

Table 5.4 Resulting percentage of the curve fitting of amide I for non-heated (NH) and heat-treated (HT) fish gelatin films as a function of lactose content.

Lactose	Amide I area (%) for NH films			Amide I area (%) for HT films		
(wt %)	1625 cm^{-1}	1652 cm^{-1}	1689 cm^{-1}	1625 cm^{-1}	1652 cm^{-1}	1689 cm^{-1}
0	41.65	53.07	5.28	51.10	39.70	9.20
10	36.03	59.48	4.49	50.24	40.15	9.62
20	36.66	58.43	4.91	53.87	36.77	9.36
30	35.38	59.68	4.93	52.18	38.49	9.33

5.2.2 Barrier properties

Protection against light plays a critical role in materials, since light can lead to oxidation reactions and deterioration (Duncan & Chang, 2012). As can be observed in **Figure 5.4**, all gelatin films exhibited a high protection against UV light in the range of 200-250 nm. The high absorption in this range is related to peptide bonds in proteins. Furthermore, it has been reported that the amino acid composition affects the non-enzymatic browning (Hong et al., 2014). The absorption in the range of 250-300 nm is

due to the presence of chromophores, such as tyrosine and phenylalanine, common aromatic amino acids found in fish gelatin. Some side chain groups in proteins, such as amino group in lysine, take part in Maillard reaction, increasing the relative proportion of aromatic amino acids and the UV absorption in the range of 250-300 nm. Moreover, an increase in the UV pattern in the range of 300-400 nm was observed for HT films, as shown in **Figure 5.4b**. The high absorption in this region can be related to the presence of conjugated structures for lactose-glycated gelatin. As the percentage of glycation is often used as a measurement of crosslinking, the high absorption at 300-400 nm would be indicative of the crosslinking reaction between gelatin and lactose, as also shown above by the changes observed in physicochemical properties. According to FTIR results, the network evolved from α-helix/unordered structures to β-sheets when lactose content was increased, indicating that electrostatic repulsions in the hydrophobic regions lead to the formation of β-sheets. It is worth noting that this high level of absorption in the UV-vis range is a desirable film characteristic for many applications.

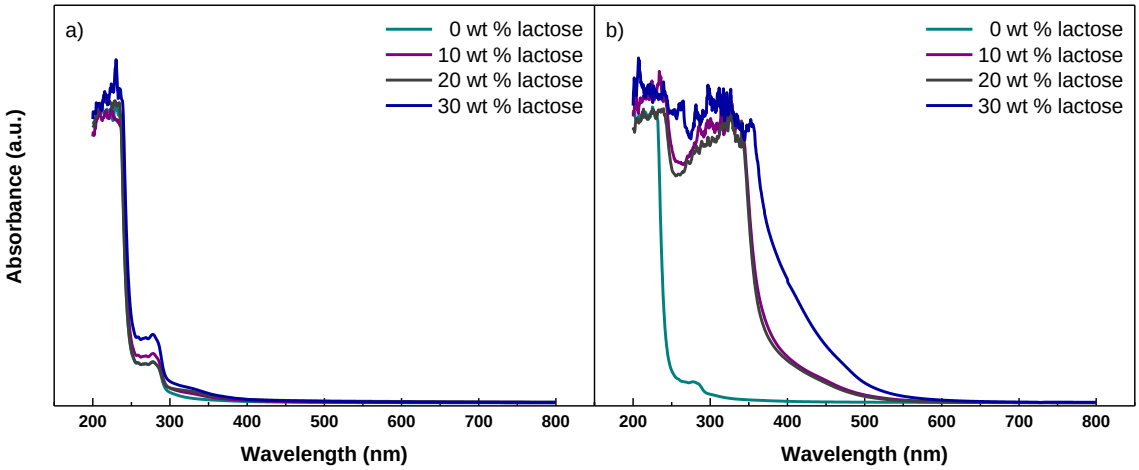

Figure 5.4 UV-vis spectra for a) non-heated (NH) and b) heat-treated (HT) fish gelatin films as a function of lactose content.

In addition to UV barrier properties, water resistance is a property required for films intended to be used in medium or high moisture conditions. Water resistance can be evaluated by measuring water contact angle (WCA), which indicates the final state of the water drop on film surface and thus, surface wettability. In order to understand the effect of lactose and temperature in surface wettability, WCA values were measured and are shown in **Table 5.5**.

Table 5.5 Water contact angle (WCA) and water vapour permeability (WVP) values for non-heated (NH) and heat-treated (HT) fish gelatin films as a function of lactose content.

Film	Lactose (wt %)	WCA (°)	WVP 10^{12} (g cm^{-1} s^{-1} Pa^{-1})
NH	0	88.61 ± 3.36^{a}	1.81 ± 0.16^{ab}
	10	107.53 ± 1.17^{b}	1.66 ± 0.11^{a}
	20	117.65 ± 0.96^{c}	2.00 ± 0.29^{ab}
	30	114.41 ± 2.41^{c}	2.15 ± 0.11^{b}
HT	0	91.13 ± 1.58^{a}	1.90 ± 0.18^{ab}
	10	104.99 ± 2.32^{b}	1.69 ± 0.09^{a}
	20	113.13 ± 0.37^{c}	1.82 ± 0.06^{ab}
	30	112.42 ± 2.35^{c}	2.18 ± 0.09^{b}

$^{a-c}$Two means followed by the same letter in the same column are not significantly ($P > 0.05$) different through the Tukey´s multiple range test.

WCA values increased ($P < 0.05$) for NH and HT films when lactose was added. In the case of NH films, this fact can be related to gelatin-lactose interactions by hydrogen bonding, which produces changes in protein structure, as shown by FTIR analysis, and the exposure of hydrophobic groups towards film surface (Jayasundera et al., 2009). For HT films, gelatin-lactose crosslinking by Maillard reaction decreased polar groups and thus, increased the hydrophobic character of films. However, no significant change ($P > 0.05$) was observed by the effect of temperature for the samples with the same composition, indicating that non polar groups tend to be oriented towards the surface and thus, all films exhibited WCA values higher than 90º and could be considered as hydrophobic films (Karbowiak et al., 2006). Additionally, water vapour permeability (WVP) values were measured and are shown in **Table 5.5**.

As can be observed, WVP was similar for all films and neither lactose nor temperature caused significant change (P > 0.05) in WVP values. Since water vapour permeability is a two-step process that includes water vapour sorption and water vapour diffusion, the increase in WCA values seems to be compensated by the changes in protein structure shown by FTIR analysis that would favoured the diffusion step.

5.2.3 Mechanical properties

Mechanical strength and flexibility are generally required for films in order to maintain integrity until usage. Mechanical properties for fish gelatin-based films are shown in **Table 5.6**. As can be seen, tensile strength (TS) and elongation at break (EB) values did not show significant change (P > 0.05) when adding lactose or heating. Tensile strength values were around 50 MPa, which are higher than the values obtained for bovine gelatin-based films (Nur Hanani, Roos, & Kerry, 2012; Nur Hanani et al., 2012; Mu et al., 2012). Since addition of plasticizers usually increases EB values but decreases TS values (Haq, Hasnain, & Azam, 2014), the low content of glycerol used in this study would explain the high TS values obtained.

Table 5.6 Tensile strength (TS) and elongation at break (EB) values for non-heated (NH) and heat-treated (HT) fish gelatin films as a function of lactose content.

Film	Lactose (wt %)	TS (MPa)	EB (%)
NT	0	52.39 ± 3.16[a]	2.88 ± 0.68[a]
	10	54.19 ± 6.19[a]	2.57 ± 0.35[a]
	20	52.14 ± 4.95[a]	2.31 ± 0.37[a]
	30	54.28 ± 4.41[a]	2.56 ± 0.35[a]
HT	0	50.63 ± 4.01[a]	2.82 ± 0.68[a]
	10	45.40 ± 5.06[a]	2.54 ± 0.32[a]
	20	44.48 ± 2.78[a]	2.94 ± 0.21[a]
	30	43.76 ± 7.53[a]	2.12 ± 0.42[a]

[a]Two means followed by the same letter in the same column are not significantly (P > 0.05) different through the Tukey´s multiple range test.

5.3 Conclusions

The addition of lactose caused changes in protein structure, which improved the hydrophobic character of the films and notably decreased the solubility of fish gelatin-

based films. Furthermore, heating promoted the glycation between reducing sugar and gelatin by non-enzymatic Maillard reaction. This reaction caused changes in protein structure from α-helix to β-sheets, as well as yellowing development due to the formation of Maillard reaction compounds. Additionally, Maillard reaction products absorbed UV light, which could promote the use of these films for food packaging in order to avoid food oxidation and contribute to extend food shelf-life. All films maintained transparency and high tensile resistance, around 50 MPa. This study demonstrates that Maillard reaction is a viable alternative to improve the functional properties of fish gelatin films. In order to improve water vapour barrier properties without impairing other functional properties, further study is required to analyse the Maillard reaction steps and the products formed through this glycation reaction.

6 The progress of Maillard reaction

6.1 Summary

As shown in the previous chapter, the structure and physical properties of gelatin can be modified by means of Maillard reaction. Furthermore, controlling those factors that affect Maillard reaction allows for tailaring gelatin properties for specific uses, such as food, medical, and industrial applications. Although fish gelatins are being increasingly researched as alternative materials to mammalian gelatins, the progress of Maillard reaction by UV-vis spectroscopy, the formation of fluorescent compounds as AGEs (Advanced Glycation End-Products), and the analysis of the protein secondary structure by FTIR spectroscopy during heating time at basic pH have not been previously reported in the literature.

In this context, the aim of this chapter was focused on analysing the Maillard reaction steps and the products formed through this glycation reaction along with the evaluation of the effect of lactose content and heating time on the morphology and physical performance of crosslinked fish gelatin films in order to select the most appropriate composition to develop technically valuable products.

6.2 Results and discussion

The heat treatment is the most widely used processing method in the industry. With this regard, one of the major chemical reactions taking place between a protein and a reducing sugar, such as the lactose used in this study, is the non-enzymatic browning, known as Maillard reaction. The analyses of Maillard reaction products (MRPs), which show great complexity and variety, have attracted the interest of scientists in different fields of research and this is the main point of this study.

6.2.1 Effect of crosslinking in the gelatin secondary structure

As explained in the previous chapter, the most relevant bands in FTIR spectra were related to the peptide bonds of the protein (**Figure 5.2**): C=O stretching at 1630 cm^{-1} (amide I), N-H bending at 1530 cm^{-1} (amide II) and C-N stretching at

1230 cm^{-1} (amide III). In this chapter, FTIR spectroscopy was used to study changes in the secondary structure of gelatin in terms of α-helix/unordered and β-sheet conformations by means of analysing the amide I band (1600-1700 cm^{-1}) at different heating times (**Figure 6.1**).

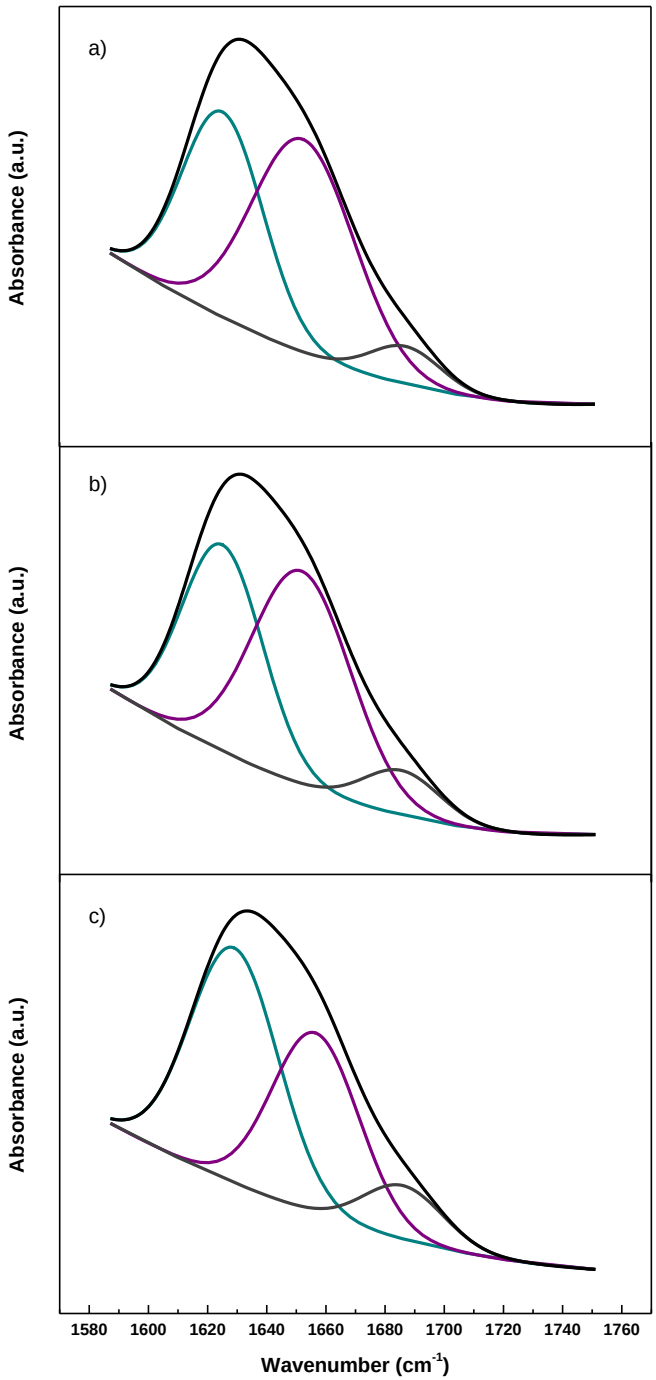

Figure 6.1 Curve fitting spectra of amide I for fish gelatin films with 30 wt % lactose content as a function of heating time: a) 0 min, b) 150 min, and c) 1440 min.

The secondary structure of gelatin-lactose films consists mainly of α-helix/unordered (1650 cm^{-1}) and antiparallel β-sheet (1630-1615 cm^{-1} and 1700-1680 cm^{-1}) conformations (Guerrero et al., 2014), where the latter is commonly found in aggregated proteins, especially in heat-denatured proteins (Susi, Timasheff, & Stevens, 1967). Regarding lactose content, similar behaviour was observed for 10, 20 (curves not shown) and 30 wt % lactose (**Figure 6.1**). As can be seen in **Figure 6.1a,** the predominant structure before heating was α-helix. However, after heating for 150 min, β-sheet was the principal structure (**Figure 6.1b**), which was maintained for the films heated for 1440 min (24 h), as shown in **Figure 6.1c**. This analysis demonstrated that there was a conversion of α-helix structure into β-sheet structure in crosslinked films with different lactose contents at different heating times. In order to carry out the quantitative analysis of FTIR spectra, the percentage of the amide I curve is shown in **Table 6.1**.

Table 6.1 Resulting percentage of the curve fitting of amide I as a function of lactose content and heating time.

		Area amide I		
Lactose (wt %)	**Time (min)**	**1625 cm^{-1}**	**1651 cm^{-1}**	**1688 cm^{-1}**
10	0	35.34	59.09	5.57
	90	38.54	52.23	9.23
	150	39.87	50.21	9.92
	210	42.21	47.74	10.05
	270	50.43	39.26	10.31
	1440	50.24	40.15	9.62
20	0	35.12	59.73	5.15
	90	37.12	57.11	5.77
	150	41.32	50.14	8.54
	210	51.23	39.38	9.39
	270	52.12	38.12	9.76
	1440	53.87	36.77	9.36
30	0	34.89	60.09	5.02
	90	40.23	52.89	6.88
	150	49.54	41.23	9.23
	210	50.12	40.23	9.65
	270	50.97	39.14	9.89
	1440	52.18	38.49	9.33

As can be seen in **Table 6.1**, the time from which the conversion of α-helix into β-sheet remains practically constant decreased when lactose content increased, being

270, 210, and 150 min for the films with 10, 20, and 30 wt % lactose, respectively. This behaviour evidenced the effect of lactose content and heating time in the secondary structure of fish gelatin.

Total soluble matter (TSM) values were measured at the times at which the conversion of α-helix into β-sheet remains practically constant. These values are shown in **Table 6.2**, where TSM values before heating (0 min) and after heating for 1440 min (24 h) are also shown for comparison. As can be seen, film solubility significantly decreased up to values around 33% when films were heated during 270, 210, and 150 min for the films with 10, 20 and 30 wt % lactose, respectively. These values indicate that crosslinking decreased solubility more rapidly for the films with higher lactose contents. Therefore, the crosslinking induced by heating and lactose addition could be an effective way to control the solubility of fish gelatin films, providing a key functional property for those films intended to be used as delivery systems in pharmaceutical or food applications.

Table 6.2 Total soluble matter (TSM) values for fish gelatin films as a function of lactose content.

Lactose (wt %)	Time (min)	TSM (%)
10	0	100^{a}
	270	31.0 ± 0.7^{b}
	1440	16.0 ± 2.4^{c}
20	0	100^{a}
	210	33.1 ± 1.1^{b}
	1440	13.0 ± 4.0^{d}
30	0	100^{a}
	150	33.1 ± 0.9^{b}
	1440	12.8 ± 3.3^{d}

$^{a-d}$Two means followed by the same letter in the same column are not significantly ($P > 0.05$) different through the Tukey´s multiple range test.

6.2.2 Pentosidine formation

UV-vis spectroscopy was carried out in order to analyse the effect of crosslinking as a function of lactose content and heating time, and spectra are shown in **Figure 6.2**. As can be seen in **Figure 6.2**, fish gelatin films before heating showed

excellent barrier properties against UV light due to the presence of peptide bonds (200-250 nm) and chromophores such as tyrosine and phenylalanine (250-300 nm) (Samira, Thuan-Chew, & Azhar, 2014; Hong et al., 2014). After heating, the formation of MRPs in the early stage is characterized by the increase of the absorption at 220 nm, related to the presence of carbonyl compounds, and the absorption around 280 nm, attributed to the presence of heterocyclic derivatives.

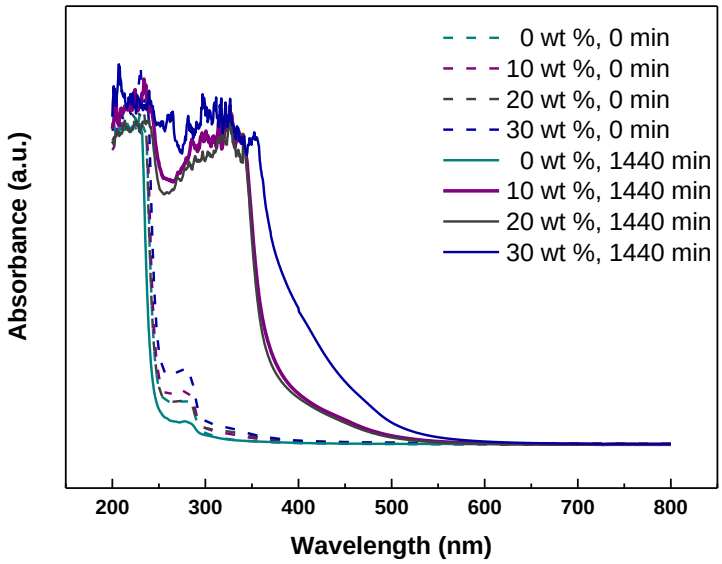

Figure 6.2 UV-vis spectra of fish gelatin films as a function of lactose content before heating (0 min) and after heating for 1440 min (24 h).

In this early stage, lactose (as an aldehyde in the open chain form) forms a Schiff base with the amino group of gelatin-bound lysine, more reactive than other amino acid residues. The formation of the Schiff base is an intermediate step in Maillard reaction, since it is rapidly transformed via the Amadori rearrangement into lactulosyl-lysine, known as the Amadori product (**Scheme 6.1**).

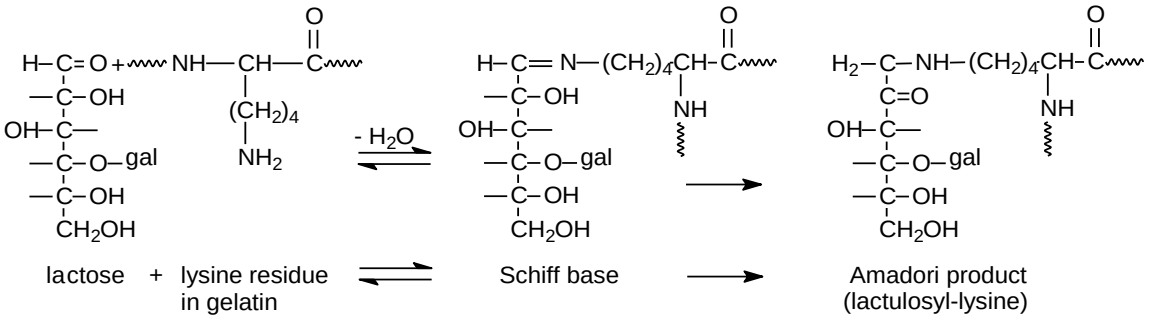

Scheme 6.1 The early stage of Maillard reaction (gal = galactose).

As the reaction proceeds, absorbance values at 280 nm progressively increased along with the appearance of the absorption at 325 nm due to the formation of more complex compounds, known as soluble premelanoidins (Cuzzoni et al., 1988; Wijewickreme, Kitts, & Durance, 1997). The formation of MRPs is greatly influenced by the reaction conditions. According to Van Boekel (1998), the degradation of the Amadori product is fast at basic conditions and Maillard reaction gives rise to browning, which can be measured as the absorption at 420 nm. Not much is known about the chemistry of the browning compounds, but the degradation route for the Amadori products, the 4-deoxyosone pathway, is significant for disaccharides under alkaline conditions (**Scheme 6.2**).

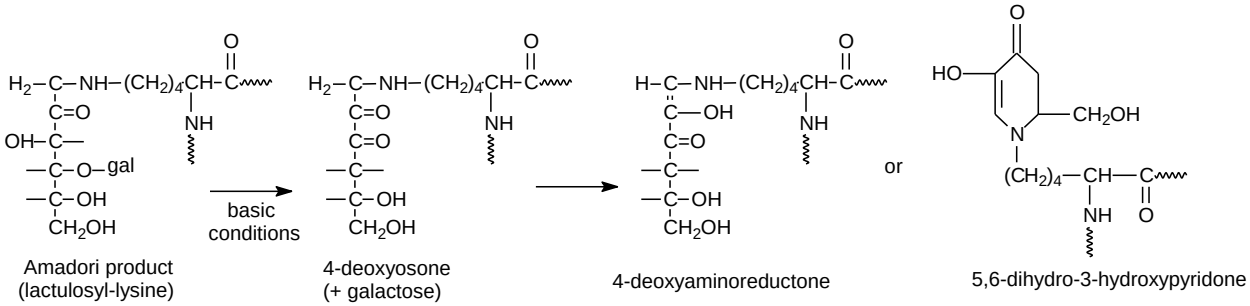

Scheme 6.2 Breakdown of the Amadori product in the advanced stage of Maillard reaction under basic conditions (gal = galactose).

The two products formed are 4-deoxyaminoreductone and 5,6-dihydro-3-hydroxypyridone (Martins, Jongen, & Van Boekel, 2001). The compounds shown above are highly reactive and take part in further reactions. In the advanced stage of Maillard reaction, a number of reactions takes place, including cyclations, dehydrations, retroaldolisations, isomerisation and further condensations, but the type and content of the products formed are difficult to determine due to their reactive nature. The final stage of Maillard reaction leads to the formation of brown nitrogenous polymers, being pentosidine one of the AGEs formed, linking lysine to arginine (**Scheme 6.3**).

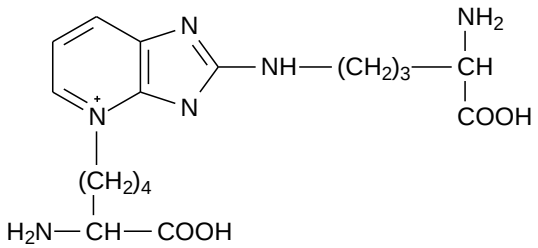

Scheme 6.3 Pentosidine formed in the advanced stage of Maillard reaction.

With the aim of following the reaction extension, **Figure 6.3** shows the UV-vis spectra of fish gelatin films with 30 wt % lactose as a function of heating time. Spectra presented a progressive increase in the absorbance at 325 nm up to 480 min and then, absorbance values were maintained for longer heating times. This behaviour indicated the improvement of UV-vis protection of fish gelatin films due to the crosslinking induced by heating and lactose addition. Heating enhanced the formation of Amadori compounds and subsequently, the formation of AGEs (Deyl et al., 1997; Morales & Van Boekel, 1997). Fluorescence AGEs, such as crossline, pentosidine and vesperlysine, and non-crosslinked AGEs without fluorescence, such as argpyrimidine, imidazolone and pyrraline, can be formed (Van Boekel, 1998; Nguyen, 2006).

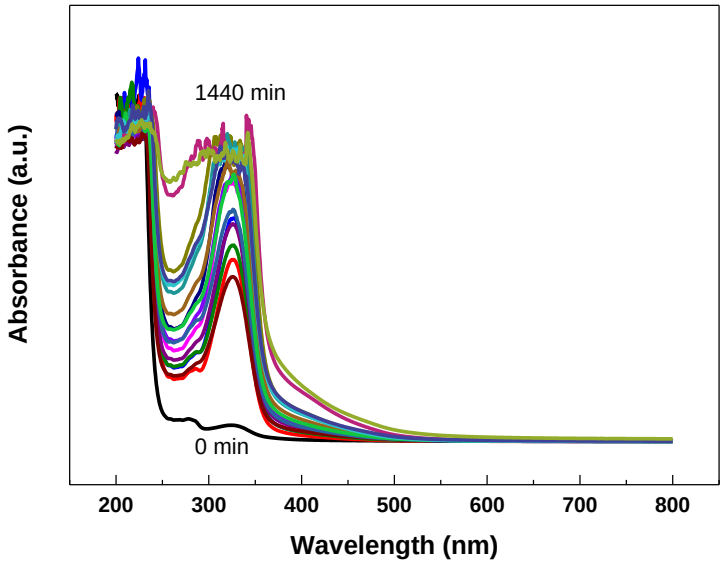

Figure 6.3 UV-vis spectra of fish gelatin films with 30 wt % lactose as a function of heating time. Measurements were collected every 30 min up to 480 min and at 1440 min.

Among fluorescence compounds, pentosidine is one of the most widely used markers to follow the reaction traceability during heating. In order to corroborate that pentosidine was generated as the first stable fluorophore product after the formation of the Amadori compound, fluorescence analysis was carried out. Fluorescence emission spectra of fish gelatin films are shown in **Figure 6.4**. On the one hand, emission spectra for the films with 30 wt % lactose excited at 335 nm are shown in **Figure 6.4a**. As can be seen, an emission peak appeared at 410 nm. These results are in agreement with other works (Morales & Van Boekel, 1997; Bhat et al., 2014), where pentosidine exhibited an excitation/emission wavelength of 335/406 nm. In addition, the area under the curves broadened with heating time, indicating the formation of higher amounts of pentosidine. On the other hand, fluorescence emission spectra of fish gelatin films after heating for 120 min are shown as a function of lactose content in **Figure 6.4b**. As can be observed, peaks were shifted toward lower wavelengths and higher intensity values were obtained as lactose percentage increased, indicating that

Maillard reaction and pentosidine formation were faster for higher lactose contents, in agreement with UV-vis results. Additionally, these results are in accordance with a faster conversion from α-helix to β-sheet observed by FTIR analysis and a faster decrease in solubility observed by TSM measurements.

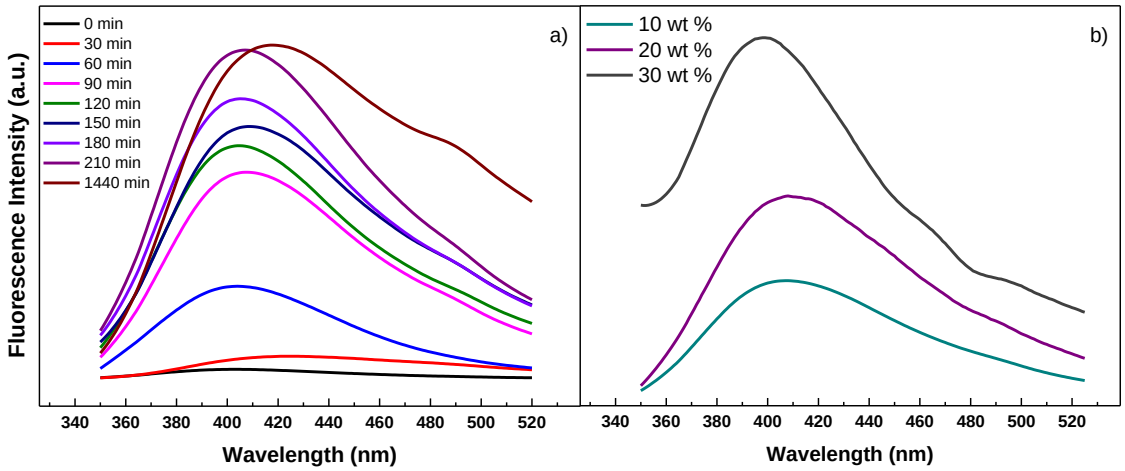

Figure 6.4 Fluorescence emission spectra of fish gelatin films a) with 30 wt % lactose as a function of heating time and b) after heating for 120 min as a function of lactose content.

6.2.3 Maillard reaction kinetics

The colour change that takes place in the films with lactose after heating can be considered as an indicator of Maillard reaction (Nursten, 1986). Fish gelatin films prepared with 30 wt % lactose as a function of heating time are shown in **Figure 6.5**.

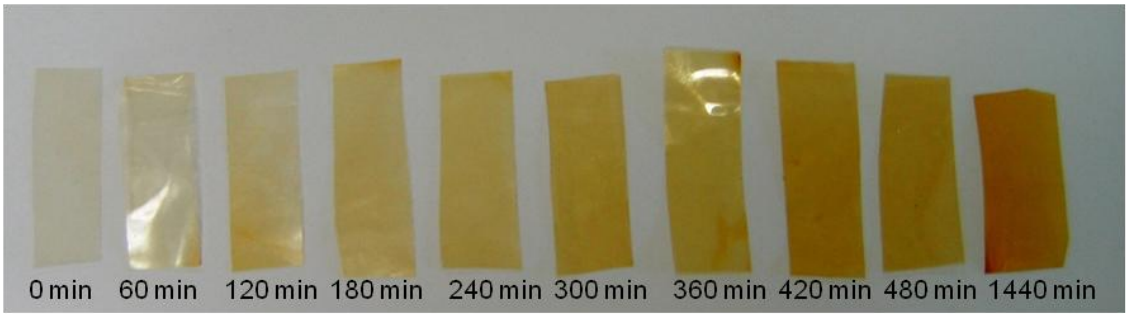

Figure 6.5 Colour change of fish gelatin films with 30 wt % lactose as a function of heating time.

All films were transparent and homogeneous, but colour change was more pronounced as heating time increased, turning toward dark yellow at longer times. Film colour was measured using CIELAB scale and L*, a* and b* parameters were used to calculate browning index (BI) value. L* and a* values (data not shown) did not present significant ($P > 0.05$) changes after heating up to 480 min, whereas b* values significantly increased ($P < 0.05$) as lactose content and heating time increased (**Table 6.3**).

Table 6.3 b* values as a function of lactose content and heating time.

Lactose (wt %)	b*					
	30 min	**60 min**	**150 min**	**210 min**	**270 min**	**480 min**
10	8.5 ± 0.5^{a}	10.2 ± 0.3^{a}	13.8 ± 0.1^{b}	18.5 ± 0.2^{c}	24.8 ± 2.6^{d}	33.8 ± 0.2^{f}
20	8.6 ± 0.3^{a}	10.2 ± 0.4^{a}	17.8 ± 1.4^{c}	24.7 ± 2.3^{d}	30.2 ± 0.7^{e}	36.5 ± 0.4^{f}
30	9.3 ± 0.1^{a}	14.0 ± 1.4^{b}	26.7 ± 1.2^{d}	31.6 ± 1.3^{e}	36.5 ± 0.4^{f}	46.1 ± 1.2^{g}

$^{a-g}$Two means followed by the same letter in the same column are not significantly ($P > 0.05$) different through the Tukey´s multiple range test.

The effect of lactose in BI values as a function of heating time is shown in **Figure 6.6**. As can be observed, BI indicated first-order kinetics, as also shown by other authors (Isleroglu et al., 2012; Jiménez et al., 2012; Gupta et al., 2011).

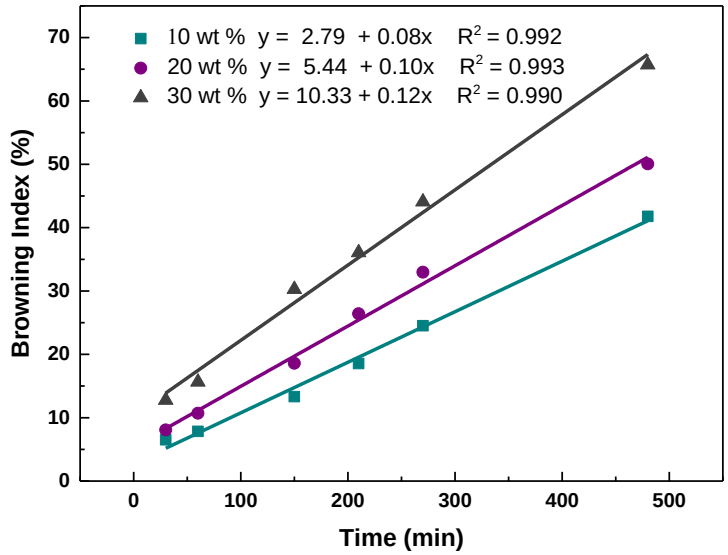

Figure 6.6 Browning index (BI) of fish gelatin films as a function of lactose content and heating time.

BI increased with heating time, showing higher values for higher lactose content. Furthermore, the slope of the line was higher for the films with higher lactose content, indicating that the formation of coloured melanoidins was faster in those systems, in accordance with previously shown UV-vis results.

On the other hand, the kinetics of pentosidine formation could be assessed by UV absorbance at 335 nm as a function of heating time and lactose content. As can be observed in **Figure 6.7**, pentosidine formation presented second order kinetics. UV absorbance increased up to a constant value for all films, regardless of lactose content. However, the rate of pentosidine formation was lower for the films prepared with lower lactose content. Pentosidine formation reached a plateau after 480, 420 and 180 min for the films with 10, 20 and 30 wt % lactose, respectively.

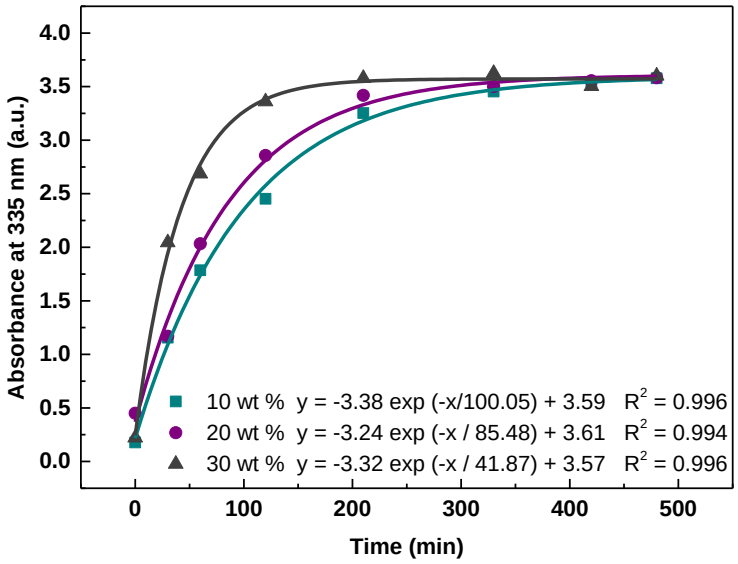

Figure 6.7 UV absorbance at 335 nm of fish gelatin films as a function of lactose content and heating time.

6.2.4 Effect of crosslinking in nanostructure

X-ray diffraction (XRD) is a common technique to determine the structure of proteins and thus, the diffraction bands of fish gelatin films as a function of lactose

content and heating time are shown in **Figure 6.8**. All patterns displayed two diffraction peaks, the peak at 21º, related to the crystallinity of gelatin, and the peak at 7.4º, corresponding to the residual triple helix from native collagen (Chen, Wang, & Jiang, 2012; Guerrero et al., 2012). When lactose content increased, gelatin crystallinity increased, indicating a more ordered structure due to the formation of new covalent bonds between lactose and gelatin. However, the content of residual triple helix decreased when films were heated, which could be related to the reduction of intermolecular interactions among protein chains due to the formation of crosslinks and glyco-conjugates through Maillard reaction, hindering the rearrangement of the typical collagen triple helix (Carvalho & Grosso, 2004; Liu & Zhong, 2012).

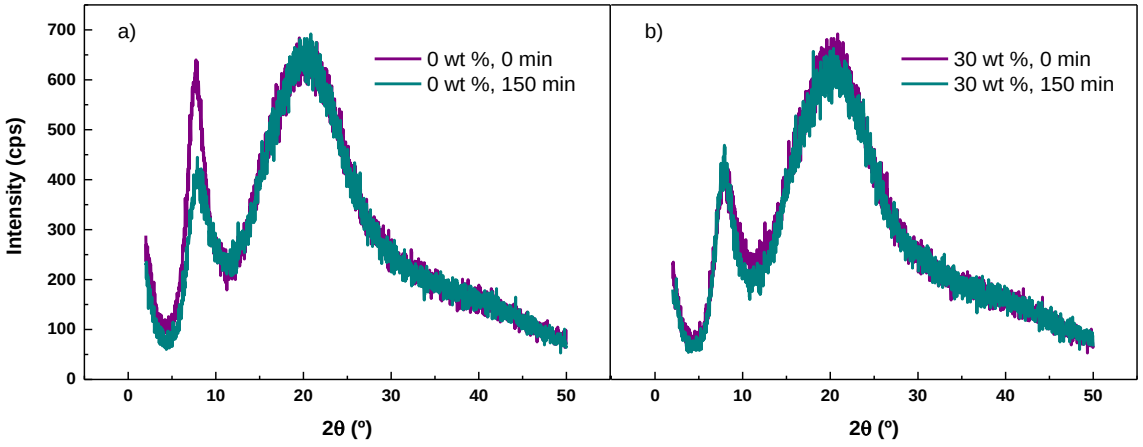

Figure 6.8 XRD patterns of fish gelatin films a) with no lactose and b) with 30 wt % lactose, before heating (0 min) and after heating (150 min).

Atomic force microscopy (AFM) measurements were conducted in order to further analyse the nanostructure of fish gelatin films, and the resulting height and phase images are depicted in **Figure 6.9**. As illustrated in **Figures 6.9a** and **6.9b** for films without lactose, gelatin showed fibril structures, as also observed by other authors (Yang et al., 2007; Wang, Yang, & Regenstein, 2008). This is in accordance with the residual triple helix structure shown by XRD.

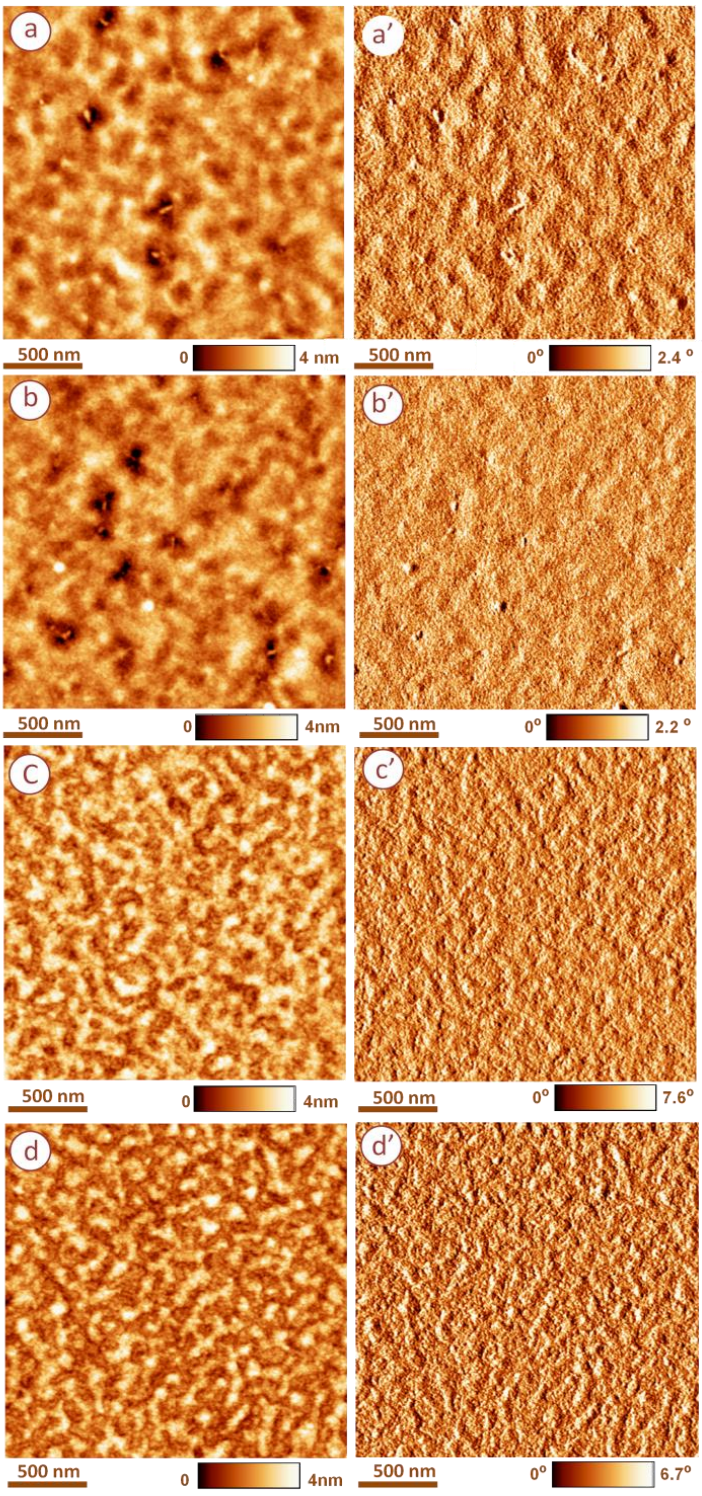

Figure 6.9 AFM images of fish gelatin films with no lactose a) before heating (0 min) and b) after heating (150 min), and with 30 wt % lactose c) before heating (0 min) and d) after heating (150 min). Height images (a, b, c, d) and phase images (a', b', c', d').

Lactose addition altered gelatin nanostructure, as can be observed in **Figure 6.9c**. As a consequence of the presence of lactose, fibres were no longer visible in the

images, in agreement with the strong reduction of the corresponding signal in XRD. Additionally, the matrix surrounding the fibrils in the films without lactose became more structured, suggesting that an aggregation occurred due to the Maillard reaction between gelatin and lactose. Subsequent heating created even more distinct features (**Figure 6.9d**), as long as Maillard reaction further progressed. In sum, AFM images evidenced that gelatin nanostructure notably changed by the addition of lactose and the effect of heating, leading to the formation of a more structured and ordered matrix, according to the lower solubility values previously shown. Therefore, AFM analysis can be used to corroborate the physicochemical changes observed by other measurements, such as solubility and XRD analyses carried out in this study.

6.2.5 Comparative analysis of the crosslinking with GTA, GP or lactose

The mechanism of the crosslinking reaction with the amino group of lysine residue in gelatin depends on the crosslinker nature. GTA is a synthetic crosslinking agent, widely used in medical research. The reaction between the carbonyl group of GTA and the amino group of lysine in gelatin leads to the formation of a Schiff base (**Figure 6.10a**), together with a yellowing process (Farris, Song, & Huang, 2010). Since GTA exhibits high cytotoxicity, GP, a natural crosslinker, can be used as an alternative. GP is known to react with the amino group of lysine residues in proteins (**Figure 6.10b**), forming blue pigments (Ali Poursamar et al., 2016; Sung et al., 1999). Although this reaction mechanism is still not well-understood, it is accepted that GP, with a hemiacetal skeleton, becomes structurally equivalent to a dialdehyde. Despite of the lower citotoxicity of GP in comparison to aldehydes, there are few reports available in the literature due to the high cost of GP (Panzavolta et al., 2011). Therefore, another natural crosslinker, lactose, was used to promote gelatin crosslinking. Heating in the presence of lactose can alter interactions within proteins and, thus, protein conformation, leading to a non-enzymatic glycation, known as Maillard reaction (**Figure 6.10c**), as previously shown in this chapter (Etxabide et al., 2015a). The films colour

changed as a function of the crosslinker used, leading to yellowish films when using lactose or GTA, whereas films were blue in the case of GP. The appearance of colour in films was considered as an indicator of crosslinking.

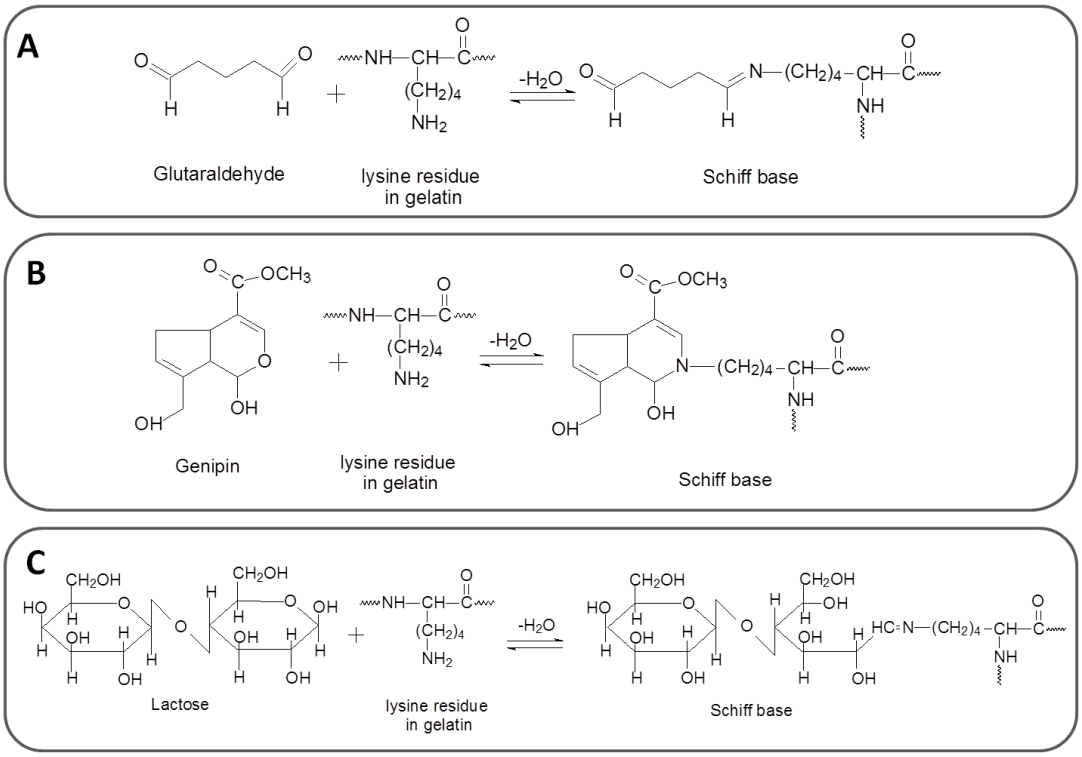

Figure 6.10 Crosslinking reactions between gelatin and (a) GTA, (b) GP, and (c) lactose.

As films hydrolytical stability is another indirect measurement of the crosslinking degree, films were immersed in a PBS solution for 3 days at 25 and 37 ºC. As can be seen in **Figure 6.11**, films stability changed as a function of the type of crosslinker and the solution temperature. After immersion in PBS at 25 ºC, the films crosslinked with GP or GTA showed a higher uptake of aqueous solution than the films crosslinked with lactose (**Figure 6.11a-b**). This behaviour indicates that a higher degree of crosslinking was reached when using lactose as a crosslinker and, therefore, the liquid uptake capacity of this film was reduced (Saarai et al., 2013). A higher liquid retention in the films crosslinked with GP or GTA led to sticky and brittle films, which were too weak to

handle. In contrast, films crosslinked with lactose did not present any handling problems.

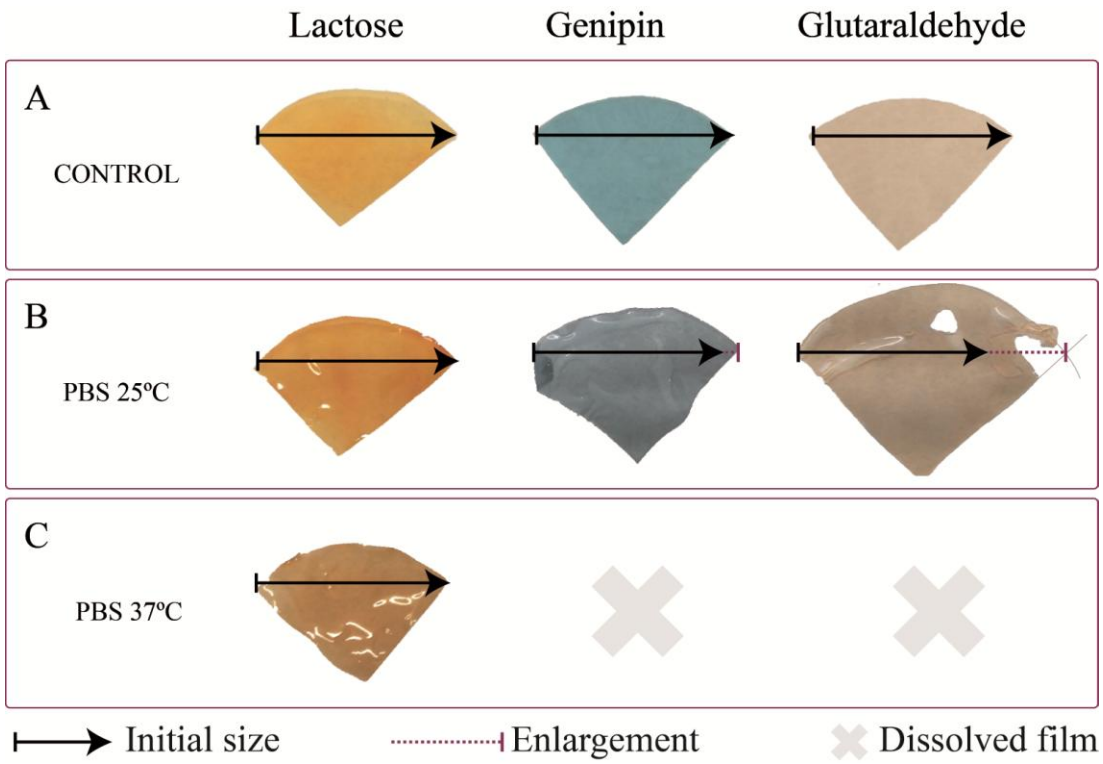

Figure 6.11 Visual aspect of the films crosslinked with lactose, GP, and GTA (a) before immersion in PBS buffer and after immersion in PBS buffer (b) at 25 ºC and (c) at 37 ºC for 3 days.

When the temperature of the PBS solution was increased up to 37 ºC, gelatin films crosslinked with GP or GTA became totally soluble after 24 and 20 h of immersion, respectively (**Figure 6.11c**). However, the increase of temperature did not affect the integrity of lactose-crosslinked films. Furthermore, lactose-crosslinked films maintained their initial appearance after immersion and showed no handling problems. These results indicate that lactose caused a higher crosslinking degree than GP or GTA. Considering these results, the films crosslinked with lactose were the samples selected for further biological analyses. In particular, these films showed an excellent biocompatibility, according to the ISO 10993-5:2009 guidelines for biological evaluation of medical devices, and film surface supported high values of cell adhesion, spreading

and proliferation (data not shown). Considering these results, lactose-crosslinked gelatin films are promising candidates for tissue engineering applications, such as wound healing.

6.3 Conclusions

Modified fish gelatin films were prepared by crosslinking with lactose during different heating times in order to promote Maillard reaction and improve functional properties. It was demonstrated that lactose content and heating time can be used to control the film solubility, which is desirable for biomedical applications such as drug delivery systems or food applications such as bioactive films. Additionally, the formation of coloured compounds, which present first order kinetics, can be used as an indicator of the reaction extension. With this regard, the formation of a fluorescence compound, which presents second order kinetics, can also be considered as a marker of the reaction extension. Interestingly, the reaction kinetics provide the knowledge to control the extension of crosslinking and thus, those functional properties directly related to the nanostructure formed during this non-enzymatic reaction.

Taking the results of the last three chapters into account, it is worth noting that HT films with 20 wt % lactose prepared at basic pH showed the lowest solubility values indicating that further addition of lactose did not promote further reaction. Furthermore, these films presented high WCA values, excellent barrier properties against UV light and tensile strength values around 50 MPa. Therefore, this formulation was considered the most suitable for further assessment.

7 Antioxidant activity of gelatin films

7.1 Summary

Currently, naturally occurring bioactives are preferred by both consumers and companies due to concerns over the potential risks of synthetic compounds. In this context, plants are a valuable source of antioxidants, such as polyphenols, used for pharmaceutical, medical and food applications (Bandyopadhyay, Ghosh, & Ghosh, 2012; Freile-Pelegrín & Robledo, 2014; Gómez-Guillén et al., 2009; Ozdal, Capanoglu, & Altay, 2013; Rao & Ravishankar, 2002). Among plant-derived antioxidant compounds, tetrahydrocurcumin (THC), a hydrogenated metabolite of curcumin (*Curcuma longa* L.), is attracting more and more interest within food, pharmaceutical and cosmetic industries due to a greater antioxidant capacity than curcumin, vitamin E, and α-tocopherol (Mehanny et al., 2016; Priyadarsini, 2014; Venkatesen et al., 2003). Furthermore, in contrast to curcumin, THC is colourless and tasteless (Portes, Gardrat, & Castellan, 2007). Besides the antioxidant capacity of THC (Somporn et al., 2007), this compound has showed antidiabetic (Murugan & Pari, 2006), anticancer (Plyduang et al., 2014), and antiinflammatory activities (Murakami et al., 2008). Therefore, the incorporation of THC into film forming solutions could lead to the development of active films, providing health benefits for consumers.

In previous chapters, the characterization of lactose-incorporated gelatin films was carried out and the crosslinking reaction between lactose and gelatin was assessed. Since the formation of phenolic compounds was found and these compounds are believed to show antioxidant activity, the aim of this work was to analyse the antioxidant capacity of those crosslinked gelatin films with 20 wt % lactose content. Additionally, the incorporation of a bio-based antioxidant, such as THC, to improve the antioxidant capacity of gelatin films was analysed, as well as the surface properties of the THC-incorporated films.

7.2 Results and discussion

First of all, the thickness of films was measured and the average value obtained was 54 ± 5 μm for all films which were designated as: G films (gelatin films without lactose), G-THC films (gelatin films with THC but without lactose), GL films (gelatin films with lactose), and GL-THC films (gelatin films with lactose and THC).

7.2.1 Characterization of films

Film colour was quantified by L*, a* and b* values, shown in **Table 7.1**. The addition of lactose caused a decrease in L* values attributed to the darkening of films. In fact, GL-THC films showed a dark yellowing colour, evidenced by a* and b* values, which increased with lactose addition. Lactose addition and subsequent heating changed film colour, which turned yellowish, and reduced lightness. This darkening and yellowing effect was related to the crosslinking reaction between gelatin and lactose. As a consequence, total colour difference (ΔE*) increased for GL-THC films in comparison with G-THC films.

Table 7.1 L*, a*, b* and ΔE* values for THC-incorporated fish gelatin films.

Film	L*	a*	b*	ΔE*	$Gloss_{60°}$ (GU)
G-THC	93.79 ± 0.29	-0.42 ± 0.02	13.54 ± 0.79		35 ± 1
GL-THC	83.06 ± 1.41	3.43 ± 1.25	58.74 ± 3.49	46.59 ± 3.80	25 ± 2

Gloss values of THC-incorporated films are also shown in **Table 7.1**. As can be seen, GL-THC films showed lower gloss and, thus, rougher surface than G-THC films. This change in surface structure could be explained by interaction among the components of the film forming solutions.

In order to analyse those interactions, FTIR analysis was carried out and spectra are shown in **Figure 7.1**. The characteristic bands of THC appeared at 1598 cm^{-1} (C-C stretching of benzene ring skeleton), 1511 cm^{-1} (C-O stretching), and 1425 cm^{-1} (C-H in-plane bending) (Souguir et al., 2013). As can be observed in **Figure 7.1a** for the films without lactose, the band corresponding to amide II (N-H bending at

1530 cm^{-1}) showed a shoulder at higher frequencies, attributed to the hydrogen bonding between the hydroxyl groups of THC and the amino groups of proline and hydroxyproline in gelatin (Rao et al., 2015). However, in the films with lactose (**Figure 7.1b**), the bands in the range of 1100-1000 cm^{-1} (related to C-O bonds) tend to become a single band, indicating the chemical reaction between gelatin and lactose, as also shown in previous works (Etxabide et al., 2015a; Etxabide et al., 2015b). In these lactose-incorporated films, the abovementioned shoulder of the amide II band was not observed, suggesting that the chemical reaction between gelatin and lactose hindered the hydrogen bonding between THC and gelatin.

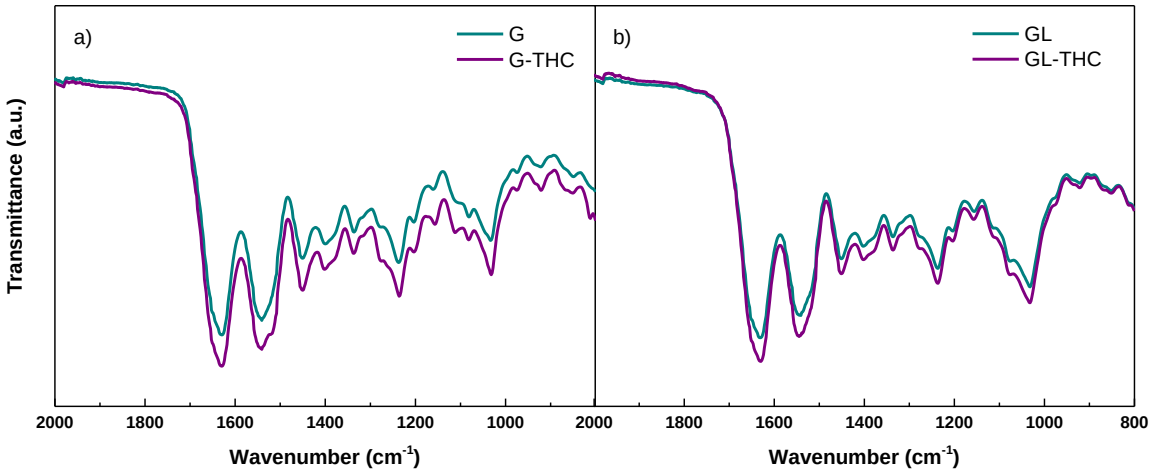

Figure 7.1 FTIR spectra of a) G and G-THC and b) GL and GL-THC fish gelatin films.

The changes that interactions caused in film surface were analysed by XPS and are shown in **Figure 7.2a**. As can be seen, C 1s (284.6 eV), N 1s (398.8 eV) and O 1s (532.0 eV) peaks can be identified. Due to the absence of lactose and, thus, due to the absence of crosslinking reaction, there was no significant difference between the two sides of G-THC films (**Figure 7.2a**). However, it is worth noting that changes were observed between the air-facing side (**Figure 7.2b**) and the plate-facing side (**Figure 7.2c**) of GL-THC films. In fact, the N 1s photoelectron peak, typical for nitrogen in organic matrices, practically disappeared in the plate-facing side of GL-THC films. The disappearance of this peak could be related to the chemical reaction of the N-

containing groups in gelatin with carbonyl groups in lactose, which may alter the protein conformation, leading to significant changes in the surface structure, as shown above by gloss results.

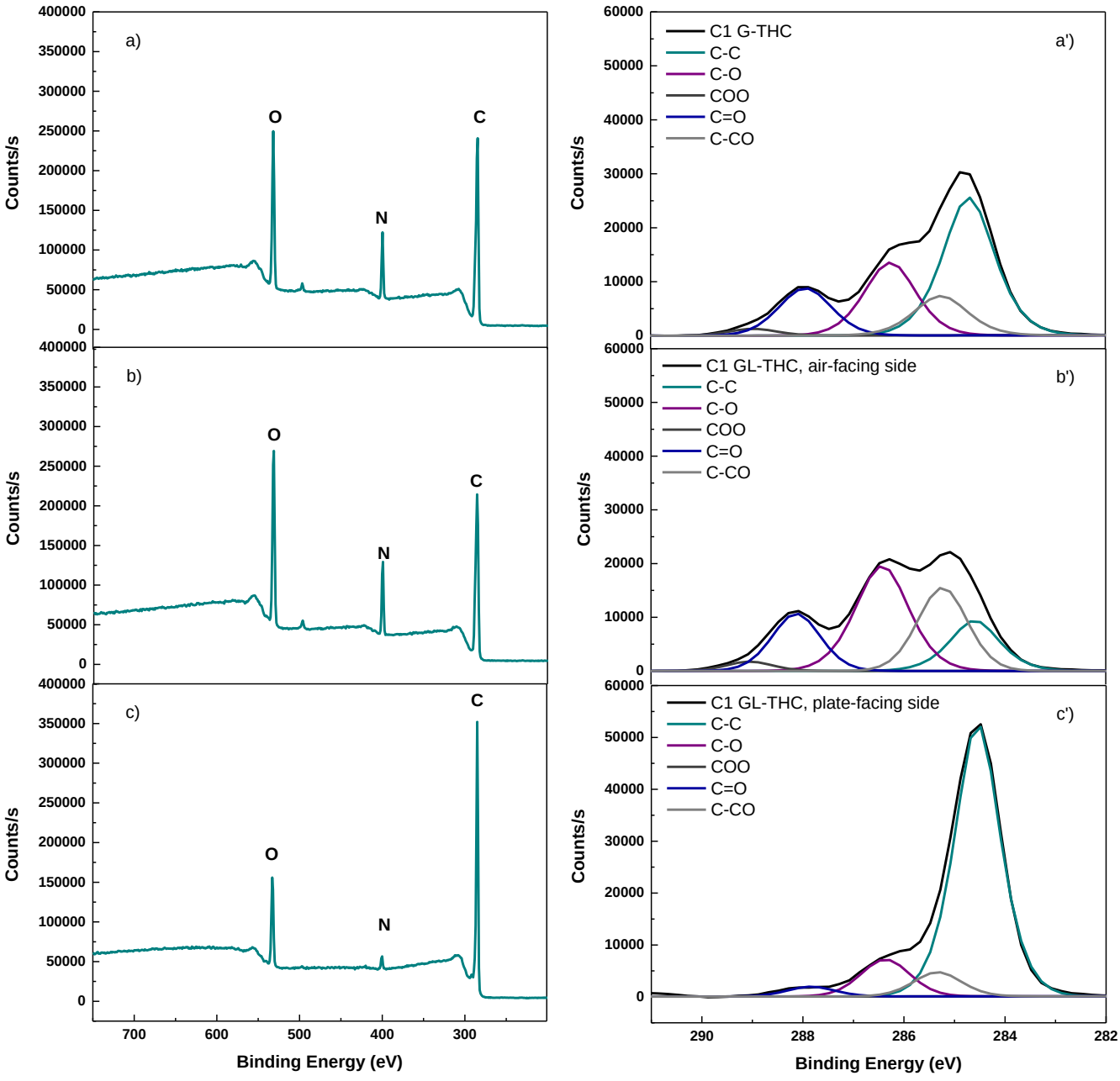

Figure 7.2 XPS survey spectra of a) G-THC (air-facing and plate-facing sides), b) air-facing side of GL-THC, and c) plate-facing side of GL-THC fish gelatin films, and XPS of C 1s features of a') G-THC (air-facing and plate-facing sides), b') air-facing side of GL-THC, and c') plate-facing side of GL-THC fish gelatin films.

These differences could be due to the fact that a higher amount of THC was accumulated on the air-facing side during the film forming process as a consequence of the low solubility of THC in water. As a result, the accumulation of THC on the air-facing side would hinder the chemical reaction between gelatin and lactose. However, when this chemical reaction occurred, an increase of C 1s and a decrease of O 1s were observed. For further analysis, the spectrum corresponding to C was fitted. The C 1s peak was decomposed in the peaks corresponding to C-C (284.60 eV), C-C=O (285.28 eV), C-O (286.28 eV), C=O (287.88 eV) and O-C=O (288.88 eV) bonds, as shown in **Figures 7.2a', 7.2b',** and **7.2c'**. The main peak occurring at 284.60 eV corresponds to the aliphatic carbons of side groups in gelatin, the peak at 285.9 eV is assigned to NH–CHR–CO carbons of the protein backbone, and the peak at 287.7 eV is assigned to –CO–NH– peptidic carbons (Deligianni et al., 2001; Guerrero et al., 2014). When comparing both sides of GL-THC films, it can be observed that the plate-facing side is mainly composed of C-C functions, whereas C-CO, C-O, C=O and COO bonds decreased. These results are due to the formation of nitrogenous compounds of high molecular weight as a consequence of the chemical reaction between gelatin and lactose (Etxabide et al., 2015b).

Although G-THC and GL-THC films showed similar XPS survey spectra (**Figure 7.2a** and **7.2b**), it is worth noting that the spectra fitting showed some differences between them due to the presence of lactose (**Figure 7.2a'** and **7.2b'**). In order to further study these differences optical microscopy was used (**Figure 7.3**). On the one hand, for the films without lactose (**Figure 7.3a**), in which chemical reaction did not occur and, thus, there were more amino groups available in gelatin for hydrogen bonding with THC (as shown by FTIR results, **Figure 7.1a**), the agglomerate size was bigger, leading to a smoother surface, as evidenced by higher gloss values (**Table 7.1**). On the other hand, the chemical reaction between gelatin and lactose led to a lower availability of amino groups to interact with THC by hydrogen bonds and, thus, the

number of agglomerates increased while their size decreased (**Figure 7.3b**), causing rougher surfaces and lower values of gloss (**Table 7.1**).

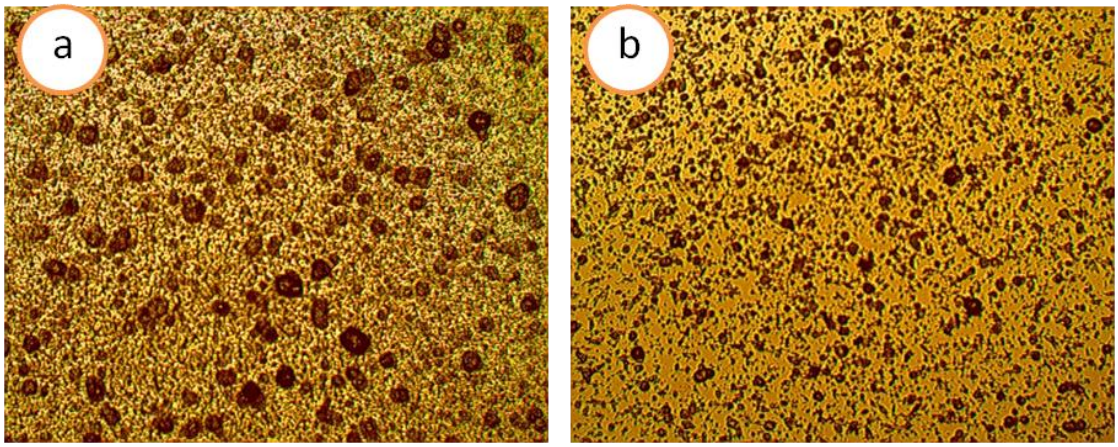

Figure 7.3 Optical micrographs of air-facing side for a) G-THC and b) GL-THC fish gelatin films. Magnification 40X.

7.3.2 Antioxidant activity

First of all, stability of THC under film preparation conditions was analysed. For that, THC powders wetted with water at basic pH were frozen and freeze-dried (THC*). Thermal stability of THC* under the conditions used in this study (105 ºC, 24 h) was analysed. TGA was used to determine weight loss under those conditions and no significant difference was observed (0.4% weight loss, data not shown). In fact, this weight loss could correspond to the evaporation of water that was not completely removed from the sample. Furthermore, solutions of THC and THC* in MeOH (209.5 µM) were prepared and their antioxidant properties were analysed by DPPH assay. Although THC* showed lower inhibition values (86 ± 2) than THC (90 ± 2), there was no difference in the antioxidant activity.

Once verified the THC stability under film preparation conditions, the release of antioxidant compounds was analysed for gelatin films without (G and GL films) and with THC (G-THC and GL-THC films). As shown in **Figure 7.4a** and **7.4b**, a slight increase of light absorption around 280 nm was observed for GL films in comparison

with G films. This increase could be related to the release of phenolic compounds formed during the chemical reaction between gelatin and lactose (Monti et al., 2000; Monti et al., 1999). It is worth noting that there was no increase of absorbance over time (**Figure 7.4b**), indicating no further release after the first day of immersion. When THC was incorporated into film forming solutions (G-THC and GL-THC films), a considerable increase of light absorption was observed (**Figure 7.4c** and **7.4d**), indicating the release of THC from films. In fact, the band with a maximum absorbance at 280 nm corresponds to THC (Portes et al., 2009). In a similar way as the results observed for the films without THC, higher absorbance values were observed for GL-THC films in comparison with G-THC films.

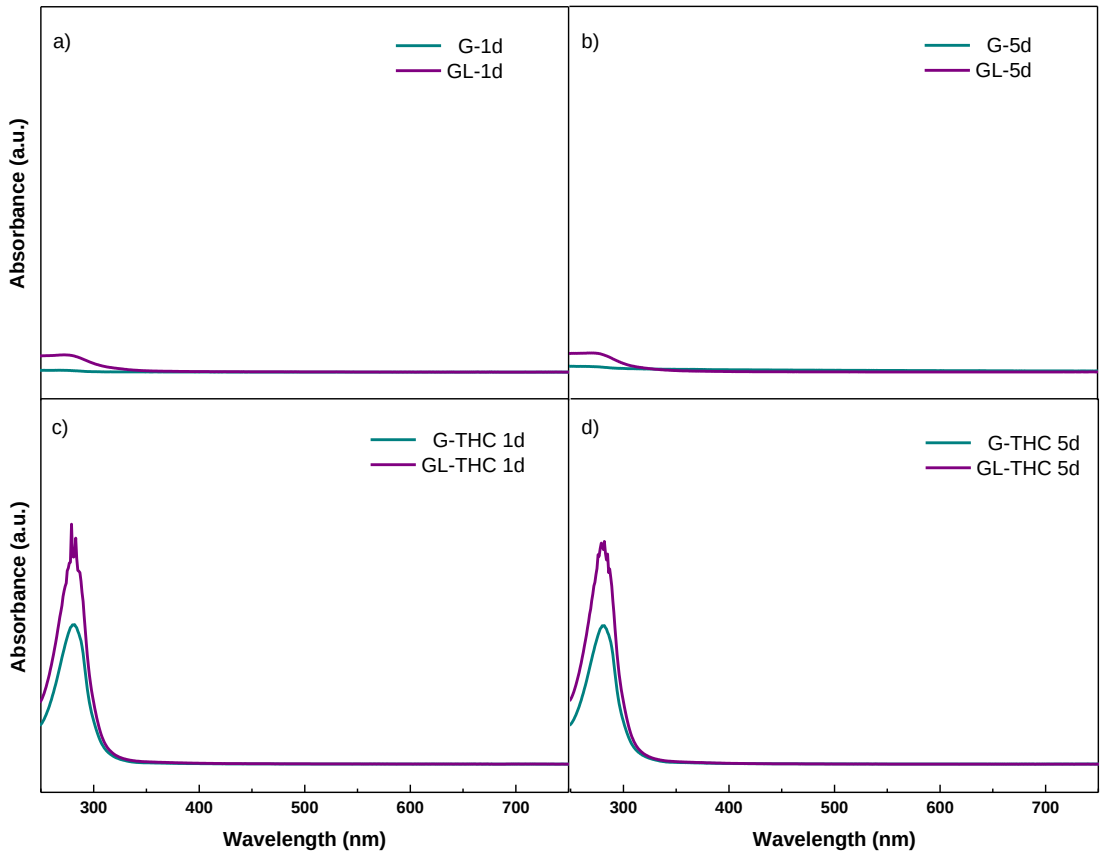

Figure 7.4 UV–vis absorbance for G and GL fish gelatin films after a) 1 day and b) 5 days of immersion, and for G-THC and GL-THC fish gelatin films after c) 1 day and d) 5 days of immersion.

These results are in accordance with the values of mass loss measured and shown in **Table 7.2**. As can be seen, the values for the films with lactose (GL and GL-THC films) were two-fold higher, irrespective of THC incorporation. This increase might be due to the soluble reaction products formed in the early stages of the reaction between gelatin and lactose, but also to the non-reacted lactose, as shown in a previous work (Etxabide et al., 2015b).

Table7.2 Values of mass loss, gallic acid equivalent (GAE), inhibition (I) and butylated hydroxytoluene equivalent (BHTE) for fish gelatin films without THC (G and GL films) and with THC (G-THC and GL-THC films).

Film	Mass loss (%)	GAE (mg/L)	I (%)	BHTE (mg/L)
G	7.93 ± 0.39^{a}	12.8 ± 1.1^{a}	-	-
GL	14.15 ± 0.42^{b}	14.4 ± 0.8^{a}	27.2 ± 1.4^{a}	5.6 ± 0.5^{a}
G-THC	8.20 ± 0.01^{a}	29.7 ± 1.4^{b}	84.5 ± 1.5^{b}	198.0 ± 1.1^{b}
GL-THC	15.14 ± 0.02^{c}	43.2 ± 2.3^{c}	88.5 ± 0.3^{c}	425.7 ± 17.1^{c}

[a-c]Two means followed by the same letter in the same column are not significantly different ($P > 0.05$) through the Tukey's multiple range test.

As also shown in **Table 7.2**, G films exhibited similar values of the total phenolic content as the ones found by other authors (Wu et al., 2013), and GL films did not show significant difference ($P > 0.05$), suggesting that the nature of the soluble compounds released after the chemical reaction between gelatin and lactose might be mainly the non-reacted lactose. The incorporation of THC caused an increase of GAE values, especially for those films prepared with lactose, in which the microstructure formed may favour the THC release. Regarding DPPH radical scavenging capacity, no antioxidant activity was detected for G films, while GL films showed an inhibition value of 27%. These results indicate that new compounds with antioxidant activity were formed due to the chemical reaction between gelatin and lactose (Serpen et al., 2007). The addition of THC significantly increased the antioxidant properties of gelatin films. Furthermore, higher antioxidant activity was observed for GL-THC films than for G-THC films.

7.3 Conclusions

Chemical reaction between gelatin and lactose affected the structure of THC-incorporated gelatin films, leading to less glossy and rougher surfaces. XPS analysis of the films prepared by solution casting showed some changes between the two sides of film surface, attributed to certain agglomeration of THC on the air-facing side. Regarding the antioxidant activity of these films, lactose-incorporated gelatin films showed certain antioxidant capacity due to the phenolic compounds formed as a consequence of the chemical reaction between the amino groups in gelatin and the carbonyl groups in lactose. However, the incorporation of THC into film forming solutions significantly increased the antioxidant capacity of the films developed. Therefore, these gelatin films containing THC have a great potential to be used in food preservation to enhance food safe and quality, also contributing to the development of eco-friendly food packaging. Furthermore, considering that lactose-crosslinked gelatin films are promising candidates for tissue engineering applications, as shown in chapter 6, the addition of a curcuma derivative compound which presents health benefits, could notably improve the healing effects of films.

8 Manufacturing gelatin biocomposites

8.1 Summary

Once processed and characterized films, some manufacturing methods currently employed in plastics industry were used in order to prepare biocomposites. Considering the low melting point of gelatin as an advantage, gelatin was processed by extrusion. Extrusion is a versatile, highly efficient and continuous manufacturing technology in which a wide range of thermo-mechanical and thermo-chemical processes are involved, resulting in physical and chemical modifications of the extruded materials (Hernández-Izquierdo & Krochta, 2009; Fakhouri et al., 2013). Although extrusion is a well-established industrial technique, it has not been widely used for proteins. However, some recent works focused on the extrusion of soy protein (Guerrero, Kerry, & de la Caba, 2014), whey protein (Nor Afizah & Rizvi, 2014) and pea protein (Osen et al., 2014) suggest the possibility of extrusion as a suitable processing method for proteins, which could promote their commercial feasibility.

The novelty of this chapter lies in the use of extrusion and injection as processing methods to manufacture fish gelatin biocomposites. Furthermore, different contents of lactose were incorporated into the formulations to give rise to chemical crosslinking by a non-enzymatic reaction, promoted by heating biocomposites. Functional properties, such as solubility, swelling and mechanical properties, were analysed and related to the changes observed in gelatin structure by differential scanning calorimetry (DSC), X-ray diffraction (XRD), scanning electron microscopy (SEM), and Fourier transform infrared spectroscopy (FTIR).

8.2 Results and discussion

A co-rotating conical twin screw extruder was used to produce gelatin sheets, as explained in chapter 2. The thickness and width of the sheets obtained by extrusion (**Figure 8.1a**) were 1.06 ± 0.19 mm and 3.79 ± 0.33 mm, respectively. These sheets were subsequently cut, injected and heated at 105 ºC for 270 min (**Figure 8.1b**) according to a previous work (Etxabide et al., 2015b).

a)

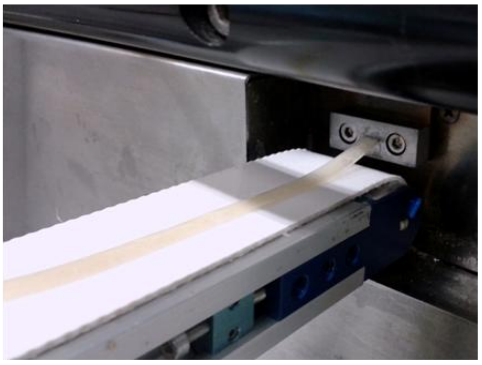

b)

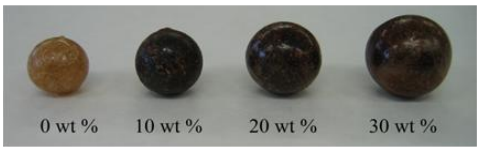

Figure 8.1 a) Continuous production of fish gelatin sheets by extrusion and b) fish gelatin biocomposites obtained by injection after being heated at 105 ºC for 270 min.

8.3.1 Thermal properties

TGA and DTG thermograms of fish gelatin biocomposites as a function of lactose content are shown in **Figures 8.2a** and **8.2b**, respectively. As can be seen, all biocomposites presented similar behaviour with three weight loss stages. The first stage up to 100 ºC was related to the loss of free and absorbed water. The second stage, appeared as a shoulder in the region of 190-260 ºC, was most likely associated with the loss of low molecular weight protein fractions, plasticizer and structurally bounded water directly involved in the triple helix conformation (Wetzel et al., 1987). This second stage appeared at temperatures higher than the glycerol boiling point (182 ºC), suggesting the existence of some kind of interactions, such as hydrogen bonds, between gelatin and glycerol (Guerrero et al., 2011a). Furthermore, the shoulder at about 250 ºC disappeared as lactose content increased, probably due to the formation of high molecular weight reaction products, which could hinder the glycerol release (Pastoriza & Rufián-Henares, 2014). Finally, the third stage was observed at 310 ºC and was related to the degradation of the larger size or highly associated gelatin fractions (Biscarat et al., 2015).

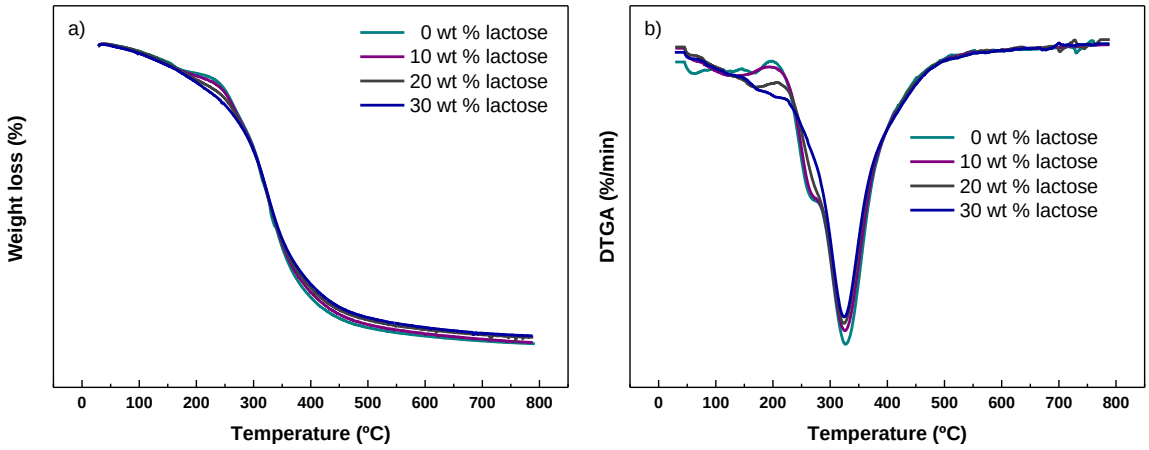

Figure 8.2 a) TGA results as weight loss curves and b) TGA results as derivative curves of fish gelatin biocomposites as a function of lactose content.

Additionally, DSC was carried out and the thermograms are shown in **Figure 8.3**. As can be seen, biocomposites without lactose presented two endothermic peaks: a small peak at 69 ºC, related to random coil region, and a narrow melting peak at 160 ºC, corresponding to the crystallization temperature of gelatin (Coppola, Djabourov, & Ferrad, 2008). In fact, gelatin is denatured collagen obtained by a partial hydrolysis, which breaks the triple helix structure and forms random coils. However, collagen is able to recover its native structure at temperatures below 35-40 ºC, phenomenon known as coil-to-helix transition (Ghoshal, Stapf, & Mattea, 2014). When lactose was added, a noticeable reduction of gelatin melting peak happened, regardless of lactose content, indicating the crosslinking of fish gelatin by the effect of lactose and heating. Furthermore, a small peak at 137 ºC, corresponding to the crystallization temperature of lactose, was observed, especially for the biocomposites with 30 wt % lactose, suggesting the presence of non-reacted lactose (Islam & Langrish, 2010).

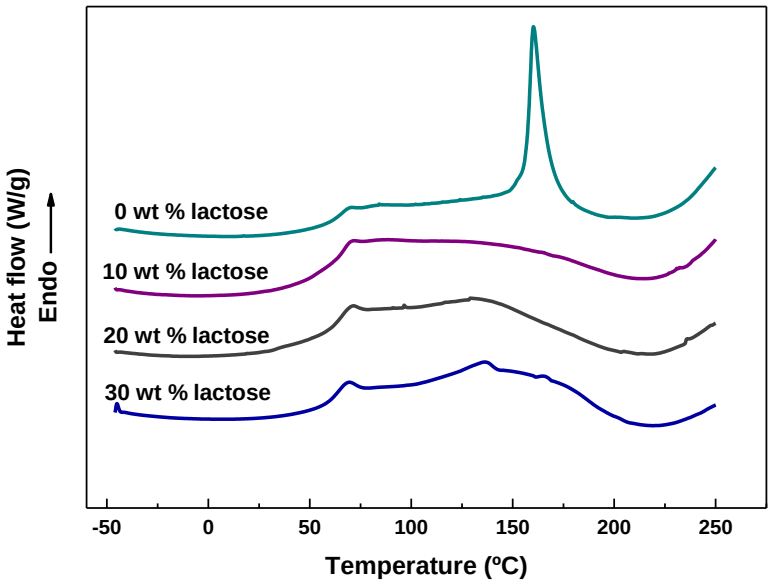

Figure 8.3 DSC thermograms of fish gelatin biocomposites as a function of lactose content.

8.3.2 Mechanical properties

The transition from the glassy to the rubbery state was analysed by DMA. The glass transition temperature (T_g), the storage modulus (E′) and the loss factor (tan δ) were measured. As shown in **Figure 8.4** for the biocomposites with 10 wt % lactose, the first T_g (T_{g1}) was observed from -100 to -55 ºC, corresponding to the glycerol bound to gelatin by physical interactions, such as hydrogen bonds, and indicating that there is no chemical reaction between gelatin and glycerol (Mathew & Dufresne, 2002). Increasing temperature up to 45 ºC caused a gradual decrease of E′ due to the helix-to-coil transition (Bigi, Panzavolta, & Rubini, 2004), while a rapid decline of E′ and a narrow peak of tan δ were observed at 45-75 ºC, related to the glass transition of fish gelatin (T_{g2}) (Ghanbarzadeh & Oromiehi, 2009), previously observed by DSC at 69 ºC. In the range from 70 to 100 ºC, a rubbery plateau was shown.

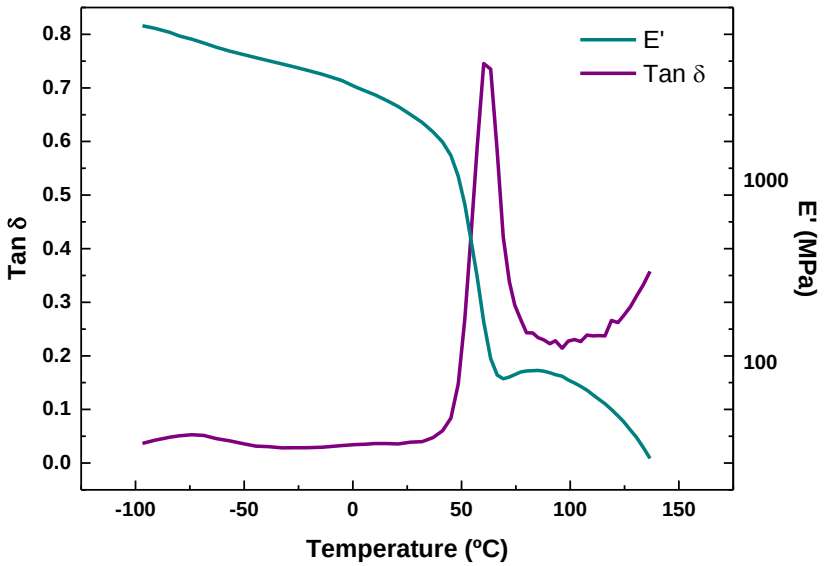

Figure 8.4 Storage modulus (E′) and loss factor (tan δ) values of fish gelatin biocomposites with 10 wt % lactose.

This range of temperatures could be selected when intending to process fish gelatin materials modified with lactose, as performed in this work. Similar graphs were obtained for the biocomposites with higher lactose contents, and T_g values as a function of lactose content are shown in **Table 8.1**. As lactose content increased, T_g values decreased, probably due to the plasticizer effect of non-reacted lactose (Suyatma, Tighzert, & Copinet, 2005). This non-reacted lactose could absorb humidity from the environment due to its hygroscopic character and form crystals, as shown by DSC. Thus, free volume would be higher, increasing chain mobility and decreasing T_g.

Table 8.1 Glass transition temperature of glycerol (T_{g1}) and gelatin (T_{g2}) as a function of lactose content.

Lactose (wt %)	T_{g1} (ºC)	T_{g2} (ºC)
0	-71.1	69.0
10	-74.1	66.4
20	-71.7	60.6
30	-72.9	58.3

In order to analyse the mechanical properties of fish gelatin biocomposites, tensile tests were carried out and stress-strain curves were analysed as a function of lactose content. Despite the fact that there was no significant difference ($P > 0.05$) in the value of tensile strength at break, regardless of lactose content, a noticeable change in the mechanical response was observed when lactose was added (**Figure 8.5**). The plastic behaviour of the biocomposites without lactose, associated with the physical interactions by hydrogen bonds between gelatin and glycerol, resulted in a rigid material undergoing deformation, in accordance with the porous structure of the biocomposites (Gibson & Ashby, 1999), as shown below. The stress-strain curve in lactose-modified biocomposites was comprised of three distinct regimes: a linear-elastic regime followed by a rigid one consisted of a plateau and the final linear rising of stress associated with the reduction of the biocomposite density induced by chemical crosslinking.

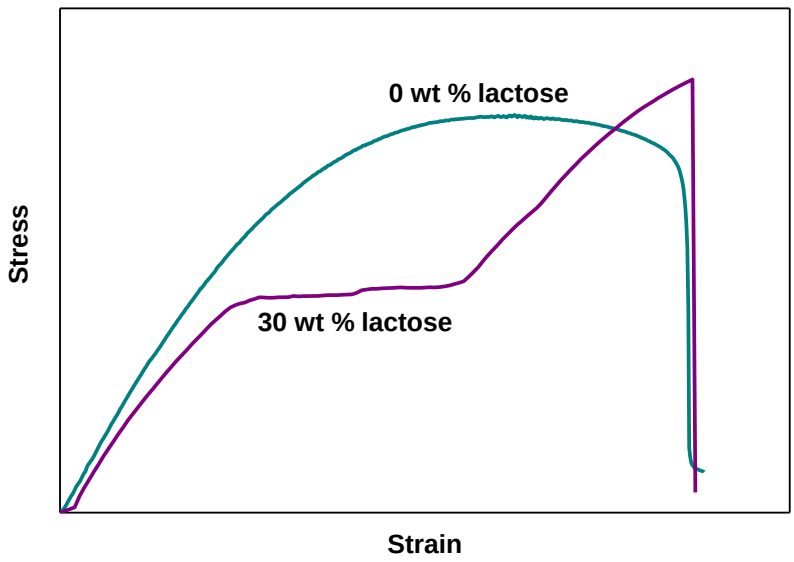

Figure 8.5 Stress-strain curves of fish gelatin biocomposites with lactose.

Besides the stress-strain behaviour, Young's modulus (E), tensile strength (TS) and elongation at break (EB) were measured and the values are shown in **Table 8.2**.

When lactose was added, E values decreased ($P < 0.05$), regardless of sugar content. As shown by DSC results, lactose addition promoted crosslinking, reducing intermolecular interactions among protein chains and hindering the rearrangement of the typical collagen triple helix (Zaman & Beg, 2015). Thus, stiffness of fish gelatin biocomposites decreased, in accordance with DMA results. In relation to tensile strength, the addition of lactose had no significant ($P > 0.05$) effect on those values, which remained constant around 20 MPa. Regarding elongation at break, these values increased ($P < 0.05$) by 5%, probably due to the plasticizing effect of non-reacted lactose, as also shown by DMA.

Table 8.2 Mechanical properties of fish gelatin biocomposites as a function of lactose content.

Lactose (wt %)	E (MPa)	TS (MPa)	EB (%)
0	1396 ± 120^{a}	20 ± 2^{a}	1.9 ± 0.1^{a}
10	906 ± 107^{b}	22 ± 1^{a}	5.6 ± 0.4^{b}
20	857 ± 70^{b}	20 ± 3^{a}	5.4 ± 1.1^{b}
30	925 ± 147^{b}	18 ± 2^{a}	4.8 ± 0.2^{b}

[a-b]Two means followed by the same letter in the same column are not significantly ($P > 0.05$) different through the Tukey's multiple range test.

8.3.3 Biocomposite structure

The biocomposite structure is a key aspect to explain the effect of lactose content on the biocomposite properties and thus, XRD and SEM analyses were carried out to study the crystallinity and morphology of fish gelatin biocomposites. As can be observed in **Figure 8.6**, diffractograms displayed two diffraction peaks: the peak at 21 º related to the crystallinity of gelatin, and the peak at 7.4 º corresponding to the residual triple helix from native collagen (Bigi, Panzavolta, & Rubini, 2004). When lactose content increased, gelatin crystallinity increased, indicating a higher order in the structure due to the formation of new covalent bonds between lactose and gelatin (Etxabide et al., 2015b). Moreover, non-reacted lactose can absorb moisture and crystallize, in agreement with the increase of the crystalline peak at 137 ºC observed by DSC as lactose content increased. In contrast, the residual triple helix decreased, in

accordance with the decrease of intermolecular interactions among protein chains due to the crosslinking, which hindered the rearrangement of the triple helix. These results agree with the decrease in Young's modulus measured by tensile tests.

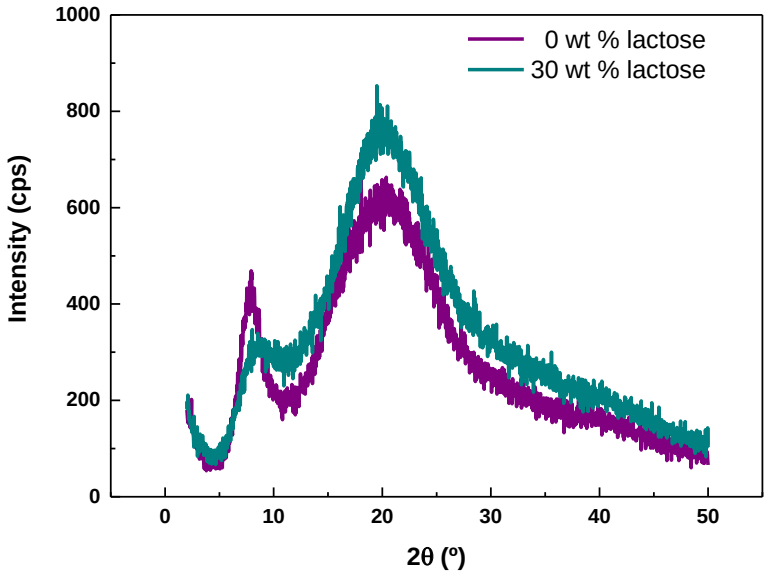

Figure 8.6 XRD results of fish gelatin biocomposites with 0 wt % and 30 wt % lactose.

In order to further analyse the structure of fish gelatin biocomposites, SEM micrographs were taken at the break surface (**Figure 8.7**).

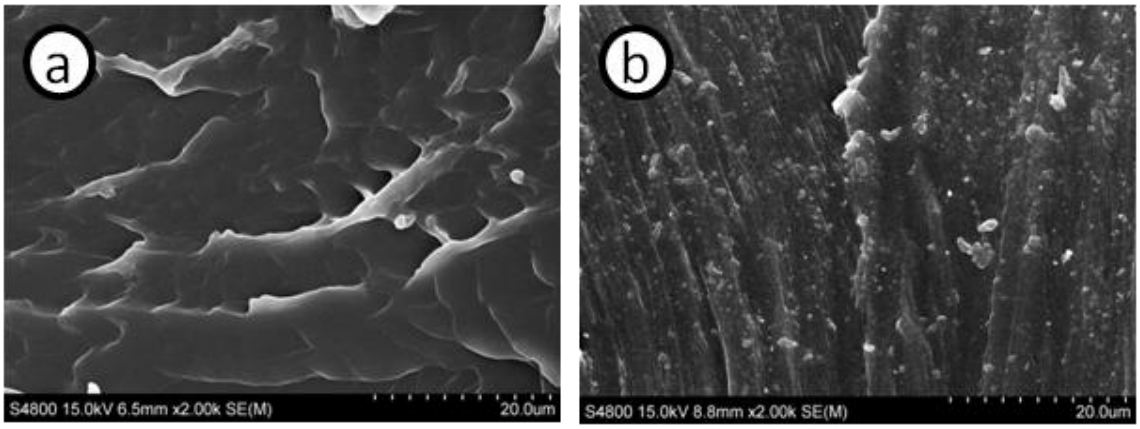

Figure 8.7 SEM images of fish gelatin biocomposites with a) 0 wt % lactose and b) 30 wt % lactose.

The biocomposite morphology changed from a flake-like structure (**Figure 8.7a**) to a fibre-like structure (**Figure 8.7b**) with non-reacted lactose crystals around the fibres when lactose was added, consistent with the more ordered structure observed by XRD.

8.3.4 Biocomposite swelling

Swelling tests were carried out and samples before and after immersion are shown in **Figure 8.8**. As can be observed, samples with lactose showed brown colour due to the formation of brown insoluble pigments, known as melanoidins (Jiang & Brodkorb, 2012). It is worth noting that all biocomposites maintained their structural integrity after immersion for 4320 min (3 days). However, the swelling of the samples with lactose was lower than the swelling observed for the biocomposites without lactose, indicating that the reaction affected the liquid uptake capacity. When lactose was added, crosslinking increased and thus, liquid diffusion through the sample decreased (Saarai et al., 2013).

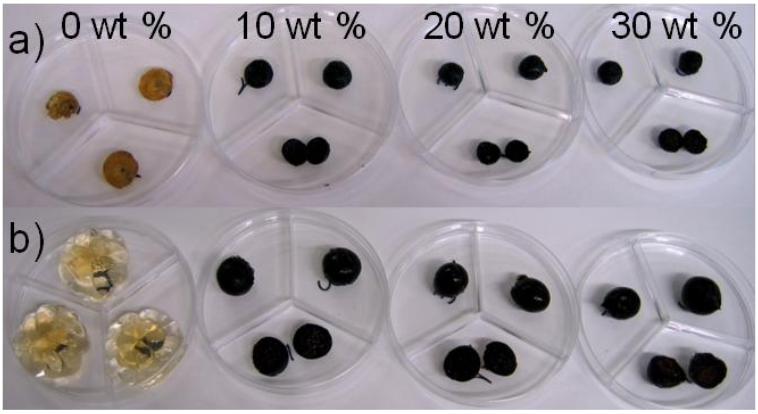

Figure 8.8 Fish gelatin biocomposites as a function of lactose content a) before and b) after swelling for 4320 min.

Additionally, swelling kinetics was determined and results are displayed in **Figure 8.9a** and **8.9b**. Samples presented second order kinetics up to 4320 min (**Figure 8.9a**), while first order kinetics was observed up to 480 min (**Figure 8.9b**). On the one hand, fish gelatin samples without lactose considerably swelled up to 230%

after 480 min and up to 1500% after 4320 min, showing a lineal increase of swelling over time. On the other hand, lactose addition induced a significant reduction of swelling up to 150% after 480 min and around 250% after 4320 min, when swelling values remained constant as a consequence of the chemical crosslinking, as explained above. However, swelling slightly increased when lactose content increased due to non-reacted lactose, which is a hygroscopic compound. These observations agreed with the results obtained by DSC and DMA.

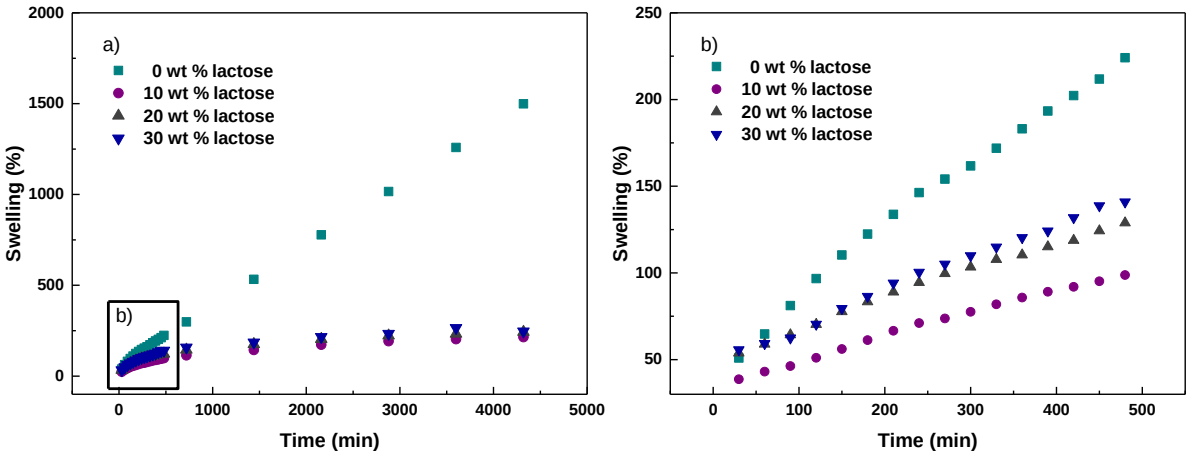

Figure 8.9 Swelling values up to a) 4320 min (3 days) and b) 480 min (8 h) for fish gelatin biocomposites as a function of lactose content.

As mass and volume changes occurred during crosslinking and swelling processes, density and porosity values were calculated and presented in **Table 8.3**. As can be seen, control biocomposites (non-heated biocomposites) and the HT biocomposite without lactose showed similar ($P > 0.05$) density, higher than water density at ambient temperature (0.997 g/mL). However, a significant ($P < 0.05$) decrease of density was observed after heating, as lactose content increased, and density was lower than water density. This behaviour could be due to the migration of glycerol and non-reacted lactose during swelling and also to the volume increase

caused by the change in gelatin structure as a consequence of the chemical crosslinking (Learner et al., 2008).

Table 8.3 Density and porosity values of fish gelatin biocomposites as a function of lactose content.

Lactose (wt %)	$\rho_{control}$ (g/mL)	ρ_x (g/mL)	Porosity (%)
0	1.34 ± 0.06[a]	1.20 ± 0.04[a]	---
10	1.33 ± 0.04[a]	0.87 ± 0.01[b]	36.54 ± 1.53[d]
20	1.29 ± 0.12[a]	0.58 ± 0.01[c]	53.83 ± 4.43[e]
30	1.32 ± 0.09[a]	0.41 ± 0.03[c]	68.78 ± 0.45[f]

[a-f]Two means followed by the same letter are not significantly (P > 0.05) different through the Tukey's multiple range test.

Since porosity values increased, SEM analysis was carried out in order to analyse the changes on the structure of fish gelatin biocomposites. As can be seen, a homogeneous and smooth surface with some cavities was obtained for the samples without lactose (**Figure 8.10a**), whereas a highly porous structure could be observed when 30 wt % lactose was added (**Figure 8.10b)**. This behaviour agrees with the migration of glycerol and non-reacted lactose during swelling tests, since more pores were observed when lactose content was higher. These porous structures with low density could be of great interest as carriers of active compounds.

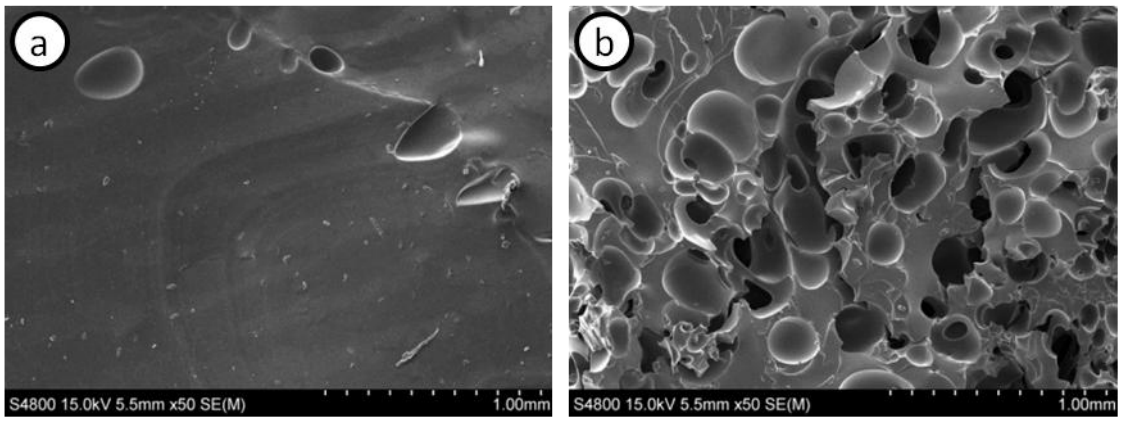

Figure 8.10 SEM images of fish gelatin biocomposites with a) 0 wt % lactose and b) 30 wt % lactose, after swelling in PBS for 4320 min.

In order to support the migration of low molecular weight components during swelling, fish gelatin biocomposites were analysed by FTIR spectroscopy. The FTIR

spectra of the biocomposites before and after immersion in PBS for 4320 min are shown in **Figure 8.11**. As can be observed, the characteristic bands of glycerol disappeared in the samples without lactose, suggesting the plasticizer migration and the fact that glycerol-gelatin interactions were mainly hydrogen-bonds (Guerrero et al., 2011b). On the other hand, a noticeable decrease in the intensity of the lactose bands was observed in **Figure 8.11b** due to the migration of non-reacted lactose.

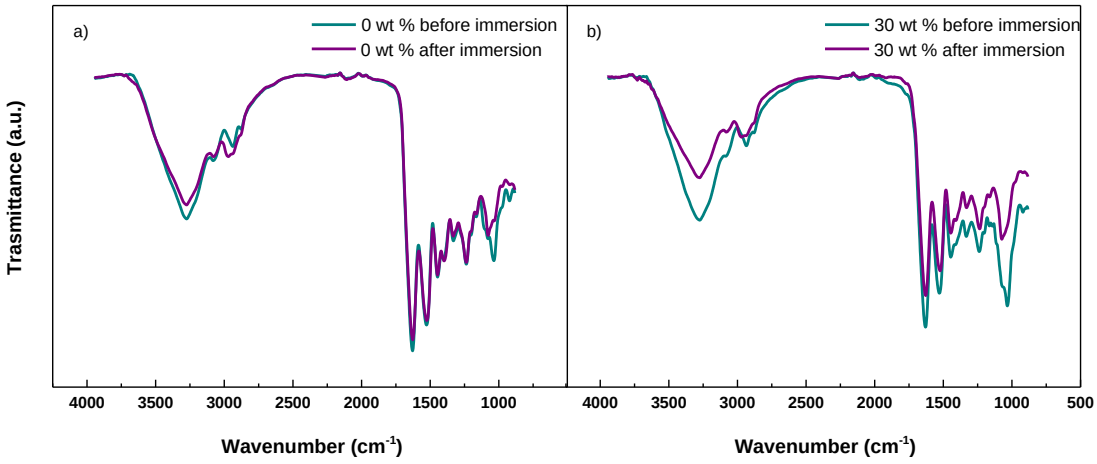

Figure 8.11 FTIR spectra of fish gelatin biocomposites with a) 0 wt % lactose and b) 30 wt % lactose, before and after immersion in PBS.

8.3 Conclusions

Gelatin pellets were obtained by extrusion and they were subsequently injected to manufacture gelatin-based biocomposites. Chemical crosslinking was caused by a non-enzymatic reaction, promoted by lactose addition and heating. This crosslinking decreased solubility, swelling and density of gelatin biocomposites due to the formation of porous structures, as shown by SEM analysis. Furthermore, increasing lactose content caused an increase of crystallinity, observed by DSC, and a reduction of the triple helix structure, supported by XRD results, in agreement with the decrease of the elastic modulus found by tensile tests. Finally, the increase of elongation at break and the decrease of the glass transition temperature as lactose content increased showed

that non-reacted lactose could act as a plasticizer in the biocomposites prepared. These results demonstrate that non-enzymatic crosslinked gelatins provide a new approach to the development of biocomposites with improved properties.

.

9 General conclusions

In this chapter, the general conclusions based on the findings of the studies presented in this thesis are described:

- Homogeneous and transparent fish gelatin films with high UV resistance and tensile strength were developed. These functional properties highlighted the potential of these films to be used for food packaging applications to extend food shelf-life.
- The positive environmental impact of composting as the end of life of films promoted their use for short-term packaging application in order to facilitate waste management but also to reduce the consumption of non-biodegradable materials.
- Lactose addition affected gelatin structure, especially after heating, which promoted Maillard reaction, whose extent could be controlled by solution pH, according to the requirements for specific applications.
- At acid pH, the extent of crosslinking reaction was low, resulting in totally soluble films, which could be used as active films in contact with gastrointestinal fluids.
- At basic pH, the extent of crosslinking reaction was high, resulting in UV-vis protective films with high water resistance, appropriate for packaging, but also excellent biocompatibility and cell proliferation properties, which enabled films to be used for pharmaceutical applications (e.g. wound healing).
- Lactose-incorporated gelatin films showed antioxidant capacity due to the phenolic compounds formed as a consequence of Maillard reaction.
- The incorporation of THC into film forming solutions significantly increased the antioxidant capacity of the films developed, showing a great potential to be used in active packaging in order to enhance food quality.

- Extrusion and injection parameters were optimised to obtain gelatin sheets and biocomposites, in which solubility, swelling and density decreased due to the formation of porous structures.
- Both formulations and processing conditions were optimised in order to produce gelatin materials by means of the techniques currently available at industrial scale.

10 References

Ahmad, M., Benjakul, S., Prodpran, T., & Agustini, T.W. (2012). Physico-mechanical and antimicrobial properties of gelatin film from the skin of unicorn leatherjacket incorporated with essential oils. *Food Hydrocolloids*, 28, 189-199.

Ali Poursamar, S., Lehner, A.N., Azami, M., Ebrahimi-Barough, S., Samadikuchaksaraei, A., & Antunes, A.P.M. (2016). The effects of crosslinkers on physical, mechanical, and cytotoxic properties of gelatin sponge prepared *via in-situ* gas foaming method as a tissue engineering scaffold. *Mater Sci Eng*, 63, 1-9.

Ali, J., Md, S., Baboota, S., & Sahni, J.K. (2012). Polymeric nanoparticles, magnetic nanoparticles and quantum dots: current future perspectives. In *Patenting nanomedicines*. Souto, E.B. (Ed.). Berlin, Springer-Verlag, pp. 107-110.

Amado, I.R., Franco, D., Sánchez, M., Zapata, C., & Vázquez, J.A. (2014). Optimisation of antioxidant extraction from *Solanum tubersum* potato peel waste by surface response methodology. *Food Chem*, 165, 290-299.

Anbinder, P.S., Peruzzo, P.J., Martino, M.N., & Amalvy, J.I. (2015). Effect of antioxidant active films on the oxidation of soybean oil monitored by Fourier infrared spectroscopy. *J Food Eng*, 151, 43-50.

Araújo, M., Pimentel, F.B., Alves, R.C., & Oliveira, M.B.P.P. (2015). Phenolic compounds from olive mill wastes: health effects, analytical approach and application as food antioxidants. *Trends Food Sci Technol*, 45, 200-211.

Arfat, Y.A., Benjakul, S., Vongkamjan, K., Sumpavapol, P., & Yarnpakdee, S. (2015). Shelf-life extension of refrigerated sea bass slices wrapped with fish protein isolate/fish skin gelatin-ZnO nanocomposite film incorporated with basil leaf essential oil. *J Food Sci Technol*, 52, 6182-6193.

Arrieta, M.P., Fortunati, E., Dominici, F., Rayón, E., López, J., & Kenny, J.M. (2014). PLA-PHB/cellulose based films: mechanical, barrier and disintegration properties. *Polym Degrad Stab*, 107, 139-149.

ASTM D1708-93 (1993). Standard test method for tensile properties of plastics by use of microtensile specimens. In *Annual Book of ASTM Standards*. Philadelphia: American Society for Testing Materials.

ASTM D523-14 (2014). Standard test method for specular gloss. In *Annual Book of ASTM Standards*. Philadelphia: American Society for Testing Materials.

ASTM D570-98 (1998). Standard test method for water absorption of plastics. In *Annual Book of ASTM Standards*. Philadelphia: American Society for Testing Materials.

ASTM E96-00 (2000). Standard test methods for water vapour transmission of material. In *Annual Book of ASTM Standards.* Philadelphia: American Society for Testing Materials.

Atarés, L. & Chiralt, A. (2016). Essential oils as additives in biodegradable films and coatings for active food packaging. *Trends Food Sci Technol*, 48, 51-62.

Bandyopadhyay, P., Ghosh, A.K., & Ghosh, C. (2012). Recent developments on polyphenol-protein interactions: effects on tea and coffee taste, antioxidant properties and the digestive system. *Food Funct*, 3, 592-605.

Bare, J.C., Hofstetter, P., Pennington, D.W., & Udo de Haes, H.A. (2000). Midpoints versus endpoints: the sacrifices and benefits. *Int J Life Cycle Assess*, 5, 319-326.

Basu, S., Shivhare, U.S., Singh, T.V., & Beniwal, V.S. (2011). Rheological, texture and spectral characteristics of sorbitol substituted mango jam. *J Food Eng*, 105, 503-512.

Benbettaïeb, N., Assifaoui, A., Karbowiak, T., Debeaufort, F., & Chambin, O. (2016a). Controlled release of tryrosol and ferulic acid encapsulated in chitosan-gelatin films after electron beam irradiation. *Radiat Phys Chem*, 118, 81-86.

Benbettaïeb, N., Chambin, O., Assifaoui, A., Al-Assaf, S., Karbowiak, T., & Debeaufort, F. (2016b). Release of coumarin incorporated into chitosan-gelatin irradiated films. *Food Hydrocolloids*, 56, 266-276.

Benbettaïeb, N., Chambin, O., Karbowiak, T., & Debeaufort, F. (2016c). Release behavior of quercetin from chitosan-fish gelatin edible films influenced by electron beam irradiation. *Food Control*, 66, 315-319.

Benetto, E., Jury, C., Igos, E., Carton, J., Hild, P., Vergne, C., & Di Martino, J. (2015). Using atmospheric plasma to design multilayer film from polylactic acid and thermoplastic starch: a screening life cycle assessment. *J Cleaner Prod*, 87, 953-960.

Benjakul, S., Kittiphattanabawon, P., & Regenstein, J.M. (2012). Fish gelatin. In *Food Biochemistry and Food*. Simpson, B.K., Nollet, L.M.L., & Toldrae, F. (Eds). John Wiley & Sons Inc, Ames, IA, USA, pp. 388-405.

Bergo, P. & Sobral, P.J.A. (2007). Effects of plasticizer on physical properties of pigskin gelatin films. *Food Hydrocolloids*, 12, 1285-1289.

Bhat, R. & Karim, A.A. (2014). Towards producing novel fish gelatin films by combination treatments of ultraviolet radiation and sugars (ribose and lactose) as cross-linking agents. *J Food Sci Technol*, 51, 1329-1333.

Bhat, S.A., Sohail, A., Siddiqui, A.A., & Bano, B. (2014). Effect of non-enzymatic glycation on cystatin: a spectroscopy study. *J Fluoresc*, 24, 1107-1117.

Bhutani, U., Laha, A., Mitra, K., & Majumdar, S. (2016). Sodium alginate and gelatin hydrogels: viscosity effect on hydrophobic drug release. *Mater Lett*, 164, 76-79.

Bigi, A., Panzavolta, S., & Rubini, K. (2004). Relationship between triple-helix content and mechanical properties of gelatin films. *Biomaterials*, 25, 5675-5680.

Biscarat, J., Charmette, C., Sanchez, J., & Pochat-Bohatier, C. (2015). Preparation of dense gelatin membranes by combining temperature induced gelation and dry-casting. *J Membr Sci*, 473, 45-53.

Bitencourt, C.M., Fávaro-Trindade, C.S., Sobral, P.J.A., & Carvalho, R.A. (2014). Gelatin-based films additivated with curcuma ethanol extract: antioxidant activity and physical properties of films. *Food Hydrocolloids*, 40, 145-152.

Bolumar, T., Andersen, M.L., & Orlien, V. (2011). Antioxidant active packaging for chicken meat processed by high pressure treatment. *Food Chem*, 129, 1406-1412.

Bosso, A., Guaita, M., & Petrozziello, M. (2016). Influence of solvents on the composition of condensed tannins in grape pomace seed extracts. *Food Chem*, 207, 162-169.

Boulekbache-Makhlouf, L., Slimani, S., & Madani, K. (2013). Total phenolic content, antioxidant and antibacterial activities of fruits of *Eucalyptus globulus* cultivated in Algeria. *Ind Crops Prod*, 41, 85-89.

Bower, C.K., Avena-Bustillos, R.J., Olsen, C.W., Mchugh, T.H., & Bechtel, P.J. (2006). Characterization of fish-skin gelatin gels and films containing the antimicrobial enzyme lysozyme. *J Food Sci*, 71, 141-145.

Bravin, B., Pressini, D., & Sensidoni, A. (2006). Development and application of polysaccharide-lipid edible coating to extend shelf-life of dry bakery products. *J Food Eng*, 76, 280-290.

Calderón, L.A., Iglesias, L., Laca, A., Herrero, M., & Díaz, M. (2010). The utility of life cycle assessment in the ready meal food industry. *Resour Conserv Recycl*, 54, 1196-1207.

Cardinali, A., Pati, S., Minervini, F., D'Antuono, I., Linsalata, V., & Lattanzio, V. (2012). Verbascoside, isoverbascoside, and their derivatives recovered from olive mill wastewater as possible food antioxidant. *J Agric Food Chem*, 60, 1822-1829.

Carlsen, M.H., Halvorsen, B.L., Holte, K., Bøhn, S.K., Dragland, S., Sampson, L., Willey, C., Senoo, H., Umezono, Y., Sanada, C., Barikmo, I., Berhe, N., Willett, W.C., Phillips, K.M., Jacobs, D.R., & Blomhoff, R. (2010). The total antioxidant content of more than 3100 foods, beverages, spices, herbs and supplements used worldwide. *Nutr J*, 9, 1-11.

Carvalho, R.A. & Grosso, C.R.F. (2004). Characterization of gelatin based films modified with transglutaminase, glyoxal and formaldehyde. *Food Hydrocolloids*, 18, 717-726.

Ćetković, G., Savatović, S., Čanadanović-Brunet, J., Djilas, S., Vulić, J., Mandić, A., & Cetojević-Simin, D. (2012). Valorization of phenolic composition, antioxidant and cell growth activities of tomato waste. *Food Chem*, 133, 938-945.

Chen, Z., Wang, L., & Jiang, H. (2012). The effect of procyanidine crosslinking on the properties of the electrospun gelatin membranes. *Biofabrication*, 4, 1-11.

Chiou, B., Avena-Bustillos, R.J., Bechtel, P.J., Jafri, H., Narayan, R., Imam, S.H., Glenn, G.M., & Orts, W.J. (2008). Cold water fish gelatin films: Effects of cross-linking on thermal, mechanical, barrier, and biodegradation properties. *Eur Polym J*, 44, 3748-3753.

Chiou, B.S., Avena-Bustillos, R.J., Shey, J., Yee, E., Bechtel, P.J., & Imam, S.H. (2006). Rheological and mechanical properties of cross-linked fish gelatins. *Polymer*, 47, 6379-6386.

Coppola, M., Djabourov, M., & Ferrand, M. (2008). Phase diagram of gelatin plasticized by water and glycerol. *Macromol Symp*, 273, 56-65.

Costa, D.C., Costa, H.S., Albuquerque, T.G., Ramos, F., Castilho, M.C., & Sanches-Silva, A. (2015). Advances in phenolic compounds analysis of aromatic plants and their potential applications. *Trends Food Sci Technol*, 45, 336-354.

Crizel, T.M., Costa, T.M.H., Rios, A.O., & Flôres, S.H. (2016). Valorization of food-grade industrial waste in the obtaining active biodegradable films for packaging. *Ind Crops Prod*, 87, 218-228.

Cuq, B., Gontard, N., Cuq, J.L., & Guilbert, S. (1996). Functional properties of myofibrillar protein-based biopackaging as affected by film thickness. *J Food Sci*, 61, 580-584.

Cuzzoni, M.T., Stoppini, G., Gazzani, G., & Mazza, P. (1988). Influence of water activity and reaction temperature of ribose-lysine and glucose-lysine Maillard systems on mutagenicity, absorbance and content of furfurals. *Food Chem Toxicol*, 26, 815-822.

Da Silva, B.V., Barreira, J.C.M., & Oliveira, M.B.P.P. (2016). Natural phytochemicals and probiotics as bioactive ingredients for functional foods: extraction, biochemistry and protected-delivery technologies. *Trends Food Sci Technol*, 50, 144-158.

Da Silva, G. P., Mack, M., & Contiero, J. (2009). Glycerol: a promising and abundant carbon source for industrial microbiology. *Biotechnol Adv*, 1, 30-39.

Deligianni, D.D., Katsala, N., Ladas, S., Sotiropoulou, D., Amedee, J., & Missirlis, Y.F. (2001). Effect of surface roughness of the titanium alloy Ti-6Al-4V on human bone marrow cell response and on protein adsorption. *Biomaterials*, 22, 1241-1251.

Deng, Y., Achten, W.M.J., Van Acker, K., & Duflou, J.R. (2013). Life cycle assessment of wheat gluten powder and derived packaging film. *Biofuels Bioprod Biorefin*, 7, 429-458.

Deyl, Z., Mikšík, I., Zicha, J., & Jelínková, D. (1997). Reversed-phase chromatography of pentosidine-containing CNBr peptides from collagen. *Anal Chim Acta*, 352, 257-270.

Díaz-Visurraga, J., Meléndrez, M.F., García, A., Paulraj, M., & Cárdenas, G. (2010). Semitransparent chitosan-TiO_2 nanotubes composite film for food package applications. J *Appl Polym Sci*, 116, 3503-3515.

Djilani, A. & Dicko, A. (2012). The therapeutic benefits of essential oils. INTECH.

Duconseille, A., Astruc, T., Quintana, N., Meersman, F., & Sante-Lhoutellier, V. (2015). Gelatin structure and composition linked to hard capsule dissolution: A review. *Food Hydrocolloids*, 43, 360-376.

Duncan, S.E. & Chang, H.H. (2012). Implications of light energy on food quality and packaging selection. In *Advances in Food and Nutrition Research.* Taylor, S. (Ed.). Elsevier, San Diego, pp. 25-73.

El Asbahani, A., Milada, K., Badri, W., Sala, M., Addi, E.H.A., Casabianca, H., El Mousadik, A., Hartmann, D., Jilale, A., Renaud, F.N.R., & Elaissari, A. (2015). Essential oils: From extraction to encapsulation. *Int J Pharm*, 483, 220-243.

Embuscado, M.E. (2015). Spices and herbs: natural sources of antioxidants - a mini review. *J Funct Foods*, 18, 811-819.

Etxabide, A., Guerrero, P., & de la Caba, K. (2016). A novel approach to manufacture porous biocomposites using extrusion and injection moulding. *Eur Polym J*, 82, 324-333.

Etxabide, A., Leceta, I., Cabezudo, S., Guerrero, P., & de la Caba, K. (2016a). Sustainable fish gelatin films: from food processing waste to compost. *ACS Sustainable Chem Eng*, 4, 4626-4634.

Etxabide, A., Uranga, J., Guerrero, P., & de la Caba, K. (2015a). Improvement of barrier properties of fish gelatin films promoted by gelatin glycation with lactose at high temperatures. *LWT-Food Sci Technol*, 63, 315-321.

Etxabide, A., Uranga, J., Guerrero, P., & de la Caba, K. (2016). Development of active gelatin films by means of valorisation of food processing waste: a review. *Food Hydrocolloids*, 68, 192-198.

Etxabide, A., Urdanpilleta, M., Guerrero, P., & de la Caba, K. (2015b). Effects of cross-linking in nanostructure and physicochemical properties of fish gelatin for bio-applications. *React Funct Polym*, 94, 55-62.

Fabian, H. & Mäntele, W. (2002). Infrared spectroscopy of proteins. In *Handbook of Vibrational Spectroscopy*. Chalmer, J.M. & Griffiths, P.R. (Eds.). John Wiley & Sons, Chichester, UK, pp. 3399-3426.

Fakhouri, F.M., Costa, D., Yamashita, F., Martelli, S.M., Jesus, R.C., Alganer, K., Collares-Queiroz, F., & Innocentini-Mei, L.H. (2013). Comparative study of processing methods for starch/gelatin films. *Carbohydr Polym*, 20, 681-689.

Farris, S., Song, J., & Huang, Q. (2010). Alternative reaction mechanism for the cross-linking of gelatin with glutaraldehyde. *J Agric Food Chem*, 58, 998-1003.

Farvin, K.H.S., Grejsen, H.D., & Jacobsen, C. (2012). Potato peel extract as a natural antioxidant in chilled storage of minced horse mackerel (*Trachurus trachurus*): effect on lipid and protein oxidation. *Food Chem*, 131, 843-851.

Freile-Pelegrín, Y. & Robledo, D. (2014). Bioactive phenolic compounds from algae. In *Bioactive compounds from marine foods: plant and animal sources*. Hernández-Ledesma, B. & Herrero, M. (Eds.) John Wiley & Sons, Ltd., Chichester, UK, pp. 131-152.

Garrido, T., Etxabide, A., Leceta, I., Cabezudo, S., de la Caba, K., & Guerrero, P. (2014). Valorization of soya by-products for sustainable packaging. *J Cleaner Prod*, 64, 228-233.

Garrido, T., Etxabide, A., Peñalba, M., de la Caba, K., & Guerrero, P. (2013). Preparation and characterization of soy protein thin films: processing-properties correlation. *Mater Lett*, 105, 110-112.

Ghanbarzadeh, B. & Oromiehi, A.R. (2009). Thermal and mechanical behavior of laminated protein films. *J Food Eng*, 90, 517-524.

Ghoshal, S., Stapf, S., & Mattea, C. (2014). Protein renaturation in the gelatin film formation process. *Appl Magn Reson*, 45, 145-154.

Gibson, L.J. & Ashby, M.F. (1999). Cellular solids: structure and properties. Cambridge University Press, Cambridge.

Giménez, B., Gómez-Guillén, M.C., López-Caballero, M.E., Gómez-Estaca, J., & Montero, P. (2012). Role of sepiolite in the release of active compounds from gelatin-egg white films. *Food Hydrocolloids*, 27, 475-486.

Giménez, B., López de Lacey, A., Pérez-Santín, E., López-Caballero, M.E., & Montero, P. (2013). Release of active compounds from agar and agar-gelatin films with green tea extract. *Food Hydrocolloids*, 30, 264-271.

Gómez-Estaca, J., Giménez, B., Gómez-Guillén, C., & Montero, P. (2010a). Influence of frozen storage on aptitude of sardine and dolphinfish for cold-smoking process. *LWT-Food Sci Technol*, 43, 1246-1252.

Gómez-Estaca, J., Gómez-Guillén, M.C., Fernández-Martin, F., & Montero, P. (2011). Effect of gelatin origin, bovine-hide and tuna-skin, on the properties of compound gelatin-chitosan films. *Food Hydrocolloids*, 25, 1461-1469.

Gómez-Estaca, J., López de Lacey, A., López-Caballero, M.E., Gómez-Guillén, M.C., & Montero, P. (2010b). Biodegradable gelatin-chitosan films incorporated with essential oils as antimicrobial agents for fish preservation. *Food Microbiol*, 27, 889-896.

Gómez-Guillén, M.C., Giménez, B., López-Caballero, M.E., & Montero, M.P. (2011). Functional and bioactive properties of collagen and gelatin from alternative sources: a review. *Food Hydrocolloids*, 25, 1813-1827.

Gómez-Guillén, M.C., Pérez-Mateos, M., Gómez-Estaca, J., López-Caballero, E., Giménez, B., & Montero, P. (2009). Fish gelatin: a renewable material for developing active biodegradable films. *Trends Food Sci Technol*, 20, 3-16.

Gómez-Guillén, M.C., Turnay, J., Fernandez-Diaz, M.D., Ulmo, N., Lizarbe, M.A., & Montero, P. (2002). Structural and physical properties of gelatin extracted from different marine species: a comparative study. *Food Hydrocolloids*, 16, 25-34.

Guadipati, V. (2013). Fish gelatin: a versatile ingredient for the food and pharmaceutical industries. In *Marine Proteins and Peptides-Biological activities and applications*. Kim, S.K. (Ed.). John Wiley & Sons, Ltd, West Sussex, UK, Chapter 13.

Guerrero, P., Beatty, E., Kerry, J.P., & de la Caba, K. (2012). Extrusion of soy protein with gelatin and sugars at low moisture content. *J Food Eng*, 110, 53-59.

Guerrero, P., Etxabide, A., Leceta, I., Peñalba, M., & de la Caba, K. (2014). Extraction of agar from *Gelidium sesquipedale* (*Rodhopyta*) and surface characterization of agar based films. *Carbohydr Polym*, 99, 491-489.

Guerrero, P., Kerry, J.P., & de la Caba, K. (2014). Characterization of protein-polysaccharide interactions in extruded blends. *Carbohyd Polym*, 111, 598-605.

Guerrero, P., Nur Hanani, Z.A., Perry, J.P., & de la Caba, K. (2011a). Characterization of soy protein-based films prepared with acids and oils by compression. *J Food Eng*, 107, 41-49.

Guerrero, P., Stefani, P.M., Ruseckaite, R., & de la Caba, K. (2011b). Functional properties of films based on soy protein isolate and gelatin processed by compression molding. *J Food Eng*, 105, 65-72.

Gullon, B., Pintado, M.E., Pérez-Álvarez, J.A., & Viuda-Martos, M. (2016). Assessment of polyphenolic profile and antibacterial activity of pomegranate peel (*Punica granatum*) flour obtained from co-product of juice extraction. *Food Control*, 59, 94-98.

Günkaya, Z. & Banar, M. (2016). An environmental comparison of biocomposite film based on orange peel-derived pectin jelly-corn starch and LDPE film: LCA and biodegradability. *Int J Life Cycle Asses*, 21, 465-475.

Gupta, R.K., Kumar, P., Sharma, A., & Patil, R.T. (2011). Color kinetics of aonla shreds with amalgamated blanching during drying. *Int J Food Prop*, 14, 1232-1240.

Haddar, A., Sellimi, S., Ghannouchi, R., Alvarez, O.M., Nasri, M., & Bougatef, A. (2012). Functional, antioxidant and film-forming properties of tuna-skin gelatin with a brown algae extract. *Int J Biol Macromol*, 51, 477-483.

Hammann, F. & Schmid, M. (2014). Determination and quantification of molecular interactions in protein films: a review. *Materials*, 7, 7975-7996.

Haq, M.A., Hasnain, A., & Azam, M. (2014). Characterization of edible gum cordia film: effects of plasticizers. *LWT-Food Sci Technol*, 55, 163-169.

He, J., Yin, T., Chen, Y., Cai, L., Tai, Z., Li, Z., Liu, C., Wang, Y., & Ding, Z. (2015). Phenolic compounds and antioxidant activities of edible flowers of *Pyrus pashia*. *J Funct Foods*, 17, 371-379.

Hernández-Izquierdo, V.M. & Krochta, J.M. (2009). Thermal transitions and heat-sealing of glycerol-plasticized whey protein films. *Packag Technol Sci*, 22, 255-260.

Hong, P.K., Gottardi, D., Ndagijimana, M., & Betti, M. (2014). Glycation and transglutaminase mediated glycosylation of fish gelatin peptides with glucosamine enhance bioactivity. *Food Chem*, 142, 285-293.

Hoque, S. (2011). Improvement of properties of edible film based on gelatin from cuttlefish (*Sepia pharaonis*) skin. PhD. Dissertation, Prince of Songkla University.

Hoque, S., Benjakul, S., & Prodpran, T. (2011). Properties of film from cuttlefish (*Sepia pharaonis*) skin gelatin incorporated with cinnamon, clove and star anise extracts. *Food Hydrocolloids*, 25, 1085-1097.

Hu, X., Lu, Q., Sun, L., Cebe, P., Wang, X., Zhang, X., & Kaplan, D.L. (2010). Biomaterials from ultrasonication-induced silk fibroin-hyaluronic acid hydrogels. *Biomacromolecules*, 11, 3178-3188.

Iahnke, A.O.S., Costa, T.M.H., Rios, A.O., & Flôres, S.H. (2015). Residues of minimally processed carrot and gelatin capsules: potential materials for packaging films. *Ind Crops Prod*, 76, 1071-1078.

Ingrao, C., Lo Giudice, A., Bacenetti, J., Khaneghah, A.M., Sant'Ana, A.S., Rana, R., & Siracusa, V. (2015). Foamy polystyrene trays for fresh-meat packaging: life-cycle inventory data collection and environmental impact assessment. *Food Res Int*, 76, 418-426.

Islam, M.I.U. & Langrish, T.A.G. (2010). An investigation into lactose crystallization under high temperature conditions during spray drying. *Food Res Int*, 43, 46-56.

Isleroglu, H., Kemerli, T., Sakin-Yilmazer, M., Guven, G., Ozdestan, O., Uren, A., & Kaymak-Ertekin, F. (2012). Effect of steam baking on acrylamide formation and browning kinetics of cookies. *J Food Sci*, 77, 257-263.

ISO 10993-5 (2009). Biological evaluation of medical devices - Part 5: Tests for in vitro cytotoxicity.

ISO 14040 (2006). Environmental Management - Life Cycle Assessment - Principals and Framework.

Iturriaga, L., Olabarrieta, I., & de Marañón, I.M. (2012). Antimicrobial assays of natural extracts and their inhibitory effect against *Listeria innocua* and fish spoilage bacteria, after incorporation into biopolymer edible films. *Int J Food Microbiol*, 158, 58-64.

Jara-Palacios, M.J., Hernanz, D., Cifuentes-Gomez, T., Escudero-Gilete, M.L., Heredia, F.J., & Spencer, J.P.E. (2015). Assessment of white grape pomace from winemaking as source of bioactive compounds, and its antiproliferative activity. *Food Chem*, 183, 78-82.

Jayasundera, M., Adhikari, B., Aldred, P., & Ghandi, A. (2009). Surface modification of spray dried food and emulsion powders with surface-active proteins: a review. *J Food Eng*, 93, 266-277.

Jiang, Z. & Brodkorb, A. (2012). Structure and antioxidant activity of Maillard reaction products from α-lactalbumin and β-lactoglobulin with ribose in an aqueous model system. *Food Chem*, 133, 960-968.

Jiménez, N., Bohuon, P., Donier, M., Bonazzi, C., Pérez, A.M., & Vaillant, F. (2012). Effect of water activity on anthocyanin degradation and browning kinetics at high temperatures (100-140 ºC). *Food Res Int*, 47, 106-115.

Kadam, S.U., Pankaj, S.K., Tiwari, B.K., Cullen, P.J., & O'Donnell, C.P. (2015). Development of biopolymer-based gelatin and casein films incorporating brown seaweed *Ascophyllum nodosum* extract. *Food Packing and Shelf Life*, 6, 68-74.

Kaewprachu, P. & Rawdkuen, S. (2016). Application of active edible films as food packaging for food preservation and extending shelf life. In *Microbes in food and health*. Garg, N., Abdel-Aziz, S.M., & Aeron, A. (Eds.). Springer-Verlag, Berlin, Germany, pp. 185-205.

Kaewprachu, P., Osako, K., Benjakul, S., & Rawdkuen, S. (2015). Quality attributes of minced pork wrapped with catechin-lysozyme incorporated gelatin film. *Food Packaging and Shelf Life*, 3, 88-96.

Kallel, F., Driss, D., Chaari, F., Belghith, L., Bouaziz, F., Ghorbel, R., & Chaabouni, S.E. (2014). Garlic (*Allium sativum* L.) husk waste as a potential source of phenolic compounds: influence of extracting solvents on its antimicrobial and antioxidant properties. *Ind Crops Prod*, 62, 34-41.

Kalogeropoulos, N., Chiou, A., Pyriochou, V., Peristeraki, A., & Karathanos, V.T. (2012). Bioactive phytochemicals in industrial tomatoes and their processing byproducts. *LWT-Food Sci Technol*, 49, 213-216.

Karbowiak, T., Debeaufort, F., Champion, D., & Voilley, A. (2006). Wetting properties at surface of iota-carrageenan-based edible films. *J Colloid Interface Sci*, 294, 400-410.

Karim, A.A. & Bhat, R. (2008). Gelatin alternatives for the food industry: recent development challenges and prospects. *Trends Food Sci Tehcnol*, 19, 644-656.

Karnjanapratum, S., O'Callaghan, Y.C., Benjakul, S., & O'Brien, N.M. (2016). *In vitro* cellular bioactivities of Maillard reaction products from sugar-gelatin hydrolysate of unicorn leatherjacket skin system. *Funct Foods*, 23, 87-94.

Kavoosi, G., Rahmatallahi, A., Dadfar, S.M.M., & Purfard, A.M. (2014). Effects of essential oil on the water binding capacity, physico-mechanical properties, antioxidant and antibacterial activity of gelatin films. *LWT-Food Sci Technol*, 57, 556-561.

Keyf, F. & Etikan, I. (2004). Evaluation of gloss changes of two denture acrylic resin materials in four different beverages. *Dent Mater*, 20, 244-251.

Kijchavengkul, T. & Auras, R. (2008). Compostability of polymers. *Polym Int*, 57, 793-804.

Kim, J.S. & Lee, Y.S. (2009). Antioxidant activity of Maillard reaction products derived from aqueous gluose/glycine, diglycine, and triglycine model systems as a function of heating time. *Food Chem*, 116, 272-232.

Kittiphattanabawon, P., Benjakul, S., Visessanguan, W., Nagai, T., & Tanaka, M. (2015). Characterization of acid soluble collagen from skin and bone of bigeye snapper (*Priacanthus tayenus*). *Food Chem*, 89, 363-372.

Kowalcyzk, D. & Biendl, M. (2016). Physicochemical and antioxidant properties of biopolymer/candelilla wax emulsion films containing hop extract - A comparative study. *Food Hydrocolloids*, 60, 384-392.

Kowalczyk, D. (2016). Biopolymer/candelilla wax emulsion films as carriers of ascorbic acid - A comparative study. *Food Hydrocolloids*, 52, 543-553.

Krochta, J.M. (2002). Proteins as raw materials for films and coatings: definitions, current status, and opportunities. In *Protein-based films and coatings*. Gennadios, A. (Ed.). CRC Press, Taylor & Francis Group, New York, pp. 1-42.

Kunte, L., Gennadios, A., Cuppett, S., Hanna, M., & Weller, C. (1997). Cast films from soy protein isolates and fractions. *Cereal Chem*, 72, 115-118.

Labuza, T. P. & Baiser, W. M. (1992). The kinetics of nonenzymatic browning. In *Physical chemistry of foods*. Schwartzberg, H. G. & Hartel, R. W. (Eds.). Marcel Dekker, New York, USA, pp. 595-649

Lacroix, M. & Vu, K.D. (2014). Edible coating and film materials: proteins. In *Innovations in Food Packaging*. Han, J.H. (Ed). Academic Press, San Diego CA, USA, pp. 277-294.

Learner, T.J.S., Smithen, P., Krueger, J.W., & Schilling, M.R. (Eds.) (2008). Modern Paints Uncovered. Getty Publications, Los Angeles (US).

Leceta, I., Etxabide, A., Cabezudo, S., de la Caba, K., & Guerrero, P. (2014). Bio-based films prepared with by-products and wastes: environmental assessment. *J Cleaner Prod*, 64, 218-227.

Leceta, I., Guerrero, P., Cabezudo, S., & de la Caba, K. (2013). Environmental assessment of chitosan-based films. *J Cleaner Prod*, 41, 312-318.

Lefevre, T. & Subirade, M. (2000). Molecular differences in the formation and structure of fine-stranded and particulate β-lactoglobulin gels. *Biopolymers*, 54, 578-586.

Lefevre, T., Subirade, M., & Pezolet, M. (2005). Molecular description of the formation and structure of plasticized globular protein films. *Biomacromolecules*, 6, 3209-3219.

Li, W., Gao, H., Mu, H., Chen, H., Fang, X., Zhou, Y., & Tao, F. (2015b). Three different active aldehydes induce the production of oxidation advanced lipoxidation end

products upon incubation with bovine serum albumin. *Eur J Lipid Sci Technol*, 117, 1432-1443.

Li, Y., Li, C., Mujeeb, A., Jin, Z., & Ge, Z. (2015a). Optimization and characterization of chemically modified polymer microspheres and their effect on cell behavior. *Mater Lett*, 154, 68-72.

Lin, C.S.K., Pfaltzgraff, L.A., Herrero-Davila, L., Mubofu, E.B., Abderrahim, S., Clark, J.H., Koutines, A., Kopsahelis, N., Stamatelatou, K., Dickson, F., Thankappan, S., Mohamed, Z., Brocklesby, R., & Luque, R. (2013). Food waste as a valuable resource for the production of chemicals, materials and fuels. Current situation and global perspective. *Energy Environ Sci*, 6, 426-464.

Lin, L.H., Chen, K.M., Liu, H.J., Chu, H.W., Kuo, T.C., Hwang, M.C., & Wang, C.F. (2012). Preparation and surface activities of modified gelatin-conjugates. *Colloids Surf A: Physicochem Eng Aspects*, 408, 97-103.

Lingua, M.S., Fabani, M.P., Wunderlin, D.A., & Baroni, M.V. (2016). From grape to wine: changes in phenolic composition and its influence on antioxidant activity. *Food Chem*, 208, 228-238.

Liu, F., Avena-Bustillos, R.J., Chiou, B.S., Li, Y., Ma, Y., Williams, T.G., Wood, D.F., McHugh, T.H., & Zhong, F. (2017). Controlled-release of tea polyphenol from gelatin films incorporated with different ratios of free/nanoencapsulated polyphenols into fatty food simulants. *Food Hydrocolloids*, 62, 212-221.

Liu, F., Majeed, H., Antoniou, J., Liu, Y., Ma, J., & Zhong, F. (2016). Tailoring physical properties of transglutaminase-modified gelatin films by varying drying temperature. *Food Hydrocolloids*, 58, 20-28.

Liu, G. & Zhong, Q. (2012). Glycation of whey protein to provide steric hindrance against thermal aggregation. *J Agric Food Chem*, 60, 9754-9762.

López-Rubio, A., Lagarón, J.M., & Ocio, M.J. (2008). Active polymer packaging of non-meat food products. In *Smart packaging technologies*. Kerry J. & Butler, P. (Eds.). John Wiley & Sons Ltd, Chichester, England, pp. 19-30.

Lozano-Sánchez, J., Giambanelli, E., Quirantes-Piné, R., Cerretani, L., Bendini, A., Segura-Carretero, A., & Fernández-Gutiérrez, A. (2011). Wastes generated during the storage of extra virgin olive oil as a natural source of phenolic compounds. *J Agric Food Chem*, 59, 11491-11500.

Lu, M., Yuan, B., Zeng, M., & Chen, J. (2011). Antioxidant capacity and major phenolic compounds of spices commonly consumed in China. *Food Res Int*, 44, 530-536.

Ma, W., Tang, C.H., Yin, S.W., Yang, X.Q., & Qi, J.R. (2013). Genipin-crosslinked gelatin films as controlled releasing carriers of lysozyme. *Food Res Inter*, 51, 321-324.

Martínez-Ruvalcaba, A., Becerra-Bracamontes, F., Sánchez-Díaz, J.C., & González-Álvarez, A. (2009). Polyacrylamide-gelatin polymeric networks: effect of pH and gelatin concentration on the swelling kinetics and mechanical properties. *Polym Bull*, 62, 539-548.

Martins, I.M., Barreiro, M.F., Coelho, M., & Rodrigues, A.E. (2014). Microencapsulation of essential oils with biodegradable polymeric carriers for cosmetic applications. *Chem Eng J*, 245, 191-200.

Martins, S.I.F.S., Jongen, W.M.F., & Van Boekel, M.A.J.S. (2001). A review of Maillard reactions in food and implications to kinetic modeling. *Trends Food Sci Tech*, 11, 364-373.

Masci, A., Coccia, A., Lendaro, E., Mosca, L., Paolicelli, P., & Cesa, S. (2016). Evaluation of different extraction methods from pomegranate whole fruit or peels and the antioxidant and antiproliferative activity of the polyphenolic fraction. *Food Chem*, 202, 59-69.

Mathew, A.P. & Dufresne, A. (2002). Plasticized waxy maize starch: effect of polyols and relative humidity on material properties. *Biomacromolecules*, 3, 1101-1108.

Mehanny, M., Hathout, R.M., Geneidi, A.S., & Mansour, S. (2016). Exploring the use of nanocarrier systems to deliver the magical molecule; Curcumin and its derivatives. *J Controlled Release*, 225, 1-30.

Melo, P.S., Maddarioli, A.P., Denny, C., Ferracini dos Santos, L., Franchin, M., Pereira, G.E., Ferreira de Souza Vieira, T.M., Rosalen, P.L., & Matias de Alencar, S. (2015). Winery by-products: extraction optimization, phenolic composition and cytotoxic evaluation to act as a new source of scavenging of reactive oxygen species. *Food Chem*, 181, 160-169.

Mikšovská, J. & Larsen, R.W. (2007). Photothermal studies of pH induced unfolding of proteins. In *Protein structures: methods in protein structure and stability analysis*. Uversky V.N. & Permyakov, E.A. (Eds.). Nova Science Publishers, New York, USA, pp. 159-187.

Molyneux, P. (2004). The use of the stable free radical diphenlpicrylhydrazyl (DPPH) for estimating antioxidant activity. *Songklanakarin J Sci Technol*, 26, 211-219.

Monedero, F.M., Fabra, M.J., Talens, P., & Chiralt, A. (2009). Effect of oleic acid-beeswax mixtures on mechanical, optical and water barrier properties of soy protein isolate based films. *J Food Eng*, 91, 509-515.

Monti, S.M., Borreilli, R.C., Ritieni, A., & Fogliano, V. (2000). A comparison of color formation and Maillard reaction products of a lactose-lysine and lactose-N(alpha)-acetyllysine model system. *J Agric Food Chem*, 48, 1041-1046.

Monti, S.M., Ritieni, A., Graziani, G., Randazzo, G., Mannina, L., Segre, A.L., & Fogliano, V. (1999). LC/MS analysis and antioxidative efficiency of Maillard reaction products from a lactose-lysine model system. *J Agric Food Chem*, 47, 1506-1513.

Morales, F.J. & Van Boekel, M.A.J.S. (1997). A study on advanced Maillard reaction in heated casein/sugar solutions: fluorescence accumulation. *Int Dairy J*, 7, 675-683.

Mu, C., Guo, J., Li, X., Lin, W., & Li, D. (2012). Preparation and properties of dialdehyde carboxymethyl cellulose crosslinked gelatin edible films. *Food Hydrocolloids*, 27, 22-29.

Murakami, Y., Ishii, H., Takada, H., Tanaka, S., Machino, M., Ito, S., & Fujisawa, S. (2008). Comparative anti-inflammatory activities of curcumin and tetrahydrocurcumin based on the phenolic O-H bond dissociation enthalpy, ionization potential and quantum chemical descriptor. *Anticancer Res*, 28, 699-707.

Murugan, P. & Pari, L. (2006). Antioxidant effect of tetrahydrocurcumin in streptozotocin-nicotinamide induced diabetic rats. *Life Sci*, 79, 1720-1728.

Muyonga, J.H., Cole, C.G.B., & Duodu, K.G. (2004). Extraction and physico chemical characterisation of Nile perch (*Lates niloticus*) skin and bone gelatin. *Food Hydrocolloids*, 18, 581-592.

Nagaranjan, M., Benjakul, S., & Prodpran, T. (2015). Effects of bio-nanocomposite films from tilapia and squid skin gelatins incorporated with ethanolic extract from coconut husk on storage stability of mackerel meat powder. *Food Packaging and Shelf Life*, 6, 42-52.

Nakamatsu, J., Torres, F.G., Troncoso, O.P., Min-Lin, Y., & Boccaccini, A.R. (2006). Processing and characterization of porous structures from chitosan and starch for tissue engineering scaffolds. *Biomacromolecules*, 7, 3345-3355.

Nguyen, C.V. (2006). Toxicity of the AGEs generated from the Maillard reaction: on the relationship of food-AGEs and biological-AGEs. *Mol Nutr Food*, 50, 1140-1149.

Nollet, L.M.L. & Toldrá, F. (Eds.) (2015). Handbook of food analysis (3rd edition-Volume I). CRC-Press, Taylor & Francis group, Boca Ratón, Florida, USA, pp. 695-716.

Nor Afizah, M. & Rizvi, S.S.H. (2014). Functional properties of whey protein concentrate texturized at acidic pH: effect of extrusion temperature. *LWT-Food Sci Technol*, 57, 290-298.

Núñez-Flores, R., Giménez, B., Fernández-Martín, F., López-Caballero, M.E., Montero, M.P., & Gómez-Guillén, M.C. (2012). Role of lignosulphonate in properties of fish gelatin films. *Food Hydrocolloids*, 27, 60-71.

Núñez-Flores, R., Giménez, B., Fernández-Martín, F., López-Caballero, M.E., Montero, M.P., & Gómez-Guillén, M.C. (2013). Physical and functional characterization of active fish gelatin films incorporated with lignin. *Food Hydrocolloids*, 30, 163-172.

Nur Hanani, Z.A., McNamara, J., Roos, Y.H., & Kerry, J.P. (2013). Effect of plasticizer content on the functional properties of extruded gelatin-based composites. *Food Hydrocolloids*, 31, 264-269.

Nur Hanani, Z.A., Roos, Y.H., & Kerry, J.P. (2012). Use of beef, pork and fish gelatin sources in the manufacturing of films and assessment of their composition and mechanical properties. *Food Hydrocolloids*, 29, 144-151.

Nur Hanani, Z.A., Ross, Y.H., & Kerry, J.P. (2014). Use and applications of gelatin as potential biodegradable packaging materials for food products. *Int J Biol Macromol*, 71, 94-102.

Nursten, H.E. (Ed.) (1986). Concentration and Drying of Foods. Elsevier, London & New York.

Olivas, G.I., Mattinson, D.S., & Barbosa-Cánovas, G.V. (2007). Alginate coatings for preservation of minimally processed “gala” apples. *Postharvest Biol Technol*, 45, 89-96.

Osen, R., Toelstede, S., Wild, F., Eisner, P., & Schweiggert-Weisz, U. (2014). High moisture extrusion cooking of pea protein isolates: raw material characteristics, extruder responses, and texture properties. *J Food Eng*, 127, 67-74.

Oussalah, M., Caillet, S., Saucier, L., & Lacroix, M. (2007). Inhibitory effects of selected plant essential oils on the growth of four pathogenic bacteria: *E. coli* O157:H7, *Salmonella typhimurium*, *Staphylococcus aureus* and *Listeria monocytogenes*. *Food Control*, 18, 414-420.

Ozdal, T., Capanoglu, E., & Altay, F. (2013). A review on protein-phenolic interactions and associated changes. *Food Res Int*, 51, 954-970.

Palou, E., López-Malo, A., Barbosa-Cánovas, G.V., Welti-Chanes, J., & Swanson, B.G.J. (1999). Polyphenoloxidase activity and color of blanched and high hydrostatic pressure treated banana puree. *Food Sci*, 64, 42-45.

Panzavolta, S., Gioffrè, M., Focarete, M.L., Gualandi, C., Foroni, L., & Bigi, A. (2011). Electrospun gelatin nanofibers: optimization of genipin cross-linking to preserve fiber morphology after exposure to water. *Acta Biomater*, *7*, 1702-1709.

Pastoriza, S. & Rufián-Henares, J.A. (2014). Contribution of melanoidins to the antioxidant capacity of the Spanish diet. *Food Chem*, 164, 438-445.

Perez-Espitia, P.J., Ferreira Soares, N.F.F., Coimbra, J.S.R., Andrade, N.J., Cruz, R.S., & Medeiros, E.A.A. (2012). Bioactive peptides: synthesis, properties, and applications in the packaging and preservation of food. *Comp Rev Food Sci Food Safe*, 11, 187-204.

PlasticsEurope (2016). Plastics-the facts 2016. Brussels: PlasticsEurope.

Plyduang, T., Lomlim, L., Yuenyongsawad, S., & Wiwattanapatapee, R. (2014). Carboxymethylcellulose-tetrahydrocurcumin conjugates for colon-specific delivery of a novel anti-cancer agent, 4-amino tetrahydrocurcumin. *Eur J Pharm Biopharm*, 88, 351-360.

Portes, E., Gardrat, C., & Castellan, A. (2007). A comparative study on the antioxidant properties of tetrahydrocurcuminoids and curcuminoids. *Tetrahedron*, 63, 9092-9099.

Portes, E., Gardrat, C., Castellan, A., & Coma, V. (2009). Environmentally friendly films based on chitosan and tetrahydrocurcumoid derivative exhibiting antibacterial and antioxidative properties. *Carbohydr Polym*, 76, 578-584.

Pourali, O., Asghari, F.S., & Yoshida, H. (2010). Production of phenolic compounds from rice bran biomass under subcritical water conditions. *Chem Engi J*, 160, 259-266.

Prakash Maran, J., Sivakumar, V., Thirugnanasambandham, K., & Sridhar, R. (2014). Degradation behavior of biocomposites based on cassava starch buried under indoor soil conditions. *Carbohyd Polym*, 101, 20-28.

Priyadarsini, K.I. (2014). The chemistry of curcumin: from extraction to therapeutic agent. *Mol*, 19, 20091-20112.

Quinn, G., Monahan, F. J., O'Sullivan, M., & Langares, A. (2003). Role of covalent and noncovalent interactions in the formation of films from unheated whey protein solutions following pH adjustment. *J Food Sci*, 68, 2284-2288.

Rahman, M.S. (Ed.) (2007). Handbook of Food Preservation (2nd edition). CRC Press, Taylor & Francis Group, New York, USA.

Ramos, P., Santos, S.A.O., Guerra, Â.R., Guerreiro, O., Felício, L., Jerónimo, E., Silvestre, A.J.D., Neto, C.P., & Duarte, M. (2013). Valorization of olive mil residues:

antioxidant and breast cancer antiproliferative activities of hydroxytyrosol-rich extracts derived from olive oil by-products. *Ind Crops Prod*, 46, 359-368.

Rao, K.M., Rao, K.S.V.K., Ramanjaneyulu, G., & Ha, C.S. (2015). Curcumin encapsulated pH sensitive gelatin based interpenetrating polymeric network nanogels for anti cancer drug delivery. *Int J Pharm*, 478, 788-795.

Rao, S.R. & Ravishankar, G.A. (2002). Plant cell cultures: chemical factories of secondary metabolites. *Biotechnol Advances*, 20, 101-153.

Ravindran, R. & Jaiswal, A. (2016). Exploitation of food industry waste for high-value products. *Trends Biotechnol*, 34, 58-69.

Rawdkuen, S., Suthiluk, P., Kamhangwong, D., & Benjakul, S. (2012). Mechanical, physico-chemical, and antimicrobial properties of gelatin-based film incorporated with catechin-lysozyme. *Chem Central J*, 6, 131-140.

Reddy, N. & Yang, Y. (2013). Thermoplastic films from plant proteins. *J Appl Polym Sci*, 130, 729-736.

Rindlav-Westling, A., Standing, M., Hermansson, A.M., & Gatenholm, P. (1998). Structure, mechanical and barrier properties of amylase and amylopectin films. *Carbohydr Polym*, 36, 217-224.

Roberston, G.L. (Ed.) (2013). Food Packaging. Principles and Practice (3rd edition). CRC Press, Taylor & Francis Group, LLC, New York, USA, Chapter 1.

Saarai, A., Kasparkova, V., Sedlacek, T., & Saha, P. (2013). On the development and characterisation of crosslinked sodium alginate/gelatin hydrogels. *J Mech Behav Biomed Mater*, 18, 152-166.

Samira, S., Thuan-Chew, T.C., & Azhar, M.E. (2014). Effect of ribose-induced Maillard reaction on physical and mechanical properties of bovine gelatin films prepared by oven drying. *Int Food Res J*, 2, 269-276.

Sanches-Silva, A., Costa, D., Albuquerque, T.G., Buonocore, G.G., Ramos, F., Castilho, M.C., Machado, A.V., & Costa, H.S. (2014). Trends in the use of natural antioxidants in active food packaging: a review. *Food Addit Contam, Part A*, 31, 374-395.

Santoro, M., Tatara, A.M., & Mikos, A.G. (2014). Gelatin carriers for drug and cell delivery in tissue engineering. *J. Control. Release,* 190, 210-218.

Schmidt, V., Giacomelli, C., & Soldi, V. (2005). Thermal stability of films formed by soy protein isolate-sodium dodecyl sulfate. *Polym Degrad Stab*, 87, 25-31.

Serpen, A., Capuano, E., Fogliano, V., & Gokmen, V. (2007). A new procedure to measure the antioxidant activity of insoluble food components. *J Agric Food Chem*, 55, 7676-7681.

Shakila, R.J., Jeevithan, E., Arumugam, V., & Jeyasekaran, G. (2015). Suitability of antimicrobial grouper bone gelatin films as edible coatings for vacuum-packaged fish steaks. *J Aquat Food Prod Technol*, 25, 724-734.

Sihem, D., Samia, D., Gaetano, P., Sara, L., Giovanni, M., Hassiba, C., Laura, G., & Noureddine, H.A. (2015). *In vitro* antioxidant activities and phenolic content in crop residues of Tunisian globe artichoke. *Sci Hortic*, 190, 128-136.

Silva, N.H.C.S., Vilela, C., Marrucho, I.M., Freire, C.S.R., Neto, C.P., & Silvestre, A.J.D. (2014). Protein-based materials: from sources to innovative sustainable materials for biomedical applications. *J Mater Chem B*, 2, 3715-3740.

Singh, P.P. & Saldaña, M.D.A. (2011). Subcritical water extraction of phenolic compounds from potato peel. *Food Res Int*, 44, 2452-2458.

Singh, S., Lee, M.H., Park, I., Shin, Y., & Lee, Y.S. (2016). Antimicrobial seafood packaging: a review. *J Food Sci Technol*, 53, 2505-2518.

Somporn, P., Phisalaphong, C., Nakornchai, S., Unchern, S., & Morales, N.P. (2007). Comparative antioxidant activities of curcumin and its demethoxy and hydrogenated derivatives. *Biol Pharm Bull*, 20, 74-78.

Song, A.Y., Oh, Y.A., Roh, S.H., Kim, J.H., & Min, S.C. (2016). Cold oxygen plasma treatments for the improvement of the physicochemical and biodegradable properties of polylactic acid films for food packaging. *J Food Sci*, 81, 86-96.

Song, J.H., Murphy, R.J., Narayan R., & Davies, G.B.H. (2009). Biodegradable and compostable alternatives to conventional plastics. *Philos Trans R Soc B*, 364, 2127-2139.

Sormoli, M.E., Das, D., & Landgrish, T. (2013). Crystallization behavior of lactose/sucrose mixtures during water-induced crystallization. *J Food Eng*, 116, 873-880.

Souguir, H., Salaün, F., Douillet, P., Vroman, I., & Chatterjee, S. (2013). Nanoencapsulation of curcumin in polyurethane and polyurea shells by an emulsion diffusion method. *Chem Eng J*, 221, 133-145.

Sung, H., Huang, D., Chang, W., Huang, R., & Hsu, J. (1999). Evaluation of gelatin hydrogel crosslinked with various crosslinking agents as bioadhesives: *in vitro* study. *J Biomed Mater Res*, 46, 520-530.

Susi, H., Serge, N., Timasheff, S.N., & Stevens, L. (1967). Infrared spectra and protein conformations in aqueous solutions: I. The amide I band in H_2O and D_2O solutions. *J Biol Chem*, 242, 5460-5466.

Suyatma, N.E., Tighzert, L., & Copinet, A. (2005). Effects of hydrophilic plasticizers on mechanical, thermal, and surface properties of chitosan films. *J Agric Food Chem*, 53, 3950-3957.

Tayel, A.A., El-Tras, W.F., Moussa, S., El-Baz, A.F., Mahrous, H., Salem, M.F., & Brimer, L. (2011). Antibacterial action of zinc oxide nanoparticles against foodborne pathogens. *J Food Safe*, 3, 211-218.

Tian, F., Decker, E.A., & Goddard, J.M. (2013). Controlling lipid oxidation of food by active packaging technologies. *Food Funct*, 4, 669-680.

Tongnuanchan, P., Benjakul, S., & Prodpran, T. (2012). Properties and antioxidant activity of fish skin gelatin film incorporated with citrus essential oils. *Food Chem*, 134, 1571-1579.

Tongnuanchan, P., Benjakul, S., & Prodpran, T. (2013). Physico-chemical properties, morphology and antioxidant activity of film from fish skin gelatin incorporated with root essential oils. *J Food Eng*, 117, 350-360.

Touati, R., Santos, S.A.O., Rocha, S.M., Belhamel, K., & Silvestre, A.J.D. (2015). The potential of cork from *Quercus suber* L. grown in Algeria as a source of bioactive lipophilic and phenolic compounds. *Ind Crops Prod*, 76, 936-945.

Tovar, L., Salafranca, J., Sanchez, C., & Nerin, C. (2005). Migration studies to assess the safety in use of a new antioxidant active packaging. *J Agric Food Chem*, 53, 5270-5275.

UNE-EN 13432:2001 (2001). Requirements for packaging recoverable through composting and biodegradation. Test scheme and evaluation criteria for the final acceptance of packaging.

Uranga, J., Leceta, I., Etxabide, A., Guerrero, P., & de la Caba, K. (2016). Cross-linking of fish gelatin films to develop sustainable films with enhanced properties. *Eur Polym J*, 78, 82-90.

Van Boekel, M.A.J.S. (1998). Effect of heating on Maillard reactions in milk. *Food Chem*, 62, 403-414.

Venkatesen, P., Unnikrishnan, M.K., Kumar, M.S., & Rao, M.N.A. (2003). Effect of curcumin analogues on oxidation of haemoglobin and lysis of erythrocytes. *Curr Sci*, 84, 74-78.

Wang, S., Marcone, M.S., Barbut, S., & Lim, L.T. (2012). Formation of dietary biopolymers-based packaging material with bioactive plant extracts. *Food Res Int*, 49, 80-91.

Wang, W.Q., Bao, Y.H., & Chen, Y. (2013). Characteristics and antioxidant activity of water-soluble Maillard reaction products from interactions in a whey protein isolate and sugars system. *Food Chem*, 139, 355-361.

Wang, Y., Liu, A., Ye, R., Wang, W., & Li, X. (2015). Transglutaminase-induced crosslinking of gelatin-calcium carbonate composite films. *Food Chem*, 166, 414-422.

Wang, Y., Yang, H., & Regenstein, J.M. (2008). Characterization of fish gelatin at nanoscale using atomic force microscopy. *Food Biophysics*, 3, 269-272.

Wanyo, P., Meeso, N., & Siriamornpun, S. (2014). Effects of different treatments on the antioxidant properties and phenolic compounds of rice bran and rice husk. *Food Chem*, 157, 457-463.

Wardhani, D.H., Fuciños, P., Vázquez, J.A., & Pandiella, S.S. (2013). Inhibition kinetics of lipid oxidation of model foods by using antioxidant extract of fermented soybeans. *Food Chem*, 139, 837-844.

Wetzel, R., Buder, E., Hermel, H., & Hüttner, A. (1987). Conformations of different gelatins in solutions and in films. An analysis of circular dichroism (CD) measurements. *Colloid Polym Sci*, 265, 1036-1045.

Wihodo, M. & Moraru, C.I. (2013). Physical and chemical methods used to enhance the structure and mechanical properties of protein films: a review. *J Food Eng*, 114, 292-302.

Wijewickreme, A.N., Kitts, D.D., & Durance, T.D. (1997). Reaction conditions influence the elementary composition and metal chelating affinity of nondialyzable model Maillard reaction products. *J Agric Food Chem*, 45, 4577-4583.

Wu, J., Chen, S., Ge, S., Miao, J., Li, J., & Zhang, L.Q. (2013). Preparation, properties and antioxidant activity of an active film from silver carp (*Hypophthalmichthys molitrix*) skin gelatin incorporated with green tea extract. *Food Hydrocolloids*, 32, 42-51.

Wu, J., Liu, H., Ge, S., Wang, S., Qin, Z., Chen, L., Zheng, Q., Liu, Q., & Zhang, Q. (2015). The preparation, characterization, antimicrobial stability, and *in vitro* release evaluation of fish gelatin films incorporated with cinnamon essential oil nanoliposomes. *Food Hydrocolloids*, 43, 427-435.

Xie, Y., He, Y., Irwin, P.L., Jin, T., & Shi, X. (2011). Antibacterial activity and mechanism of action of zinc oxide nanoparticles against *Campylobacter jejuni*. *Appl Environ Microbiol*, 77, 2325-2331.

Yang, H., Wang, Y., Zhou, P., Regenstein, J.M., & Rouse, B. (2007). Nanostructural characterization of catfish skin gelatin using atomic force microscopy. *J Food Sci*, 72, 430-440.

Yates, M.R. & Barlow, C.Y. (2013). Life cycle assessments of biodegradable, commercial biopolymers - A critical review. *Resour, Conser Recycl*, 78, 54-66.

Yayalayan, V.A., Ismail, A.A., & Mandeville, S. (1993). Quantitative determination of the effect of pH and temperature on the keto form of D-fructose by FTIR spectroscopy. *Carbohydr Res,* 248, 355-360.

Yu, X., Zhao, M., Hu, J., Zeng, S., & Bai, X. (2012). Correspondence analysis of antioxidant activity and UV-Vis absorbance of Maillard reaction products as related to reactants. *LWT-Food Sci Technol*, 46, 1-9.

Yuan, Y. & Lee, T.R. (2013). Contact angle and wetting properties. In *Surface Science Techniques*. Bracco, G. & Holst, B. (Eds.). Spinger-Verlag, Berlin, Germany, pp. 3-33.

Zaman, H.U. & Beg, M.D.H. (2015). Improvement of physico-mechanical, thermomechanical, thermal and degradation properties of PCL/gelatin biocomposites: effect of gamma radiation. *Radiat Phys Chem*, 109, 73-82.

Zhang, X.L., Guo, Y.S., Wang, C.H., Li, G.Q., Xu, J.J., Chung, H.Y., Ye, W.C., Li, Y.L., & Wang, G.C. (2014). Phenolic compounds from *Origanum vulgare* and their antioxidant and antiviral activities. *Food Chem*, 152, 300-306.

Zhao, S., Yao, J., Fei, X., Shao, Z., & Chen, X. (2013). An antimicrobial film by embedding in situ synthesized silver nanoparticles in soy protein isolate. *Mater Lett*, 95, 142-144.


Cross-linking
Gelatin
Maillard reaction
Lactose
Cross-linking
Maillard
Gelatin

BioMat